DIPARTIMENTO DI SCIENZE MEDICHE
UNIVERSITA' DEL PIEMONTE ORIENTALE "A. AVOGADRO"
DOTTORATO IN MEDICINA MOLECOLARE - XVIII CICLO

TESI FINALE

NEGATIVE REGULATION OF THE RON TYROSINE KINASE RECEPTOR

Candidata: **Serena Germano**

Tutore: **Prof. Giovanni Gaudino**

Coordinatore del dottorato: **Prof. Umberto Dianzani**

ANNI ACCADEMICI: 2002-2006

Negative Regulation of RTKs Signaling

Receptor tyrosine kinases (RTKs) are involved in critical aspects of cell physiology ranging from cell survival, proliferation, growth, migration and differentiation (Ullrich & Schlessinger, 1990).

On engagement by their cognate trophic factor, RTKs become catalytically active and autophosphorylation of several tyrosine residues occurs in the cytoplasmic tail of the receptors, thus providing docking site for phosphotyrosine-binding proteins. The specific recruitment of these proteins, which are endowed with catalytic and/or scaffolding domains, determines the signaling output, initiating an intricate network of protein-protein interactions (Fiorini et al., 2001).

The signals that control cell fate determination need to be regulated in both time and space and different cellular mechanisms have evolved to ensure that the appropriate signaling thresholds are achieved and maintained during the right period of time and within precise spatial restrictions (Dikic & Giordano, 2003). Thereby, both positive signals and a complex chain of events defined as “negative signaling” are triggered upon growth factor binding to RTKs. The negative regulatory mechanisms ultimately leads to transient attenuation or termination of signal transmission and involve such diverse cellular processes as membrane trafficking, compartmentalization and regulated protein expression.

Although the molecular mediators of signal desensitization are currently under investigation, several mechanisms through which different physiological inhibitors antagonize and restrict trophic factor signaling have been identified, including ligand sequestration and binding inhibition, attenuation of RTKs autophosphorylation, induction of inhibitory proteins and ligand-induced receptor ubiquitination.

Ligand sequestration and binding inhibition

Evidence for RTKs regulation by ligand sequestration come from studies made in Drosophila, where activation of the Epidermal Growth Factor Receptor (EGFR) homologue, DER, is strictly regulated and different mechanisms have been described for modulation of this signaling.

The secreted protein **Argos** has been identified as an extracellular inhibitor of DER (Golembo et al., 1996; Wasserman & Freeman, 1998). While Argos mutant embryos show hyper-activation of DER signaling (Golembo et al., 1996), the addition of Argos resulted in the abrogation of DER activation by its ligand, Spitz (Schweitzer et al., 1995), indicating a role for Argos as a negative regulator of DER. Although several reports have argued that Argos interacts directly with DER (Jin et al., 2000; Vinos & Freeman, 2000), it has been demonstrated that Argos inhibits DER signaling by sequestering its activating ligand (Klein et al., 2004); see Figure 1).

DER activation has been shown to be inhibited also by **Kekkon1**, a single spanning transmembrane protein with leucine-rich repeats (LRR) and immunoglobulin (Ig) motifs (Musacchio & Perrimon, 1996). Indeed, developmental assays showed that loss of Kekkon1 activity results in increased DER signaling, whereas ectopic expression of the gene suppressed receptor activation. The inhibition involves a physical interaction between both the extracellular and transmembrane domains of Kekkon1 with DER that suppresses ligand binding and autophosphorylation of the receptor (Ghiglione et al., 1999); see Figure 1). Interestingly, these inhibitors of receptor function are expressed in the context of transcriptional responses triggered by DER itself, therefore representing a negative feedback mechanism.

While a mammalian Argos homologue has not been identified yet, **LRIG1** (leucine-rich repeats and immunoglobulin-like domain 1), the mammalian protein structurally related to Kekkon1, has been shown to inhibit mammalian Epidermal Growth Factor Receptor (EGFR) activation (Gur et al., 2004; Laederich et al., 2004).

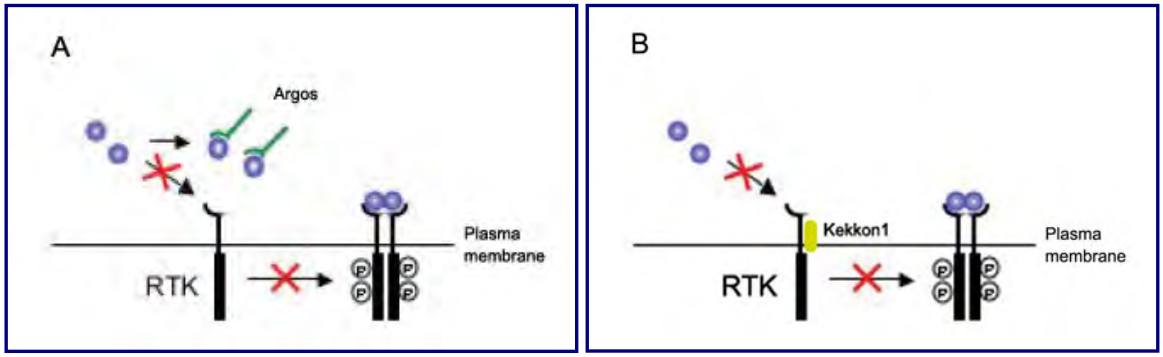

Figure 1 Different mechanisms of RTK signal attenuation: ligand-sequestration and binding inhibition. (**A**) Inhibitory role of the secreted protein Argos, which negatively regulates DER signaling sequestering the DER-activating ligand Spitz. (**B**) Kekkon1 acts as a negative regulator of DER activity, by virtue of a physical interaction with the receptor.

(*Modified form Ledda and Paratcha, 2007*)

To date few natural ligands that restrain RTKs activation have been identified, including Herstatin protein. **Herstatin** is a secreted protein, encoded by an alternatively spliced form of the ErbB2 mRNA, containing a truncated extracellular domain. Herstatin binds to ErbB2 with high affinity and has been shown to dampen receptor dimerization and catalytic activation (Doherty et al., 1999). Consistently, addition of Herstatin to the culture medium has been reported to hamper anchorage-independent growth of NIH-ErbB2 transfectants (Doherty et al., 1999). Functions similar to those of Argos have been proposed to explain Herstatin inhibition, although it is not clear whether the soluble protein inhibits binding of NDF or other ligands to ErbB heterodimers containing ErbB2.

Recently, a new mechanism of RTK negative regulation has been reported, which in contrast to ligand sequestration involves a decrease in the ligand affinity. The cell-surface glycoprotein **E-cadherin** was found to interact through its extracellular domain with EGFR, Hepatocyte Growth Factor Receptor (HGF-R/Met) and Insulin-like Growth Factor Receptor (IGFR-1), thus lessening receptor mobility and ligand binding (Andl & Rustgi, 2005).

Interference with RTKs autophosphorylation

Protein tyrosine phosphatases (PTPs) have been reported to mediate dephosphorylation of activation loop sites in RTKs, leading to inactivation of the kinase domain, while other PTPs negatively regulate RTKs activity by abrogating receptor autophosphorylation and subsequently blocking downstream signaling (Hunter et al., 1992). Several studies have shown that PTPs are able to dephosphorylate specific subsets of phosphorylated tyrosines on RTKs that have multiple phosphorylation sites, indicating a certain degree of selectivity (Kovalenko et al., 2000; Ostman et al., 2006; Persson et al., 2004). Moreover, RTKs inactivation by PTPs can be spatially partitioned in the cell, as reported for the interaction between tyrosine phosphatase **PTP1B** with activated receptors located on the inner surface of endocytic vescicles (Haj et al., 2003; Haj et al., 2002); see Figure 2). Other examples of RTK-regulating tyrosine phosphatase are the RPTPσ, whose activity has been implicated in the negative regulation of EGF receptor activation and downstream signaling (Suarez Pestana et al., 1999), the PEST-type protein-tyrosine phosphatase BDP1, emerged as a negative regulator of ErbB2 (Gensler et al., 2004) and **SHP-1**,

which has been identified as a phosphotyrosine phosphatase that negatively regulates the nerve growth factor (NGF) receptor, TrkA (Marsh et al., 2003).

During the last years **Mig6** (Mitogen-inducible gene 6, also known as **RALT**, Receptor-Associated Late Transducer) was identified as a feedback inhibitor of different RTKs. Several studies indicate that Mig6 can attenuate mitogen signaling induced by EGF, Heregulin (HRG-β) and HGF-R/Met (Fiorentino et al., 2000; Hackel et al., 2001; Pante et al., 2005; Xu et al., 2005). In the case of EGF and ErbB2 receptors, it has been reported that Mig6 is able to suppress their signaling by directly binding to the RTKs (see Figure 2) and inhibiting the EGFR/ErB2 receptor autophosphorylation, thereby attenuating the MAPK signaling (Anastasi et al., 2003). Mig6 was found to inhibit HGF-dependent signaling by indirectly binding to HGF-R/Met, through the adaptor protein Grb2 (Pante et al., 2005). Indeed, overexpression of Mig6 negatively affected the HGF-R/Met-induced cell migration.

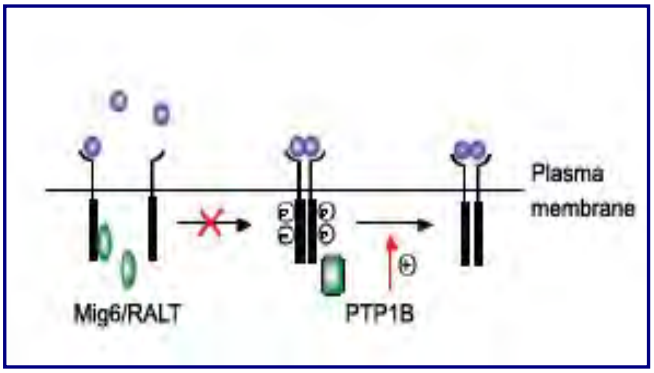

Figure 2. Different mechanisms of RTK signal attenuation: Inhibition of RTKs autophosphorylation. (**A**) Examples of this type of inhibition include the cytosolic adapter/scaffold protein Mig6/RALT and the PTP1B phosphatases.

(*Modified form Ledda and Paratcha, 2007*)

Inhibitory proteins that restrain downstream signaling

A number of intracellular inhibitors have emerged as negative regulators of specific pathways triggered by RTKs. The majority of the biological processes induced upon RTKs activation by trophic factors require the stimulation of Erk/MAP kinase family members and activation of PI3K and Akt kinases.

Increasing evidence highlights the role of Sprouty, Sef and PTEN proteins as both selective and physiological inhibitors of Erk/MAPK and PI3K-Akt signaling pathways respectively.

The mammalian **Sprouty** (Spry) family of proteins represents the major class of trophic factor-inducible antagonists of RTK signaling. In particular, Sprouty proteins have been reported to specifically inhibit the Ras-Raf-Erk1/2 pathway, leaving the PI3K and other MAPK pathways unaffected (Gross et al., 2001; Hanafusa et al., 2002; Yusoff et al., 2002); see Figure 3). All family members share a highly conserved cystein-rich domain, believed to be critical for targeting them to the inner surface of the plasma membrane, where they can bind to Grb2 and displace Grb2-Sos complexes from activated receptors. The inhibitory role of Sprouty on downstream signaling has been characterized for several mammalian RTKs, including Fibroblast Growth Factor Receptor (FGFR), HGF-R/Met, Vascular Endothelial Growth Factor Receptor (VEGFR) and Glial Cell-line Derived Neurotrophic Factor (GDNF) Receptor and RET (Impagnatiello et al., 2001; Kramer et al., 1999; Reich et al., 1999; Sasaki et al., 2003). As a negative regulator, Sprouty itself is subjected to tight control at multiple levels. Evidence indicate an increase in the levels of the *Sprouty* transcripts upon growth factors stimulation, as well as a regulated recruitment of Sprouty proteins to the plasma membrane and their tyrosine phosphorylation (Mason et al., 2004; Rubin et al., 2003). It has been suggested that

phosphorylation-dependent degradation of an active Sprouty protein might limit its inhibitory effects to a defined period after receptor engagement (Fong et al., 2003; Hall et al., 2003).

A newly identified protein that acts as signaling inhibitor is **Sef** (Similar expression to *fgf* genes). *Sef* gene encodes a putative Type I transmembrane protein highly conserved across species (Kovalenko et al., 2003). Evidence support a role for Sef protein as a feedback-induced antagonist of the Ras/MAPK-mediated FGF signaling (Furthauer et al., 2002). However, the precise mechanism of the inhibitory effect of Sef remains controversial, since it has also been reported that Sef may antagonize FGF signaling by binding to and restricting FGFR tyrosine phosphorylation (Kovalenko et al., 2003).

SOCS (suppressor of cytokine signaling) proteins have also been implicated in negative regulation of a number of RTKs. In particular, SOCS-3 was identified as a feedback inhibitor of the Stat5b pathway activated by the Insulin Receptor (IR; (Emanuelli et al., 2000). SOCS-1 has been shown to bind to ligand-activated c-Kit competing compete with c-Kit effectors for binding to the receptor. Notably, SOCS-1 overexpression has been shown to ablate proliferative but not survival signals propagated by the c-Kit RTK (De Sepulveda et al., 1999).

PTEN (phosphatase and tensin homologue) is a well characterized attenuator that has been implicated in negative signaling by RTKs, specifically in inhibition of PI3K/Akt signaling pathway, a key regulator of cell proliferation, motility and survival (see Figure 3). PTEN antagonizes PI3K by degrading PIP3 to phosphatidyl-inositol 4, 5-biphosphate (PIP2). It has been reported that downregulation of PTEN results in an increased concentration of PIP3 and Akt hyper-activation leading to protection from

apoptotic stimuli (Stambolic et al., 1998), while overexpression of PTEN in cancer cell lines results in the inactivation of Akt and cell cycle arrest (Lu et al., 1999).

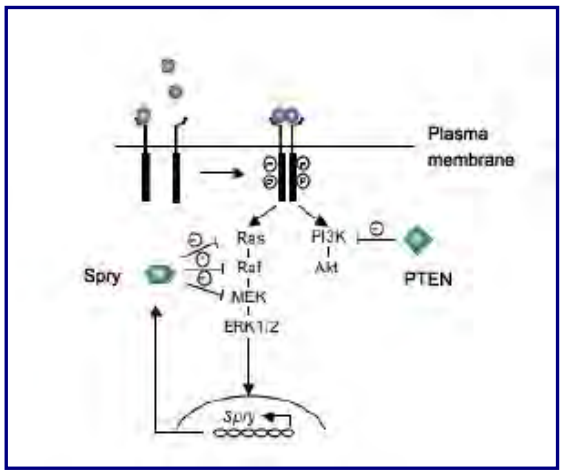

Figure 3. **Different mechanisms of RTKs signal attenuation**: negative regulation by inhibitory proteins. Growth factor stimulation activates the Ras-Erk1/2 pathway, which ends in the induction of the *Sprouty* gene. Then, Sprouty in a negative-feedback loop deactivates this cascade by inhibiting the pathway at undetermined intermediates. The role of the phosphatidylinositol phosphatase PTEN as a specific attenuator of the RTK-PI3K-Akt pathway is also indicated.

(*modified form Ledda and Paratcha, 2007*)

Ligand-induced receptor downregulation

Negative feedback provides an effective control of RTKs signaling, however other mechanisms, collectively known as receptor downregulation, have been evolved to restrict RTK signaling independently of transcription (Peschard & Park, 2003; Shtiegman & Yarden, 2003; Thien & Langdon, 2001).

This type of molecular machinery limits signal propagation by removing activated receptors from the plasma membrane, thus reducing the number of specific binding sites on the cell surface. Once activated, RTKs are ubiquitinated, internalized and targeted to degradative compartments.

Role of endocytosis in negative signaling

Activated receptors generally enter the endosomal system through incorporation into clathrin coated vesicles (CCVs). They are initially targeted to clathrin-coated membrane invaginations that pinch off to form internalizing vescicles. The AP2 adaptor complex triggers the formation of clathrin-coated vescicles, while their detachment from the plasma membrane is mediated by the GTPase dynamin. Subsequent membrane fusion and budding events drive the internalized vescicles along the endocytic pathway, from the early endosome to the late endosome. From here receptors may recycle to plasma membrane or be selected for lysosomal sorting by incorporation into small vescicles that bud off from the limiting membrane into the vacuolar lumen to generate multivescicular bodies (MBVs). Fusion of MBVs with lysosomes leads to degradation of internal vescicles and their contents by hydrolytic enzymes. Ubiquitination provides a sorting signal that is proposed to engage with the MVB sorting machinery (Hicke & Dunn, 2003; Raiborg et al., 2002; Urbe et al., 2003). It has been reported that non-ubiquitinated RTKs are not sorted in the bilayered clathrin coat, but are recycled back to the cell surface and escape lysosomal degradation (Katzmann et al., 2002); see Figure 4)

Growing evidence indicate that membrane trafficking plays an important role in controlling the localization of signaling interactions and in regulating degradation and recycling of activated receptors. Since RTKs can transmit signals from the membrane of the endosomes, the molecular machinery that regulate trafficking of receptors from early endosomes to degradative lysosomes plays an important role in controlling the localization of signaling interactions and in regulating degradation and recycling of activated receptors.

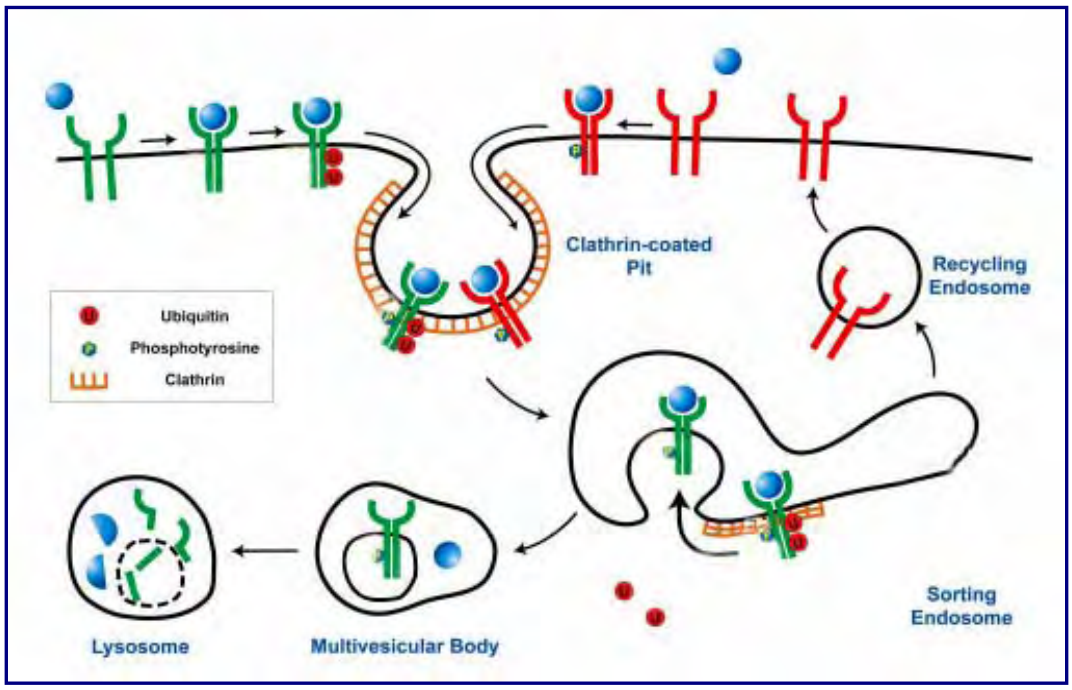

Figure 4 Model for clathrin dependent endocytosis of activated RTKs. Activated receptors are sorted into clathrin-coated pits. Following formation of a clathrin-coated vesicle and the subsequent shedding of clathrin to from the early endosome, ubiquitinated receptors (green) receptors undergo sequestration in inner vescicular structures of multivesicular bodies (MBVs). Fusion of MBVs with lysosomes leads to the degradation of inner vesicles and their content by lysosomal proteases. RTKs that are not ubiquitinated (red) are not sequestered in the bilayered clathrin coat of the sorting endosomes and can be recycled to the cell surface where they can be reactivated.

(*Modified form Peschard and Park, 2003*)

Clathrin dependent endocytosis represents the best characterized endocytic pathway involved in downregulation of a number of RTKs. Less well characterized are clathrin-independent endocytic pathways, including caveolae/raft-dependent. Caveolae are cholesterol- and sphingolipid-rich small uncoated invaginations of the plasma membrane that partition into raft fractions and whose expression is associated with caveolin-1 (Parton, 1996). Caveolae are thus considered a subdomain of the biochemically defined glycolipid raft.

The caveolae- and raft- dependent endocytic pathways differ from clathrin-mediated endocytosis for a number of components of the endocytic machinery, like adaptor

proteins, involvement of cytoskeletal proteins (Pelkmans & Helenius, 2002). As for calthrin-madiated endocytosis, the **caveolae/raft-dependent endocyto**sis of various molecules has been reported to be inhibited by microinjection of anti-dynamin antibodies or by overexpression of a dominant-negative dynamin K44A mutant devoid of GTP hydrolytic activityand (Dessy et al., 2000; Lamaze et al., 2001; Pelkmans et al., 2002). Other features typical of these pathways are the sensitivity to cholesterol depletion and the morphology and lipid composition of the vescicular intermediates. The internalization of caveolae may be facilitated by disruption of the actin cytoskeleton and by inhibition of phosphatases, while it is prevented by kinase inhibitors (Mundy et al., 2002; Thomsen et al., 2002).

Growing evidence indicate that caveolin-1 acts not as determinant of caveolae invagination and internalization, but rather as a regulator that stabilizes caveolae at the plasma membrane and reduces the endocytic potential of caveolae/raft domains (Le et al., 2002; Oh & Schnitzer, 2001). Moreover, internalization of some caveolar ligands is a signal-mediated process that requires caveolin-1 expression (Minshall et al., 2000; Razani et al., 2001). This observation together with the existence of multiple caveolin-1 partners (Liu et al., 2002) implicates caveolin-1 as a scaffolding molecule that determines the cargos for caveolae/raft-dependent endocytosis.

Interesting insights into the function of caveolar/raft-dependent endocytosis have come from studies following endocytosis and signaling of the Transforming Growth Factor-β (TGF-β) receptor (Di Guglielmo et al., 2003). TGF- β receptor has been found in both clathrin-coated pits and caveolae at the cell surface and after internalization the receptor is localized in non-acidic caveolin-1 associated vescicles (caveosomes) as well in endosomes. The clathrin-dependent entry has been associated with increased receptor signaling, while the caveolar pathway has been

reported to lead to receptor degradation and turnover (Di Guglielmo et al., 2003). TGF- β receptor can bind directly to caveolin-1 and this interaction may play a role in targeting of receptor to caveolin-1-positive organelles (Razani et al., 2001).

Association with caveolin-1 has been described for other signaling receptors to interact with, including the RTKs EphB1 receptor and Insulin Receptor (Bickel, 2002; Vihanto et al., 2006). Interestingly, in caveolin-1 null mice any alterations in insulin tolerance were detected but they were characterized by significantly low levels of Insulin Receptor (Cohen et al., 2003). Studies on EGFR have led to a model according which low concentrations of EGF lead to receptor internalization by clathrin-coated pits, while high doses of the ligand stimulate receptor internalization and degradation through a raft-dependent mechanism (Aguilar & Wendland, 2005; Sigismund et al., 2005); see Figure 5). However, it has been recently demonstrated by live-cell microscopy that incubating cells with high doses of EGF did not increase the mobility of caveolae (Kazazic et al., 2006). These findings prompt a role for caveolar/raft-dependent endocytosis in the regulation of turnover, rather than signaling.

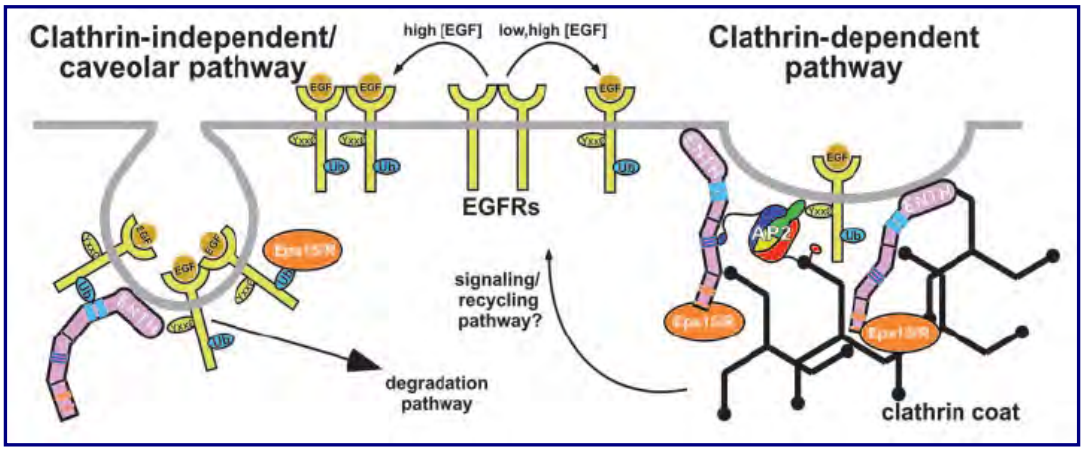

Figure 5 Model for ligand-induced EGFR downregulation. High [EGF] induces Ub modification and degradation through a clathrin-independent caveolar pathway. Low [EGF] promotes recognition by the AP2 cargo adaptor and internalization via clathrin-coated vesicles, leading to efficient signal transduction.

(*Modified form (Aguilar & Wendland, 2005)*

Role of ubiquitination in negative signaling

Ligand-induced RTKs downregulation is controlled by protein ubiquitination, an evolutionarily conserved post-translational modification where the small protein ubiquitin is covalently conjugated to a lysine residue within the substrate (Pickart, 2001). Protein ubiquitination is mediated by an enzymatic cascade composed of a ubiquitin-activating enzyme (E1), a ubiquitin-conjugating enzyme (E2), and a ubiquitin-ligase (E3). Multiple classes of E3 ubiquitin-ligases provide the specificity of ubiquitination reaction by binding substrates (Weissman, 2001). These include HECT domain-containing proteins, such as Nedd4 family, proteins containing RING finger domains, such as Cbl family and U-box containing proteins, such as CHIP.

When a single or multiple 76 amino acid ubiquitin moiety is appended to the lysine residue of substrate proteins monoubiquitination or multiple monoubiquitination occur, respectively. Ubiquitin itself contains seven lysine residues that can be substrate for the conjugation of other ubiquitin molecules, allowing the formation of polyubiquitin chains (see Figure 6). It has been reported that all seven lysine residue can be involved in chain formation *in vivo*.

The functional relevance of differential ubiquitination is not yet completely understood. However, the consensus view is that mono- and multi-ubiquitination are non-proteolytic signals involved in endocytosis, endosomal sorting, histone regulation, DNA repair and nuclear export (Mukhopadhyay & Riezman, 2007). Polyubiquitination through Lys48 linkage is involved in targeting for degradation via the proteasome 26S (Pickart & Fushman, 2004). Much less is known about specific functions of chains linked through other lysine residues. In addition, recent studies have reported the identification of branched chains containing different types of linkages, but their function is still unclear (Kirkpatrick et al., 2006).

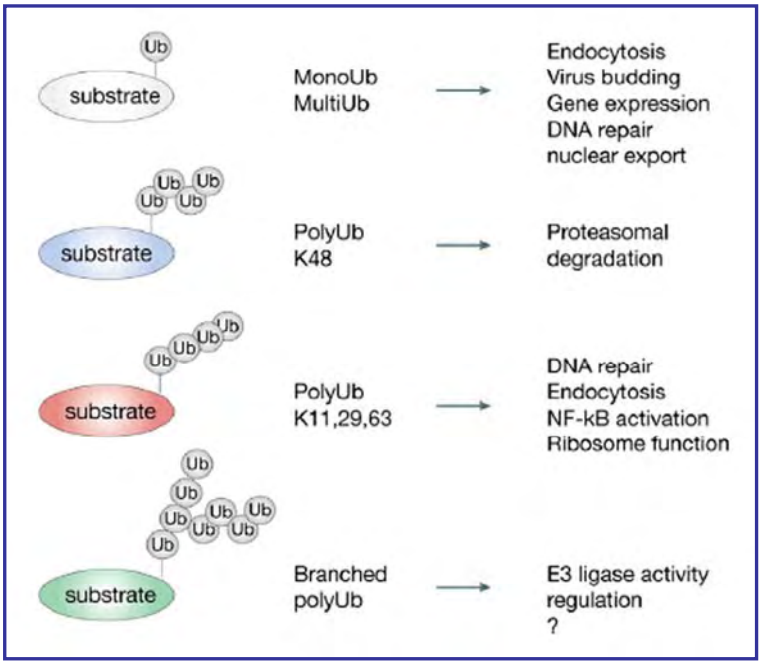

Figure 6 Schematic representation of different ubiquitin modifications with their functional roles.

(*Modified form (Woelk et al., 2007)*

Several different families of ubiquitin-protein ligases, including Cbl, Nedd4 and CHIP have been reported to regulate ubiquitination of RTKs in mammalian cells (Joazeiro & Weissman, 2000; Katz et al., 2002; Xu et al., 2002). The Hsp70/Hsp90-associated **U-box ubiquitin ligase CHIP** is preferentially involved in degradative pathways initiated by receptor misfolding, and thus triggered by mutations or drug-induced misfolding (Citri et al., 2002; Germano et al., 2006). Recently, the E3 Ubiquitin ligase Nedd4-2 as been identified as an enzyme that binds specifically to the C-terminal portion of the TrkA receptor, leading to receptor downregulation, thereby modulating neuronal survival by NGF (Arevalo et al., 2006).

However, accumulating evidence suggest that the Cbl family of ubiquitin ligases plays a major role in mediating ligand-dependent downregulation of RTKs (Thien et al., 2001). Several activated receptors, such as EGFR, Platelet-Derived Growth

Factor receptor (PDGFR), RET, HGFR/MET and Ron receptors are ubiquitinated upon interaction with c-Cbl, the most studied member of the Cbl family. Cbl ubiquitin-protein ligases contain a conserved N-teminal tyrosine kinase binding (TKB) domain and a RING finger domain in addition to other protein interaction motifs (Thien & Langdon, 2001). c-Cbl can directly associate with activated receptors by binding to specific tyrosine residues on the receptor through its TKB domain. Additionally, it has been reported that c-Cbl can also interact with the SH3 domain of Grb2, an adaptor protein known to associate with phosphorylated receptors and link RTK to the activation of the Ras pathway. Thus, in mammalian cells Grb2 can indirectly recruit c-Cbl to EGFR, RET, HGFR/MET and Ron receptors (Jiang et al., 2003; Penengo et al., 2003; Peschard et al., 2001; Scott et al., 2005). It has been suggested that Cbl may sequester Grb2 from the guanine nucleotide exchange factor Sos, thus inhibiting Ras activation (Dikic & Giordano, 2003).

The precise involvement of c-Cbl in ligand-dependent downregulation remains elusive, as several evidences prompt a role for c-Cbl also in the regulation of RTKs endocytosis. The overexpression of c-Cbl has been shown to enhance the kinetic of internalization of EGFR (Soubeyran et al., 2002), whereas in c-Cbl null macrophage a slower internalization rate was detected for Colony-Stimulating Factor-1(CSF-1) Receptor (Lee et al., 1999). It has been proposed that c-Cbl promotes the internalization of RTKs by binding to the CIN-85-Endophilin complex, a step required for the invagination of the plasma membrane into the coated-pits (Petrelli et al., 2002; Soubeyran et al., 2002). Interfering with Cbl-CIN85-Endophilin interaction was sufficient to hamper RTKs endocytosis and degradation, without disrupting the ability of Cbl to ubiquitinate activated receptors (Petrelli et al., 2002; Soubeyran et al., 2002). The binding of Cbl to activated RTKs thus regulates ligand-dependent RTKs

downregulation by promoting receptor ubiquitination and by regulating the endocytic pathway through the interaction with CIN85-Endophilin complexes. However, Cbl-mediated ubiquitination of RTKs seems more critical for sorting into MBVs vescicles rather than for the initial internalization step. Indeed, it has been demonstrated that Cbl can associate with and ubiquitinated activated EGFR at the plasma membrane (Stang et al., 2000) but also remain associated with the receptor throughout the endocytic pathway. Colocalization of Cbl with activated EGFR in internal vescicles of MBVs has been reported (de Melker et al., 2001). Interestingly, dominant negative mutants of Cbl have been reported to inhibit RTKs degradation and accelerate recycling, while any effect on the internalization rate was detectable (Thien & Langdon, 2001).

Early lines of evidence indicate that ubiquitination of both receptor cargos and components of the endocytic machinery is required for correct functioning of the degradative machinery (Di Fiore et al., 2003; Marmor & Yarden, 2004). Indeed, several Ub binding domains (UBDs), have been identified in endocytic regulatory proteins, including Hrs, Eps15, Stam, Epsin and Tsg101 (Bienko et al., 2005; Hicke et al., 2005). They are responsible for ubiquitin binding and for directing self-monoubiquitination. Ubiquitin has thus emerged as a recognition element in RTKs sorting, coupling ubiquitinated cargos with the endocytic machinery and coordinating their trafficking to degradative compartments.

Moreover, ubiquitination is a dynamic and reversible process, as deubiquitinating enzymes (DUBs) can mediate the rapid removal of ubiquitin from substrate proteins (Wilkinson, 2000). The reversibility of ubiquitination thus represent an additional level of regulation and the balance between activity and subcellular localization of DUB enzymes and ubiquitin ligases allows for fine tuning of responses.

Oncogenic Deregulation of RTKs

Aberrant RTKs signaling is associate with the development and progression of many human malignancies. The dysregulation of approximately fifty percent (30 of 58) of the genes known to encode RTKs has been associated with human tumors (Blume-Jensen & Hunter, 2001) and frequently correlate with poor responsiveness to conventional therapies.

Mechanisms of uncontrolled RTKs signaling

Several mechanisms that dysregulate RTKs have been characterized, including overexpression, point mutations, partial deletions and gene rearrangements (Blume-Jensen & Hunter, 2001; Lamorte & Park, 2001). These molecular changes result in ligand-independent autophosphorylation or enhanced catalytic activity of RTKs, thus leading to prolonged cell stimulation (see Figure 7).

Gene amplification and /or overexpression of RTKs is a recurrent theme in human tumors, that leads to abnormal accumulation, dimerization and constitutive activation of the receptors resulting in dysregulated cell proliferation. Important examples can be found in EGFR and HGF-R/Met family of tyrosine kinase receptors. Overexpression and/or gene amplification of ErbB2 occurs in a significant proportion of adenocarcinomas and clinical studied have demonstrated that elevated ErbB2 expression correlates with poor prognosis in multiple malignancies, including breast and ovarian cancer (Klapper et al., 2000; Ouyang et al., 2001). In the case of EGFR the predominant mechanism leading to receptor overexpression is gene amplification with up to 60 copies per cell reported in certain tumors (Libermann et al., 1985).

As well, the *MET* gene has been found amplified in liver metastasis of colorectal carcinomas and the Met protein overexpressed in tumors of specific histotypes, including thyroid and pancreatic carcinomas (Di Renzo et al., 1995).

Activating point mutations represent another common mechanism responsible for altered RTKs signaling. They have been detected in the extracellular domain of the tyrosine kinase receptor Ret, where they are associated with multiple endocrine neoplasia (MEN) type 2A and familial medullary thyroid carcinoma (FMTC). In addition, a M→T mutation directly affecting the tyrosine kinase domain has been implicated in the MEN type 2B syndrome (Hofstra et al., 1994). Interestingly, the same conserved residue among RTKs, was found mutated in the tyrosine kinases Kit and Met and associated to human mast cell leukaemia and mastocytosis (Longley et al., 1996) and to human papillary renal carcinoma (HPRC; (Schmidt et al., 1997). Somatic mutations in the kinase domain of EGFR, including L858R point mutation and exon 19 deletion have been reported in 10% of non-small cell lung cancers (NSCLC;(Lynch et al., 2004). The oncogenic form of Neu, $p185^{neu*}$, represents a model of constitutive activation that occurs by alteration of the transmembrane domain. In this case a V→E substitution induces tyrosine kinase autophosphorylation and cell transformation (Weiner et al., 1989).

Examples of gene rearrangements can be found in the *ret* proto-oncogene. Indeed, rearrangement of the 3' sequence of *ret* with the 5' sequences of H4/D10S170, the type Iα regulatory subunit of cyclic AMP-dependent protein kinase and the ELE1 gene have been detected from DNA extracts from PTC (Papillary Thyroid Carcinoma; (Bongarzone et al., 1993). The resulting rearranged genes produce hybrid proteins with a constitutively active Ret kinase. The nerve growth factor receptor (NGF-R) can undergo a gene rearrangement with tropomyosin, in

which the extracellular domain of the receptor is lost and tropomyosin is fused to the kinase domain (Martin-Zanca et al., 1986). Similarly, the tyrosine kinase HGF-R/Met can acquire oncogenic properties by gene rearrangements with sequences from chromosome 1 called *tpr* (translocated promoter region). In the resulting Tpr-Met hybrid protein, that lacks the extracellular and transmembrane domains of Met, the leucine zipper motif of Tpr mediates the dimerization (Rodrigues & Park, 1993).

Finally, another important mechanism of constitutive RTKs signaling involves autocrine–paracrine stimulation through growth factor loops and has been described for the EGFR, PDGFR IGF-IR receptor families. This potent mechanism of activation, reported in many solid tumors, occurs when RTKs are overexpressed in the presence of their cognate ligands, or when overexpression of the ligand occurs in the presence of its associated receptor.

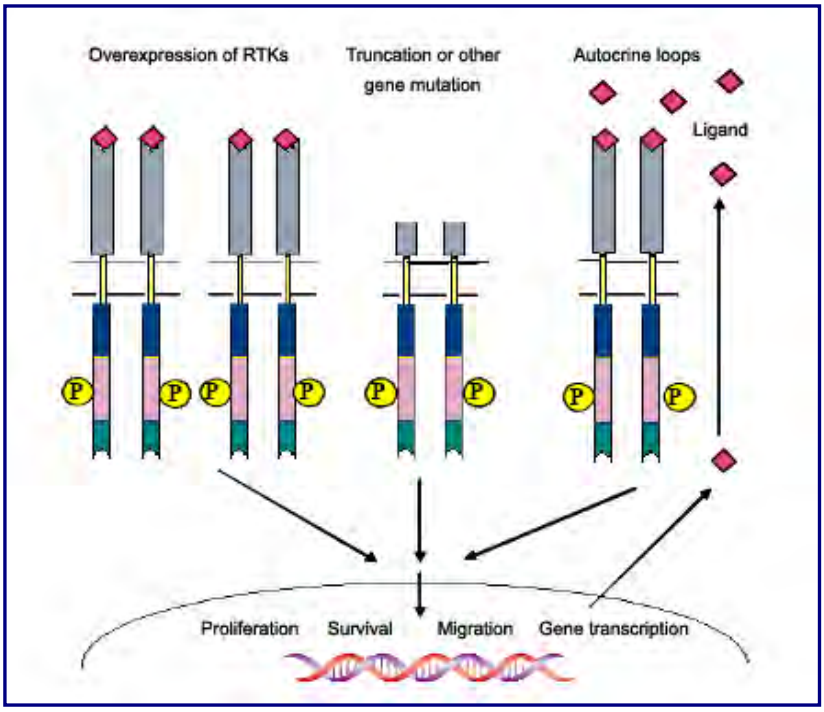

Figure 7. Schematic view of different mechanisms leading to RTKs constitutive activation.

(*Modified form Manash et al., 2004*)

Growing evidence support the idea that also failure of RTKs to be appropriately deactivated may be a cause of unrestrained proliferative ability and neoplastic growth (Dikic & Giordano, 2003). Indeed, alterations that uncouple RTKs from c-Cbl mediated ubiquitination and downregulation are strictly associated with the pathogenesis of cancer. Examples include CSF-1R, HGF-R/Met, c-Kit and EGFR. It has been reported that mutation of a C-terminal tyrosine, which is the c-Cbl direct binding site, enhances the transforming abilities of CSF-1R in fibroblasts. Moreover, mutations of the c-Cbl binding site are frequently observed in CSF-1R in human myelodysplasia and acute myeloblastic leukaemia (Ridge et al., 1990). Similarly, loss of c-Cbl recruitment and c-Cbl-mediated ubiquitination is likely to contribute to the oncogenic deregulation of Tpr-Met (Peschard et al., 2001).

The Stem Cell Factor (SCF) Receptor/c-Kit recruits c-Cbl indirectly *via* the adaptor containing PH and SH2 domains (APS). The deletion of APS binding sites in c-Kit greatly enhances its transforming potential, although part of the effect may be due to enhanced catalytic activity of the receptor (Herbst et al., 1995).

Finally, an EGFR mutant lacking only the direct c-Cbl binding site elicits stronger mitogenic signals than the wild-type receptor (Waterman et al., 2002). In addition, it has been demonstrated that EGFR/ErbB2 heterodimers recruit c-Cbl to a lesser extent than EGFR homodimers and escape form the degradative fate by rapidly being recycled at the cell surface (Muthuswamy et al., 1999). Hence, the overexpression of ErbB2 constitutes a mechanism by which EGFR avoids c-Cbl-mediated downregulation.

Together these receptors are examples of how different oncoproteins can escape from downregulation mechanisms by loss of the c-Cbl binding sites or inefficient c-Cbl recruitment.

Consistent with its role in the downregulation of RTKs, mutant c-Cbl proteins that lack ubiquitin ligase activity have been identified in mouse tumors (Thien & Langdon, 2001). Moreover, c-Cbl is itself regulated by several proteins that are implicated in potentially carcinogenic signaling pathways, including the adaptor protein Sprouty2 and the cytosolic tyrosine kinase Src (Polo et al., 2004). It was shown that active Src induce tyrosine phosphorylation and poly-ubiquitination, with consequent proteasomal degradation, of c-Cbl leading to upregulation of EGFR expression and signaling (Bao et al., 2003). Consistently, mutational activation of Src occurs in cancer and frequently correlates with simultaneous overexpression of EGFR (Summy & Gallick, 2003).

Targeting RTKs signaling

The mechanisms of altered RTK signaling that leads to cancer represent promising areas for the development of target-selective anticancer drugs. Several approaches towards the prevention or inhibition of RTKs signaling have been followed, thanks to the understanding of the mechanisms of signal generation and regulation by RTKs and of the crystallographic structure of many RTKs. Strategies include the development of selective components that target either the extracellular ligand-binding domain, the intracellular tyrosine kinase or the substrate-binding region (see Figure 8).

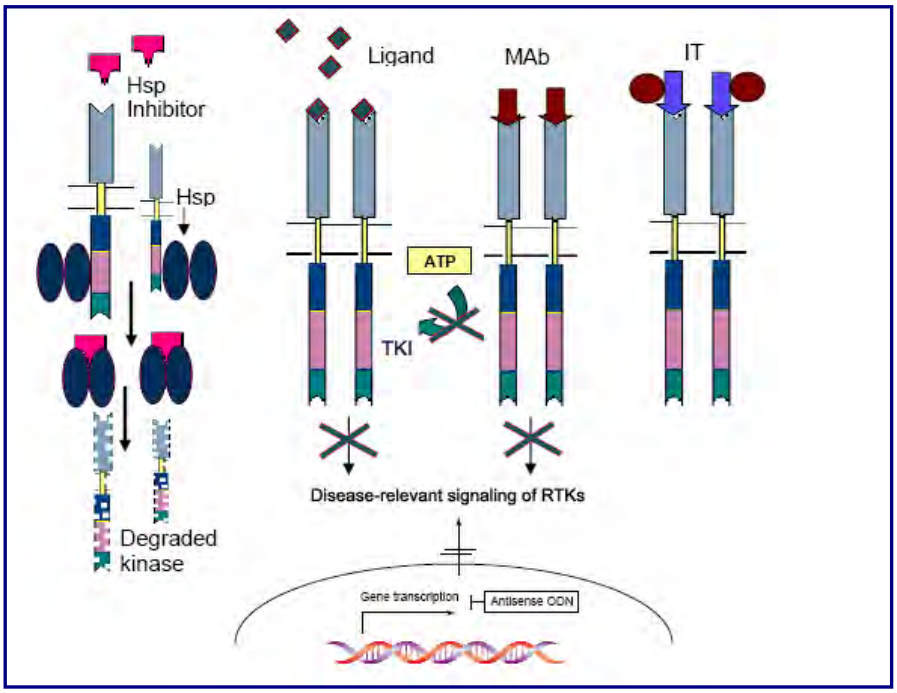

Figure 8. Schematic structure of different approaches for RTKs inhibition. Abbreviations: MAb, monoclonal antibody; ODN, oligodeoxynucleotides; IT, immunotoxin; TKI, tyrosine kinase inhibitor.

(*Modified form Manash et al., 2004*)

Recombinant antibody technology has enabled the production of humanized or human **neutralizing antibodies** directed against the extracellular domain of RTKs. They can bind to the receptor and inhibit its activation, either by blocking the interaction with the ligand or by inducing receptor internalization and degradation. The humanized monoclonal antibody against ErbB2 receptor Herceptin (Trastuzumab) mainly acts by inducing receptor downregulation and gave significant results in the treatment of metastatic breast cancers in which ErbB2 was overexpressed (Vogel et al., 2002). As well, the monoclonal antibody Cetuximab (C225), which is directed against the extracellular domain of the EGFR, has shown growth-inhibiting and anti-tumor effect in a variety of human cancer cells including

pancreatic, renal and breast carcinomas (Overholser et al., 2000). Recently, it has been reported that treatment of carcinoma cell lines with a monoclonal antibody against HGF-R/Met (DN30) resulted in impaired HGF-induced signal transduction and enhanced receptor downregulation, associated with weakened anchorage-independent growth and invasiveness (Petrelli et al., 2006).

An alternative strategy to force RTKs towards degradative pathways is based on **Heat shock protein 90 (Hsp90) inhibitors**. Indeed, many kinases require the activity of molecular chaperones to maintain their activation competent conformation (Kamal et al., 2004). Chaperone-based inhibitors other than interacting with protein kinases, prevent the associated chaperones from maintaining the activation competent conformation of the kinase. The ansamycin antibiotic geldanamycin and its derivatives are able to compete with ADP/ATP in the nucleotide binding pocket of Hsp90, inhibiting the intrinsic ATP-dependent chaperone activity and thus directing the ubiquitin-mediated proteasomal degradation of the misfolded kinases (Stebbins et al., 1997).

Another promising approach to interfere with aberrant RTKs signaling is the development of **small-molecule inhibitors** that selectively interfere with their intrinsic tyrosine kinase activity thus blocking receptor autophosphorylation and activation of downstream signal transducers (Levitzki, 1999). Several of these compounds are low molecular weight molecules that compete with the ATP-binding site of the receptor. The major examples are BCR-ABL kinase inhibitor Imatinib mesylate (Gleevec, STI 571), that also affects the activity of two related RTKs, PDGFR and c-Kit and the EGFR kinase inhibitor Iressa (ZD-1839).

Additional strategies for the inhibition of receptor tyrosine kinase signaling include immunotoxins and antisense oligonucleotides. Natural **immunotoxins** are

fused or chemically conjugated to a specific ligand, such as monoclonal antibodies, or growth factors and once internalized by cancer cells can induce apoptosis. One promising immunotoxin is the EGF fusion protein DAB389EGF, which contains domains of diphtheria toxin fuse with sequences for human EGF (Sweeney & Murphy, 1995).

Antisense oligodeoxynucleotides (ODN) are 15-25bp nucleotides designed to interact with the mRNA and inhibit RNA function in several ways including the steric block of RNA translation and the alteration of RNA processing. Preclinical studies have shown that antisense ODN targeting IGF-1R induces apoptosis in malignant melanoma and is also effective in breast cancer (Andrews et al., 2001). The silencing of HGF-R/Met expression has been achieved by using antisense ODN delivered *in vivo* through liposomes, resulting in impaired growth of different xenografts models (Stabile et al., 2004).

Another way to inhibit protein expression is represented by the **RNA interference** (RNAi) technique. Indeed, it has been proven to achieve almost complete Met silencing in vitro and in xenografts models. Although it represents a challenging and powerful technique several limitations arise form difficulties in efficient delivery. The production of chemically modified siRNAs suitable for *in vivo* administration offers new hints for clinical translation.

The Ron tyrosine kinase receptor

The product of the proto-oncogene RON has been identified as the receptor for Macrophage Stimulating Protein (MSP), belonging to the subfamily of the HGF-R/Met (Gaudino et al., 1994; Wang et al., 2005). The RON gene contains 20 exons and 19 introns and is located on chromosome 3p21, a region frequently altered in certain cancers (Zabarovsky et al., 2002). The cDNA encoding human Ron was originally cloned from keratinocytes (Ronsin et al., 1993) and its murine homologue, named stem cell-derived tyrosine kinase (Stk) was isolated from bone marrow cells (Iwama et al., 1994).

Structure and biological activities

Ron is a disulphide-linked heterodimer (p185) composed of an extracellular 35-kDa α chain and a 150-kDa transmembrane β chain with intrinsic tyrosine kinase activity. Both chains are derived from proteolytic cleavage of a single-chain precursor (pr170) by a furin-like protease (Gaudino et al., 1994; Wang et al., 1994). The extracellular moiety contains a Sema domain of 500 amino acids, which is known to be a protein-protein interaction domain, a eight-cysteine motif of 80 amino acids termed Met-related sequence (MRS) and four domains Immunoglobulin-like fold domains shared by plexin and transcription factors (IPT;(Comoglio et al., 1999). Although the functional role of these domains remains partially unknown, it has been reported that a soluble molecule representing the Sema domain of Ron negatively affects ligand-induced receptor activation, thus suggesting that this domain participate in ligand-binding by the full length receptor (Angeloni et al., 2004). The

intracellular portion of the receptor comprises a juxtamembrane region that contains a conserved tyrosine residue (T1017) which is a potent negative regulation site for Met receptor, the tyrosine kinase catalytic domain and a C-terminal docking tail comprising two conserved tyrosine residues that form the multifunctional docking site for SH2-containing proteins (Y^{1353}VQLPATY^{1360}MNL;(Ponzetto et al., 1994). By expressing active Ron with the Sf9/baculovirus system Yokoyama and co-workers presented evidence for an autoinhibitory role of the C-terminal tail, that may regulate Ron kinase activity *via* an interaction with the catalytic domain (Yokoyama e Miller 2005). This is in accordance with the observation that the C-terminal domain of Met acts as an intramolecular modulator of receptor activity (Bardelli et al., 1999). Within the HGF-R/Met subfamily, a distinctive feature of Ron is the presence of a proline/arginine-rich sequence (RRPRPLS^{1394}EPPRPT) in the last 20 amino acids of the receptor, which function as protein-protein interaction motif. Indeed, it has been reported that serine phosphorylation at residue 1394 generate a 14-3-3 binding site, connecting Ron with α6β4 integrin (Santoro et al., 2003).

The only ligand for Ron was identified as MSP, also known as HGF-like protein, a serum protein that belongs to the family of plasminogen-related growth factor (Gaudino et al., 1994; Yoshimura et al., 1993). MSP is synthesized as single-chain precursor and secreted into the plasma, where it undergoes activation by serum proteases of the intrinsic coagulation cascade, nerve growth factor-γ, epidermal growth factor-binding protein and membrane-bound proteases (Wang et al., 1994). The mature heterodimeric form of MSP consists of 65-kDa α chain, containing four disulfide loop structure called kringle domains, and a 30kDa β chain, endowed with a serine protease-like domain devoid of enzymatic activity (Yoshimura et al., 1993). As for HGF, it is established that the major receptor binding site is located on MSP β

chain (Wang et al., 1997), even though analysis of the intermolecular interactions in the crystal lattice of β-chain of MSP demonstrated the absence of a conserved mode of dimerization of the serine protease homology domains of HGF and MSP (Carafoli et al., 2005). Complete knockout of the mouse MSP gene has been reported to produce no visible phenotypic changes, implying that additional ligands for Ron might exist, which could compensate fro the loss of MSP (Bezerra et al., 1998).

On engagement by its cognate ligand, Ron activates multiple intracellular signaling pathways including Ras/MAPK (Li et al., 1995), PI-3K/Akt (Wang et al., 1996), JNK/SAPK(Chen et al., 2000), β-Catenin (Danilkovitch-Miagkova & Leonard, 2001) and NF-kB (Santoro et al., 2003), mediating cellular proliferation, survival, migration and differentiation on cells of different origins. In particular MSP has been shown to stimulate proliferation of mammary duct epithelial cells and keratinocytes, maturation of megakaryocytes, motility of keratinocytes and bone resorption and contraction of osteoclasts (Banu et al., 1996; Kurihara et al., 1996; Santoro et al., 2003; Wang et al., 1996). Ron is a critical negative regulator of macrophage function and inflammation. *In vitro* activation of Ron in macrophages has been shown to inhibit inducible nitric oxide synthase (iNOS) expression and nitric oxide (NO) production, following lipopolysaccharide (LPS) or interferon γ treatment (Wang et al., 1994). Accordingly, targeted disruption of Ron in mice leads to deregulated inflammatory responses (Correll et al., 1997). Moreover, overexpression of Ron in monocytes/macrophages has been reported to inhibit HIV-1 proviral transcription (Lee et al., 2004). The MSP-Ron pathway has been proposed as a novel regulatory mechanisms within the central nervous system (CNS), on the basis of observations in an animal model of multiple sclerosis. Indeed, neurological desease in Ron-deficient

animals showed a more rapid and severe onset after induction of experimental autoimmune encephalomyelitis (EAE;(Tsutsui et al., 2005).

Functional interaction of Ron with a number of receptors has been reported, namely erythropoietin receptor HGF-R/Met, EGFR (Follenzi et al., 2000; Peace et al., 2003). These studies highlight the importance of the extracellular and transmembrane domains of Ron beside the tyrosine kinase domain in intracellular signaling and prompt a role for Ron in complex and interacting networks.

Cell transforming and oncogenic potential

In physiological conditions Ron activation is a transient event, whereas its deregulated activation is involved in cancer progression and metastasis in humans (Wang et al., 2003) and in murine models (Peace et al., 2005). Oncogenic activation of Ron can occur through a variety of mechanisms, including overexpression, partial deletions, point mutations and gene rearrangements, resulting in constitutive activation of the kinase.

The RON gene is normally transcribed at relatively low levels in cells of epithelial origins, while overexpression and subsequent aberrant activation have been observed in primary breast carcinomas (Maggiora et al., 1998), in non-small cell lung tumors (Willett et al., 1998) and colorectal adenocarcinomas (Zhou et al., 2003). Moreover, Ron expression is positively associated with histological grading, larger size and tumor stage in bladder cancer specimens (Cheng et al., 2005).

Abnormal accumulation and activation of Ron might play a critical role *in vivo* in the progression of malignant human epithelial cancers. Indeed, studies from transgenic animals provided evidence indicating that overexpression of Ron can lead to formation of lung tumors *in vivo* (Chen et al., 2002). Additionally, silencing RON gene

expression by RNA interference has been shown to hamper *in vivo* tumor formation of established colorectal carcinoma cells (Xu et al., 2004).

Altered Ron expression is also accompanied by generation of biologically active splice variants in cancerous cells. Several Ron mRNA splicing products have been characterized so far. The first Ron variant, designated as RonΔ165 or Δ-Ron, was found in a stomach cancer cell line and in colon cancer specimens and is the result of an in frame deletion of 49 amino acid in the extracellular domain of β chain (Collesi et al., 1996). This deletion prevents the proteolytic conversion of the single chain precursor into the two-chains form and causes the protein to be retained in the cytoplasm. The intracellular activation of RonΔ165 by disulphide-linked intracellular oligomerization confers invasive properties in vitro. A second Ron variant, RonΔ160 , was cloned from colon cancer cell lines and later was found in colorectal adenocarcinoma samples (Wang 2000). The in frame deletion of 109 amino acids in the extracellular region of β chain, rather than affecting the proteolytic processing of the protein, results in abnormal dimerization due to an unbalanced number of cysteine residues. The splicing variant RonΔ155, identified in primary colorectal adenocarcinoma samples, has a deletion of 158 amino acids in the extracellular domain of β chain and is a constitutively active non-processed single-chain protein retained in the cytoplasm (Zhou et al., 2003). Even though the involvement of these Ron variants in the progression of colorectal adenocarcinomas has not been completely elucidated, they provide a molecular mechanism for post transcriptional activation of Ron in cancer. Bardella and co-workers identified a short RON mRNA in several human cancers, including ovarian carcinomas. This transcript encodes a truncated protein lacking most of the extracellular domain, but retaining the whole transmembrane and intracellular domains. Expression of this constitutively active

truncated kinase results in loss of epithelial phenotype and drives tumor cell progression (Bardella et al., 2004).

To date, naturally occurring oncogenic mutant forms of Ron have not been identified. We have demonstrated that introducing single point mutations (D1232V and M1254T) in the activation loop of the Ron kinase domain, that mimic those found in c-Kit and Ret, results in activation of its transforming and tumorigenic potential (Santoro et al., 1998). These oncogenic substitutions induce constitutive activation of the kinase and yield a dramatic increase in catalytic efficiency, suggesting a direct correlation between kinase activity and oncogenic potential. Mutational analysis revealed that the Y→F conversion of the tyrosine residue at position 1317 significantly impairs tumorigenic and metastatic properties of the oncogenic Ron^{M1254T}, indicating that the transforming activity of this mutant is dependent on Y1317 phosphorylation and suggesting a shift in intramolecular substrate specificity (Santoro et al., 2000). Moreover, Ron^{M1254T} can exert cell transforming and metastatic activities without a functional docking site, supporting the idea that increased Ron kinase activity alone is sufficient to transduce oncogenic signaling.

Altogether this evidence strongly support a role for Ron tyrosine kinase in the onset or progression of tumor, even though additional studies focusing on the cellular and molecular mechanisms of Ron-mediated biological effects are required.

Mechanisms Underlying Ligand-induced Ron Downregulation

Summary

Decoration of ligand-activated receptors by ubiquitin acts as a signal controlling receptor internalization and routing to degradative compartments. EGFR and PDGFR tyrosine kinase receptors have been shown to be primarily modified by addition of single ubiquitin moieties at different lysine residues following ligand stimulation (Haglund et al., 2003; Mosesson et al., 2003) and this kind of modification has become recognized as the principal signal responsible for receptor internalization and routing to the lysosome for degradation (Haglund et al., 2003). However, a recent study based on a mass spectrometry approach has demonstrated that, in addition to multiple monoubiquitination, the EGFR is modified by short lys63-linked polyubiquitin chains within the kinase domain (Huang et al., 2006). Similarly, Geetha and co-workers have reported that the nerve growth factor receptor TrKA requires lys63 chains for internalization (Geetha et al., 2005). The mechanism by which lys63-linked chains could regulate internalization remain unknown, even though NMR studies suggest that the extended, linear conformation of ubiquitin chains formed through this lysine residue, might be recognized and function as a signal topologically similar to monoubiquitin (Varadan et al., 2004). Different structural features have been attributed to lys48-linked chains, such as a closed conformation and contact between hydrophobic residues of adjacent ubiquitin moieties. These structural requirements seem to be essential for the recognition of the modified proteins by the proteasome 26S subunits (Eddins et al., 2006; Thrower et al., 2000).

Altogether these findings indicate the existence of multiple ubiquitin signals on activated RTKs, that might account for distinct degradative fates. Furthermore, studies on TGFβR and EGFR have demonstrated the existence of different internalization pathways (clathrin-dependent or caveolae/raft-dependent) regulated by receptor ubiquitination state, and involved in the generation of signaling diversity (Di Guglielmo et al., 2003; Sigismund et al., 2005).

Previous work in our laboratory, performed on a chimaeric receptor generated by fusing the C-terminus of the EGFR transmembrane domain with the N-terminus of the Ron intracellular domain (ER), reported that activated Ron recruits to the multifunctional docking site the E3 ubiquitin ligase c-Cbl, a critical modulator of several RTKs (Penengo et al., 2003). c-Cbl recruitment to this site, as well as to juxtamembrane tyrosine autophosphorylation site, results in receptor ubiquitination and internalization.

The aim of this study was to shed light on the molecular mechanisms involved in Ron endocytic trafficking and degradative fate following ligand-induced activation, that play a critical role in regulating signaling magnitude and specificity.

Experimental procedures

Reagents and antibodies

MG-132, lactacystin, concanamycin and bafilomycin were purchased from Alexis. MSP was obtained by R&D System; monensin was from Sigma. Monoclonal antibody against Ron extracellular domain Zt/c1 was kindly provided by M.H. Wang (Texas Tech University, Amarillo, USA). Polyclonal antibody against Ron C-terminal domain (c-20) and against EGFR (1005) were from Santa Cruz Biotechnology, Inc.;

monoclonal anti-α-tubulin (B-5-1-2), anti-phospho-Erk1/2 (MAPK-YT), and anti-Erk1/2 (ERK-NP2) were purchased from Sigma; polyclonal phospho-Akt (Ser^{473}) and polyclonal anti-Akt were from Cell Signaling Technology; monoclonal anti-Cbl (7G10) and anti-phospho-tyrosine (4G10) were from Upstate Biotechnology, Inc. Monoclonal anti ubiquitin PD41 and FK1 were from Covance and BIOMOL International, respectively. Anti-HA antibody was from Roche, anti-caveolin and anti-clathrin heavy chain antibodies from BD Transduction laboratories and anti-transferrin receptor from Zymed Laboratories, Inc. Horseradish peroxidase-conjugated anti-mouse and anti-rabbit were purchased from Cell Signaling Technology, Inc.

Plasmids

pMT2-Ron was obtained as described previously (Santoro et al., 1998), c-Cbl in pcDNA3, HA-tagged ubiquitin and its KO mutant in pMT123 were kindly provided by Y. Yarden (Weizmann Institute of Science, Rehovot, Israel). pCCLsin.PPT.hPGK.GFP.Wpre transfer plasmid was used to express three independent siRNAs (5'-GATCGACCTGGTCAACCGC-3'; 5'-GCAATGAGCTGTTTGAAGA.-3'; 5'-GAAGCGAGATATCCCTGAC-3'), targeting caveolin-1 or clathrin heavy chain transcripts or an unrelated sequence as negative control. The expression was under the transcriptional control of the H1 promoter. The vector carries an independent GFP expression cassette, to allow for the identification of transfected cells.

Cell culture and transfection

FG2 cells were maintained in RPMI-1640, Hela cells were maintained in MEM medium (Invitrogen) with non-essential amino acids and sodium pyruvate, HEK293T

and NIH-3T3 cells were maintained in Dulbecco's modified Eagle's medium (Sigma), supplemented with 10% fetal bovine serum (Invitrogen) in a 5% CO_2-humidified atmosphere. Hela stably expressing Ron were obtained by infection with a lentiviral vector (p156RRLsin.PPT.hCMVMCS.pre) encoding human Ron. NIH-3T3 stably expressing Ron were obtained as described previously (Santoro et al., 1998), NIH-3T3 stably expressing EGFR were kindly provided by L. Moro (University of Piemonte Orientale, Novara, Italy). Transient transfection of HEK293T cells was performed with calcium-phosphate using the CellPhect transfection kit (GE Healthcare). Lipofectamine was used for transfection of FG2 and Hela cells according to the manufacturer's recommendations.

Immunoprecipitation and Immunoblotting

Total cellular proteins were extracted in RIPA buffer (50 mM Tris-HCl pH 7.4, 150 mM NaCl, 0.5% sodium deoxycholate, 1% Triton X-100, 0.1% SDS) containing protease and phosphatase inhibitors (10 µg/ml aprotinin, 10 µg/ml leupeptin, 10 µg/ml pepstatin, 1 mM phenylmethylsulfonyl fluoride, 1 mM sodium orthovanadate, 2 mM sodium fluoride). Lysates were clarified by centrifugation, quantified with the BCA Protein Assay Reagent Kit (Pierce) and dissolved in Laemmli sample buffer. For immunoprecipitation, cells were lysed in Solubilization buffer (20 mM Tris-HCl pH 7.4, 5 mM EDTA, 150 mM NaCl, 10% glycerol, 1% Triton X-100) with protease inhibitors. 500-µg aliquots of clarified cell lysates were incubated with 1µg of the indicated antibody immobilized on protein A-Sepharose 4B packed beads (GE Healthcare) for 2 h at 4°C. After extensive washes, precipitated proteins were dissolved in Laemmli sample buffer. Proteins were resolved by SDS-PAGE, transferred to nitrocellulose membrane and probed with respective antibodies. For ubiquitin immunoblotting,

proteins were transferred to PVDF membranes, incubated for 30 min in 20 mM Tris-HCl containing 6 M guanidine hydrochloride and 5 mM 2-mercaptoethanol, then probed with ubiquitin antibodies. Detection was performed by the ECL system (GE Healthcare) and Chemidoc exposure system (Bio-Rad). Image analysis was performed with Quantity One (Bio-Rad).

Cell surface biotinylation assay

Surface proteins were labelled fro 30 minutes at 4°C with 0.5 mg/ml Ez-Link® sulfo-NHS-Biotin (Pierce) in buffer A (1.3 mM $CaCl_2$, 0.4 mM $MgSO_4$-$7H_2O$, 5 mM KCl, 138 mM NaCl, 5.6 mM D-glucose, 25 mM HEPES, pH 7.4). After extensive washes with Dulbecco's modified Eagle's medium containing 0.6% bovine serum albumin and 20 mM HEPES, pH 7.4, cells were lysed. Biotinylated proteins were detected by streptavidin immunoprecipitation or avidin-HRP blotting as indicated.

Immunofluorescence

Cells were plated onto glass coverslips at a density of 2 X 10^4 . After serum starvation, medium was removed by extensive washes with PBS containing 1% bovine serum albumin and labeling with the appropriate antibodies was performed on ice for 1 hour in PBS containing 3% bovine serum with or without MSP or EGF. Fixing was performed with 4% paraformaldheyde solution for 5 minutes at room temperature. Permeabilization with 0.4% Triton X-100 was followed by 30 minutes incubation with 1% normal goat serum and 30 minutes staining with HRP-linked Alexa Fluor 488 anti-mouse or Alexa Fluor 555 anti-rabbit antibodies (Invitrogen) in a humidified chamber. Coverslips were mounted with Pro-Long Gold Antifade reagent (Invitrogen). DRAQ-5 (Alexis) was added 5 minutes before fixation.

Results

Activated Ron is preferentially modified through the conjugation of ubiquitin chains.

To gain a better understanding of the physiological consequences of ligand-induced Ron ubiquitination, we characterized the type of modification occurring on the receptor following activation. To this end we made use of a previously characterized (Mosesson et al., 2003) mutant from of ubiquitin, harbouring lysine-to-arginine (K→R) substitutions at all sites involved in chain branching, thus deficient in the formation of polyubiquitin chains. We transiently expressed the HA-tagged mutant form (Ub-KO), together with Ron or EGFR and c-Cbl, in HEK293T cells and compared its ability to mediate receptor ubiquitination with that of wild type ubiquitin (Ub-WT; Figure 1A). Ron ubiquitination pattern was severely affected in Ub-KO expressing cells. In contrast, in cells transfected with EGFR as a comparison, the ubiquitination signal was only slightly influenced by expression of the mutant form of ubiquitin. As expected, in a similar experiment, Ub-KO abolished the typical ladder of ubiquitinated β-catenin, a well characterized substrate for polyubiquitination (data not shown). These results provide evidence indicating that ligand-activated Ron preferentially undergoes polyubiquitination, rather than multiple monoubiquitination.

We further investigated receptor ubiquitination in FG2 pancreatic carcinoma cells expressing endogenous Ron, by using two commercially available antibodies against ubiquitin, one recognizing polymeric chains only (FK1), the other able to detect both ubiquitin chains and single monomers (P4D1). Moreover, in line with previous reports on EGFR indicating differential effects of ligand concentrations on the ubiquitination state of the receptor (Sigismund et al., 2005), we tested increasing amount of MSP, all within the physiological range. Detectable Ron ubiquitination was observed following stimulation with doses of MSP starting from 50 ng/ml (Figure 1B).

The kind of modification entails polymeric chains conjugations, even at the highest dose of MSP tested, as it is efficiently recognized by FK1 antibodies. Interestingly, we observed a strong correlation between Ron ubiquitination and its tyrosine phosphorylation. Indeed, a marked Ron phosphorylation was detectable at a concentration of MSP of 50 ng/ml or higher, although activation of the two major downstream effectors Akt and Erk1/2 occurred even at lower doses.

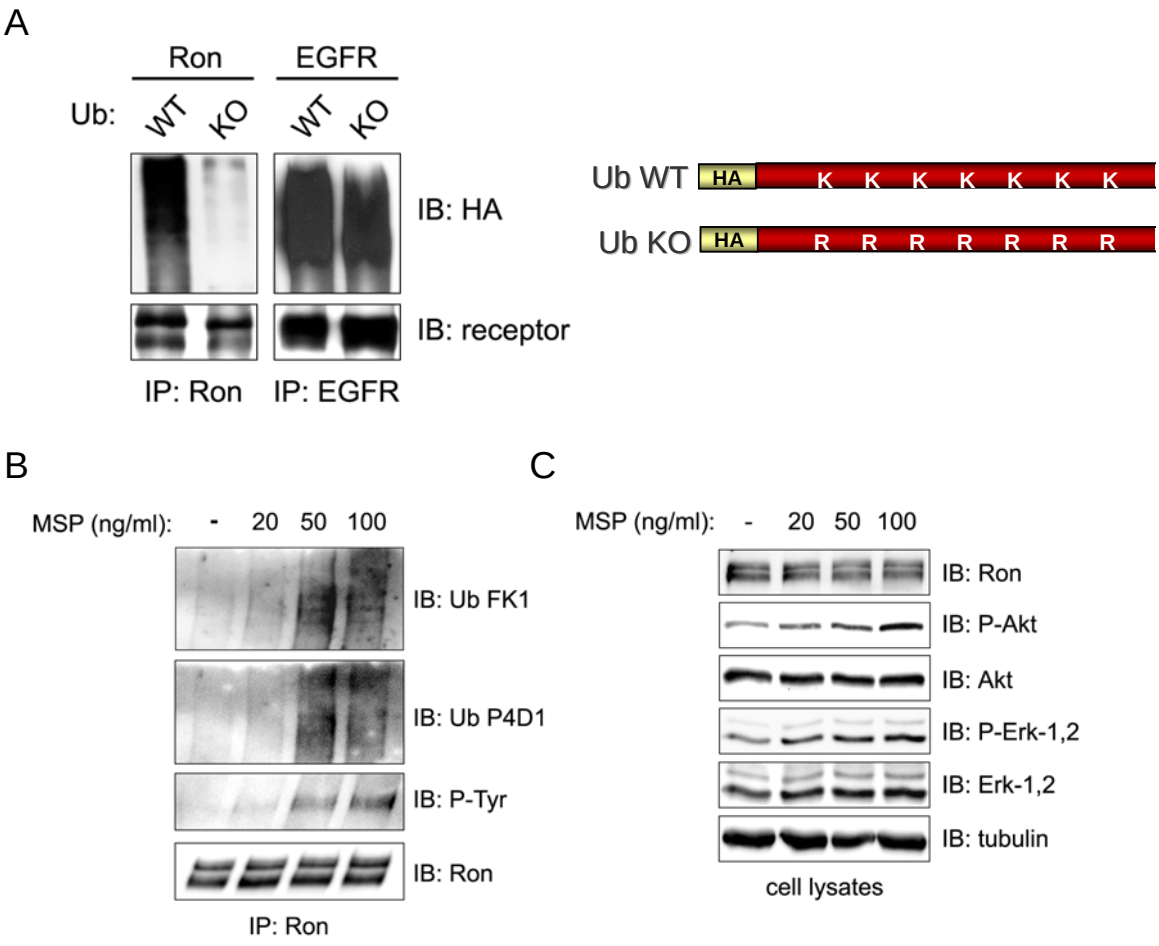

Figure 1. MSP induces Ron polyubiquitination. A) HEK293T cells expressing c-Cbl and either Ron or EGFR along with the indicated form of HA-tagged ubiquitin were stimulated with 100 ng/ml MSP or 100 ng/ml EGF and cell lysates were immunoprecitated (IP) with Ron or EGFR antibodies. HA immunoblotting (IB) was used to detect receptor ubiquitination. Receptor levels were monitored with the appropriate antibodies. **B**) FG2 cells endogenously expressing Ron were stimulated with increasing MSP concentrations. Equal protein amounts were immunoprecipitated with Ron antibodies and polyubiquitin chains were detected with FK1 antibodies. After stripping, the filter was probed P4D1. Receptor activation was monitored with phospho-tyrosine antibodies. **C**) Protein from cell lysates of FG2 cells stimulated as described in B were analyzed by IB with the indicated antibodies.

Polyubiquitination is required for MSP-induced Ron degradation.

Since ubiquitination has been shown to be critical for proper sorting of activated RTKs to degradative compartments, we characterized MSP-induced Ron degradation. At this end, cells endogenously expressing Ron were treated with increasing concentration of MSP for 8 hours and cell lysates were analyzed by immunoblotting. We observed that Ron degradation was strongly induced upon stimulation with MSP concentrations sufficient to promote receptor ubiquitination. Indeed, prolonged exposure of the cells to media containing 50-100 ng/ml of MSP resulted in a marked reduction (up to 60%) of both precursor and mature form of the receptor (figure 2A).

To address the role of polyubiquitination in controlling the fate of activated receptor, we analyzed MSP-induced Ron degradation in the presence of the Ub-KO mutant. As shown in figure 2B, in cells transfected with wild-type ubiquitin, Ron underwent time-dependent degradation, which was completely abolished in cells overexpressing Ub-KO. Thus, the mutant form of ubiquitin acted as a dominant negative, indicating that Ron polyubiquitination is required for its proper sorting to degradative compartments.

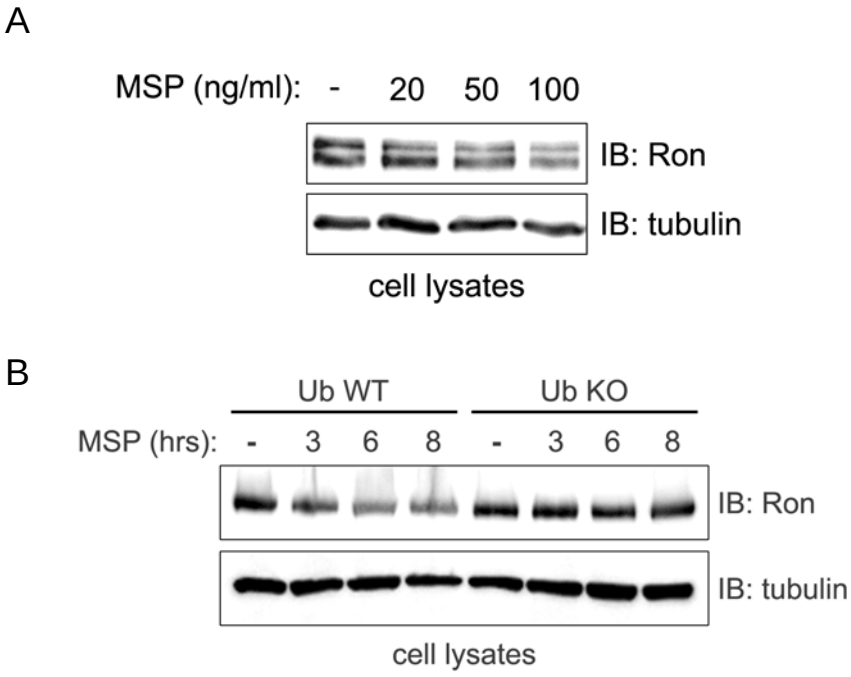

Figure 2. MSP promotes polyubiquitination-dependent Ron degradation. A) FG2 cells endogenously expressing Ron were stimulated with increasing MSP concentrations for 8 hours. Equal protein amounts were analyzed by Immunoblotting (IB) with Ron antibodies. 3T3-Ron or 3T3-EGFR cells were preincubated for 1 h with either lactacystin or concanamycin and then cultured in medium with or without MSP (100 ng/ml) or EGF (100 ng/ml) for 8 hours. Following cell surfaces biotinylation, equal amounts proteins were subjected to immunoprecipitation with the indicated antibodies. Immunoprecipitated proteins and total cell lysates were analyzed by immunoblotting. **B**) HEK293T cells expressing Ron and either wild-type (Ub WT) or mutant (Ub KO) ubiquitin were stimulated with 100 ng/ml MSP for the indicated time. Protein from cell lysates were analyzed by immunoblotting with the indicated antibodies.

Proteasome inhibition prevents MSP-dependent Ron degradation.

The major downregulation mechanism described for RTKs involves targeting of activated receptors to lysosomes for degradation and multiple monoubiquitination has became recognized as a critical sorting signal (Di Fiore et al., 2003; Haglund et al., 2003). However, at least for some receptors, it has been demonstrated that proteasomal activity is required for their proper downregulation (Pierchala et al., 2006; Sehat et al., 2007).

To identify the pathway that account for Ron degradation, a pharmacological approach was taken. In NIH-3T3 fibroblasts stably expressing Ron (3T3-Ron) or

EGFR (3T3-EGFR), here used as a prototype of RTKs undergoing lysosomal degradation, we performed a time-course ligand stimulation in presence of well-known inhibitors of lysosome or proteasome activity.

In 3T3-Ron cells pretreated with the selective inhibitor of lysosomal proteases concanamycin, the rate of MSP-induced Ron degradation was comparable to that observed in untreated cells (Figure 3A, upper panel). This was not a consequence of the ineffectiveness of the inhibitor, since when concanamycin was used under the same condition in 3T3-EGFR cells, it effectively impaired receptor degradation upon ligand stimulation (Figure 3A, lower panel). Conversely, pretreatment with the highly specific proteasome inhibitor lactacystin almost completely abolished Ron degradation, with receptor levels being significantly different when compared to stimulated control cells at all time points (figure 3B, upper panel). Since Ron was still ubiquitinated upon ligand stimulation in treated cells, we excluded the possibility that the inhibitory effect of lactacystin on receptor degradation could be due to a depletion of cellular pool of free ubiquitin (data not shown). As expected, in a parallel experiment on 3T3-EGFR cells, receptor degradation was only slightly affected (figure 3B, lower panel). Similar results were obtained on FG2 cells endogenously expressing Ron when either MG132 or bafilomycin was used to inhibit proteasome and lysosomal proteases respectively (data not shown).

Interestingly, inhibition of Ron downregulation resulted in accumulation of phosphorylated forms of Erk-1/2 and Akt, crucial mediators of two major downstream signaling pathways triggered by MSP (Figure 3B).

Taken together, these results suggest the requirement of receptor degradation for an efficient switching off of its signaling activity and indicate the proteasome as a key player in this process.

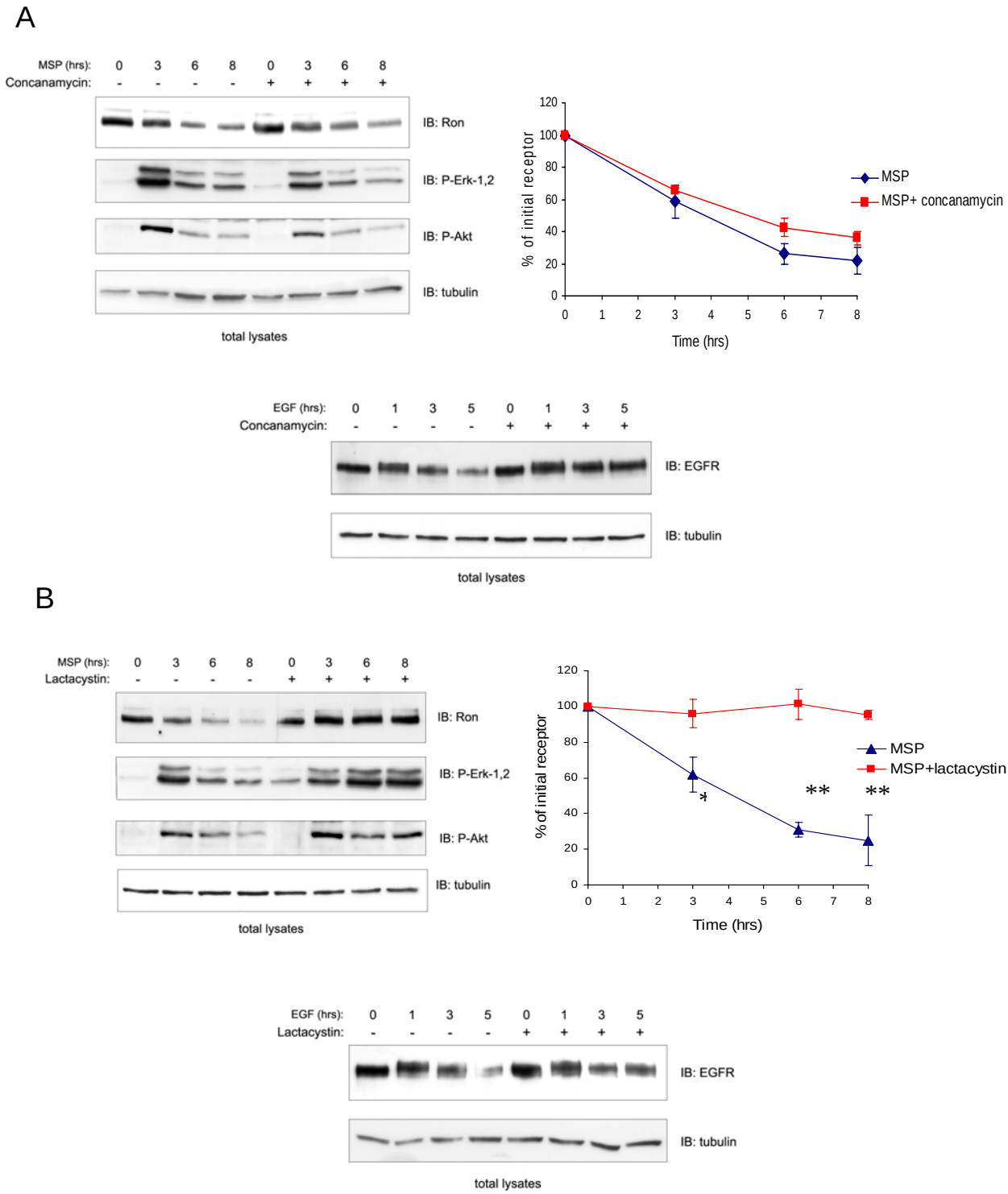

Figure 3. Proteasome is required for MSP-induced Ron degradation, whereas lysosome activity is dispensable. NIH-3T3 cells stably expressing Ron or EGFR were preincubated for 30 minutes with either 100 nM concanamycin (**A**) or 20 μM lactacystin (**B**). Cells were then cultured in medium with or without 100 ng/ml MSP or 100ng/ml EGF. Equal amounts of lysates from cells harvested at the indicated time were subjected to immunoblotting (IB) with the indicated antibodies. Densitometry on Ron Immunoblotting and values, normalized to the relative α-tubulin control bands, were plotted as percentage of vehicle treated cells. Each data point represents the mean ± S.E. of three independent experiments. **P*,< 0.05; ***P*,< 0.005.

Activated Ron accumulates at the cell surface upon proteasome inhibition

We next investigated if activated receptor molecules accumulate at the plasma membrane in conditions of impaired proteasome or lysosome activity. In a cell surface biotinylation assay, 3T3-Ron or 3T3-EGFR cells were ligand-stimulated in presence or absence of lactacystin or concanamycin, then surface protein labelled with biotin and analyzed by immunoprecipitation and avidin blotting. Prolonged MSP stimulation resulted in a measurable decrease of cell surface mature Ron when compared to unstimulated cells (Figure 4, left panel). Notably, lactacystin treatment completely prevented the MSP-dependent reduction of the amount of receptor exposed at the plasma membrane, while lysosome inhibition was almost totally ineffective. On the contrary, EGFR was efficiently removed from cell surface in all experimental conditions tested. Although concanamycin treatment prevented EGFR degradation, it could not block its removal from cells surface (Figure 4, right panel), in line with previous observations indicating that ubiquitination is necessary and sufficient to drive receptor internalization (Haglund et al., 2003).

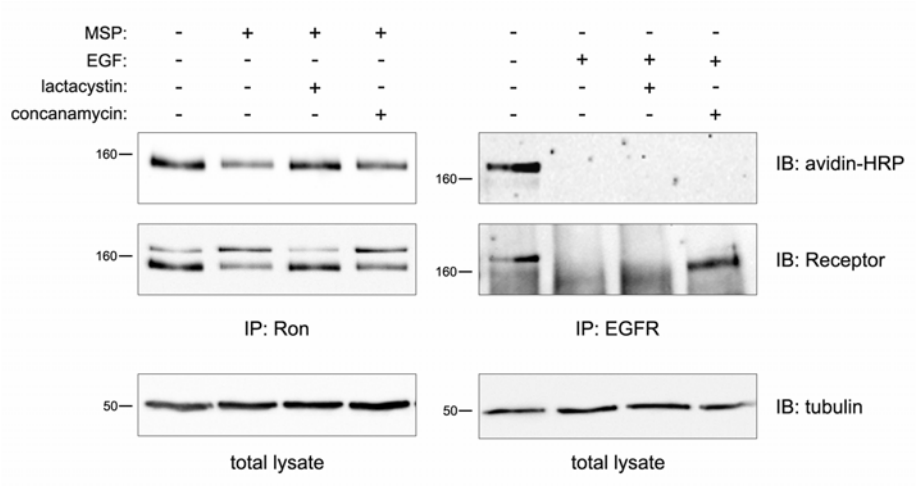

Figure 4. Proteasome inhibition stabilizes Ron at the cell surface. 3T3-Ron or 3T3-EGFR cells were preincubated for 1 h with either lactacystin or concanamycin and then cultured in medium with or without MSP (100 ng/ml) or EGF (100 ng/ml) for 8 hours. Following cell surfaces biotinylation, equal amounts proteins were subjected to immunoprecipitation with the indicated antibodies. Immunoprecipitated proteins and total cell lysates were analyzed by immunoblotting.

These findings indicate that proteasome inhibition sustains Ron downstream signaling pathways not only by preventing its degradation, but also by stabilizing activated receptor molecules at the cell surface.

Internalization is a critical step in ligand-induced Ron downregulation

The majority of growth factor receptors respond to ligand with an enhanced rate of internalization. To further assess the effect of ligand activation on Ron trafficking, the subcellular localization of receptor molecules was evaluated by immunofluorescence analysis at different time points following MSP stimulation. Staining with anti-Ron antibodies of serum starved cells kept on ice resulted in an intense fluorescent signal distributed along all the cell surface (Figure 5A). Following incubation at 37°C in the presence of MSP, the membrane associated fluorescence was decreased, with a parallel accumulation of clustered receptor molecules in the cytoplasm (Figure 5 B-D). Interestingly, we observed a delayed internalization rate for Ron, when compared to that observed for EGFR in the same cell line stimulated with EGF (Figure 5 F-H). Moreover, one hour after ligand stimulation EGFR was mainly found in large spots surrounding the cell nucleus, with a staining pattern characteristic of late endosomes (Figure 5G) and after fluorescence started to decrease most likely as a consequence of receptor degradation (Figure 5H). In contrast, Ron was still scattered as small spots in the cytoplasm even at later time points.

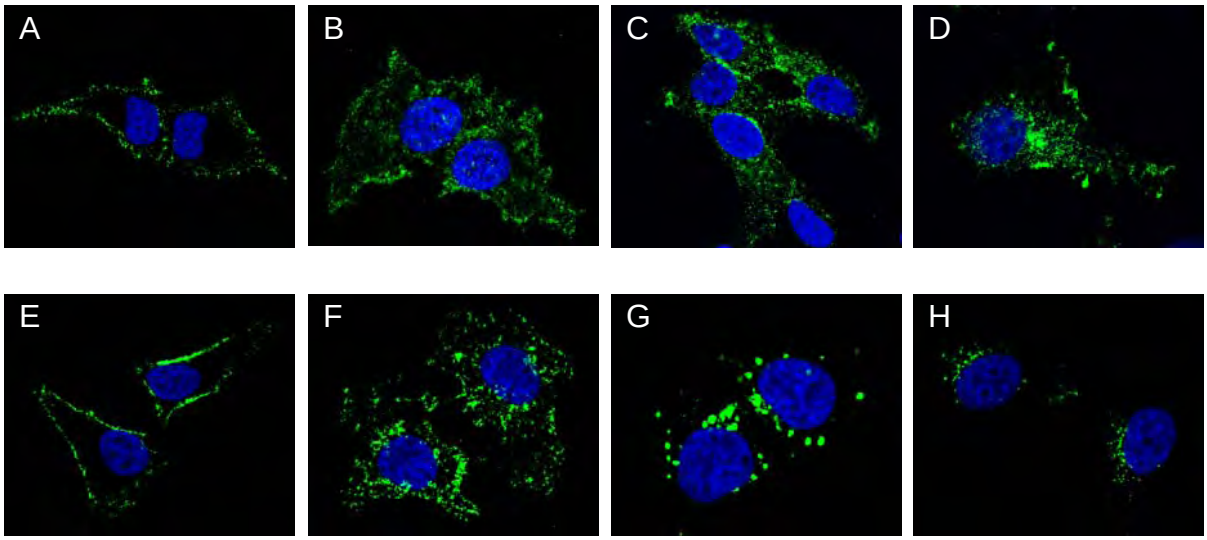

Figure 5. MSP induces Ron internalization. Serum starved HeLa-Ron cells expressing exogenous Ron and endogenous EGFR were labelled on ice with anti-Ron (upper panels) or anti-EGFR (lower panels) antibodies directed against their extracellular domains. Cells were then immediately fixed (**A** and **E**) or incubated at 37°C in medium with MSP (100 ng/ml) or EGF (100 ng/ml) for 30 minutes (**B** and **F** respectively), 1 hour (**C** and **G** respectively) or 3 hours (**D** and **H** respectively). After permeabilization and incubation with Alexa Fluor 488-conjugated secondary antibodies, cells were analyzed by a Leica LS2 laser scanning confocal microscope. Blue signal represents DraQ-5 nuclear staining.

We next addressed weather Ron internalization is required for MSP-induced receptor degradation. We performed a time course of MSP stimulation in cells expressing an HA-tagged mutant form of the GTPase dynamin II (dynamin K44A) under the control of a *tet-off* promoter. Overexpression of this dominant negative mutant acts as a general inhibitor of endocytosis (Henley et al., 1998). In cells cultured in the absence of tetracycline, and thus expressing dynamin K44A, MSP-induced Ron degradation was severely impaired, demonstrating the requirement of active endocytosis to target the activated receptor for degradation (Figure 6).

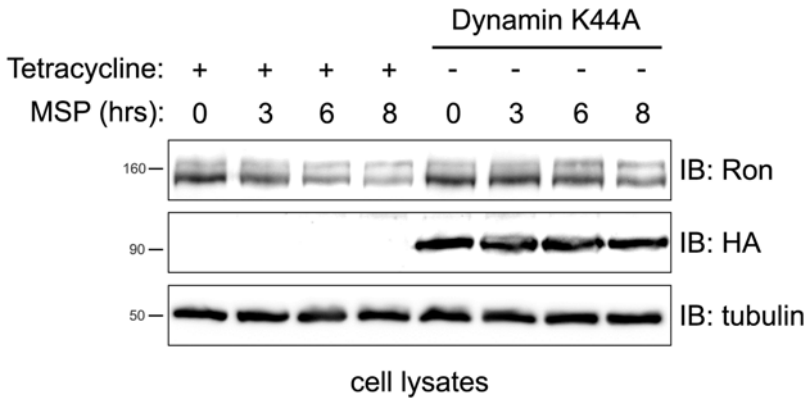

Figure 6. Ligand-induced Ron degradation is hampered in endocytosis-impaired cells. Ron cDNA was transiently transfected in HeLa cells stably transduced with a vector encoding for a dominant negative dynamin II (dynamin K44A) under the control of a *tet-off* promoter. Cells were cultured in the presence or absence of tetracycline for 48 hours and then stimulated with 100 ng/ml MSP for the indicated time. Equal amount of proteins from cell lysates were analyzed by immunoblotting with the indicated antibodies.

Since confocal microscopy analysis indicated that Ron undergoes internalization upon MSP stimulation in a process that does not involve substantial translocation to late endosomes at time points as long as 3 hours, we tested the hypothesis that the receptor could be recycled back to cell surface before degradation. Thus, we treated cells with the carboxylic ionophore monensin, which mediates proton movement across membranes and has been shown to allow receptor internalization but not the traffic of intracellular vesicles, leading to the inhibition of both routing to the lysosomes and recycling to the plasma membrane (Wang et al., 2002). Indeed, it was shown that cell treatment with monensin could block shuttling back to the cell membrane of the transferrin receptor (Tfr), which recycles for the purpose of transporting critical nutrients into the cells (Moos & Morgan, 2000).

In unstimulated cells we observed a reduction in the amount of cell surface Ron following monensin treatment, at a similar extent of that detected for transferrin

receptor, indicating that Ron displays an increased degradation rate in condition of impaired recycling (Figure 7). The effect of monensin on Ron levels were only slightly augmented in MSP stimulated cells.

These results suggest that Ron undergoes recycling both in the presence and absence of ligand activation.

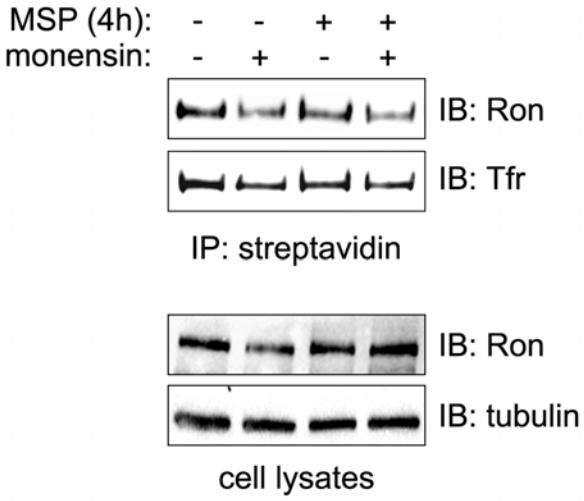

Figure 7. Monensin treatment results increased Ron degradation. FG2 cells were preincubated for 1 hour with 100μM monensin and subjected to cell surfaces biotinylation. Cells were then cultured in medium with or without MSP (100 ng/ml) for 4 hours. Equal amounts proteins from cell lysates were subjected to streptavidin immunoprecipitation. Immunoprecipitated proteins and total cell lysates were analyzed by immunoblotting. α-tubulin immunoblotting was used as loading control.

Caveolae/raft-dependent endocytosis mediates MSP-induced Ron degradation

Based on observations indicating dynamin as a major player in both clathrin- and caveolae/raft-dependent endocytosis (Oh et al., 1998), we tested the involvement of these endocytic pathways in Ron downregulation. To address this issue, we made use of gene silencing approach, analyzing Ron expression following MSP stimulation in cells infected with lentiviral vectors that encode siRNAs designed to selectively target clathrin heavy chain or caveolin-1 expression.

In cells depleted of clathrin, we could not observed any significant perturbation in ligand-induced receptor degradation (Figure 8A). Conversely, caveolin-1 gene siliencing severely impaired ligand-induced Ron downregulation, that was not clearly detectable even at later time points of MSP stimulation. To exclude the possibility that the involvement of the two endocytic pathways could diverge at different ligand concentration, we performed a similar experiment by using lower MSP doses, down to 20 ng/ml. Caveolin-1 depletion resulted in impaired receptor degradation at all concentration of MSP tested (Figure 8C), suggesting that caveolar endocytosis is a general mechanism involved in ligand-induced Ron downregulation.

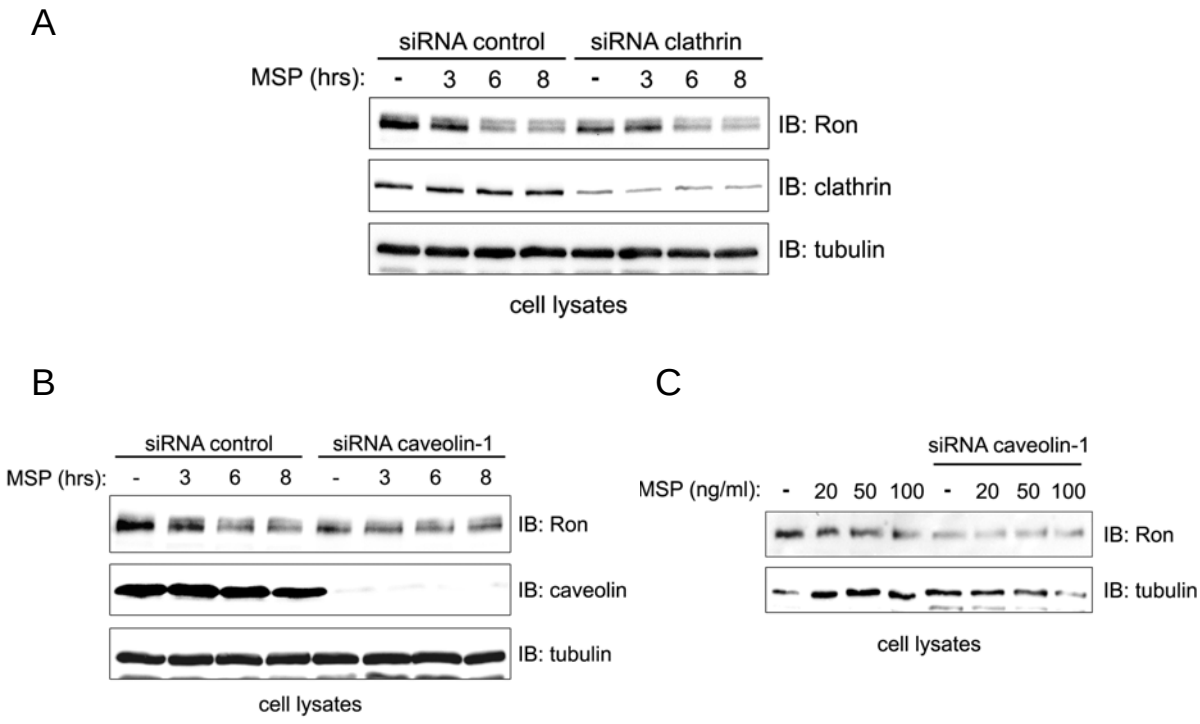

Figure 8. Caveolar endocytosis is involved in MSP-induced Ron downregulation. FG2 cells were transfected siRNA targeted to clathrin (**A**) or caveolin-1 (**B** and **C**) transcript or to an unrelated sequence. 72h after transfection, cells were stimulated with 100 ng/ml MSP for the indicated times (**A** and **B**) or with different MSP concentrations for 8 hours (**C**). Equal quantities of cell lysates were analyzed by Immunoblotting with the indicated antibodies. α-tubulin immunoblotting was used as loading control.

To go better inside in the role of caveolin-1 in the regulation of ligand-induced Ron downregulation, we tested the possibility that the receptor could be found in complex with caveolin-1. By co-immunoprecipitation experiments we observed association between Ron and caveolin-1, already present in unstimulated cells and increased upon MSP stimulation (Figure 9A). Moreover, confocal microscopy analysis revealed a partial overlay of Ron and caveolin-1 signals in untreated cells and a clear relocalization of Ron in structures containing caveolin-1 upon ligand stimulation (Figure 9B). Our findings thus reveal that Ron can directly interact with caveolin-1 and interference with caveolae/raft-dependent endocytosis affects Ron degradation.

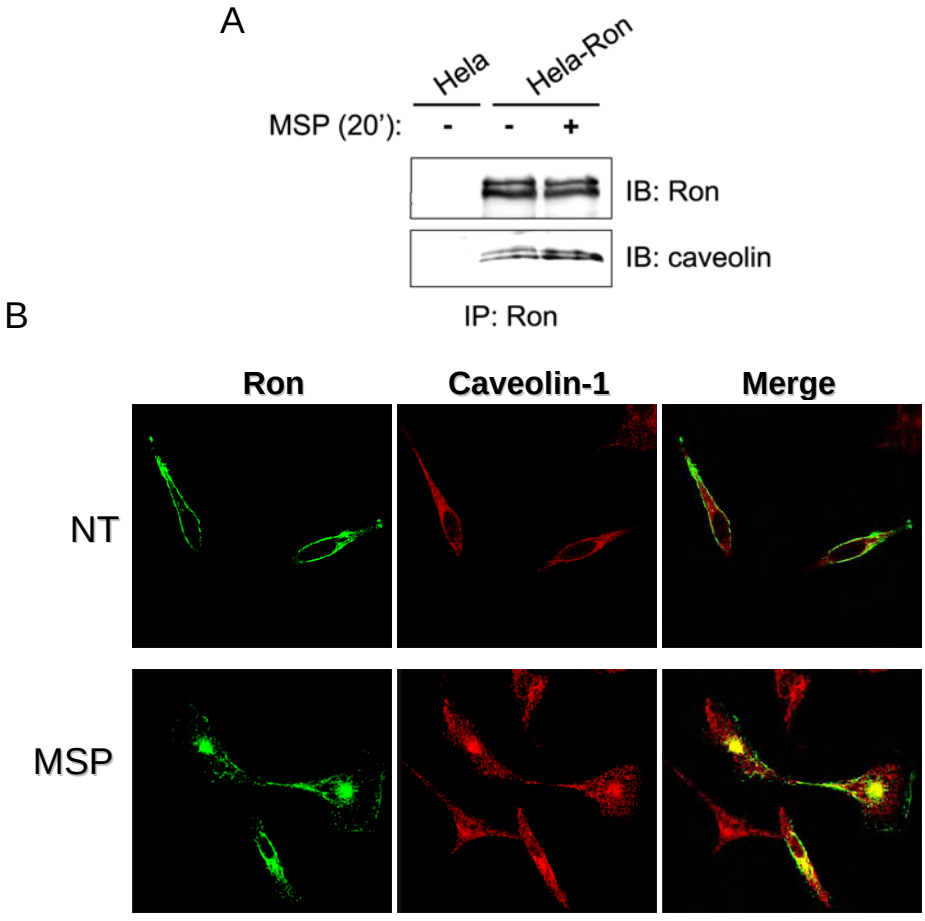

Figure 9. Ron associates with caveolin-1. (**A**) HeLa-Ron cells stably expressing Ron were stimulated or not with 100 ng/ml MSP for 20 minutes. Equal protein amounts were immunoprecipitated with Ron antibodies and association of caveolin-1 to the Ron immunocomplex was detected by immunoblotting. (**B**) The same cells were treated as described above and then fixed and permeabilized. After incubation with primary antibodies, Alexa Fluor 488- or 555-conjugated antibodies were added to detect antigen bounds anti-Ron (green signal) or anti-caveolin-1 (red signals) antibodies. In yellow, superimposition of the two signals.

Discussion

Ligand-induced downregulation of RTKs as emerged as a key negative regulatory mechanism that can achieve long-lasting signalling attenuation by removing activated receptor from the cell surface and committing them to degradation. The maintenance of the appropriate extent and duration of signals elicited by activated RTKs is critical for preventing over-stimulation, that could potentially lead to cellular transformation (Di Fiore & Gill, 1999). Studies on the ErbB family of RTKs have provided important hints on how controlled receptor trafficking to degradative compartments regulate the potency of mitogenic signalling. It has been reported that different ErbB receptor ligands, namely EGF and TGF-α, invoke distinct signalling potencies in term of mitogenic potential. High mitogenic responses correlate with increased recycling and decreased downregulation that occur in the presence of TGF-α (Waterman et al., 1998). Moreover, considerable evidence suggests that escape from ligand-induced downregulation plays an important role in RTKs deregulation and may be mechanism in cancer (Peschard & Park, 2003).

Several reports have established that ubiquitination plays a major role in RTKs downregulation, by driving activated receptors throughout the endocytic route to degradative compartments. Some evidence supports that EGFR, PDGFR and HGF-R/Met undergo multiple monoubiquitination following ligand stimulation (Carter et al., 2004; Haglund et al., 2003; Mosesson et al., 2003) and a single ubiquitin moiety has been demonstrated to be sufficient to drive receptor internalization (Haglund et al., 2003). While the requirement of ubiquitination at the initial step of internalization remains still controversial, the best characterized role for RTKs ubiquitination is to regulate their sorting to lysosome for degradation. The identification of ubiquitin-binding proteins (Ub-receptors) compartmentalized along the endocytic pathway has

lead to hypothesize that multiple monoubiquitin signals on activated RTKs might determine the specificity and the strength of their interactions with Ub-receptors (Haglund et al., 2003). This contention has been challenged by recent reports, in which authors used ubiquitin-containing reporter proteins to argue that low-affinity interactions via monoubiquitin are not sufficient for endocytosis, whereas polyubiquitin chains are preferentially recognized by the endocytic machinery (Barriere et al., 2006; Madshus, 2006). In addition, Carter and co-workers indicated a requirement of Lys-48-linked polyubiquitin chains for HGF-R/Met endosomal trafficking, even though activted receptor undergoes multiple monoubiquitination (Carter et al., 2004). More recently, mass spectrometry analysis of immunopurified EGFR demonstrated the occurrence of Lys63-linked polyubiquitin chains within the kinase domain of the receptor following stimulation (Huang et al., 2006). Thus, in addition to multiple monoubiquitination the EGFR is modified also by polyubiquitination, although the mechanism through which Lys63-linked chains could regulate internalization and sorting of activated receptor is not known. At present the functional relevance of different lysine linkages *in vivo* is a matter of debate and growing evidence points to additional levels of complexity in the ubiquitin system.

Moreover, the accepted view that activated RTKs are ultimately sorted to lysosome for degradation has been challenged by several observations indicating a role for proteasome 26S in downregulation of some RTKs, including IGF-1R and Ret (Pierchala et al., 2006; Sehat et al., 2007), and cytokine receptors such as the erythropoietin receptor (EpoR; (Walrafen et al., 2004).

The Ron tyrosine kinase receptor has been implicated in cancer progression and malignancy (Wang et al., 2006). The mechanisms by which Ron can acquire oncogenic potential has been extensively characterized, including overexpression,

point mutations and truncations (reviewed in (Wang et al., 2003). Much less is known about the negative regulation of Ron signalling and its alterations in human cancers.

We have previously identified the E3 ubiquitin ligase c-Cbl as a critical modulator of Ron, as it mediates ligand-induced receptor ubiquitination and downregulation (Penengo et al., 2003). In the present work we characterized the role of ubiquitination and endocytic trafficking in the negative regulation of Ron. Our findings indicate that the type of modification occurring on activated Ron involves the conjugation of polyubiquitin chains, rather than single ubiquitin moiety at multiple sites. At present the nature of lysine linkages of polyubiquitin chains as well as the lysine residues specifically modified by ubiquitin remain obscure. Ubiquitin mutants harbouring single lysine to arginine substitutions and mass spectrometry analysis will help us to verify the occurrence of specific lysine-linked chains on Ron, like lys63 chains, as reported for EGFR and TrkA (Geetha et al., 2005; Huang et al., 2006), or others never identified on activated RTKs so far.

The different ubiquitination pattern displayed by activated Ron, with respect to that generally described for RTKs, may account for the peculiar degradative fate of this receptor. Indeed, our results indicate that lysosomal activity is dispensable and identify the proteasome 26S as the major player in MSP-induced Ron degradation. Moreover we present evidence indicating that recycling back to cell surfaceis a critical mechanism in Ron downregulation, that might regulate the amount of receptor exposed at the plasma membrane either at steady-state and following ligand stimulation. The decrease in receptor expression level observed upon treatment with monensin suggests that Ron is continuously internalized, even in absence of ligand activation, and when the internalized receptor is kept inside the cell by impaired recycling, it is forced to proteasome degradation. Although the ultimate and long-

lasting effect of endocytosis is to terminate signalling, several evidences for signaling within endosomal compartments have emerged. Based on these findings, it will be of interest to assess whether recycling is a mechanism through which activated Ron might regulate duration and compartmentalization of signals. Our recent observations suggest that in conditions of impaired recycling MSP-dependent signaling to PI3K/Akt pathway.

Although the existence of different endocytic routes is well known, how they orchestrate distinct biochemical pathways and biological behaviour remains still elusive. Studies on TGF-β receptor have reported that clathrin-mediated endocytosis sustains continuous shuttling of the receptor between the plasma membrane, whereas the fraction of receptors internalized through caveolae/raft- dependent endocytosis is delivered to a degradative compartment (Di Guglielmo et al., 2003). Moreover, it has been demonstrated that while the raft-dependent pathway is preferentially associated with EGFR degradation, clathrin-dependent internalization appears to contribute primarily to EGFR recycling and signaling (Sigismund et al., 2005). In line with these observations, we found that caveolae/raft-dependent endocytosis is required for MSP-induced Ron degradation, even with low doses of ligand. This is further confirmed by the enhanced association between the receptor and caveolin-1 observed following MSP stimulation. Although our data clearly indicate that clathrin-mediated endocytosis is not involved in the degradative fate of activated Ron, we cannot exclude a role for this endocytic pathway in the regulation of MSP-dependent signaling. A complete understanding of these pathways is of great importance to highlight the role of ubiquitination and endocytic trafficking in the negative regulation of Ron, thereby providing novel attractive approaches to target altered Ron signaling in cancer.

Ligand-independent Downregulation of Ron and its Oncogenic Variant

Summary

RTKs downregulation can be induced by ligand-stimulation but also by activating mutations that lead to accelerated turnover. In these conditions, the mechanisms controlling receptor degradation can be partially independent from the activity of the RING finger E3 ligase c-Cbl and require the activity of other ubiquitin ligases such as the chaperone-interacting protein CHIP. The carboxyl-terminal U-box domain of the protein is endowed with ubiquitin ligase activity, while the amino-terminal tetratricopeptide (TPR) domain mediates binding to the chaperones Hsp70 and Hsp90 (Jiang et al., 2001).

A wide array of proteins involved in signal transduction pathways depend on Hsp90 and other chaperone components for functional maturation, regulation and stability (Pratt & Toft, 2003). CHIP has been reported to associate with and convert Hsp90 multichaperone complexes from a chaperone function to one that promotes ubiquitination and degradation of client proteins (Connell et al., 2001). A role for CHIP in mediating proteasomal degradation of Hsp90 client proteins has been demonstrated in the case of the glucocorticoid receptor (Connell et al., 2001), the cystic fibrosis transmembrane-conductance regulator (Meacham et al., 2001), c-Raf kinase and both wild-type and mutant p53 proteins (Esser et al., 2005). Moreover, it has been reported that ErbB2 tyrosine kinase receptor, which is resistant to c-Cbl mediated downregulation, requires association with the Hsp90 for its stability and is efficiently ubiquitinated and degraded by the E3 ligase CHIP (Xu et al., 2002).

CHIP-mediated ubiquitination thus seems critical in all the situations where receptors are conformationally altered, such as point mutations or rearrangement. It is also conceivable that CHIP plays a role in down-regulation of receptors that are unable to interact with Cbl, as a consequence of mutation of the Cbl tyrosine kinase domain, Cbl sequestration by intracellular proteins or receptor mutation in the Cbl-interaction site.

In addition, CHIP has been proposed to mediate the effects of geldanamycins, a class of Hsp90 inhibitors that compete with ADP/ATP for the nucleotide binding pocket of Hsp90 and restrain its ATP-dependent chaperone activity and thus directing the proteasomal degradation of the client proteins (Schneider et al., 1996; Zhou et al., 2003). Sensitivity to geldanamycins has been described for several RTKs. Treatment of breast and other cancer cells with geldanamycin has been reported to cause ubiquitination of cell surface ErbB2 molecules, followed by their proteasome-dependent degradation (Mimnaugh et al., 1996). Moreover, geldanamycins have been shown to downregulate HGF-R/Met preventing HGF-mediated tumor cell motility and invasion (Xie et al., 2005) and to deplete mature EGFR proteins harbouring mutations in the kinase domain (Shimamura et al., 2005).

Based on preliminary observations suggesting the ability of an oncogenic Ron variant harbouring a single point mutation (Ron^{M1254T}) in kinase domain to escape from c-Cbl mediated downregulation, we addresses the possibility of alternative degradative pathways triggered by different E3 ligase such as CHIP.

In this context we explored the effects of geldanamycin and its derivatives on Ron stability and on deregulated signalling triggered by the oncogenic mutant.

Experimental procedures

Reagents and antibodies

Geldanamycin and 17-AAG were purchased from Alexis. MSP was obtained by R&D System. Polyclonal antibody against Ron C-terminal domain (c-20) and monoclonal anti Hsc-70 (B-6) were from Santa Cruz Biotechnology, Inc.; monoclonal anti-α-tubulin (B-5-1-2), anti-phospho-Erk1/2 (MAPK-YT), and anti-Erk1/2 (ERK-NP2) and anti-FLAG (M2) were purchased from Sigma; polyclonal phospho-Akt (Ser^{473}) and polyclonal anti-Akt were from Cell Signaling Technology; monoclonal anti-Cbl (7G10) was from Upstate Biotechnology, Inc. and monoclonal anti-Hsp90 antibody from BD Transduction laboratories; monoclonal anti ubiquitin (FK2) was from Stressgen and CHIP rabbit polyclonal antiserum was from Calbiochem (Merck). Horeseradish peroxidase-conjugated anti-mouse and anti-rabbit were purchased from Cell Signaling Technology, Inc.

Plasmids

pMT2-Ron and pMT2-Ron^{M1254T} were described previously (Santoro et al., 1998), c-Cbl, c-Cbl70z, CHIP, CHIPK30A and CHIPΔU-box were in pcDNA3 (Ballinger et al., 1999; Waterman et al., 1999). GST-CHIP and GST-CHIPΔU-box in pGEX4T-2 vector were kindly provided by H. Band (Brigham and women's Hospital, Boston, MA). pCCLsin.PPT.hPGK.GFP.Wpre transfer plasmid was used to express two independent siRNAs (5'-ACCACGAGGGTGATGAGGA-3'; 5'-GAAGCGAGATATCCC TGAC-3'), targeting CHIP transcript or an unrelated sequence as negative control.

Cell culture and transfection

FG2 cells were maintained in RPMI-1640, COS-7 and NIH-3T3 cells were maintained in Dulbecco's modified Eagle's medium (Sigma), supplemented with 10% fetal bovine serum (Invitrogen) in a 5% CO_2-humidified atmosphere. NIH-3T3 stably expressing Ron or Ron^{M1254T} were obtained as described previously (Santoro et al., 1998). Transient transfection of COS-7 cells was performed with DEAE-dextran using the CellPhect transfection kit (GE Healthcare). Transfection of FG2 cells was performed as described in Experimental Procedures of Section I.

Biochemical assays

Immunoprecipitation, immunoblotting and cell surface biotinylation assay were performed as described previously (see Experimental Procedures, Section I). For *in vitro* ubiquitination assay GST-CHIP and GST-CHIPΔU-box were expressed in *E.coli* and affinity-purified according to the manufacturer's recommendations. Receptors were immunoprecipitated from 800 µg aliquots of cell lysates with protein A-Sepharose beads. Following purification Sepharose beads were extensively washed and incubated in a 50 µl reaction for 90 min at 37 °C with 275 ng purified E1, 400 ng E2 (UbcH5a), 5 ng/µl biotin Nterminal ubiquitin, 10 ng/µl ubiquitin (Boston Biochem Inc.) and 5 µg of the indicated GST fusion proteins in a buffer containing 50 mM Tris-HCl pH 7.5, 2.5 mM MgCl2, 2 mM ATP, 2 mM DTT. After extensive washes the ubiquitylated receptors were detected by SDS-PAGE and Western Blotting with HRPconjugated streptavidin (GE Healthcare).

Cell proliferation assay

Cells were plated on 96-well plates at a density of 4 x 10^3/ well and cultured in appropriate medium supplemented with 10% fetal bovine serum in presence or absence of 100 nM 17-AAG. Cells were fixed in 11% glutaraldehyde 0, 24, 48 and 72 hours after drug addition and stained in Crystal Violet. Staining was solubilized in 10% acetic acid and absorbance at 595nm was measured with a microplate reader.

Cell migration assay

Cell motility was assayed using 8 µM pore size Transwell® chambers (Corning). The lower side of the membrane was coated with 10 µg/ml fibronectin for 2 hours, and then blocked with 0.2% BSA. Cells were detached with 1 mM EDTA and resuspended with 2% fetal bovine serum. 1 x 10^5 cells were plated on the upper side and allowed to migrate for 6 hours in presence of 100 nM 17-AAG towards the lower chamber containing appropriate medium supplemented with 10% fetal bovine serum. Cells remaining in the upper chamber were mechanically removed and those migrated to the lower side were fixed and stained as described above.

Transforming assay

Focus forming assay was performed on NIH-3T3 fibroblasts (5 x 10^5 cells) with 5 µg of recombinant plasmid as described previously (Santoro et al., 1998). Two days after transfection, 17-AAG were added to cultures and renewed every 48 hours. Cell cultures were maintained at confluence and screened for *foci* formation 10 ± 18 days after transfection. Spontaneous formation of foci was negligible.

Results

Oncogenic mutant Ron^{M1254T} displays c-Cbl-independent ubiquitination

According to our previous results, indicating that E3 ubiquitin ligase c-Cbl physically interacts with Ron and promotes its ligand-dependent ubiquitination and degradation, we sought to determine if a similar mechanism could be involved in downregulation of the oncogenic mutant Ron^{M1254T}. Interestingly, in COS-7 cells co-expressing c-Cbl and Ron^{M1254T}, the mutant receptor failed to coimmunoprecipitate the ubiquitin ligase, even upon MSP stimulation (Figure 1A upper panel). Likewise, in the reciprocal experiment, wild-type Ron, but not Ron^{M1254T}, was present in c-Cbl immunoprecipitates of the same cells (Figure 1A lower panel).

On the basis of these results, we evaluated if the lack of association with c-Cbl could affect Ron^{M1254T} ubiquitination. In COS-7 cells co-transfected with wild-type or mutant receptor along with c-Cbl and a flag-tagged form of ubiquitin, the ubiquitination of Ron^{M1254T} was preserved and was ligand independent (Figure 1B).

These data suggest that also c-Cbl independent mechanisms might responsible for receptor ubiquitination, at least for mutant Ron^{M1254T}. This oncogenic variant harbours a point mutation responsible for constitutive activation of the kinase and for overcoming the requirement for the multifunctional docking site. The subversion of substrate specificity that characterize this mutant might thus account for its c-Cbl independent ubiquitination.

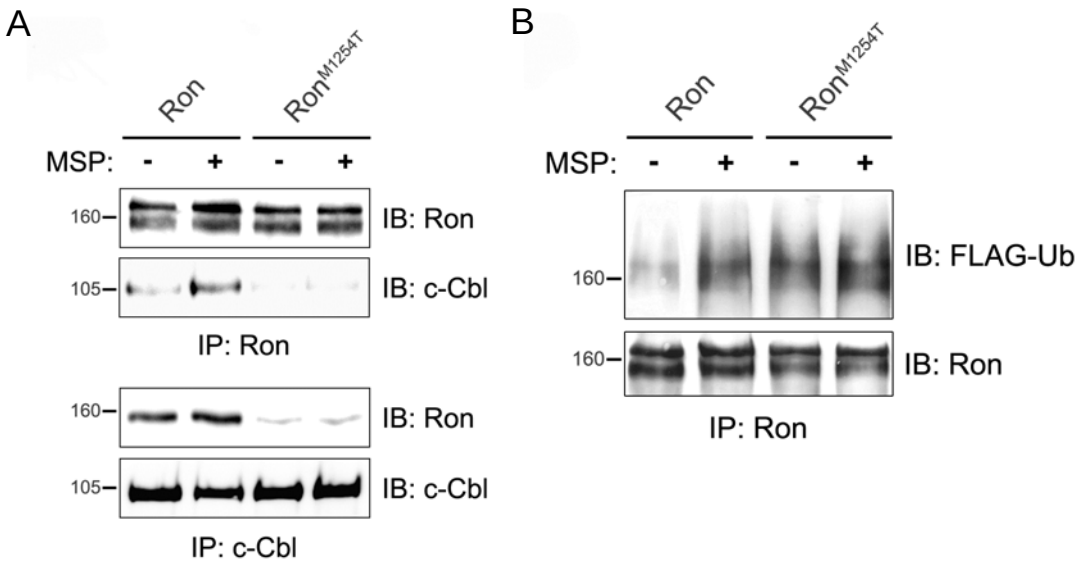

Figure 1. Oncogenic mutant Ron^{M1254T} escape from cCbl-dependent ubiquitination. A) COS-7 cells were transiently transfected with Ron or Ron^{M1254T}, along with c-Cbl and FLAG-tagged ubiquitin. 72 hours after transfection, serum starved cells were stimulated with 100 ng/ml MSP for 20 min and equal protein amounts of cell lysates were immunoprecipitated with Ron (upper panel) or c-Cbl (lower panel) antibodies. Associated c-Cbl or Ron were detected with the appropriate antibodies. **B**) Ron immunoprecipitation described in A was followed by immunoblotting with FLAG antibodies to detect ubiquitylated receptors. The immunoprecipitated receptor was detected by Ron Immunoblotting.

Ron and Ron^{M1254T} associate with a chaperone complex containing CHIP E3 ligase

Among several ubiquitin ligases, we focused our attention on CHIP (C-terminal Hsc70-interacting protein), as it has been involved in the negative regulation of molecules responsible for oncogenic transformation. This E3 ligase has been reported to mediate degradation of signaling proteins, relying on the association with chaperone proteins Hsp90 and Hsc70. Based on these indications, we sought evidence of the association of Ron and Ron^{M1254T} with the chaperone complex

containing CHIP. We co-transfected COS-7 cells with cDNAs encoding either Ron^{M1254T} or wild-type Ron and CHIP. Endogenous Hsp90 and Hsc70, as well as CHIP, were detected in Ron immunocomplexes and were more abundant in immunocomplexes from cells expressing the oncogenic receptor (Figure 2A). The stronger interaction between CHIP and Ron^{M1254T} was confirmed by the reciprocal experiment.

CHIP has the ability to bind Hsc70 by means of the amino-terminal tetratricopeptide (TPR) domain, while its E3 ubiquitin ligase activity is mediated by its C-terminal U-box domain (Jiang et al., 2001). To better characterize the interaction between the receptor and the ubiquitin ligase we tested the ability of CHIP proteins harboring a mutation in the TPR (K30A) or lacking the U-box (ΔU-box) domain to interact with Ron. The K30A mutant, which does not bind to either Hsp90 or Hsc70 (Xu et al., 2002), failed to co-immunoprecipitate with Ron. This suggests that these chaperone intermediates are involved in the Ron-CHIP interaction. Conversely, the deletion of the U-box domain did not impair the complex formation (Figure 2B).

Taken together, these results indicate that in live cells Ron and its oncogenic variant Ron^{M1254T} forms a complex with the chaperones Hsp90 and Hsc70, which mediate receptor association with the E3 ubiquitin ligase CHIP.

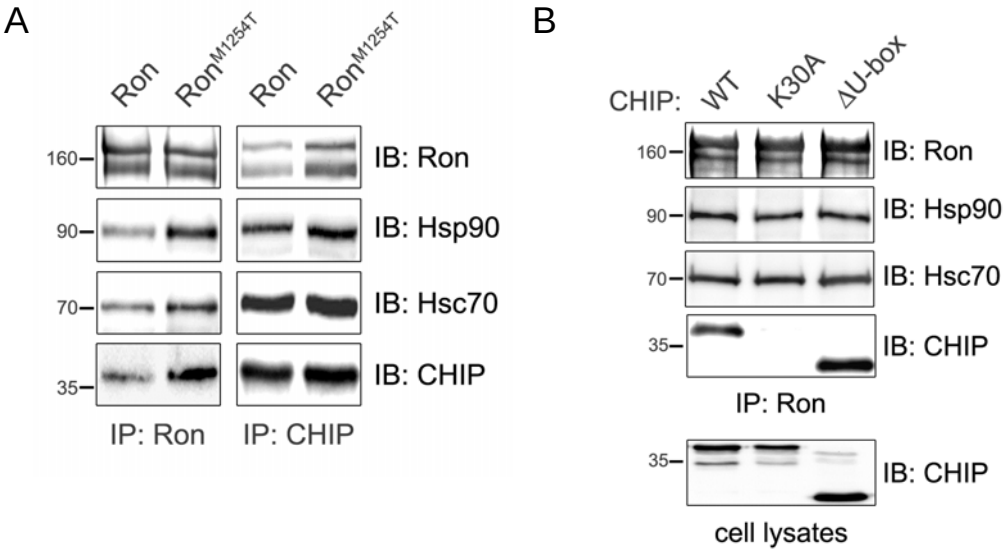

Figure 2. CHIP interacts with Ron and Ron^{M1254T} by a chaperone intermediate. A) COS-7 cells were transiently transfected with Ron or Ron^{M1254T} along with CHIP. 72 hours after transfection equal protein amounts of cell lysates were immunoprecipitated with Ron or CHIP antibodies and presence of CHIP, Ron, Hsp90, Hsc70 in the immunocomplexes was detected with the appropriate antibodies. Ron, Ron^{M1254T} and CHIP expression was monitored by immunoblotting. **B**) COS-7 cells were transiently transfected with Ron and either CHIP or different CHIP mutants. Cells were lysed and equal protein amounts were immunoprecipitated with Ron antibodies. Association of Hsp90, Hsc70 and CHIP to the Ron immunocomplex was detected with the appropriate antibodies. Anti-CHIP immunoblotting of cell lysates was used to control transfection efficiency.

Ron and Ron^{M1254T} associate with a chaperone complex containing CHIP E3 ligase

To verify whether CHIP could directly mediate Ron ubiquitination, we performed an *in vitro* ubiquitination assay on immunocomplexes from 3T3-Ron fibroblasts, by using purified GST-CHIP fusion proteins in the presence of biotinylated ubiquitin and E1 and E2 enzymes. Wild type (GST-CHIP), but not U-box-deleted (GST-CHIP ΔU-box), fusion protein catalyzed the receptor ubiquitination. No ubiquitination was observed in the presence of GST protein alone, as well as when the reaction was performed in absence of immunoprecipitated Ron (Figure 3A). These data indicate that CHIP can serve *in vitro* as an E3 ligase for Ron.

We next addressed whether Ron^{M1254T} ubiquitination *in vivo* could rely on the ubiquitin ligase activity of CHIP. We over-expressed CHIP or the defective ligase CHIP ΔU-box in COS-7 cells. Endogenous CHIP was sufficient to promote Ron^{M1254T} ubiquitination, which was increased by overexpression of recombinant CHIP and almost totally abrogated in cells overexpressing CHIP ΔU-box (Figure 3B). This demonstrates that CHIP is a functional E3 ubiquitin ligase for this oncogenic receptor.

These data altogether indicate that Ron and Ron^{M1254T} differentially interact with the E3 ligase CHIP, which is responsible for the c-Cbl and ligand independent ubiquitINation of the oncogenic receptor.

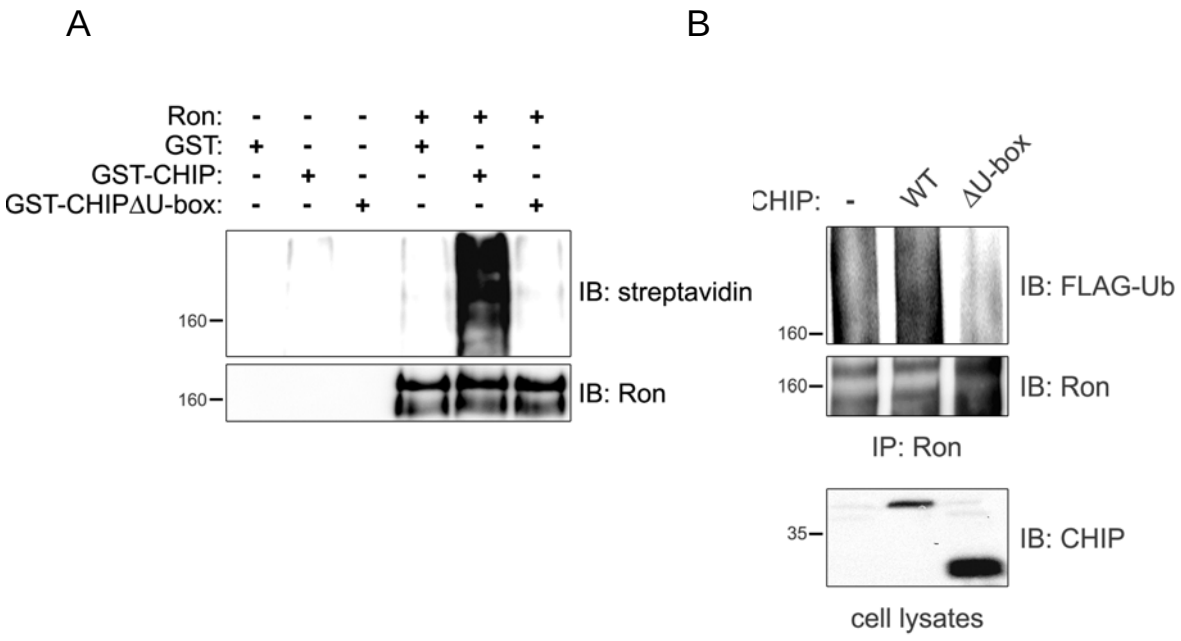

Figure 3. CHIP serves as an E3 ligase for Ron *in vitro* and *in vivo*. A) Proteins from 3T3-Ron cell lysates were immunoprecipitated with Ron antibodies or pre-immune rabbit serum. Immunoprecipitates were subjected to *in vitro* ubiquitination assay in the presence of GST or GST-CHIP fusion proteins, biotin-labeled ubiquitin, E1 and E2 enzymes. The ubiquitinated receptors were detected by immunoblotting with streptavidin-HRP. **B**) Proteins from cell lysates of COS-7 transiently transfected with Ron^{M1254T} and FLAG-tagged ubiquitin, along with CHIP or CHIP ΔU-box or empty vector, were subjected to immunoprecipitation with Ron antibodies and analyzed by anti-FLAG and anti-Ron immunoblotting. Anti-CHIP immunoblotting on cell lysates was used to control transfection efficiency.

CHIP regulates Ron and Ron^{M1254T} turnover

A number of reports assigned a role for CHIP in the regulation of the turnover of several Hsp90 client proteins (Connell et al., 2001). We have thus investigated the possibility that CHIP may normally regulate Ron and Ron^{M1254T} stability. To address this issue, NIH-3T3 fibroblasts stably expressing Ron (3T3-Ron) or the oncogenic mutant (3T3-Ron^{M1254T}) were transfected with a vector encoding a siRNA to target CHIP expression and cicloheximide was used to evaluate the half-life of the receptor in condition of impaired *de novo* synthesis (Figure 4). In cells transfected with a control vector, 8 hours treatment with cicloheximide were sufficient to observe a marked reduction of Ron expression, due to concomitant block of neosynthesis and degradation of mature receptor. Even more pronounced was the decrease of Ron^{M1254T} protein levels, suggesting the oncogenic receptor undergoes a more rapid turnover. Conversely, in cells expressing CHIP targeted siRNAs, we could not observe any significant reduction in receptor level upon cicloheximide treatment, demonstrating CHIP ubiquitin ligase plays an essential role in the regulation of the turnover of both wild-type and mutant Ron.

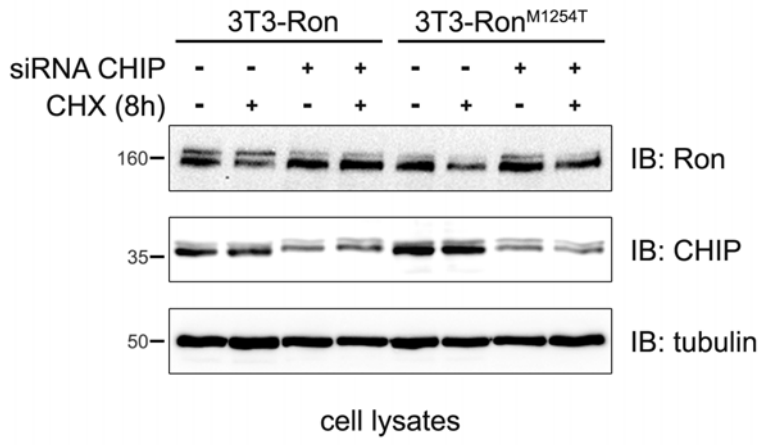

Figure 4. CHIP controls Ron and Ron^{M1254T} stability. 3T3-Ron or 3T3-Ron^{M1254T} cells were transfected with siRNA targeted to CHIP transcript or to an unrelated sequence. 72h after transfection, cells were treated with cicloheximide or vehicle for 8 hours. Equal quantities of lysates were analyzed by immunoblotting with Ron antibodies.

CHIP mediates Ron degradation induced by geldanamycins

It has been reported that CHIP mediates the effects of the Hsp90 inhibitor geldanamycin (GA), by promoting ubiquitination and degradation of Hsp90 client proteins.

We first investigated the sensitivity of Ron to GA, by performing a time-course experiment on 3T3-Ron cells and FG2 cells, expressing recombinant and endogenous Ron, respectively. After cell exposure to GA for different times, we observed a robust reduction of both precursor and mature form of the receptor within 6 hours. Noteworthy, Ron protein levels declined with similar rates in both cell lines, upon GA treatment. Similar effects, at a slightly lesser extent, were observed with the same concentration of the less toxic GA derivative 17-AAG, (Figure 5A). Ron destabilization upon Hsp90 inhibition was obtained also by using a chemically unrelated Hsp90 inhibitor, the macrolactone antibiotic radicicol (data not shown).

We further investigated if Ron depletion following GA or 17-AAG exposure was due to impaired maturation of the nascent chains only, or also cell-surface exposed receptors were targeted for degradation. By surface biotinylation of 3T3-Ron and FG2 cells, followed by Ron immunoprecipitation, we observed an accelerated decrease of cell surface mature Ron after exposure to GA or 17-AAG for 6 hours (Figure 5B). This indicates that GA and 17-AAG, albeit with minor efficacy, are able to destabilize the receptor even after its exposure to the plasma membrane.

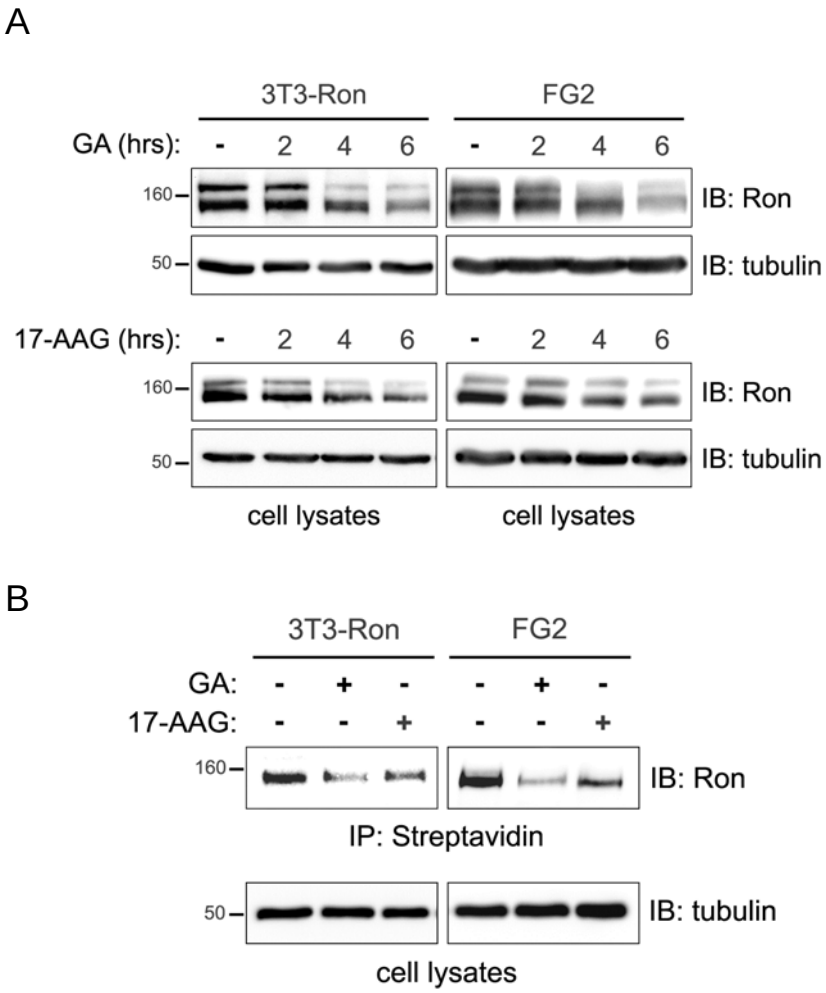

Figure 5. Geldanamycins induce degradation of both precursor and mature cell surface Ron. **A**) 3T3-Ron and FG2 cells were treated with or without 1 μM GA or 1 μM 17-AAG for the indicated times. Cell lysates were analyzed by immunoblotting with Ron antibodies. α-tubulin immunoblotting was used as loading control. **B**) 3T3-Ron and FG2 cells were cell-surface biotinylated and then cultured in medium with or without 1 μM GA or 1 μM 17-AAG for 6 hours. After immunoprecipitation of cell lysates with streptavidin-Sepharose surface-labeled mature Ron was detected by anti-Ron Immunoblotting.

Since GA-induced degradation of the client proteins is reported to involve the ubiquitin-proteasome pathway (Sepp-Lorenzino et al., 1995), we analyzed Ron ubiquitination upon GA or 17-AAG treatment of 3T3-Ron of FG2 cells. In these conditions a marked ubiquitylation of the receptor was observed as early as 15 minutes after drug addition (Figure 6A). This indicates that receptor ubiquitylation is an early step in GA-induced Ron degradation.

Moreover, pre-treatment of both cell lines with the proteasome inhibitor MG-132 impaired Ron depletion induced by geldanamycins (Figure 6B), indicating that this destabilizing effect on Ron requires proteasomal activity. Conversely, when cells were pre-treated with the lysosomal inhibitor Concanamycin A, GA retained full activity on Ron (data not shown).

Taken together these results show that cell-surface exposed mature Ron is destabilized by GA-induced degradation, involving the ubiquitin proteasome pathway.

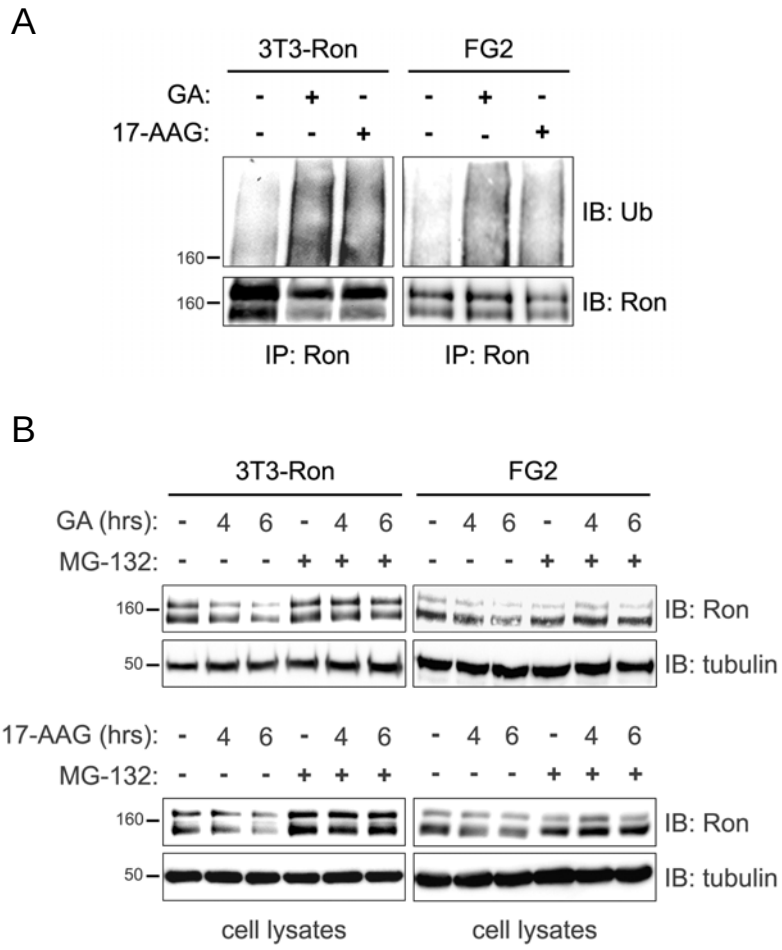

Figure 6. The ubiquitin-proteasome pathway is involved in Ron degradation induced by geldanamycins. **A**) Proteins from lysates of 3T3-Ron and FG2 cells treated with or without 1μM GA, or 1 μM 17-AAG for 15 minutes were immunoprecipitated with Ron antibodies. Anti-ubiquitin immunoblotting was used to detect the ubiquitinated receptor molecules. The immunoprecipitated receptor was detected by Ron immunoblotting. **B**) 3T3-Ron and FG2 cells were treated with or without 1 μM GA, or 1 μM 17-AAG in presence or absence of the proteasome inhibitor MG-132 (20 μM). Cells were incubated with MG-132 for 1 hour before drugs addition. Equal quantities of lysates from cells harvested at the indicated times were analyzed by anti-Ron immunoblotting.

Based on these observations we evaluated the involvement of CHIP in GA-induced Ron degradation. To this end we made use of COS-7 cells expressing the wild-type E3 ligase or the deletion mutant CHIP ΔU-box, which despite its lack of ubiquitin ligase activity still associates with the receptor. Overexpression of the dominant negative CHIP ΔU-box resulted in abrogation of GA-induced Ron degradation (Figure 7A).

We previously reported that the E3 ubiquitin ligase c-Cbl physically interacts with Ron, promoting its ligand-dependent ubiquitylation and downregulation. To verify the role for c-Cbl in receptor destabilization driven by GA, we performed the parallel experiment in COS-7 transfected with c-Cbl or the dominant negative c-Cbl-70Z (Weissman, 2001). Impairment of c-Cbl activity had no effect on GA-induced Ron degradation (Figure 7B).

To confirm the key role of CHIP in GA mediated Ron destabilization, we analyzed cells deprived of CHIP by expression of targeted siRNAs sequences. FG2 cells were engineered by means of vectors to express siRNAs designed to selectively inactivate CHIP transcripts or targeted to an unrelated sequence as control. Cells expressing CHIP-targeted siRNAs displayed markedly reduced levels of CHIP. In these conditions, Ron was refractory to the degradation induced by GA, whereas in cells expressing control siRNAs receptor degradation still occurred. Similar results were obtained with the same concentration of 17-AAG. (Figure 6C).

We conclude that the ubiquitin ligase activity of CHIP is necessary to mediate Ron degradation induced by geldanamycins.

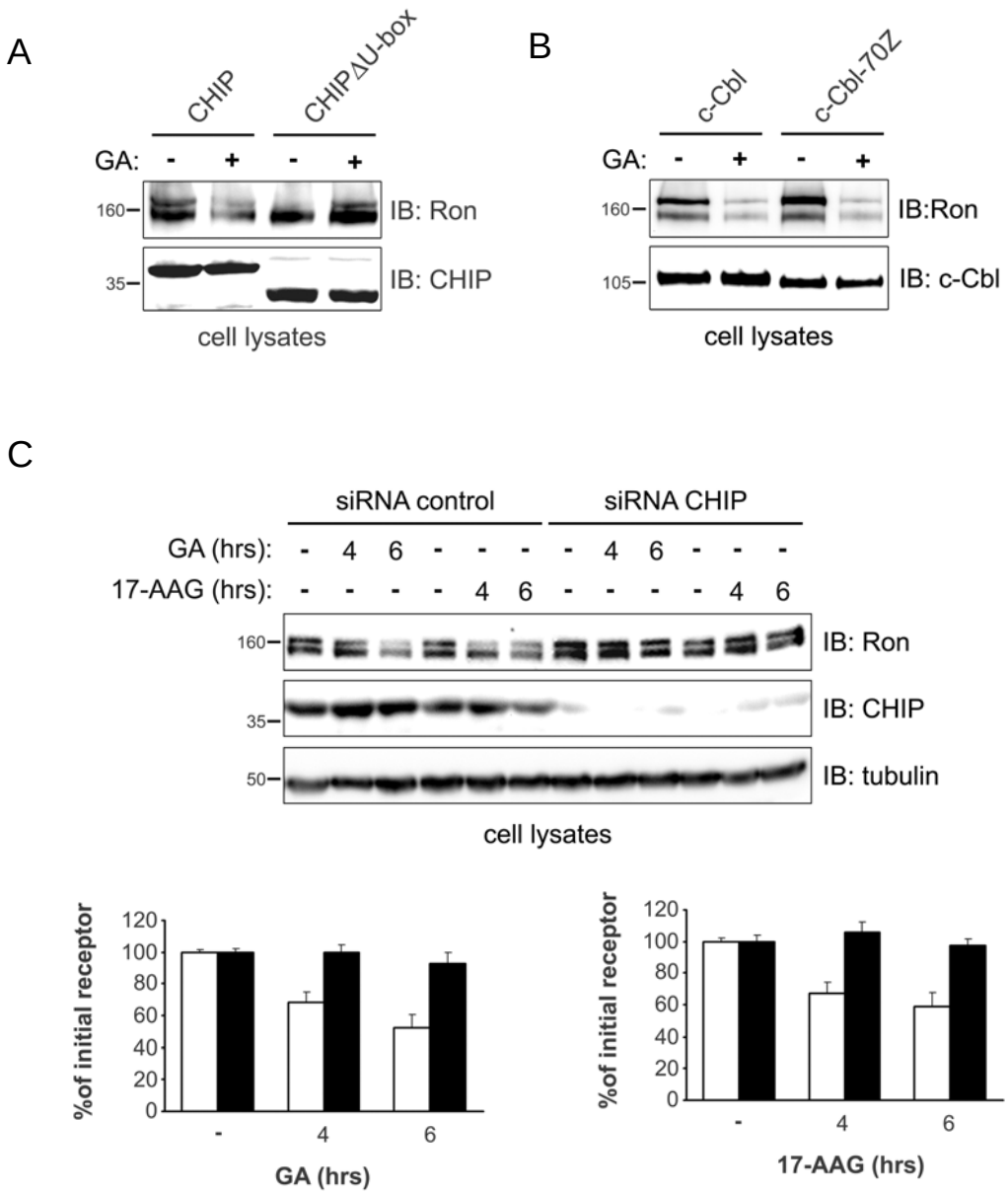

Figure 7. The ubiquitin ligase activity of CHIP is necessary to mediate Ron degradation induced by geldanamycins. **A**) COS-7 cells were transiently transfected with Ron and either CHIP or CHIP ΔU-box. 72 hours after transfection cells were treated with or without 1 μM GA for 6 hours and equal amounts of cell lysates were analyzed by immunoblotting with Ron and CHIP antibodies. **B**) COS-7 cells were transiently transfected with Ron and either c-Cbl or c-Cbl-70Z. Lysates from cells treated with or without 1 μM GA for 6 hours were analyzed by immunoblotting with Ron and c-Cbl antibodies. **C**) FG2 cells were transfected with siRNAs targeted to CHIP transcript or to an unrelated sequence. Cells were treated with or without 1 μM GA, or 1 μM 17-AAG. Equal quantities of lysates from cells harvested at the indicated times were analyzed by immunoblotting with Ron antibodies. Densitometry of Ron immunoblotting was performed and values, normalized to the relative α-tubulin control bands, were plotted as percentages of vehicle-treated cells. Unrelated siRNA: white columns; CHIP siRNA: black columns. Each data point represents the mean ±SE of three independent experiments.

Oncogenic M1254T substitution increases Ron sensitivity to geldanamycins.

As oncogenic Ron^{M1254T} is recruited into the CHIP-chaperone complex more efficiently than wild-type Ron, we tested the activity of GA and 17-AAG on the stability of the wild-type Ron and of its oncogenic counterpart. The treatment with both inhibitors revealed an accelerated degradation rate for the mutant receptor, as compared to wild-type Ron (Figure 8A). Interestingly, Ron^{M1254T} degradation was paralleled by an evident de-phosphorylation of Akt and Erk1/2 effectors. We next evaluated the relative sensitivity of wild-type and oncogenic Ron to these inhibitory drugs in a dose-response experiment. GA or 17-AAG concentration as low as 0.1 μM was efficient in degrading the mutant Ron^{M1254T}, while at least 1μM concentration was required to induce detectable degradation of the wild-type receptor (Figure 8B).

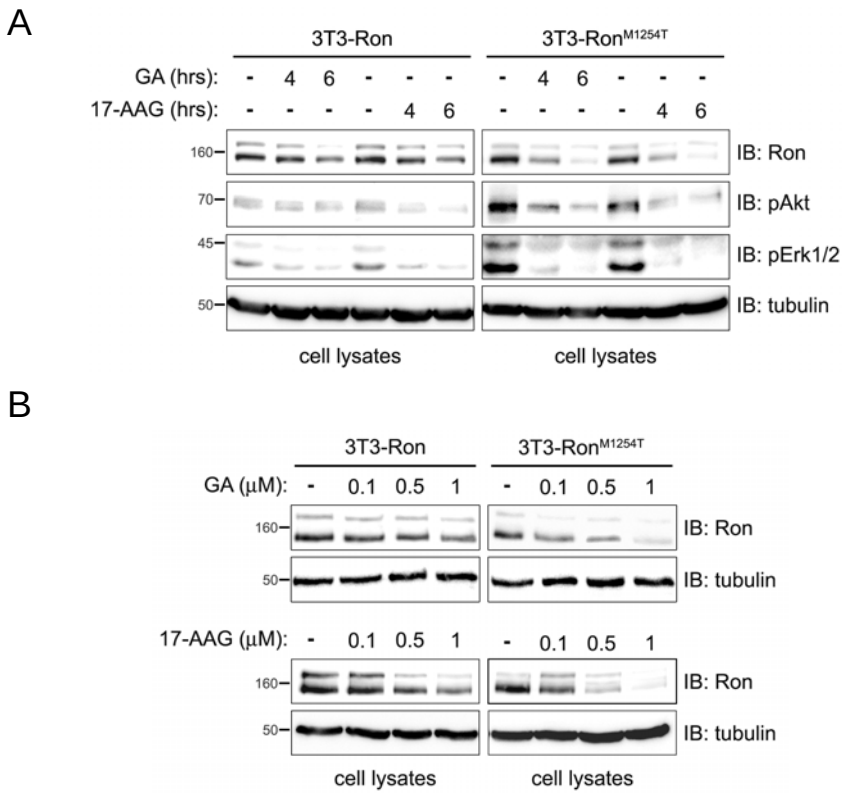

Figure 7. Ron^{M1254T} displays higher sensitivity to geldanamycins than wild-type receptor. **A**) 3T3-Ron and 3T3-Ron^{M1254T} cells were treated with or without 1 μM GA or 1 μM 17-AAG for the indicated times. Equal amounts of cell lysates were analyzed by immunoblotting with Ron, phospho-Akt and phospho-Erk1/2 antibodies. **B**) 3T3-Ron and 3T3-Ron^{M1254T} cells treated with increasing amounts of GA or of 17-AAG for 6 hours. Equal amounts of cell lysates were analyzed by immunoblotting with Ron antibodies.

The destabilizing effects of GA have been attributed to altered association of Hsp90 with its client proteins (Xu et al., 2001)). Therefore, we tested Ron interaction with Hsp90 upon GA or 17-AAG treatment of 3T3-Ron and 3T3-Ron^{M1254T} cells in a short term experiment. In both cell types the receptor co-precipitated with Hsp90, and geldanamycins caused an evident decrease in the amount of Hsp90 associated with Ron immunocomplexes. However, the dissociation of the Ron-Hsp90 complex occurs earlier, starting within 15 minutes of drugs exposure, as compared to the Ron-Hsp90 complex (Figure 9A). Consistently, by using the lowest effective concentration of GA and 17-AAG (0.1 μM) able to induce degradation of Ron^{M1254T} but not of wildtype Ron, we observed dissociation of Hsp90 from the mutant receptor only (Figure 9B). These results indicate that the oncogenic M1254T substitution in the Ron receptor is associated with increased sensitivity to geldanamycins, and with a more dynamic interaction with Hsp90.

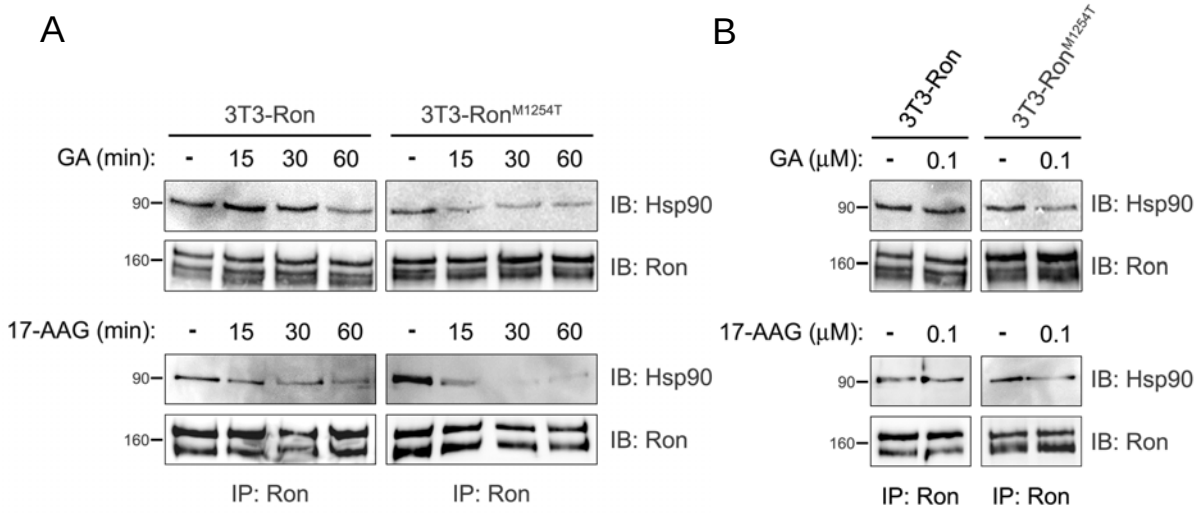

Figure 7. Hsp90 dissociation from Ron^{M1254T} is more rapid and occurs at lower geldanamycins concentrations compared to wild-type receptor. **A**) 3T3-Ron and 3T3-Ron^{M1254T} cells were treated with or without 1 μM GA, or 1 μM 17-AAG for the indicated times. Equal protein amounts of cell lysates were subjected to immunoprecipitation with Ron antibodies and associated Hsp90 was detected by immunoblotting with the appropriate antibodies. The immunoprecipitated receptor was detected by Ron immunoblotting. **B**) Proteins from cell lysates of 3T3-Ron and 3T3-Ron^{M1254T} treated with increasing amounts of GA, or of 17-AAG for 6 hours were subjected to Ron immunoprecipitation. Associated Hsp90 was detected by immunoblotting with the appropriate antibodies. The immunoprecipitated receptor was detected by Ron immunoblotting

Geldanamycins hamper growth, migration and transforming activity of Ron^{M1254T}.

The M1254T substitution confers to Ron *in vitro* transforming potential, including growth and migration in ligand-independent way (Santoro et al., 1998). Therefore, we tested if the GA-derivative suitable for clinical use 17-AAG, could hamper these biological effects in 3T3-Ron^{M1254T} cells. In a 72 hours proliferation assay, the higher proliferation rate of 3T3-Ron^{M1254T} cells compared to 3T3-Ron cells was considerably reduced in the presence of low concentrations (0.1 μM) of 17-AAG (Figure 10A). As expected, the growth rates of non transformed 3T3 and 3T3-Ron cells were similar and, consistently, the reduction of growth rate observed in these cells upon 17-AAG was comparable.

Similarly, in a migration assay, performed in the presence of serum, the presence of 17-AAG hampered the haptotactic migration of both 3T3-Ron And 3T3-RonM1254T, but the inhibition was by far more evident in cells expressing the Ron oncogenic form (Figure 10B).

We have previously shown that Ron^{M1254T} has a strong transforming activity when expressed in NIH-3T3 fibroblasts (Santoro et al., 1998). We performed a focus forming assay in presence or absence of low doses of 17-AAG. As expected, Ron^{M1254T} transfected cells displayed a high transforming activity, which was completely abolished by 17-AAG treatment (Figure 10C).

We conclude that the clinically relevant inhibitor 17-AAG is a potent negative regulator of cell proliferation, migration and transformation, typically induced by the Ron^{M1254T} oncogenic form.

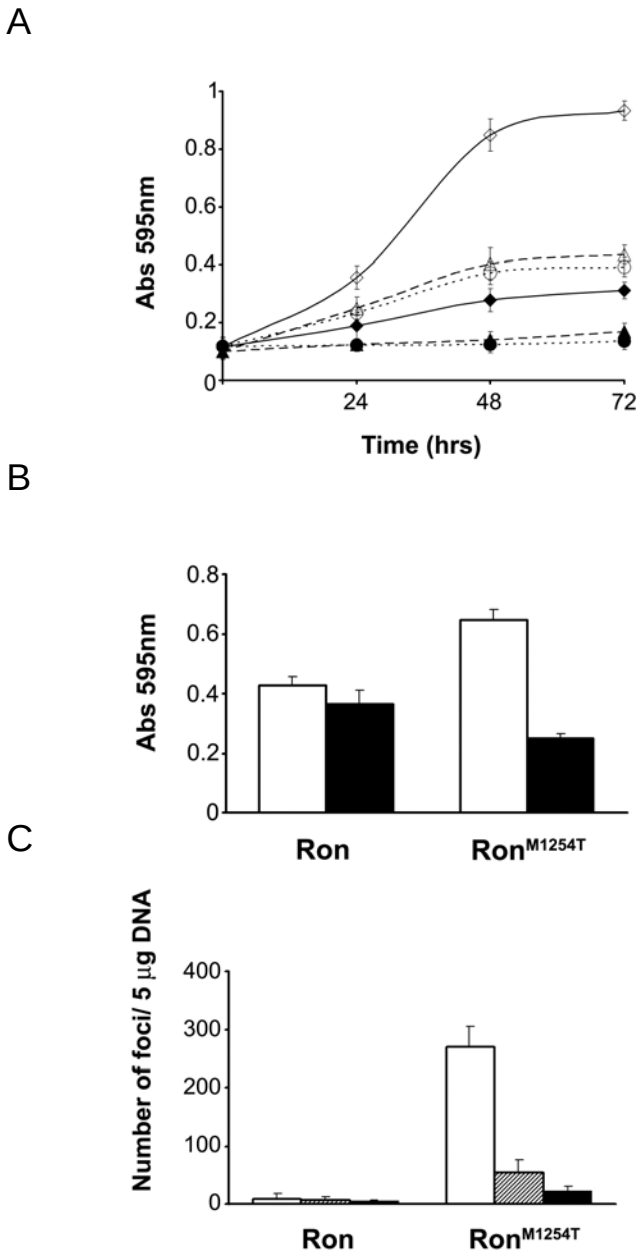

Figure 7. 17-AAG potently affects growth, migration and transformation of cells expressing oncogenic Ron^{M1254T}. **A**) NIH-3T3 fibroblasts (dotted curve), 3T3-Ron (dashed curve) and 3T3-Ron^{M1254T} (plain curve) cells were plated on 96-well plates and cultured in medium supplemented with 10% fetal bovine serum in presence of vehicle (white symbols) or 100 nM 17-AAG (black symbols). After 0, 24, 48 and 72 hours drug addition cells were fixed, stained in Crystal Violet and absorbance at 595 nm was measured. O.D. is expressed as mean A_{595}± SE of three independent experiments. **B**) 3T3-Ron and 3T3-Ron^{M1254T} cells were plated on the upper side of 8 μM pore size Transwell® chambers and allowed to migrate for 6 hours in presence of vehicle (white columns) or 100 nM 17-AAG (black columns) towards the lower chamber containing appropriate medium supplemented with 10% fetal calf serum and coated with fibronectin. Cells migrated towards the lower chamber were fixed and stained as described in A. O.D. is expressed as mean A_{595}± SE of three independent experiments. **C**) NIH-3T3 fibroblasts were transfected as described in Experimental Procedures with Ron or Ron^{M1254T} encoding plasmid. Two days after transfection, vehicle (white columns), 10 nM 17-AAG (hatched columns) or 50 nM 17-AAG (black columns) were added and renewed every 48 hours. Cell cultures were maintained at confluence and screened for *foci* formation 10 ± 18 days after transfection. Spontaneous formation of foci was negligible. All the experiments were performed in triplicate and mean ± SE number of foci is displayed.

Discussion

We have previously demonstrated a ligand induced c-Cbl dependent mechanism for the downregulation of Ron. In this work we identified a novel degradative pathway for Ron that involves the Hsp90/Hsc70 chaperones and the U-box E3 ubiquitin ligase CHIP.

It has been reported that Hsp90 and its cohort of co-chaperones play a regulatory role in conformational maturation and in maintenance of structural integrity of a variety of cellular proteins (Wegele et al., 2004). By remodelling Hsp90 heterocomplexes to favour substrate degradation, CHIP has been shown to regulate the balance between protein folding and degradation of chaperone substrates (Connell et al., 2001). In this context, it has been reported that CHIP regulates ErbB2 receptor stability, being recruited to the ErbB2-chaperone complex and promoting receptor ubiquitination and degradation. Moreover, CHIP over-expression has been shown to efficiently downregulate ErbB2 protein in vivo (Xu et al., 2002).

Our results demonstrate that Ron is present in a stable but dynamic complex with the Hsp90/Hsc70-based chaperone machinery, also containing the E3 ligase CHIP. Interestingly the oncogenic form of Ron harbouring the M1254T substitution in the kinase domain that shifts substrate specificity and overcomes the requirement fro the multifunctional docking site, displayed a stronger interaction with Hsp90 and CHIP. This is in accordance with similar observations on EGFR mutants (Shimamura et al., 2005), v-Src (Xu et al., 1999) and mutated p53 (Esser et al., 2005). As hypothesized for other kinases, the reason for the greater association of the mutated receptor to the chaperone complex, may reside more on a inherently less stable structure, rather than on its altered phosphorylation state. By an *in vitro* ubiquitination assay we demonstrated that CHIP may serve as an E3 ligase for Ron. More

intriguingly, we found that the oncogenic Ron^{M1254T}, which escapes from c-cbl mediated downregulation, is efficiently ubiquitinated *in vivo* by this E3 ligase.

Our findings revealed that CHIP is involved in the regulation of turnover of both wild-type Ron and Ron^{M1254T}. Indeed, silencing CHIP expression dramatically prolonged the half-life of the receptors. The requirement of the Hsp90 chaperone complex for Ron stability is confirmed by the destabilizing effects triggered by the small molecule inhibitors of Hsp90 geldanamycins. These inhibitory drugs, namely geldanamycin and 17-AAG, have been shown to force disruption of the Ron-Hsp90 interaction, followed by receptor ubiquitination and proteasomal degradation.

The effect of geldanamycins has been restricted to the ability of destabilizing newly synthesized EGFR or PDGFR molecules (Supino-Rosin et al., 2000). On the other hand, it has been also demonstrated that geldanamycin enhances the loss of mature cell surface ErbB2 protein (Zhou et al., 2003), suggesting a lack of univocal mean to target different receptors. Our results clearly indicate that mature Ron exposed at plasma membrane is a target of geldanamycin, as in the case of ErbB2, even if we cannot exclude that also the uncleaved precursor of the receptor may be affected. Moreover, by CHIP RNA interference and by use of a truncated CHIP mutant, we demonstrated that CHIP is necessary for Ron degradation, following Hsp90 inhibition by geldanamycins. A destabilizing effect of geldanamycins has been described for HGF-R/Met, homologous to Ron (Webb et al., 2000), but the E3 ligase regulating this process has not been identified yet.

Interestingly, geldanamycins-induced degradation of the oncogenic Ron^{M1254T} occured even more rapidly than for the non mutated receptor and at lower doses of the Hsp90 inhibitor. The effect of Hsp90 inhibition by geldanamycin has been thoroughly investigated and clarified in terms of altered association of the chaperone

to its client proteins, which are thus degraded. In the case of ErbB2, geldanamycin activity has been associated to a parallel increase of Hsp/Hsc70 association to the receptor (Xu et al., 2002). We did not observe any reciprocal exchange between Hsp90 and Hsc70 in the binding to either Ron or Ron^{M1254T}. On the other hand, we reported a significant difference in dissociation rate from Hsp90, between wild-type and oncogenic Ron receptors, upon geldanamycins treatment. We hypothesize that the ADP/ATP cycling rate of the Hsp90/RonM1254T complex is higher than that of Hsp90 complex containing Ron. This may explain the higher sensitivity of the oncogenic mutant to geldanamycins, highlighting Ron^{M1254T} as an ideal target for the antioncogenic activity of these drugs.

The very high sensitivity of the oncogenic receptor and of its signaling to geldanamycins resulted in robust inhibition of dysregulated biological activities. Indeed, the less toxic geldanamycin derivative 17-AAG markedly inhibited growth and migration rates induced by oncogenic Ron^{M1254T} signaling. Recently, it has been demonstrated that geldanamycins inhibit HGF/SF-dependent, uPA (urokinase-type plasminogen activator) mediated cell scattering and invasion, thus affecting typical tumor cell properties (Xie et al., 2005). Consistently, 17-AAG was able to abrogate the transforming ability of oncogenic Ron, suggesting that Ron-dependent tumorigenesis might be a sensitive target of geldanamycin or its derivatives.

In this work we have described a novel pathway that mediates Ron stability, amenable to pharmacologic manipulation. Indeed, ansamycin antibiotics have emerged as suitable pharmacological tools to force downregulation of Ron and its oncogenic variant.

MicroRNAs and post-transcriptional regulation of Ron expression

Summary

RTKs activity is tightly controlled within the cell, through the coordinated action of several negative protein regulators that function at multiple levels of the signaling cascade, and at different time-points after receptor engagement. In addition to protein attenuators, microRNAs (miRNAs) have emerged as an abundant class of small non-protein-coding RNAs molecules that play an important role in the negative regulation of gene expression, controlling the translational efficiency of target mRNAs (Esquela-Kerscher & Slack, 2006). miRNAs have been shown to regulate a wide range of developmental processes modulated by RTKs, like proliferation, survival and differentiation.

The biogenesis of miRNAs has only recently been elucidated. miRNAs are transcribed by RNA polymerase II, and the primary transcripts contain hairpin–loop domains that fold back into duplex-like structures (Lee et al., 2004). The hairpin–loop region is cleaved in the nucleus by the RNase III enzyme Drosha in complex with a double-strand RNA-binding protein termed DGCR8/Pasha (Gregory et al., 2004). The resulting hairpin–loop fragment is then exported by the RAN GTP-dependent transporter Exportin-5 from the nucleus to the cytoplasm where where it is cleaved by the RNase III enzyme Dicer. The fully mature miRNA accumulates as a single-stranded species comprising one arm of each miRNA hairpin precursor, and it incorporates into a ribonucleoprotein complex (RISC) that carries out its function of silencing gene expression (Du & Zamore, 2005).

Most miRNAs in animals are thought to exert their regulatory effects by binding to imperfect complementary sites within the 3' untranslated regions (UTRs) of target mRNAs (Bartel, 2004). The mechanism by which miRNAs silence gene expression is still poorly understood, but it appears to involve the inhibition of translational initiation (Pillai et al., 2005) or to affects the stability (Bagga et al., 2005; Jing et al., 2005) and compartmentalization of mRNAs (Liu et al., 2005). It is also conceivable that miRNAs act through multiple cooperative mechanisms to repress their targets.

There are estimated to beat least 300 miRNAs in the human genome (http://www.sanger.ac.uk/Software/Rfam/mirna/index.shtml), comprising 1-4% of all expressed human genes, which makes miRNAs one of the largest classes of gene regulator. A major question about miRNAs concerns the extent of their regulation of animal genomes. Computational methods estimated that approximately 20 to 30% of all human genes are targets of miRNA regulation, and there is an average of 200 targets per miRNA.

Mutations that abrogate miRNAs function or lead to their dysregulation are associated with a variety of diseases, including cancer.

The findings that RON gene is normally transcribed at low levels in cells from epithelial origin, while the protein is abnormally expressed, activated and generated in epithelial cancers prompted us to investigate whether aberrant expression of miRNA genes may contribute to Ron dysregulation. In this preliminary work we sought to determine if any of all known miRNAs gene could participate in the post-transcriptional regulation of Ron expression.

Experimental procedures

Reagents and antibodies

The following pre-miR miRNA Precursor molecules, hsa-miR-198, hsa-miR-214 and miRNA Negative Control #1 were obtained from Ambion. The miRNA inhibitors miRCURY LNA Knockdown probes LNA-198, LNA-124 and the scramble-5'FITC control probe were from Exiqon. Polyclonal anti-Ron antibody (c-20) and anti-Met antibody were purchased from Santa Cruz Biotechnology, Inc. Monoclonal anti-α-tubulin (B-5-1-2) was from Sigma. Horeseradish peroxidase-conjugated anti-mouse and anti-rabbit were purchased from Cell Signaling Technology, Inc.

Cell culture and transfection

Immortalized epithelial cell line HaCaT and human gastric carcinoma cell line GTL16 were maintained in Dulbecco's modified Eagle's medium (Sigma), supplemented with 10% fetal bovine serum (Invitrogen) in a 5% CO_2-humidified atmosphere. Transfection of all cell lines with small RNAs were performed with Siport Neo*Fx* reagent (Ambion) according to the manufacturer's instructions.

Immunoblotting and immunofluorescence

Immunoblotting was performed as described previously (see Experimental Procedures, Section I). For immunofluorescence analysis, cells were plated onto glass coverslips and 48 hours after transfection were fixed with Fixing was performed with 4% paraformaldheyde solution for 5 minutes at room temperature. Coverslips were mounted with Pro-Long Gold Antifade reagent (Invitrogen). Images were acquired with a Leica LS2 laser scanning confocal microscope.

Quantitative Real-time PCR

Total RNA was extracted from cells 48 hours after transfection by using miRNeasy mini kit (Qiagen). 50 ng of RNA from each sample was retrotranscribed with specific primers for mature hsa-miR198, hsa-miR214 or U6 RNA with microRNA reverse transcription kit (Applied Biosystems). The TaqMan microRNA Assays (Applied Biosystems) were used to quantify the expression of mature hsa-miR198 and hsa-miR214 according to manufacturer's protocol on a Stratagene Mx3000 Real-Time PCR thermocycler. Relative miRNA expression was calculated with the –ddCt method, with U6 RNA as the housekeeping gene.

To quantify Ron transcript levels, total RNA was extracted as described above. 1µg RNA was retrotranscribed with RevertAid H-minus first strand synthesis kit (Fermentas) by using random nonamers. The analysis of Ron gene expression was performed using commercial gene expression assay from Applied Biosystems (Assay-on-Demand: MSPR1). The housekeeping gene beta-actin (Assay-on-Demand: ACTB, Applied Biosystems) was used to normalize for variations in cDNA. Relative miRNA expression was calculated with the –ddCt method.

Results

RON transcript is a potential target of hsa-miR-198 and hsa-miR-214 miRNAs

Several computational target prediction programs have been developed so far to allow for identification of mammalian miRNA targets. Most bioinformatics algorithms use a "miRNA seed" that encompasses the first 2-8 bases of the mature miRNA sequence to search for complementarity to sequences in the 3'UTR of all

expressed genes. They identify potential miRNA binding sites according to specific base-pairing rules and implement cross-species conservation requirements (Sethupathy et al., 2006).

An on-line search of the miRBase Target database (http://www.sanger.ac.uk) demonstrated that 15 putative miRNA target sites were harbored in the 3'UTR of RON transcript and identified 17 human miRNA genes as potential regulator of Ron expression (Figure 1A). We then cross-checked the results with other target prediction programs, including DIANA-microT (http://www.diana.pcbi.upenn.edu), PicTar (http://www.pictar.bio.nyu.edu) and MiRanda (http://www.microrna.org). For this study we have focused on 2 of 17 miRNA genes identified with miRBase, that were predicted also by these programs, namely hsa-miR-198 and hsa-miRNA-214. Notably, these predicted miRNAs displayed the highest score when analyzed by the RNAhybrid algorithm (http://www.bbserv.techfak.uni-bielefeld.de), which calculates the thermodynamic stability of the duplex formed when miRNA are hybridized to 3'UTR of target transcript (Figure 1B). Interestingly, two different target sites for hsa-miR-198 have been found on 3'UTR of RON transcript and one of them overlaps with has-miR-214 target site.

A

Rfam ID	Score	Energy	Base P	Poisson P	Org P	Start	End	Alignment
hsa-miR-18a*	19.5466	-24.81	2.362340e-03	5.391240e-04	3.793950e-04	158	179	UCUUCCUC-GUGAAUCCCGUCA |||: ||| || | |||||||| AGAGTGAGCCAGTGAGGGCAGT
hsa-miR-214	18.2893	-22.53	6.023470e-03	6.005370e-03	6.258440e-03	191	211	gacggacagaCACGGACGACA ||||||||||| tatttatggaGTGCCTGCTGT
hsa-miR-659	17.8514	-19.7	3.738430e-03	6.484020e-04	5.134210e-04	255	276	accccugggaGGGACUUGGUUc ||:|||||||| caacactgacCCTTGAACCAAt
hsa-miR-324-3p	17.7377	-29.27	9.162650e-03	9.120800e-03	9.979070e-03	62	83	gGUCGUCGUGGACCCCGUCACC :: ||| | ||||||||| aTGCCAGGCCAGAGGGCAGTGG
hsa-miR-198	16.9977	-23.05	1.794750e-02	3.197750e-04	3.197750e-04	44	61	GGAUAGAGGGGAGACCUGG || | || |||||||:|| CCAAGCT-GCCTCTGGGCC
hsa-miR-565	16.9418	-21.68	2.056610e-02	2.035610e-02	2.035610e-02	150	171	uuugucUGUAGCGCUCGGUCG ||| |:|||||||: cactccACAGAGTGAGCCAGT
hsa-miR-198	16.6508	-21.67	2.550500e-02	3.197750e-04	3.197750e-04	212	230	ggauaGAGGGGAGACCUG || :|:|||||:| ggaccCTGTCTTCTGGGC
hsa-miR-136	16.6303	-16.21	2.945910e-02	2.902940e-02	3.046240e-02	112	136	AGGUAGUAGU--UUUGUUUACCUCa |:|| : || |:::||||||:| TTCAGAGGCAATAGGTAAATGGGGc
hsa-miR-149	16.3733	-18.16	4.760780e-02	4.649230e-02	5.319120e-03	149	170	ccUCACUUCUGUGCCUCGGUC | | | | | ||||||| tcACTCCACAGAGTGAGCCAG
hsa-miR-587	16.346	-14.98	3.173860e-02	3.124020e-02	3.124020e-02	181	202	cACUGAGUA-GUGGAUACCUU || ||| :|::||||||: cTGCAACATGTATTTATGGAG
hsa-miR-627	16.2596	-17.42	2.071500e-02	2.050190e-02	2.050190e-02	220	242	AGGAGAAAAGAAUC-UCUGAGUg ||:||| | || :|||||| TCTTCTGGGCACAGTGGACTCAg
hsa-miR-137	16.1459	-10.08	2.892280e-02	2.850850e-02	3.000110e-02	103	124	gaugcgcauAAGAAUUCGUUAU ||| |:|||||| cctttaactTTCAGAGGCAATA
hsa-miR-492	15.8384	-18.19	3.657490e-02	3.591410e-02	8.278450e-04	126	148	uucUUAGAACAGGGCGUCCAGGa ||| | || :|||||| gtaAATGGGGCCCATTAGGTCCc
hsa-miR-633	15.8384	-5.81	4.037510e-02	3.957090e-02	4.030960e-02	275	297	aaauaacaccaucuaUGAUAAU ||||||| ataaaggaacaaatgACTATTA
hsa-miR-124a	15.8047	-16.19	4.363490e-02	4.476540e-02	7.809580e-03	15	36	ACC-GUAAGUGGCGCACGGAAUU ||| | | | : || ||||||:| TGGACCTGCTTAGC-TGCCTTGA
hsa-miR-24	15.8047	-20.06	6.290750e-02	3.989270e-03	4.340360e-03	20	40	GACAAGGACGACUUGACUCGGU ||| | : |||| :|||||:| CTGCT-TAGCTGCCTTGAGCTA
hsa-miR-650	15.7745	-17.44	9.227800e-02	4.004540e-03	4.405110e-03	37	57	caggacucucgCGACGGAGG ||||||||: gctaaccccaaGCTGCCTCT
hsa-miR-639	15.7253	-18.34	3.426150e-02	3.368120e-02	3.744260e-02	230	249	UGUCGCGAGCGUUGGCGUCGCUa ||||:| | || ||||:|| ACAGTGGACTCA---GCAGTGAc

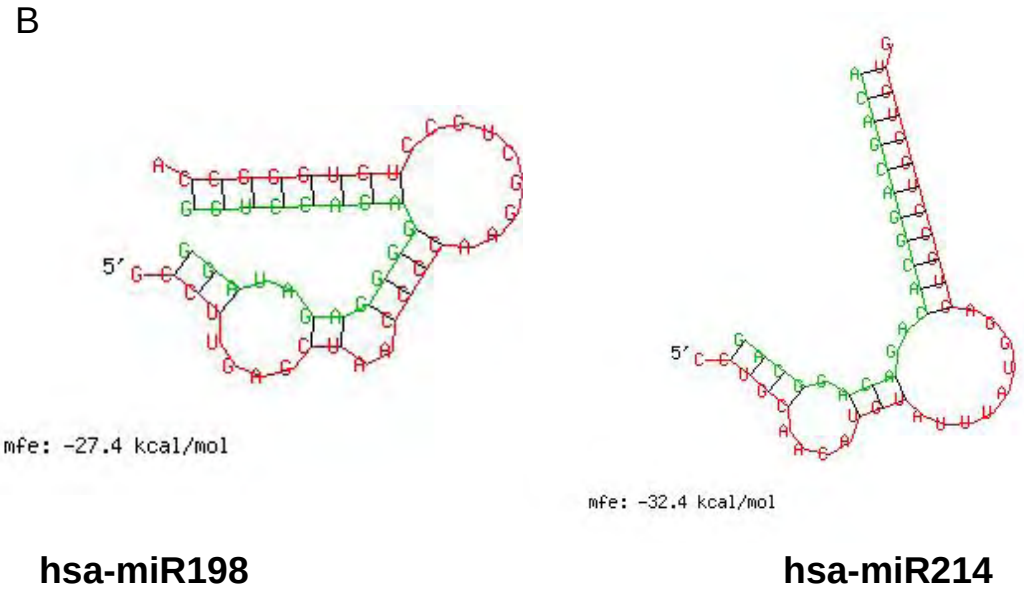

Figure 1. *In silico* analysis of miRNAs potentially targeting Ron transcript. (**A**) 3'UTR of RON transcript was used as input to search potential human miRNA targets in the microRNA registry at the Sanger Institute by the miRBase algorithm. (**B**) Thermodynamic stability analysis of miRNA by RNAHybrid program. The potential structure and energy of hsa-miR-198- and hsa-miR–214- RON 3'UTR hybrid are shown.

Human miRNAs hsa-miR-198 and hsa-miR-214 regulate Ron expression

We next moved to experimental validation of the computational data obtained. Chemically synthesized double stranded RNAs, that mimic endogenous mature miRNA sequences, can be used in biological assays to asses the function of specific miRNAs. We verified if overexpression of hsa-miR-198 or hsa-miR-214 could alter receptor levels in cells expressing endogenous Ron, namely the immortalized epithelial cell line HaCaT and the human gastric carcinoma cell line GTL16.

Quantitative real-time RT-PCR analysis demonstrated that hsa-miR-198 or hsa-miR-214 levels were increased to a very high extent upon transfection of HaCaT cells with the respective precursor molecule. As expected, expression of the two miRNAs did

not change following transfection with a control pre-miR precursor targeting no known human sequence (Figure 2A).

In the same cells, receptor levels were analyzed by immunoblotting. Ron expression was nearly unaffected in cells transfected with control RNA at all conditions tested (Figure 2B). In contrast, we observed a significant decrease in both precursor and mature Ron in cells were overexpression of hsa-miR198 was achieved with a higher efficiency. Similar results, albeit to a lower extent, were obtained upon transfection of hsa-miR-214. Noteworthy, overexpression of both miRNAs did not alter expression of the related family member HGF-R/Met.

A

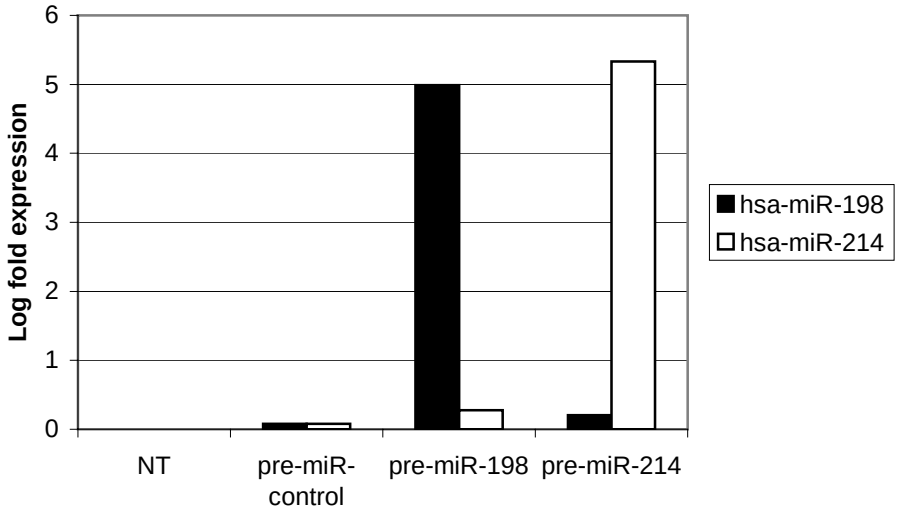

B

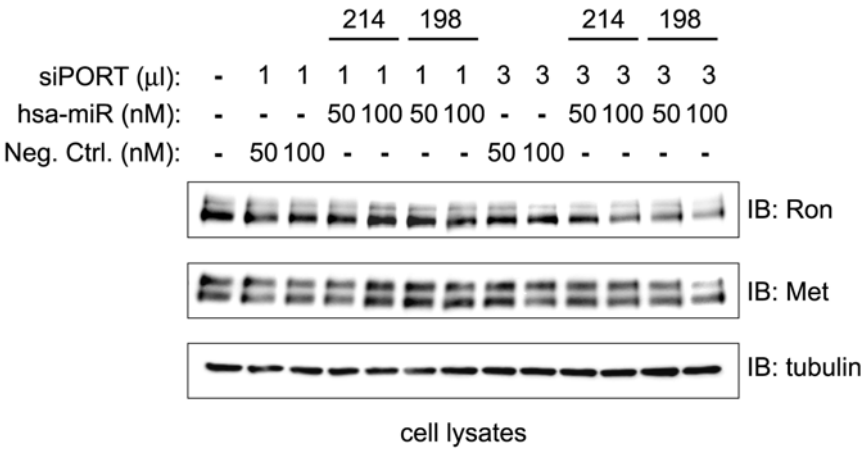

Figure 2. Overexpression of human miRNA hsa-miR-198 or -214 reduces Ron protein levels. (**A**) HaCaT cells were transfected with 30 nM hsa-pre-miRNA negative control, hsa-miRNA-198 or hsa-miRNA-214 with 3 μl di siPORT-NeoFX Transfection Reagent. Twenty-four hours post transfection, miRNA levels were analyzed by quantitative PCR with TaqMan probes. (**B**)) HaCaT cells were transfected as described in A with the indicated amount of pre-miRNA precursors and transfection reagent. Forty-eight hours post transfection cell were lysed and immunoblotting analysis was performed with the indicated antibody.

To confirm the data obtained by gain-of-function experiments, we used antisense oligonucleotides (LNA probes), that form stable complexes with target miRNA thus inhibiting mature miRNAs. Since it has been reported that LNA probes block miRNA function without affecting their expression level, quantitative PCR could not be used to verify the cellular uptake of the transfected oligonucleotides. Fluorescence analysis was therefore used to monitor the transfection efficiency, exploiting a FITC-conjugated LNA probe. Twenty-four hours after transfection, accumulation of the LNA probes in the cytoplasm was clearly visible in nearly 60% of cells (Figure 3A). We next addressed whether functional inhibition of hsa-miR-198 or hsa-miR-214 could affect Ron expression. Interestingly, depletion of either hsa-miR-198 or hsa-miR-214 resulted in a consistent increase in Ron protein level, when compared to that observed in cell transfected with the same amount of control LNA probe (Figure 3B). In line with the observation obtained by gain-of-function experiments, Met expression was not significantly altered by transfection of any LNA-probe.

A

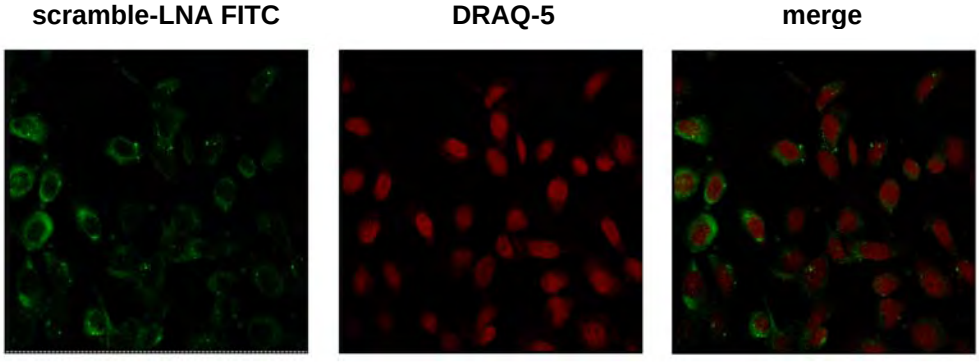

B

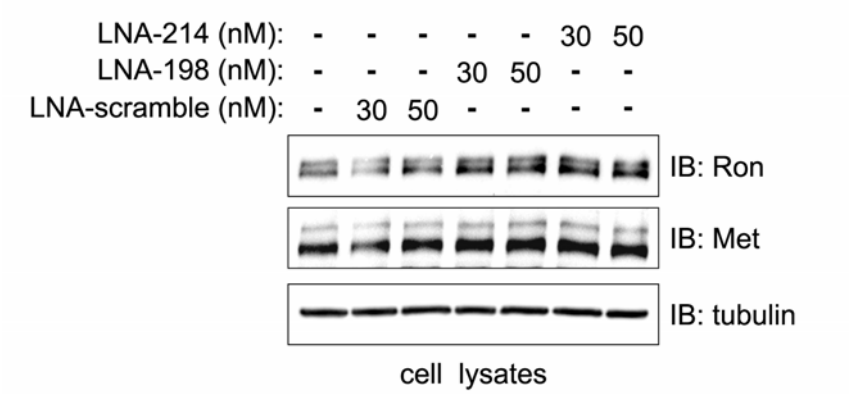

Figure 3. Depletion of has-miR-198 or -214 upregulate Ron expression. (**A**) HaCaT cells were transfected with miRCURY LNA Knockdown FITC-conjugated control probe (scramble-LNA FITC). Twenty-four hors post transfection cells were analyzed by confocal microscopy analysis. Red signals represent DRAQ-5 nuclear staining. (**B**) HaCaT cells were transfected as described in A with the indicated amount of miRCURY LNA Knockdown probe. Forty-eight hours post transfection cell were lysed and immunoblotting analysis was performed with the indicated antibodies.

Most miRNAs are reported to exert their activity through the inhibition of translational initiation. Consistent with translational control, miRNAs that use this mechanism reduce the protein levels of their target genes, but the mRNA levels of these genes are barely affected. We thus verified if this mechanisms could account for regulation of Ron expression by hsa-miR-198 and hsa-miR-214. We performed Real Time PCR to quantify RON transcript level in cells transfected with pre-miR precursor or LNA probes. No significant modulation of RON mRNA was observed in any condition tested (Figure 4). This demonstrates that hsa-miR-198 and hsa-miR-214 play their inhibitory role on Ron expression without affecting the corresponding mRNA stability.

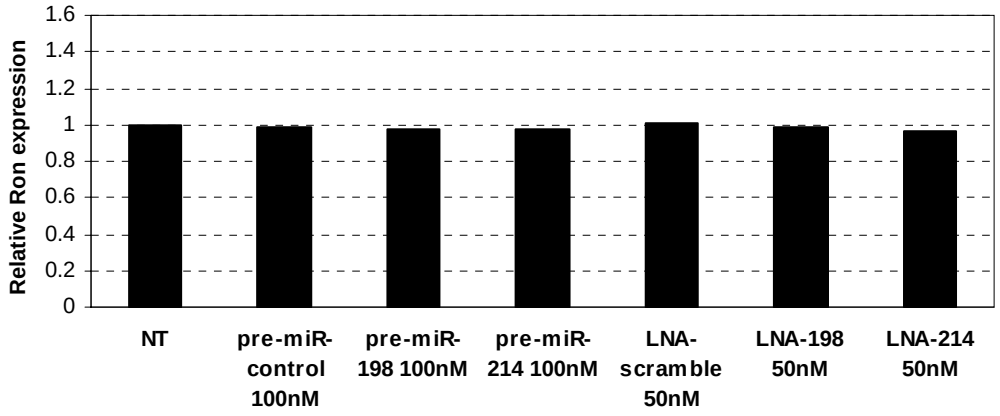

Figure 4. RON transcript levels are not affected by hsa-miR-198 or -214. HaCaT cells were transfected with the indicated oligonucleotides. Twenty-four hours post transfection, RON mRNA levels were analyzed by quantitative PCR with TaqMan probes.

These results, together with similar observations obtained in GTL16 cells (data not shown), prompt for a role of hsa-miR-198 or hsa-miR-214 in the post-tanscriptional regulation of Ron expression.

Discussion

MiRNAs have been recognized as a very large gene family conserved among many species. The precise biological effects of miRNAs are yet to be elucidated in detail, partly because each miRNA is believed to negative regulate the expression of hundreds of target genes. The deletion or dysregulation of these small RNAs is thus

likely to contribute to pathological conditions. Among human diseases, it has been shown that miRNAs are aberrantly expressed in cancer, suggesting that may play a role as a novel class of oncogenes or tumor suppressor genes. The findings that miRNAs have a role in cancer are supported by the fact that about 50% of miRNA genes are localized in cancer-associated genomic regions or fragile sites (Calin et al., 2004). For instance miRNAs miR-155, miR-21 and cluster miR-17-92, whose expression is enhanced in tumors, might be considered as oncogenes and their targets as tumor suppressors. Under-expressed miRNAs, such as *let-7*, probably act as tumor-suppressor genes and their modulation more likely reflects the loss of differentiation typical for tumor cells.

The biological role of only a small fraction of identified miRNAs have been elucidated to date and future studies will help to elucidate whether miRNAs could represent a new and alternative mechanism to downregulate RTK signaling during normal development and disease. This has been proved for EGFR, whose signaling pathway has been reported to be modulated by miR-7 in *Drosophila* (Li et al., 2005). Moreover it has been demonstrated that hsa-miR-221 and hsa-miR-222 affect c-Kit expression and, as a consequence, the angiogenic properties of its ligand Stem Cell Factor (Poliseno et al., 2006).

Our preliminary results indicate that translational repression by miRNA provides yet another mechanism by which Ron expression can be modulated. Indeed at least two miRNAs encoded by the human genome, namely hsa-miR-198 and hsa-miR-214, participate in post-transcriptional regulation of Ron expression. The observation the expression of closely related Met receptor is not affected by this two miRNAs suggests that this novel regulatory mechanism is not shared by other members of the HGF-R/Met subfamily. This is likely a consequence of the low homology in the

3'UTR of the Ron and Met transcripts, as well as in the murine Ron counterpart Stk. However further studies are required to better elucidate the mechanism underlying Ron regulation by hsa-miR-198 and hsa-miR-214. In particular it will be of interest to experimentally support miRNA-Ron 3'UTR interaction with *in vitro* reporter silencing assays. This will be useful to rule out the possibility that hsa-miR-198 and hsa-miR-214 could indirectly exert their activity on Ron by affecting the expression of proteins involved in negative regulation of the receptor.

No biological functions have been assigned to hsa-miR-198 and hsa-miR-214 to date, nor other mRNA targets were previously identified. A single report indicate that zebrafish miR-214 modulate the expression of genes regulated by Hedgehog signaling (Flynt et al., 2007). Therefore future studies will help to characterize the activity of these two miRNAs in modulating the biological response triggered by activated Ron. Moreover it will be of extreme interest to evaluate whether aberrant expression of miRNA genes may contribute to Ron dysregulation in human cancer. Analysis of the variations in miRNA levels between normal primary cells and epithelial cancer cell lines from breast, colon and prostate in which aberrant Ron expression has been described will provide evidence for the role of specific miRNAs in targeting Ron expression, which downregulation may contribute to altered Ron signaling in human tumors.

REFERENCES

Aguilar, R.C. & Wendland, B. (2005). Endocytosis of membrane receptors: two pathways are better than one. *Proc Natl Acad Sci U S A*, **102,** 2679-80.

Anastasi, S., Fiorentino, L., Fiorini, M., Fraioli, R., Sala, G., Castellani, L., Alema, S., Alimandi, M. & Segatto, O. (2003). Feedback inhibition by RALT controls signal output by the ErbB network. *Oncogene*, **22,** 4221-34.

Andl, C.D. & Rustgi, A.K. (2005). No one-way street: cross-talk between e-cadherin and receptor tyrosine kinase (RTK) signaling: a mechanism to regulate RTK activity. *Cancer Biol Ther*, **4,** 28-31.

Andrews, D.W., Resnicoff, M., Flanders, A.E., Kenyon, L., Curtis, M., Merli, G., Baserga, R., Iliakis, G. & Aiken, R.D. (2001). Results of a pilot study involving the use of an antisense oligodeoxynucleotide directed against the insulin-like growth factor type I receptor in malignant astrocytomas. *J Clin Oncol*, **19,** 2189-200.

Angeloni, D., Danilkovitch-Miagkova, A., Miagkov, A., Leonard, E.J. & Lerman, M.I. (2004). The soluble sema domain of the RON receptor inhibits macrophage-stimulating protein-induced receptor activation. *J Biol Chem*, **279,** 3726-32.

Arevalo, J.C., Waite, J., Rajagopal, R., Beyna, M., Chen, Z.Y., Lee, F.S. & Chao, M.V. (2006). Cell survival through Trk neurotrophin receptors is differentially regulated by ubiquitination. *Neuron*, **50,** 549-59.

Bagga, S., Bracht, J., Hunter, S., Massirer, K., Holtz, J., Eachus, R. & Pasquinelli, A.E. (2005). Regulation by let-7 and lin-4 miRNAs results in target mRNA degradation. *Cell*, **122,** 553-63.

Ballinger, C.A., Connell, P., Wu, Y., Hu, Z., Thompson, L.J., Yin, L.Y. & Patterson, C. (1999). Identification of CHIP, a novel tetratricopeptide repeat-containing protein that interacts with heat shock proteins and negatively regulates chaperone functions. *Mol Cell Biol*, **19,** 4535-45.

Banu, N., Price, D.J., London, R., Deng, B., Mark, M., Godowski, P.J. & Avraham, H. (1996). Modulation of megakaryocytopoiesis by human macrophage-stimulating protein, the ligand for the RON receptor. *J Immunol*, **156,** 2933-40.

Bao, J., Gur, G. & Yarden, Y. (2003). Src promotes destruction of c-Cbl: implications for oncogenic synergy between Src and growth factor receptors. *Proc Natl Acad Sci U S A*, **100,** 2438-43.

Bardella, C., Costa, B., Maggiora, P., Patane, S., Olivero, M., Ranzani, G.N., De Bortoli, M., Comoglio, P.M. & Di Renzo, M.F. (2004). Truncated RON tyrosine kinase drives tumor cell progression and abrogates cell-cell adhesion through E-cadherin transcriptional repression. *Cancer Res*, **64,** 5154-61.

Bardelli, A., Longati, P., Williams, T.A., Benvenuti, S. & Comoglio, P.M. (1999). A peptide representing the carboxyl-terminal tail of the met receptor inhibits kinase activity and invasive growth. *J Biol Chem*, **274,** 29274-81.

Barriere, H., Nemes, C., Lechardeur, D., Khan-Mohammad, M., Fruh, K. & Lukacs, G.L. (2006). Molecular basis of oligoubiquitin-dependent internalization of membrane proteins in Mammalian cells. *Traffic*, **7,** 282-97.

Bartel, D.P. (2004). MicroRNAs: genomics, biogenesis, mechanism, and function. *Cell*, **116,** 281-97.

Bezerra, J.A., Carrick, T.L., Degen, J.L., Witte, D. & Degen, S.J. (1998). Biological effects of targeted inactivation of hepatocyte growth factor-like protein in mice. *J Clin Invest*, **101,** 1175-83.

Bickel, P.E. (2002). Lipid rafts and insulin signaling. *Am J Physiol Endocrinol Metab*, **282,** E1-E10.

Bienko, M., Green, C.M., Crosetto, N., Rudolf, F., Zapart, G., Coull, B., Kannouche, P., Wider, G., Peter, M., Lehmann, A.R., Hofmann, K. & Dikic, I. (2005). Ubiquitin-binding domains in Y-family polymerases regulate translesion synthesis. *Science*, **310,** 1821-4.

Blume-Jensen, P. & Hunter, T. (2001). Oncogenic kinase signalling. *Nature*, **411,** 355-65.

Bongarzone, I., Monzini, N., Borrello, M.G., Carcano, C., Ferraresi, G., Arighi, E., Mondellini, P., Della Porta, G. & Pierotti, M.A. (1993). Molecular characterization of a thyroid tumor-specific transforming sequence formed by the fusion of ret tyrosine kinase and the regulatory subunit RI alpha of cyclic AMP-dependent protein kinase A. *Mol Cell Biol*, **13,** 358-66.

Calin, G.A., Sevignani, C., Dumitru, C.D., Hyslop, T., Noch, E., Yendamuri, S., Shimizu, M., Rattan, S., Bullrich, F., Negrini, M. & Croce, C.M. (2004). Human microRNA genes are frequently located at fragile sites and genomic regions involved in cancers. *Proc Natl Acad Sci U S A*, **101,** 2999-3004.

Carafoli, F., Chirgadze, D.Y., Blundell, T.L. & Gherardi, E. (2005). Crystal structure of the beta-chain of human hepatocyte growth factor-like/macrophage stimulating protein. *Febs J*, **272,** 5799-807.

Carter, S., Urbe, S. & Clague, M.J. (2004). The met receptor degradation pathway: requirement for Lys48-linked polyubiquitin independent of proteasome activity. *J Biol Chem*, **279,** 52835-9.

Chen, Y.Q., Zhou, Y.Q., Angeloni, D., Kurtz, A.L., Qiang, X.Z. & Wang, M.H. (2000). Overexpression and activation of the RON receptor tyrosine kinase in a panel of human colorectal carcinoma cell lines. *Exp Cell Res*, **261,** 229-38.

Chen, Y.Q., Zhou, Y.Q., Fu, L.H., Wang, D. & Wang, M.H. (2002). Multiple pulmonary adenomas in the lung of transgenic mice overexpressing the RON receptor tyrosine kinase. Recepteur d'origine nantais. *Carcinogenesis*, **23,** 1811-9.

Cheng, H.L., Liu, H.S., Lin, Y.J., Chen, H.H., Hsu, P.Y., Chang, T.Y., Ho, C.L., Tzai, T.S. & Chow, N.H. (2005). Co-expression of RON and MET is a prognostic indicator for patients with transitional-cell carcinoma of the bladder. *Br J Cancer*, **92,** 1906-14.

Citri, A., Alroy, I., Lavi, S., Rubin, C., Xu, W., Grammatikakis, N., Patterson, C., Neckers, L., Fry, D.W. & Yarden, Y. (2002). Drug-induced ubiquitylation and degradation of ErbB receptor tyrosine kinases: implications for cancer therapy. *Embo J*, **21,** 2407-17.

Cohen, A.W., Combs, T.P., Scherer, P.E. & Lisanti, M.P. (2003). Role of caveolin and caveolae in insulin signaling and diabetes. *Am J Physiol Endocrinol Metab*, **285,** E1151-60.

Collesi, C., Santoro, M.M., Gaudino, G. & Comoglio, P.M. (1996). A splicing variant of the RON transcript induces constitutive tyrosine kinase activity and an invasive phenotype. *Mol Cell Biol*, **16,** 5518-26.

Comoglio, P.M., Tamagnone, L. & Boccaccio, C. (1999). Plasminogen-related growth factor and semaphorin receptors: a gene superfamily controlling invasive growth. *Exp Cell Res*, **253,** 88-99.

Connell, P., Ballinger, C.A., Jiang, J., Wu, Y., Thompson, L.J., Hohfeld, J. & Patterson, C. (2001). The co-chaperone CHIP regulates protein triage decisions mediated by heat-shock proteins. *Nat Cell Biol*, **3,** 93-6.

Correll, P.H., Iwama, A., Tondat, S., Mayrhofer, G., Suda, T. & Bernstein, A. (1997). Deregulated inflammatory response in mice lacking the STK/RON receptor tyrosine kinase. *Genes Funct*, **1,** 69-83.

Danilkovitch-Miagkova, A. & Leonard, E.J. (2001). Anti-apoptotic action of macrophage stimulating protein (MSP). *Apoptosis*, **6,** 183-90.

de Melker, A.A., van der Horst, G., Calafat, J., Jansen, H. & Borst, J. (2001). c-Cbl ubiquitinates the EGF receptor at the plasma membrane and remains receptor associated throughout the endocytic route. *J Cell Sci*, **114,** 2167-78.

De Sepulveda, P., Okkenhaug, K., Rose, J.L., Hawley, R.G., Dubreuil, P. & Rottapel, R. (1999). Socs1 binds to multiple signalling proteins and suppresses steel factor-dependent proliferation. *Embo J*, **18,** 904-15.

Dessy, C., Kelly, R.A., Balligand, J.L. & Feron, O. (2000). Dynamin mediates caveolar sequestration of muscarinic cholinergic receptors and alteration in NO signaling. *Embo J*, **19,** 4272-80.

Di Fiore, P.P. & Gill, G.N. (1999). Endocytosis and mitogenic signaling. *Curr Opin Cell Biol*, **11,** 483-8.

Di Fiore, P.P., Polo, S. & Hofmann, K. (2003). When ubiquitin meets ubiquitin receptors: a signalling connection. *Nat Rev Mol Cell Biol*, **4,** 491-7.

Di Guglielmo, G.M., Le Roy, C., Goodfellow, A.F. & Wrana, J.L. (2003). Distinct endocytic pathways regulate TGF-beta receptor signalling and turnover. *Nat Cell Biol*, **5,** 410-21.

Di Renzo, M.F., Poulsom, R., Olivero, M., Comoglio, P.M. & Lemoine, N.R. (1995). Expression of the Met/hepatocyte growth factor receptor in human pancreatic cancer. *Cancer Res*, **55,** 1129-38.

Dikic, I. & Giordano, S. (2003). Negative receptor signalling. *Curr Opin Cell Biol*, **15,** 128-35.

Doherty, J.K., Bond, C., Jardim, A., Adelman, J.P. & Clinton, G.M. (1999). The HER-2/neu receptor tyrosine kinase gene encodes a secreted autoinhibitor. *Proc Natl Acad Sci U S A*, **96,** 10869-74.

Du, T. & Zamore, P.D. (2005). microPrimer: the biogenesis and function of microRNA. *Development*, **132,** 4645-52.

Eddins, M.J., Carlile, C.M., Gomez, K.M., Pickart, C.M. & Wolberger, C. (2006). Mms2-Ubc13 covalently bound to ubiquitin reveals the structural basis of linkage-specific polyubiquitin chain formation. *Nat Struct Mol Biol*, **13,** 915-20.

Emanuelli, B., Peraldi, P., Filloux, C., Sawka-Verhelle, D., Hilton, D. & Van Obberghen, E. (2000). SOCS-3 is an insulin-induced negative regulator of insulin signaling. *J Biol Chem*, **275,** 15985-91.

Esquela-Kerscher, A. & Slack, F.J. (2006). Oncomirs - microRNAs with a role in cancer. *Nat Rev Cancer*, **6,** 259-69.

Esser, C., Scheffner, M. & Hohfeld, J. (2005). The chaperone-associated ubiquitin ligase CHIP is able to target p53 for proteasomal degradation. *J Biol Chem*, **280,** 27443-8.

Fiorentino, L., Pertica, C., Fiorini, M., Talora, C., Crescenzi, M., Castellani, L., Alema, S., Benedetti, P. & Segatto, O. (2000). Inhibition of ErbB-2 mitogenic and transforming activity by RALT, a mitogen-induced signal transducer which binds to the ErbB-2 kinase domain. *Mol Cell Biol*, **20,** 7735-50.

Fiorini, M., Alimandi, M., Fiorentino, L., Sala, G. & Segatto, O. (2001). Negative regulation of receptor tyrosine kinase signals. *FEBS Lett*, **490,** 132-41.

Follenzi, A., Bakovic, S., Gual, P., Stella, M.C., Longati, P. & Comoglio, P.M. (2000). Cross-talk between the proto-oncogenes Met and Ron. *Oncogene*, **19,** 3041-9.

Fong, C.W., Leong, H.F., Wong, E.S., Lim, J., Yusoff, P. & Guy, G.R. (2003). Tyrosine phosphorylation of Sprouty2 enhances its interaction with c-Cbl and is crucial for its function. *J Biol Chem*, **278,** 33456-64.

Furthauer, M., Lin, W., Ang, S.L., Thisse, B. & Thisse, C. (2002). Sef is a feedback-induced antagonist of Ras/MAPK-mediated FGF signalling. *Nat Cell Biol*, **4,** 170-4.

Gaudino, G., Follenzi, A., Naldini, L., Collesi, C., Santoro, M., Gallo, K.A., Godowski, P.J. & Comoglio, P.M. (1994). RON is a heterodimeric tyrosine kinase receptor activated by the HGF homologue MSP. *Embo J*, **13,** 3524-32.

Geetha, T., Jiang, J. & Wooten, M.W. (2005). Lysine 63 polyubiquitination of the nerve growth factor receptor TrkA directs internalization and signaling. *Mol Cell*, **20,** 301-12.

Gensler, M., Buschbeck, M. & Ullrich, A. (2004). Negative regulation of HER2 signaling by the PEST-type protein-tyrosine phosphatase BDP1. *J Biol Chem*, **279,** 12110-6.

Germano, S., Barberis, D., Santoro, M.M., Penengo, L., Citri, A., Yarden, Y. & Gaudino, G. (2006). Geldanamycins trigger a novel Ron degradative pathway hampering oncogenic signaling. *J Biol Chem*.

Ghiglione, C., Carraway, K.L., 3rd, Amundadottir, L.T., Boswell, R.E., Perrimon, N. & Duffy, J.B. (1999). The transmembrane molecule kekkon 1 acts in a feedback loop to negatively regulate the activity of the Drosophila EGF receptor during oogenesis. *Cell*, **96,** 847-56.

Golembo, M., Schweitzer, R., Freeman, M. & Shilo, B.Z. (1996). Argos transcription is induced by the Drosophila EGF receptor pathway to form an inhibitory feedback loop. *Development*, **122,** 223-30.

Gregory, R.I., Yan, K.P., Amuthan, G., Chendrimada, T., Doratotaj, B., Cooch, N. & Shiekhattar, R. (2004). The Microprocessor complex mediates the genesis of microRNAs. *Nature*, **432,** 235-40.

Gross, I., Bassit, B., Benezra, M. & Licht, J.D. (2001). Mammalian sprouty proteins inhibit cell growth and differentiation by preventing ras activation. *J Biol Chem*, **276,** 46460-8.

Gur, G., Rubin, C., Katz, M., Amit, I., Citri, A., Nilsson, J., Amariglio, N., Henriksson, R., Rechavi, G., Hedman, H., Wides, R. & Yarden, Y. (2004). LRIG1 restricts growth factor signaling by enhancing receptor ubiquitylation and degradation. *Embo J*, **23,** 3270-81.

Hackel, P.O., Gishizky, M. & Ullrich, A. (2001). Mig-6 is a negative regulator of the epidermal growth factor receptor signal. *Biol Chem*, **382,** 1649-62.

Haglund, K., Di Fiore, P.P. & Dikic, I. (2003). Distinct monoubiquitin signals in receptor endocytosis. *Trends Biochem Sci*, **28,** 598-603.

Haglund, K., Sigismund, S., Polo, S., Szymkiewicz, I., Di Fiore, P.P. & Dikic, I. (2003). Multiple monoubiquitination of RTKs is sufficient for their endocytosis and degradation. *Nat Cell Biol*, **5,** 461-6.

Haj, F.G., Markova, B., Klaman, L.D., Bohmer, F.D. & Neel, B.G. (2003). Regulation of receptor tyrosine kinase signaling by protein tyrosine phosphatase-1B. *J Biol Chem*, **278,** 739-44.

Haj, F.G., Verveer, P.J., Squire, A., Neel, B.G. & Bastiaens, P.I. (2002). Imaging sites of receptor dephosphorylation by PTP1B on the surface of the endoplasmic reticulum. *Science*, **295,** 1708-11.

Hall, A.B., Jura, N., DaSilva, J., Jang, Y.J., Gong, D. & Bar-Sagi, D. (2003). hSpry2 is targeted to the ubiquitin-dependent proteasome pathway by c-Cbl. *Curr Biol*, **13,** 308-14.

Hanafusa, H., Torii, S., Yasunaga, T. & Nishida, E. (2002). Sprouty1 and Sprouty2 provide a control mechanism for the Ras/MAPK signalling pathway. *Nat Cell Biol*, **4,** 850-8.

Henley, J.R., Krueger, E.W., Oswald, B.J. & McNiven, M.A. (1998). Dynamin-mediated internalization of caveolae. *J Cell Biol*, **141,** 85-99.

Herbst, R., Munemitsu, S. & Ullrich, A. (1995). Oncogenic activation of v-kit involves deletion of a putative tyrosine-substrate interaction site. *Oncogene*, **10,** 369-79.

Hicke, L. & Dunn, R. (2003). Regulation of membrane protein transport by ubiquitin and ubiquitin-binding proteins. *Annu Rev Cell Dev Biol*, **19,** 141-72.

Hicke, L., Schubert, H.L. & Hill, C.P. (2005). Ubiquitin-binding domains. *Nat Rev Mol Cell Biol*, **6,** 610-21.

Hofstra, R.M., Landsvater, R.M., Ceccherini, I., Stulp, R.P., Stelwagen, T., Luo, Y., Pasini, B., Hoppener, J.W., van Amstel, H.K., Romeo, G. & et al. (1994). A mutation in the RET proto-oncogene associated with multiple endocrine neoplasia type 2B and sporadic medullary thyroid carcinoma. *Nature*, **367,** 375-6.

Huang, F., Kirkpatrick, D., Jiang, X., Gygi, S. & Sorkin, A. (2006). Differential regulation of EGF receptor internalization and degradation by multiubiquitination within the kinase domain. *Mol Cell*, **21,** 737-48.

Hunter, T., Lindberg, R.A., Middlemas, D.S., Tracy, S. & van der Geer, P. (1992). Receptor protein tyrosine kinases and phosphatases. *Cold Spring Harb Symp Quant Biol*, **57,** 25-41.

Impagnatiello, M.A., Weitzer, S., Gannon, G., Compagni, A., Cotten, M. & Christofori, G. (2001). Mammalian sprouty-1 and -2 are membrane-anchored phosphoprotein inhibitors of growth factor signaling in endothelial cells. *J Cell Biol*, **152,** 1087-98.

Iwama, A., Okano, K., Sudo, T., Matsuda, Y. & Suda, T. (1994). Molecular cloning of a novel receptor tyrosine kinase gene, STK, derived from enriched hematopoietic stem cells. *Blood*, **83,** 3160-9.

Jiang, J., Ballinger, C.A., Wu, Y., Dai, Q., Cyr, D.M., Hohfeld, J. & Patterson, C. (2001). CHIP is a U-box-dependent E3 ubiquitin ligase: identification of Hsc70 as a target for ubiquitylation. *J Biol Chem*, **276,** 42938-44.

Jiang, X., Huang, F., Marusyk, A. & Sorkin, A. (2003). Grb2 regulates internalization of EGF receptors through clathrin-coated pits. *Mol Biol Cell*, **14,** 858-70.

Jin, M.H., Sawamoto, K., Ito, M. & Okano, H. (2000). The interaction between the Drosophila secreted protein argos and the epidermal growth factor receptor inhibits dimerization of the receptor and binding of secreted spitz to the receptor. *Mol Cell Biol*, **20,** 2098-107.

Jing, Q., Huang, S., Guth, S., Zarubin, T., Motoyama, A., Chen, J., Di Padova, F., Lin, S.C., Gram, H. & Han, J. (2005). Involvement of microRNA in AU-rich element-mediated mRNA instability. *Cell*, **120,** 623-34.

Joazeiro, C.A. & Weissman, A.M. (2000). RING finger proteins: mediators of ubiquitin ligase activity. *Cell*, **102,** 549-52.

Kamal, A., Boehm, M.F. & Burrows, F.J. (2004). Therapeutic and diagnostic implications of Hsp90 activation. *Trends Mol Med*, **10,** 283-90.

Katz, M., Shtiegman, K., Tal-Or, P., Yakir, L., Mosesson, Y., Harari, D., Machluf, Y., Asao, H., Jovin, T., Sugamura, K. & Yarden, Y. (2002). Ligand-independent degradation of epidermal growth factor receptor involves receptor ubiquitylation and Hgs, an adaptor whose ubiquitin-interacting motif targets ubiquitylation by Nedd4. *Traffic*, **3,** 740-51.

Katzmann, D.J., Odorizzi, G. & Emr, S.D. (2002). Receptor downregulation and multivesicular-body sorting. *Nat Rev Mol Cell Biol*, **3,** 893-905.

Kazazic, M., Roepstorff, K., Johannessen, L.E., Pedersen, N.M., van Deurs, B., Stang, E. & Madshus, I.H. (2006). EGF-induced activation of the EGF receptor does not trigger mobilization of caveolae. *Traffic*, **7,** 1518-27.

Kirkpatrick, D.S., Hathaway, N.A., Hanna, J., Elsasser, S., Rush, J., Finley, D., King, R.W. & Gygi, S.P. (2006). Quantitative analysis of in vitro ubiquitinated cyclin B1 reveals complex chain topology. *Nat Cell Biol*, **8,** 700-10.

Klapper, L.N., Kirschbaum, M.H., Sela, M. & Yarden, Y. (2000). Biochemical and clinical implications of the ErbB/HER signaling network of growth factor receptors. *Adv Cancer Res*, **77,** 25-79.

Klein, D.E., Nappi, V.M., Reeves, G.T., Shvartsman, S.Y. & Lemmon, M.A. (2004). Argos inhibits epidermal growth factor receptor signalling by ligand sequestration. *Nature*, **430,** 1040-4.

Kovalenko, D., Yang, X., Nadeau, R.J., Harkins, L.K. & Friesel, R. (2003). Sef inhibits fibroblast growth factor signaling by inhibiting FGFR1 tyrosine phosphorylation and subsequent ERK activation. *J Biol Chem*, **278,** 14087-91.

Kovalenko, M., Denner, K., Sandstrom, J., Persson, C., Gross, S., Jandt, E., Vilella, R., Bohmer, F. & Ostman, A. (2000). Site-selective dephosphorylation of the platelet-derived growth factor beta-receptor by the receptor-like protein-tyrosine phosphatase DEP-1. *J Biol Chem*, **275,** 16219-26.

Kramer, S., Okabe, M., Hacohen, N., Krasnow, M.A. & Hiromi, Y. (1999). Sprouty: a common antagonist of FGF and EGF signaling pathways in Drosophila. *Development*, **126,** 2515-25.

Kurihara, N., Iwama, A., Tatsumi, J., Ikeda, K. & Suda, T. (1996). Macrophage-stimulating protein activates STK receptor tyrosine kinase on osteoclasts and facilitates bone resorption by osteoclast-like cells. *Blood*, **87,** 3704-10.

Laederich, M.B., Funes-Duran, M., Yen, L., Ingalla, E., Wu, X., Carraway, K.L., 3rd & Sweeney, C. (2004). The leucine-rich repeat protein LRIG1 is a negative regulator of ErbB family receptor tyrosine kinases. *J Biol Chem*, **279,** 47050-6.

Lamaze, C., Dujeancourt, A., Baba, T., Lo, C.G., Benmerah, A. & Dautry-Varsat, A. (2001). Interleukin 2 receptors and detergent-resistant membrane domains define a clathrin-independent endocytic pathway. *Mol Cell*, **7,** 661-71.

Lamorte, L. & Park, M. (2001). The receptor tyrosine kinases: role in cancer progression. *Surg Oncol Clin N Am*, **10,** 271-88, viii.

Le, P.U., Guay, G., Altschuler, Y. & Nabi, I.R. (2002). Caveolin-1 is a negative regulator of caveolae-mediated endocytosis to the endoplasmic reticulum. *J Biol Chem*, **277,** 3371-9.

Lee, E.S., Kalantari, P., Tsutsui Section, S., Klatt, A., Holden, J., Correll, P.H., Power Section, C. & Henderson, A.J. (2004). RON receptor tyrosine kinase, a negative regulator of inflammation, inhibits HIV-1 transcription in monocytes/macrophages and is decreased in brain tissue from patients with AIDS. *J Immunol*, **173,** 6864-72.

Lee, P.S., Wang, Y., Dominguez, M.G., Yeung, Y.G., Murphy, M.A., Bowtell, D.D. & Stanley, E.R. (1999). The Cbl protooncoprotein stimulates CSF-1 receptor multiubiquitination and endocytosis, and attenuates macrophage proliferation. *Embo J*, **18,** 3616-28.

Lee, Y., Kim, M., Han, J., Yeom, K.H., Lee, S., Baek, S.H. & Kim, V.N. (2004). MicroRNA genes are transcribed by RNA polymerase II. *Embo J*, **23,** 4051-60.

Levitzki, A. (1999). Protein tyrosine kinase inhibitors as novel therapeutic agents. *Pharmacol Ther*, **82,** 231-9.

Li, B.Q., Wang, M.H., Kung, H.F., Ronsin, C., Breathnach, R., Leonard, E.J. & Kamata, T. (1995). Macrophage-stimulating protein activates Ras by both activation and translocation of SOS nucleotide exchange factor. *Biochem Biophys Res Commun*, **216,** 110-8.

Libermann, T.A., Nusbaum, H.R., Razon, N., Kris, R., Lax, I., Soreq, H., Whittle, N., Waterfield, M.D., Ullrich, A. & Schlessinger, J. (1985). Amplification, enhanced expression and possible rearrangement of EGF receptor gene in primary human brain tumours of glial origin. *Nature*, **313,** 144-7.

Liu, J., Valencia-Sanchez, M.A., Hannon, G.J. & Parker, R. (2005). MicroRNA-dependent localization of targeted mRNAs to mammalian P-bodies. *Nat Cell Biol*, **7,** 719-23.

Liu, P., Rudick, M. & Anderson, R.G. (2002). Multiple functions of caveolin-1. *J Biol Chem*, **277,** 41295-8.

Longley, B.J., Tyrrell, L., Lu, S.Z., Ma, Y.S., Langley, K., Ding, T.G., Duffy, T., Jacobs, P., Tang, L.H. & Modlin, I. (1996). Somatic c-KIT activating mutation in urticaria pigmentosa and aggressive mastocytosis: establishment of clonality in a human mast cell neoplasm. *Nat Genet*, **12,** 312-4.

Lu, Y., Lin, Y.Z., LaPushin, R., Cuevas, B., Fang, X., Yu, S.X., Davies, M.A., Khan, H., Furui, T., Mao, M., Zinner, R., Hung, M.C., Steck, P., Siminovitch, K. & Mills, G.B. (1999). The PTEN/MMAC1/TEP tumor suppressor gene decreases cell growth and induces apoptosis and anoikis in breast cancer cells. *Oncogene*, **18,** 7034-45.

Lynch, T.J., Bell, D.W., Sordella, R., Gurubhagavatula, S., Okimoto, R.A., Brannigan, B.W., Harris, P.L., Haserlat, S.M., Supko, J.G., Haluska, F.G., Louis, D.N., Christiani, D.C., Settleman, J. & Haber, D.A. (2004). Activating mutations in the epidermal growth factor receptor underlying responsiveness of non-small-cell lung cancer to gefitinib. *N Engl J Med*, **350,** 2129-39.

Madshus, I.H. (2006). Ubiquitin binding in endocytosis--how tight should it be and where does it happen? *Traffic*, **7,** 258-61.

Maggiora, P., Marchio, S., Stella, M.C., Giai, M., Belfiore, A., De Bortoli, M., Di Renzo, M.F., Costantino, A., Sismondi, P. & Comoglio, P.M. (1998). Overexpression of the RON gene in human breast carcinoma. *Oncogene*, **16,** 2927-33.

Marmor, M.D. & Yarden, Y. (2004). Role of protein ubiquitylation in regulating endocytosis of receptor tyrosine kinases. *Oncogene*, **23,** 2057-70.

Marsh, H.N., Dubreuil, C.I., Quevedo, C., Lee, A., Majdan, M., Walsh, G.S., Hausdorff, S., Said, F.A., Zoueva, O., Kozlowski, M., Siminovitch, K., Neel, B.G., Miller, F.D. & Kaplan, D.R. (2003). SHP-1 negatively regulates neuronal survival by functioning as a TrkA phosphatase. *J Cell Biol*, **163,** 999-1010.

Martin-Zanca, D., Hughes, S.H. & Barbacid, M. (1986). A human oncogene formed by the fusion of truncated tropomyosin and protein tyrosine kinase sequences. *Nature*, **319,** 743-8.

Mason, J.M., Morrison, D.J., Bassit, B., Dimri, M., Band, H., Licht, J.D. & Gross, I. (2004). Tyrosine phosphorylation of Sprouty proteins regulates their ability to inhibit growth factor signaling: a dual feedback loop. *Mol Biol Cell*, **15,** 2176-88.

Meacham, G.C., Patterson, C., Zhang, W., Younger, J.M. & Cyr, D.M. (2001). The Hsc70 co-chaperone CHIP targets immature CFTR for proteasomal degradation. *Nat Cell Biol*, **3,** 100-5.

Mimnaugh, E.G., Chavany, C. & Neckers, L. (1996). Polyubiquitination and proteasomal degradation of the p185c-erbB-2 receptor protein-tyrosine kinase induced by geldanamycin. *J Biol Chem*, **271,** 22796-801.

Minshall, R.D., Tiruppathi, C., Vogel, S.M., Niles, W.D., Gilchrist, A., Hamm, H.E. & Malik, A.B. (2000). Endothelial cell-surface gp60 activates vesicle formation and trafficking via G(i)-coupled Src kinase signaling pathway. *J Cell Biol*, **150,** 1057-70.

Moos, T. & Morgan, E.H. (2000). Transferrin and transferrin receptor function in brain barrier systems. *Cell Mol Neurobiol*, **20,** 77-95.

Mosesson, Y., Shtiegman, K., Katz, M., Zwang, Y., Vereb, G., Szollosi, J. & Yarden, Y. (2003). Endocytosis of receptor tyrosine kinases is driven by monoubiquitylation, not polyubiquitylation. *J Biol Chem*, **278,** 21323-6.

Mukhopadhyay, D. & Riezman, H. (2007). Proteasome-independent functions of ubiquitin in endocytosis and signaling. *Science*, **315,** 201-5.

Mundy, D.I., Machleidt, T., Ying, Y.S., Anderson, R.G. & Bloom, G.S. (2002). Dual control of caveolar membrane traffic by microtubules and the actin cytoskeleton. *J Cell Sci*, **115,** 4327-39.

Musacchio, M. & Perrimon, N. (1996). The Drosophila kekkon genes: novel members of both the leucine-rich repeat and immunoglobulin superfamilies expressed in the CNS. *Dev Biol*, **178,** 63-76.

Muthuswamy, S.K., Gilman, M. & Brugge, J.S. (1999). Controlled dimerization of ErbB receptors provides evidence for differential signaling by homo- and heterodimers. *Mol Cell Biol*, **19,** 6845-57.

Oh, P., McIntosh, D.P. & Schnitzer, J.E. (1998). Dynamin at the neck of caveolae mediates their budding to form transport vesicles by GTP-driven fission from the plasma membrane of endothelium. *J Cell Biol*, **141,** 101-14.

Oh, P. & Schnitzer, J.E. (2001). Segregation of heterotrimeric G proteins in cell surface microdomains. G(q) binds caveolin to concentrate in caveolae, whereas G(i) and G(s) target lipid rafts by default. *Mol Biol Cell*, **12,** 685-98.

Ostman, A., Hellberg, C. & Bohmer, F.D. (2006). Protein-tyrosine phosphatases and cancer. *Nat Rev Cancer*, **6,** 307-20.

Ouyang, X., Gulliford, T., Zhang, H., Smith, G., Huang, G. & Epstein, R.J. (2001). Association of ErbB2 Ser1113 phosphorylation with epidermal growth factor receptor co-expression and poor prognosis in human breast cancer. *Mol Cell Biochem*, **218,** 47-54.

Overholser, J.P., Prewett, M.C., Hooper, A.T., Waksal, H.W. & Hicklin, D.J. (2000). Epidermal growth factor receptor blockade by antibody IMC-C225 inhibits growth of a human pancreatic carcinoma xenograft in nude mice. *Cancer*, **89,** 74-82.

Pante, G., Thompson, J., Lamballe, F., Iwata, T., Ferby, I., Barr, F.A., Davies, A.M., Maina, F. & Klein, R. (2005). Mitogen-inducible gene 6 is an endogenous inhibitor of HGF/Met-induced cell migration and neurite growth. *J Cell Biol*, **171,** 337-48.

Parton, R.G. (1996). Caveolae and caveolins. *Curr Opin Cell Biol*, **8,** 542-8.

Peace, B.E., Hill, K.J., Degen, S.J. & Waltz, S.E. (2003). Cross-talk between the receptor tyrosine kinases Ron and epidermal growth factor receptor. *Exp Cell Res*, **289,** 317-25.

Peace, B.E., Toney-Earley, K., Collins, M.H. & Waltz, S.E. (2005). Ron receptor signaling augments mammary tumor formation and metastasis in a murine model of breast cancer. *Cancer Res*, **65,** 1285-93.

Pelkmans, L. & Helenius, A. (2002). Endocytosis via caveolae. *Traffic*, **3,** 311-20.

Pelkmans, L., Puntener, D. & Helenius, A. (2002). Local actin polymerization and dynamin recruitment in SV40-induced internalization of caveolae. *Science*, **296,** 535-9.

Penengo, L., Rubin, C., Yarden, Y. & Gaudino, G. (2003). c-Cbl is a critical modulator of the Ron tyrosine kinase receptor. *Oncogene*, **22,** 3669-79.

Persson, C., Savenhed, C., Bourdeau, A., Tremblay, M.L., Markova, B., Bohmer, F.D., Haj, F.G., Neel, B.G., Elson, A., Heldin, C.H., Ronnstrand, L., Ostman, A. & Hellberg, C. (2004). Site-selective regulation of platelet-derived growth factor beta receptor tyrosine phosphorylation by T-cell protein tyrosine phosphatase. *Mol Cell Biol*, **24,** 2190-201.

Peschard, P., Fournier, T.M., Lamorte, L., Naujokas, M.A., Band, H., Langdon, W.Y. & Park, M. (2001). Mutation of the c-Cbl TKB domain binding site on the Met receptor tyrosine kinase converts it into a transforming protein. *Mol Cell*, **8,** 995-1004.

Peschard, P. & Park, M. (2003). Escape from Cbl-mediated downregulation: a recurrent theme for oncogenic deregulation of receptor tyrosine kinases. *Cancer Cell*, **3,** 519-23.

Petrelli, A., Circosta, P., Granziero, L., Mazzone, M., Pisacane, A., Fenoglio, S., Comoglio, P.M. & Giordano, S. (2006). Ab-induced ectodomain shedding mediates hepatocyte growth factor receptor down-regulation and hampers biological activity. *Proc Natl Acad Sci U S A*, **103,** 5090-5.

Petrelli, A., Gilestro, G.F., Lanzardo, S., Comoglio, P.M., Migone, N. & Giordano, S. (2002). The endophilin-CIN85-Cbl complex mediates ligand-dependent downregulation of c-Met. *Nature*, **416,** 187-90.

Pickart, C.M. (2001). Ubiquitin enters the new millennium. *Mol Cell*, **8,** 499-504.

Pickart, C.M. & Fushman, D. (2004). Polyubiquitin chains: polymeric protein signals. *Curr Opin Chem Biol*, **8,** 610-6.

Pierchala, B.A., Milbrandt, J. & Johnson, E.M., Jr. (2006). Glial cell line-derived neurotrophic factor-dependent recruitment of Ret into lipid rafts enhances signaling by partitioning Ret from proteasome-dependent degradation. *J Neurosci*, **26,** 2777-87.

Pillai, R.S., Bhattacharyya, S.N., Artus, C.G., Zoller, T., Cougot, N., Basyuk, E., Bertrand, E. & Filipowicz, W. (2005). Inhibition of translational initiation by Let-7 MicroRNA in human cells. *Science*, **309,** 1573-6.

Polo, S., Pece, S. & Di Fiore, P.P. (2004). Endocytosis and cancer. *Curr Opin Cell Biol*, **16,** 156-61.

Ponzetto, C., Bardelli, A., Zhen, Z., Maina, F., dalla Zonca, P., Giordano, S., Graziani, A., Panayotou, G. & Comoglio, P.M. (1994). A multifunctional docking site mediates signaling and transformation by the hepatocyte growth factor/scatter factor receptor family. *Cell*, **77,** 261-71.

Pratt, W.B. & Toft, D.O. (2003). Regulation of signaling protein function and trafficking by the hsp90/hsp70-based chaperone machinery. *Exp Biol Med (Maywood)*, **228,** 111-33.

Raiborg, C., Bache, K.G., Gillooly, D.J., Madshus, I.H., Stang, E. & Stenmark, H. (2002). Hrs sorts ubiquitinated proteins into clathrin-coated microdomains of early endosomes. *Nat Cell Biol*, **4,** 394-8.

Razani, B., Zhang, X.L., Bitzer, M., von Gersdorff, G., Bottinger, E.P. & Lisanti, M.P. (2001). Caveolin-1 regulates transforming growth factor (TGF)-beta/SMAD signaling through an interaction with the TGF-beta type I receptor. *J Biol Chem*, **276,** 6727-38.

Reich, A., Sapir, A. & Shilo, B. (1999). Sprouty is a general inhibitor of receptor tyrosine kinase signaling. *Development*, **126,** 4139-47.

Ridge, S.A., Worwood, M., Oscier, D., Jacobs, A. & Padua, R.A. (1990). FMS mutations in myelodysplastic, leukemic, and normal subjects. *Proc Natl Acad Sci U S A*, **87,** 1377-80.

Rodrigues, G.A. & Park, M. (1993). Dimerization mediated through a leucine zipper activates the oncogenic potential of the met receptor tyrosine kinase. *Mol Cell Biol*, **13,** 6711-22.

Ronsin, C., Muscatelli, F., Mattei, M.G. & Breathnach, R. (1993). A novel putative receptor protein tyrosine kinase of the met family. *Oncogene*, **8,** 1195-202.

Rubin, C., Litvak, V., Medvedovsky, H., Zwang, Y., Lev, S. & Yarden, Y. (2003). Sprouty fine-tunes EGF signaling through interlinked positive and negative feedback loops. *Curr Biol*, **13,** 297-307.

Santoro, M.M., Gaudino, G. & Marchisio, P.C. (2003). The MSP receptor regulates alpha6beta4 and alpha3beta1 integrins via 14-3-3 proteins in keratinocyte migration. *Dev Cell*, **5,** 257-71.

Santoro, M.M., Penengo, L., Minetto, M., Orecchia, S., Cilli, M. & Gaudino, G. (1998). Point mutations in the tyrosine kinase domain release the oncogenic and metastatic potential of the Ron receptor. *Oncogene*, **17,** 741-9.

Santoro, M.M., Penengo, L., Orecchia, S., Cilli, M. & Gaudino, G. (2000). The Ron oncogenic activity induced by the MEN2B-like substitution overcomes the requirement for the multifunctional docking site. *Oncogene*, **19,** 5208-11.

Sasaki, A., Taketomi, T., Kato, R., Saeki, K., Nonami, A., Sasaki, M., Kuriyama, M., Saito, N., Shibuya, M. & Yoshimura, A. (2003). Mammalian Sprouty4 suppresses Ras-independent ERK activation by binding to Raf1. *Cell Cycle*, **2,** 281-2.

Schmidt, L., Duh, F.M., Chen, F., Kishida, T., Glenn, G., Choyke, P., Scherer, S.W., Zhuang, Z., Lubensky, I., Dean, M., Allikmets, R., Chidambaram, A., Bergerheim, U.R., Feltis, J.T., Casadevall, C., Zamarron, A., Bernues, M., Richard, S., Lips, C.J., Walther, M.M., Tsui, L.C., Geil, L., Orcutt, M.L., Stackhouse, T., Lipan, J., Slife, L., Brauch, H., Decker, J., Niehans, G., Hughson, M.D., Moch, H., Storkel, S., Lerman, M.I., Linehan, W.M. & Zbar, B. (1997). Germline and somatic mutations in the tyrosine kinase domain of the MET proto-oncogene in papillary renal carcinomas. *Nat Genet*, **16,** 68-73.

Schneider, C., Sepp-Lorenzino, L., Nimmesgern, E., Ouerfelli, O., Danishefsky, S., Rosen, N. & Hartl, F.U. (1996). Pharmacologic shifting of a balance between protein refolding and degradation mediated by Hsp90. *Proc Natl Acad Sci U S A*, **93,** 14536-41.

Schweitzer, R., Shaharabany, M., Seger, R. & Shilo, B.Z. (1995). Secreted Spitz triggers the DER signaling pathway and is a limiting component in embryonic ventral ectoderm determination. *Genes Dev*, **9,** 1518-29.

Scott, R.P., Eketjall, S., Aineskog, H. & Ibanez, C.F. (2005). Distinct turnover of alternatively spliced isoforms of the RET kinase receptor mediated by differential recruitment of the Cbl ubiquitin ligase. *J Biol Chem*, **280,** 13442-9.

Sehat, B., Andersson, S., Vasilcanu, R., Girnita, L. & Larsson, O. (2007). Role of Ubiquitination in IGF-1 Receptor Signaling and Degradation. *PLoS ONE*, **2,** e340.

Sepp-Lorenzino, L., Ma, Z., Lebwohl, D.E., Vinitsky, A. & Rosen, N. (1995). Herbimycin A induces the 20 S proteasome- and ubiquitin-dependent degradation of receptor tyrosine kinases. *J Biol Chem*, **270,** 16580-7.

Sethupathy, P., Megraw, M. & Hatzigeorgiou, A.G. (2006). A guide through present computational approaches for the identification of mammalian microRNA targets. *Nat Methods*, **3,** 881-6.

Shimamura, T., Lowell, A.M., Engelman, J.A. & Shapiro, G.I. (2005). Epidermal growth factor receptors harboring kinase domain mutations associate with the heat shock protein

90 chaperone and are destabilized following exposure to geldanamycins. *Cancer Res*, **65,** 6401-8.

Shtiegman, K. & Yarden, Y. (2003). The role of ubiquitylation in signaling by growth factors: implications to cancer. *Semin Cancer Biol*, **13,** 29-40.

Sigismund, S., Woelk, T., Puri, C., Maspero, E., Tacchetti, C., Transidico, P., Di Fiore, P.P. & Polo, S. (2005). Clathrin-independent endocytosis of ubiquitinated cargos. *Proc Natl Acad Sci U S A*, **102,** 2760-5.

Soubeyran, P., Kowanetz, K., Szymkiewicz, I., Langdon, W.Y. & Dikic, I. (2002). Cbl-CIN85-endophilin complex mediates ligand-induced downregulation of EGF receptors. *Nature*, **416,** 183-7.

Stabile, L.P., Lyker, J.S., Huang, L. & Siegfried, J.M. (2004). Inhibition of human non-small cell lung tumors by a c-Met antisense/U6 expression plasmid strategy. *Gene Ther*, **11,** 325-35.

Stambolic, V., Suzuki, A., de la Pompa, J.L., Brothers, G.M., Mirtsos, C., Sasaki, T., Ruland, J., Penninger, J.M., Siderovski, D.P. & Mak, T.W. (1998). Negative regulation of PKB/Akt-dependent cell survival by the tumor suppressor PTEN. *Cell*, **95,** 29-39.

Stang, E., Johannessen, L.E., Knardal, S.L. & Madshus, I.H. (2000). Polyubiquitination of the epidermal growth factor receptor occurs at the plasma membrane upon ligand-induced activation. *J Biol Chem*, **275,** 13940-7.

Stebbins, C.E., Russo, A.A., Schneider, C., Rosen, N., Hartl, F.U. & Pavletich, N.P. (1997). Crystal structure of an Hsp90-geldanamycin complex: targeting of a protein chaperone by an antitumor agent. *Cell*, **89,** 239-50.

Suarez Pestana, E., Tenev, T., Gross, S., Stoyanov, B., Ogata, M. & Bohmer, F.D. (1999). The transmembrane protein tyrosine phosphatase RPTPsigma modulates signaling of the epidermal growth factor receptor in A431 cells. *Oncogene*, **18,** 4069-79.

Summy, J.M. & Gallick, G.E. (2003). Src family kinases in tumor progression and metastasis. *Cancer Metastasis Rev*, **22,** 337-58.

Supino-Rosin, L., Yoshimura, A., Yarden, Y., Elazar, Z. & Neumann, D. (2000). Intracellular retention and degradation of the epidermal growth factor receptor, two distinct processes mediated by benzoquinone ansamycins. *J Biol Chem*, **275,** 21850-5.

Sweeney, E.B. & Murphy, J.R. (1995). Diphtheria toxin-based receptor-specific chimaeric toxins as targeted therapies. *Essays Biochem*, **30,** 119-31.

Thien, C.B. & Langdon, W.Y. (2001). Cbl: many adaptations to regulate protein tyrosine kinases. *Nat Rev Mol Cell Biol*, **2,** 294-307.

Thien, C.B., Walker, F. & Langdon, W.Y. (2001). RING finger mutations that abolish c-Cbl-directed polyubiquitination and downregulation of the EGF receptor are insufficient for cell transformation. *Mol Cell*, **7,** 355-65.

Thomsen, P., Roepstorff, K., Stahlhut, M. & van Deurs, B. (2002). Caveolae are highly immobile plasma membrane microdomains, which are not involved in constitutive endocytic trafficking. *Mol Biol Cell*, **13,** 238-50.

Thrower, J.S., Hoffman, L., Rechsteiner, M. & Pickart, C.M. (2000). Recognition of the polyubiquitin proteolytic signal. *Embo J*, **19,** 94-102.

Tsutsui, S., Noorbakhsh, F., Sullivan, A., Henderson, A.J., Warren, K., Toney-Earley, K., Waltz, S.E. & Power, C. (2005). RON-regulated innate immunity is protective in an animal model of multiple sclerosis. *Ann Neurol*, **57,** 883-95.

Ullrich, A. & Schlessinger, J. (1990). Signal transduction by receptors with tyrosine kinase activity. *Cell*, **61,** 203-12.

Urbe, S., Sachse, M., Row, P.E., Preisinger, C., Barr, F.A., Strous, G., Klumperman, J. & Clague, M.J. (2003). The UIM domain of Hrs couples receptor sorting to vesicle formation. *J Cell Sci*, **116,** 4169-79.

Varadan, R., Assfalg, M., Haririnia, A., Raasi, S., Pickart, C. & Fushman, D. (2004). Solution conformation of Lys63-linked di-ubiquitin chain provides clues to functional diversity of polyubiquitin signaling. *J Biol Chem*, **279,** 7055-63.

Vihanto, M.M., Vindis, C., Djonov, V., Cerretti, D.P. & Huynh-Do, U. (2006). Caveolin-1 is required for signaling and membrane targeting of EphB1 receptor tyrosine kinase. *J Cell Sci*, **119,** 2299-309.

Vinos, J. & Freeman, M. (2000). Evidence that Argos is an antagonistic ligand of the EGF receptor. *Oncogene*, **19,** 3560-2.

Vogel, C.L., Cobleigh, M.A., Tripathy, D., Gutheil, J.C., Harris, L.N., Fehrenbacher, L., Slamon, D.J., Murphy, M., Novotny, W.F., Burchmore, M., Shak, S., Stewart, S.J. & Press, M. (2002). Efficacy and safety of trastuzumab as a single agent in first-line treatment of HER2-overexpressing metastatic breast cancer. *J Clin Oncol*, **20,** 719-26.

Walrafen, P., Verdier, F., Kadri, Z., Chretien, S., Lacombe, C. & Mayeux, P. (2004). Both proteasomes and lysosomes degrade the activated erythropoietin receptor. *Blood*, **in press**.

Wang, D., Shen, Q., Xu, X.M., Chen, Y.Q. & Wang, M.H. (2005). Activation of the RON receptor tyrosine kinase attenuates transforming growth factor-beta1-induced apoptotic death and promotes phenotypic changes in mouse intestinal epithelial cells. *Carcinogenesis*, **26,** 27-36.

Wang, M.H., Dlugosz, A.A., Sun, Y., Suda, T., Skeel, A. & Leonard, E.J. (1996). Macrophage-stimulating protein induces proliferation and migration of murine keratinocytes. *Exp Cell Res*, **226,** 39-46.

Wang, M.H., Julian, F.M., Breathnach, R., Godowski, P.J., Takehara, T., Yoshikawa, W., Hagiya, M. & Leonard, E.J. (1997). Macrophage stimulating protein (MSP) binds to its receptor via the MSP beta chain. *J Biol Chem*, **272,** 16999-7004.

Wang, M.H., Montero-Julian, F.A., Dauny, I. & Leonard, E.J. (1996). Requirement of phosphatidylinositol-3 kinase for epithelial cell migration activated by human macrophage stimulating protein. *Oncogene*, **13,** 2167-75.

Wang, M.H., Ronsin, C., Gesnel, M.C., Coupey, L., Skeel, A., Leonard, E.J. & Breathnach, R. (1994). Identification of the ron gene product as the receptor for the human macrophage stimulating protein. *Science*, **266,** 117-9.

Wang, M.H., Wang, D. & Chen, Y.Q. (2003). Oncogenic and invasive potentials of human macrophage-stimulating protein receptor, the RON receptor tyrosine kinase. *Carcinogenesis*, **24,** 1291-300.

Wang, M.H., Yao, H.P. & Zhou, Y.Q. (2006). Oncogenesis of RON receptor tyrosine kinase: a molecular target for malignant epithelial cancers. *Acta Pharmacol Sin*, **27,** 641-50.

Wang, Y., Pennock, S., Chen, X. & Wang, Z. (2002). Internalization of inactive EGF receptor into endosomes and the subsequent activation of endosome-associated EGF receptors. Epidermal growth factor. *Sci STKE*, **2002,** PL17.

Wasserman, J.D. & Freeman, M. (1998). An autoregulatory cascade of EGF receptor signaling patterns the Drosophila egg. *Cell*, **95,** 355-64.

Waterman, H., Katz, M., Rubin, C., Shtiegman, K., Lavi, S., Elson, A., Jovin, T. & Yarden, Y. (2002). A mutant EGF-receptor defective in ubiquitylation and endocytosis unveils a role for Grb2 in negative signaling. *Embo J*, **21,** 303-13.

Waterman, H., Levkowitz, G., Alroy, I. & Yarden, Y. (1999). The RING finger of c-Cbl mediates desensitization of the epidermal growth factor receptor. *J Biol Chem*, **274,** 22151-4.

Waterman, H., Sabanai, I., Geiger, B. & Yarden, Y. (1998). Alternative intracellular routing of ErbB receptors may determine signaling potency. *J Biol Chem*, **273,** 13819-27.

Webb, C.P., Hose, C.D., Koochekpour, S., Jeffers, M., Oskarsson, M., Sausville, E., Monks, A. & Vande Woude, G.F. (2000). The geldanamycins are potent inhibitors of the hepatocyte growth factor/scatter factor-met-urokinase plasminogen activator-plasmin proteolytic network. *Cancer Res*, **60,** 342-9.

Wegele, H., Muller, L. & Buchner, J. (2004). Hsp70 and Hsp90--a relay team for protein folding. *Rev Physiol Biochem Pharmacol*, **151,** 1-44.

Weiner, D.B., Kokai, Y., Wada, T., Cohen, J.A., Williams, W.V. & Greene, M.I. (1989). Linkage of tyrosine kinase activity with transforming ability of the p185neu oncoprotein. *Oncogene*, **4,** 1175-83.

Weissman, A.M. (2001). Themes and variations on ubiquitylation. *Nat Rev Mol Cell Biol*, **2,** 169-78.

Wilkinson, K.D. (2000). Ubiquitination and deubiquitination: targeting of proteins for degradation by the proteasome. *Semin Cell Dev Biol*, **11,** 141-8.

Willett, C.G., Wang, M.H., Emanuel, R.L., Graham, S.A., Smith, D.I., Shridhar, V., Sugarbaker, D.J. & Sunday, M.E. (1998). Macrophage-stimulating protein and its receptor in non-small-cell lung tumors: induction of receptor tyrosine phosphorylation and cell migration. *Am J Respir Cell Mol Biol*, **18,** 489-96.

Woelk, T., Sigismund, S., Penengo, L. & Polo, S. (2007). The ubiquitination code: a signalling problem. *Cell Div*, **2,** 11.

Xie, Q., Gao, C.F., Shinomiya, N., Sausville, E., Hay, R., Gustafson, M., Shen, Y., Wenkert, D. & Vande Woude, G.F. (2005). Geldanamycins exquisitely inhibit HGF/SF-mediated tumor cell invasion. *Oncogene*, **24,** 3697-707.

Xie, X., Lu, J., Kulbokas, E.J., Golub, T.R., Mootha, V., Lindblad-Toh, K., Lander, E.S. & Kellis, M. (2005). Systematic discovery of regulatory motifs in human promoters and 3' UTRs by comparison of several mammals. *Nature*, **434,** 338-45.

Xu, D., Makkinje, A. & Kyriakis, J.M. (2005). Gene 33 is an endogenous inhibitor of epidermal growth factor (EGF) receptor signaling and mediates dexamethasone-induced suppression of EGF function. *J Biol Chem*, **280,** 2924-33.

Xu, W., Marcu, M., Yuan, X., Mimnaugh, E., Patterson, C. & Neckers, L. (2002). Chaperone-dependent E3 ubiquitin ligase CHIP mediates a degradative pathway for c-ErbB2/Neu. *Proc Natl Acad Sci U S A*, **99,** 12847-52.

Xu, W., Mimnaugh, E., Rosser, M.F., Nicchitta, C., Marcu, M., Yarden, Y. & Neckers, L. (2001). Sensitivity of mature Erbb2 to geldanamycin is conferred by its kinase domain and is mediated by the chaperone protein Hsp90. *J Biol Chem*, **276,** 3702-8.

Xu, X.M., Wang, D., Shen, Q., Chen, Y.Q. & Wang, M.H. (2004). RNA-mediated gene silencing of the RON receptor tyrosine kinase alters oncogenic phenotypes of human colorectal carcinoma cells. *Oncogene*, **23,** 8464-74.

Xu, Y., Singer, M.A. & Lindquist, S. (1999). Maturation of the tyrosine kinase c-src as a kinase and as a substrate depends on the molecular chaperone Hsp90. *Proc Natl Acad Sci U S A*, **96,** 109-14.

Yoshimura, T., Yuhki, N., Wang, M.H., Skeel, A. & Leonard, E.J. (1993). Cloning, sequencing, and expression of human macrophage stimulating protein (MSP, MST1) confirms MSP as a member of the family of kringle proteins and locates the MSP gene on chromosome 3. *J Biol Chem*, **268,** 15461-8.

Yusoff, P., Lao, D.H., Ong, S.H., Wong, E.S., Lim, J., Lo, T.L., Leong, H.F., Fong, C.W. & Guy, G.R. (2002). Sprouty2 inhibits the Ras/MAP kinase pathway by inhibiting the activation of Raf. *J Biol Chem*, **277,** 3195-201.

Zabarovsky, E.R., Lerman, M.I. & Minna, J.D. (2002). Tumor suppressor genes on chromosome 3p involved in the pathogenesis of lung and other cancers. *Oncogene*, **21,** 6915-35.

Zhou, P., Fernandes, N., Dodge, I.L., Reddi, A.L., Rao, N., Safran, H., DiPetrillo, T.A., Wazer, D.E., Band, V. & Band, H. (2003). ErbB2 degradation mediated by the co-chaperone protein CHIP. *J Biol Chem*, **278,** 13829-37.

Zhou, Y.Q., He, C., Chen, Y.Q., Wang, D. & Wang, M.H. (2003). Altered expression of the RON receptor tyrosine kinase in primary human colorectal adenocarcinomas: generation of different splicing RON variants and their oncogenic potential. *Oncogene*, **22,** 186-97.

THE JOURNAL OF BIOLOGICAL CHEMISTRY VOL. 281, NO. 31, pp. 21710–21719, August 4, 2006

Geldanamycins Trigger a Novel Ron Degradative Pathway, Hampering Oncogenic Signaling*[S]

Received for publication, March 2, 2006, and in revised form, June 1, 2006 Published, JBC Papers in Press, June 1, 2006, DOI 10.1074/jbc.M602014200

Serena Germano[‡], Davide Barberis[‡], Massimo M. Santoro[‡], Lorenza Penengo[‡1], Ami Citri[§], Yosef Yarden[§], and Giovanni Gaudino[‡2]

From the [‡]Department DISCAFF and DFB Center, University of Piemonte Orientale "A. Avogadro," Novara 28100, Italy and the [§]Department of Biological Regulation, Weizmann Institute of Science, Rehovot 76100, Israel

Ron, the tyrosine kinase receptor for macrophage-stimulating protein is responsible for proliferation and migration of cells from different tissues. Ron can acquire oncogenic potential by single point mutations in the kinase domain, and dysregulated Ron signaling has been involved in the development of different human cancers. We have previously shown that ligand-activated Ron recruits the negative regulator c-Cbl, which mediates its ubiquitylation and degradation. Here we report that Ron is ubiquitylated also by the U-box E3 ligase C-terminal Hsc70-interacting protein (CHIP), recruited via chaperone intermediates Hsp90 and Hsc70. Gene silencing shows that CHIP activity is necessary to mediate Ron degradation upon cell treatment with Hsp90 inhibitors geldanamycins. The oncogenic Ron^{M1254T} receptor escapes from c-Cbl negative regulation but retains a strong association with CHIP. This constitutively active mutant of Ron displays increased sensitivity to geldanamycins, enhanced physical interaction with Hsp90, and more rapid degradation rate. Cell growth and migration, as well as the transforming potential evoked by Ron^{M1254T}, are abrogated upon Hsp90 inhibition. These data highlight a novel mechanism for Ron degradation and propose Hsp90 antagonists like geldanamycins as suitable pharmacological agents for therapy of cancers where altered Ron signaling is involved.

Dysregulated activation of receptor tyrosine kinases (RTKs)[3] has been extensively documented in different types of human tumors (1) and frequently correlates with poor responsiveness to conventional therapies, pointing at RTKs as potential targets for molecule-based cancer therapy (2, 3). Among the different therapeutic approaches a promising strategy relies on forcing RTKs toward degradative pathways (4).

The Ron tyrosine kinase, receptor for macrophage-stimulating protein (MSP), is a member of the hepatocyte growth factor (HGF) receptor subfamily (5, 6). Ron is expressed in a variety of human tissues, and the engagement by its cognate ligand activates multiple intracellular signaling pathways controlling normal cell proliferation, migration, and adhesion-dependent survival (7–9). A single point mutation (M1254T), targeted to a conserved residue of the tyrosine kinase domain is oncogenic (Ron^{M1254T}), by increasing kinase efficiency and subverting substrate specificity (10, 11). Growing evidence indicates that Ron can be involved in cancer development and progression in humans (12, 13) and in murine models (14, 15). Therefore, targeting Ron expression by forcing its down-regulation may help to elucidate its role in tumor development and progression.

It has been reported that many kinases that are deregulated in human cancers are dependent on the chaperone activity of the Heat shock protein 90 (Hsp90) for their conformational maturation and stability (16). Hsp90 is a ubiquitous chaperone protein abundantly expressed in mammalian cells, where it performs housekeeping functions assisting in the folding, activation, and assembly of a variety of proteins (17). Hsp90 functions in concert with several co-chaperone proteins that modulate its chaperone activity (18). The co-chaperone E3 ubiquitin ligase C-terminal Hsc70-interacting protein (CHIP) has been reported to participate in Hsp90 multichaperone complexes, being involved in ubiquitylation and degradation of client proteins (19, 20).

Geldanamycins are a class of benzoquinone ansamycin antibiotics, able to compete with ADP/ATP in the nucleotide binding pocket of Hsp90, inhibiting its ATP-dependent chaperone activity and thus directing the ubiquitin-mediated proteasomal degradation of the client proteins (21, 22). By leading to depletion of important effector proteins that contribute to deregulated signaling, geldanamycin (GA) and its less toxic derivative 17-allylamino-17-demethoxygeldanamycin (17-AAG) exhibit potent anti-tumor activity against human cancer cells, both *in vitro* and in tumor xenografts (23, 24). Indeed, based on promising preclinical evaluations, 17-AAG is currently in clinical trials as a single agent or in combination with other chemotherapeutics (25, 26).

Sensitivity to benzoquinone ansamycins has been described for several RTKs. It has been reported that treatment of breast

* This work was supported by research grants from Associazione Italiana per la Ricerca sul Cancro (AIRC), from the Italian Department of University (COFIN-PRIN), and from the Buzzi Unicem Foundation (to G. G.). The costs of publication of this article were defrayed in part by the payment of page charges. This article must therefore be hereby marked "*advertisement*" in accordance with 18 U.S.C. Section 1734 solely to indicate this fact.

[S] The on-line version of this article (available at http://www.jbc.org) contains supplemental Figs. 1–3.

[1] Present address: IFOM, The FIRC Institute for Molecular Oncology, Via Adamello 16, Milano 20139, Italy.

[2] To whom correspondence should be addressed: DISCAFF and DFB Center, University of Piemonte Orientale "A. Avogadro," via Bovio 6, Novara 28100, Italy. Tel.: 39-0321-375-815; Fax: 39-0321-375-821; E-mail: giovanni.gaudino@unipmn.it.

[3] The abbreviations used are: RTK, receptor tyrosine kinase; MSP, macrophage-stimulating protein; HGP, hepatocyte growth factor; CHIP, C-terminal Hsc70-interacting protein; GA, geldanamycin; 17-AAG, 17-allylamino-17-demethoxygeldanamycin; E1, ubiquitin-activating enzyme; E2, ubiquitin carrier protein; E3, ubiquitin-protein isopeptide ligase; siRNA, small interfering RNA; GST, glutathione *S*-transferase; EGFR, epidermal growth factor receptor.

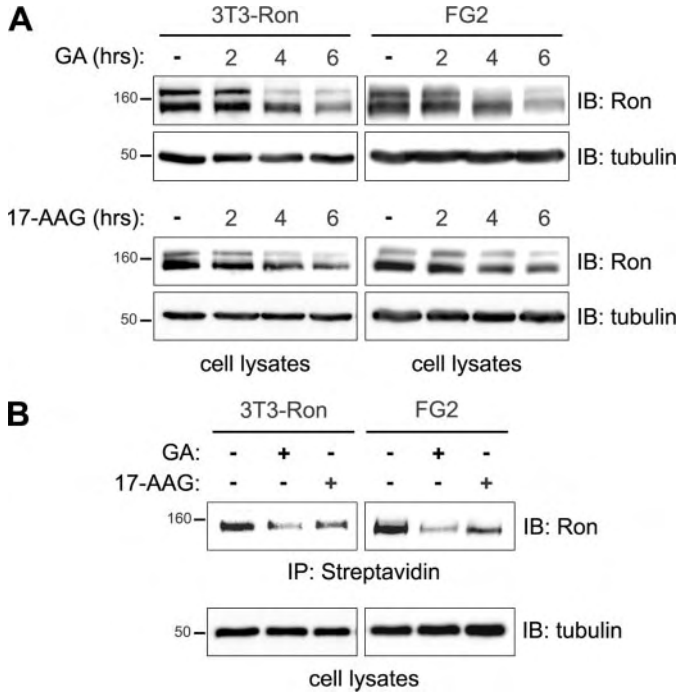

FIGURE 1. **Geldanamycins induce degradation of both precursor and mature cell surface Ron.** *A*, 3T3-Ron and FG2 cells were treated with vehicle (−) or 1 μM GA or 1 μM 17-AAG for the indicated times. Cell lysates were analyzed by immunoblotting (*IB*) with a polyclonal antibody against Ron C-terminal domain, recognizing both the 170-kDa precursor and the 150-kDa β-chain of the receptor. α-Tubulin immunoblotting was used as loading control. *B*, 3T3-Ron and FG2 cells were cell surface-biotinylated and then cultured in medium with vehicle (−) or 1 μM GA, or 1 μM 17-AAG for 6 h. After immunoprecipitation (*IP*) of cell lysates with streptavidin-Sepharose, surface-labeled mature Ron was detected by anti-Ron immunoblotting. All results shown are representative of at least four independent experiments.

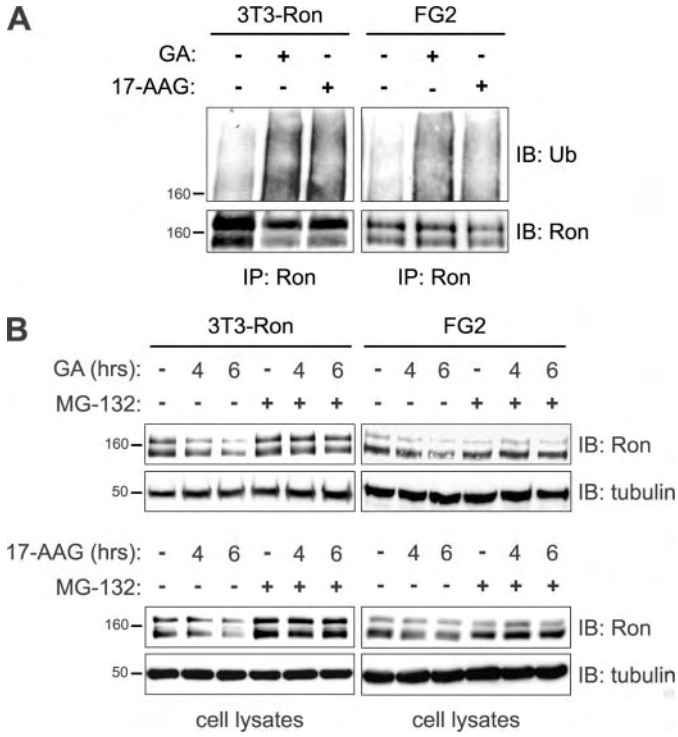

FIGURE 2. **The ubiquitin-proteasome pathway is involved in Ron degradation induced by geldanamycins.** *A*, proteins from lysates of 3T3-Ron and FG2 cells treated with vehicle (−) or 1 μM GA, or 1 μM 17-AAG for 15 min were immunoprecipitated with Ron antibodies. Anti-ubiquitin immunoblotting (*IB*) was used to detect the ubiquitylated receptor molecules. The immunoprecipitated (*IP*) receptor was detected by Ron immunoblotting. *B*, 3T3-Ron and FG2 cells were treated with vehicle (−) or 1 μM GA or 1 μM 17-AAG in the presence or absence of the proteasome inhibitor MG-132 (20 μM). Cells were incubated with MG-132 for 1 h before drug addition. Equal quantities of lysates from cells harvested at the indicated times were analyzed by anti-Ron immunoblotting. Anti-α-tubulin immunoblotting was used as loading control. Representative results from three independent experiments are shown.

and other cancer cells with GA causes rapid ubiquitylation of cell surface HER2/ErbB2 molecules, followed by their proteasome-dependent degradation (27). A recent study demonstrated the ability of GA to deplete mature EGFR protein harboring kinase domain mutations (28). Moreover, geldanamycins have been shown to down-regulate the HGF receptor (Met) and to prevent HGF-mediated tumor cell motility and invasion (29, 30).

We have previously shown that activated Ron recruits to its multifunctional docking site the negative regulator c-Cbl, which mediates ligand-dependent Ron ubiquitylation and down-regulation, through its E3 ubiquitin ligase activity (31). Here we report that Ron forms a multichaperone complex containing Hsp90, Hsc70, and the E3 ligase CHIP. We also show that GA and its derivative 17-AAG induce degradation of both precursor and membrane-exposed forms of Ron. This occurs by impairing Ron association with Hsp90 and by promoting CHIP-mediated receptor ubiquitylation.

The oncogenic Ron^{M1254T} escapes from c-Cbl-mediated negative regulation but is efficiently destabilized by geldanamycins, which hinder growth and migration as well as transforming activity of the oncogenic receptor.

EXPERIMENTAL PROCEDURES

Reagents and Antibodies—Geldanamycin, 17-AAG, MG-132, and concanamycin A were purchased from Alexis (Montreal, Canada). Human recombinant MSP was obtained by R&D Systems (Minneapolis, MN). Polyclonal antibodies against Ron C-terminal domain (c-20) and monoclonal anti-Hsc70 (B-6) were obtained from Santa Cruz Biotechnology, Inc. (Santa Cruz, CA). Monoclonal anti-Hsp90 antibody was from BD Transduction Laboratories; monoclonal anti-α-tubulin (B-5-1-2), anti-phospho-Erk1/2 (MAPK-YT), and anti-FLAG (M2) were from Sigma; polyclonal phospho-Akt (Ser^{473}) was from Cell Signaling Technology (Beverly, MA); monoclonal anti-Cbl (7G10) was from Upstate Biotechnology, Inc. (Charlottesville, VA), monoclonal anti-ubiquitin (FK2) was from Stressgen (San Diego, CA); and CHIP rabbit polyclonal antiserum was from Calbiochem (Merck). Horseradish peroxidase-conjugated anti-mouse and anti-rabbit were purchased from GE Healthcare (Uppsala, Sweden).

Preparation of Plasmid Constructs—pMT2-Ron and pMT2-Ron^{M1254T} were described previously (10). c-Cbl, c-Cbl70z, CHIP, CHIPK30A, and CHIPΔU-box were prepared in pcDNA3 (32, 33). GST-CHIP and GST-CHIPΔU-box in pGEX4T-2 vector were kindly provided by Dr. H. Band (Brigham and Women's Hospital, Boston, MA). pCCLsin-.PPT.hPGK.GFP.Wpre transfer plasmid was used to express two independent small interfering RNAs (siRNAs) (5′-ACCACGAGGGTGATGAGGA-3′ and 5′-GAAGCGAGATATCCCTGAC-3′), targeting CHIP transcripts or an unrelated

sequence as negative control. The expression was under the transcriptional control of the H1 promoter derived from pSUPER plasmid (34). The vector carries an independent GFP expression cassette, to allow for the identification of transfected cells.

Cell Culture and Transfection—Cells were purchased from American Type Culture Collection. FG2 cells were maintained in RPMI 1640, COS-7, and NIH-3T3 cells in Dulbecco's modified Eagle's medium (Sigma), supplemented with 10% fetal bovine serum (Invitrogen) in a 5% CO_2-humidified atmosphere. NIH-3T3 cells stably expressing Ron or Ron^{M1254T} were obtained as described previously (10). Transient transfection of COS-7 cells was performed with DEAE-dextran using the CellPhect transfection kit (GE Healthcare). LipofectaminePlus (Invitrogen) was used for transfection of FG2 cells with siRNAs constructs according to the manufacturer's recommendations.

Immunoprecipitation and Immunoblotting—Total cellular proteins were extracted by solubilizing the cells in radioimmune precipitation buffer (50 mM Tris-HCl, pH 7.4, 150 mM NaCl, 0.5% sodium deoxycholate, 1% Triton X-100, 0.1% SDS) containing protease and phosphatase inhibitors (10 μg/ml aprotinin, 10 μg/ml leupeptin, 10 μg/ml pepstatin, 1 mM phenylmethylsulfonyl fluoride, 1 mM sodium orthovanadate, and 2 mM sodium fluoride). Whole-cell lysates were clarified by centrifugation (14,000 $\times$ *g*, 10 min), quantified with the BCA protein assay reagent kit (Pierce) and dissolved in Laemmli sample buffer. For immunoprecipitation, cells were lysed in solubilization buffer (20 mM Tris-HCl, pH 7.4, 5 mM EDTA, 150 mM NaCl, 10% glycerol, 1% Triton X-100) with protease inhibitors. 500-μg aliquots of clarified cell lysates were incubated with 1 μg of the indicated antibody immobilized on protein A-Sepharose 4B packed beads (GE Healthcare) for 2 h at 4 °C. After extensive washes with lysis buffer, precipitated proteins were dissolved in Laemmli sample buffer. Proteins were resolved by 10% SDS-PAGE, transferred to nitrocellulose membrane, and probed with respective antibodies. For ubiquitin immunoblotting, proteins were transferred to polyvinylidene difluoride membranes, incubated for 30 min in 20 mM Tris-HCl containing 6 M guanidine hydrochloride and 5 mM 2-mercaptoethanol, and then probed with ubiquitin antibodies. Detection was performed by the ECL system (GE Healthcare) and the Chemidoc exposure system (Bio-Rad). Image analysis was performed with Quantity One (Bio-Rad).

In Vitro Ubiquitylation Assay—The GST-CHIP and GST-CHIPΔU-box fusion proteins were expressed in *E. coli* and affinity-purified as described by the manufacturer's protocol. Receptors were immunoprecipitated from 800-μg aliquots of cell lysates with protein A-Sepharose beads. Following purification, Sepharose beads were extensively washed and incubated in a 50-μl reaction for 90 min at 37 °C with 275 ng of purified E1, 400 ng of E2 (UbcH5a), 5 ng/μl biotin NH_2-terminal ubiquitin, 10 ng/μl ubiquitin (Boston Biochem Inc., Cambridge, MA), and 5 μg of the indicated GST fusion proteins in a buffer containing 50 mM Tris-HCl, pH 7.5, 2.5 mM $MgCl_2$, 2 mM ATP, 2 mM dithiothreitol. After extensive washes the ubiquitylated receptors were detected by SDS-PAGE and Western blotting with horseradish peroxidase-conjugated streptavidin (GE Healthcare).

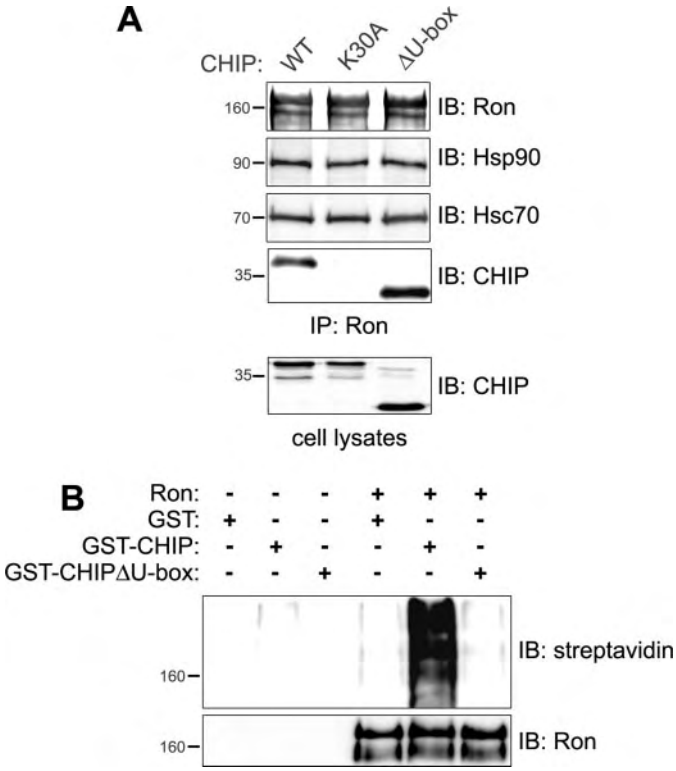

FIGURE 3. **CHIP serves as an E3 ligase for Ron and interacts with the receptor by a chaperone intermediate.** *A*, COS-7 cells were transiently transfected with Ron and either CHIP or different CHIP mutants. 72 h after transfection, cells were lysed, and equal protein amounts were immunoprecipitated (*IP*) with Ron antibodies. Association of Hsp90, Hsc70, and CHIP to the Ron immunocomplex was detected with the appropriate antibodies. Anti-CHIP immunoblotting (*IB*) of cell lysates was used to control transfection efficiency. *B*, proteins from 3T3-Ron cell lysates were immunoprecipitated with Ron antibodies or preimmune rabbit serum. Immunoprecipitates were subjected to *in vitro* ubiquitylation assay in the presence of GST or GST-CHIP fusion proteins, biotin-labeled ubiquitin, E1 and E2 enzymes. The ubiquitylated receptors were detected by Western blotting with streptavidin-horseradish peroxidase. All results shown are representative of at least three independent experiments. *WT*, wild type.

Cell Surface Biotinylation Assay—Surface proteins were labeled for 30 min at 4 °C with 0.5 mg/ml Ez-Link® sulfo-NHS-Biotin (Pierce) in buffer A (1.3 mM $CaCl_2$, 0.4 mM $MgSO_4$-$7H_2O$, 5 mM KCl, 138 mM NaCl, 5.6 mM D-glucose, 25 mM HEPES, pH 7.4). After extensive washes with Dulbecco's modified Eagle's medium containing 0.6% bovine serum albumin and 20 mM HEPES, pH 7.4, cells were lysed, and proteins were subjected to immunoprecipitation with streptavidin-Sepharose (GE Healthcare). Protein samples were analyzed by SDS-PAGE and immunoblotting.

Cell Proliferation Assay—Cells were plated on 96-well plates at a density of 4×10^4/well and cultured in appropriate medium supplemented with 10% fetal bovine serum in the presence or absence of 100 nM 17-AAG. Cells were fixed in 11% glutaraldehyde 0, 24, 48, and 72 h after drug addition and stained in crystal violet. Staining was solubilized in 10% acetic acid, and absorbance at 595 nm was measured with a microplate reader.

Cell Migration Assay—Cell motility was assayed using 8-μm pore size Transwell® chambers (Corning Glass). The lower side of the membrane was coated with 10 μg/ml fibronectin for 2 h and then blocked with 0.2% bovine serum albumin. Cells were

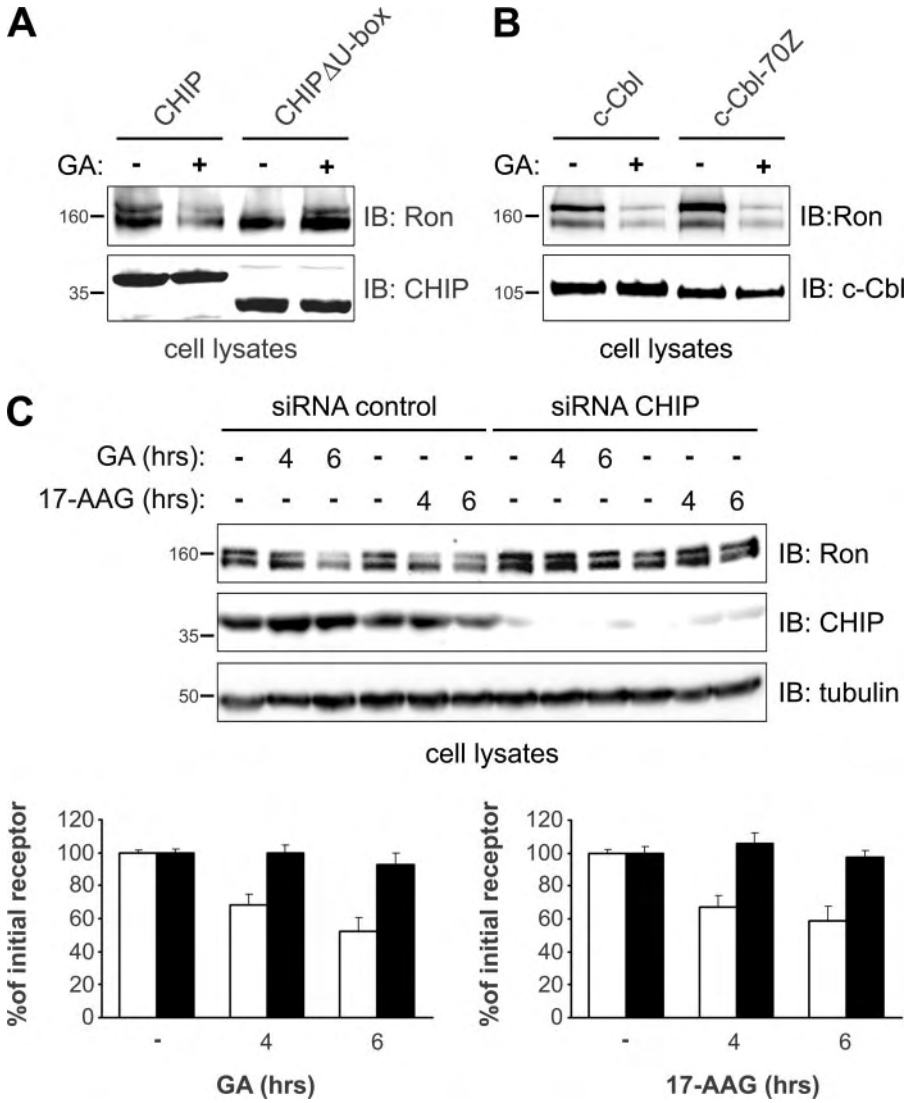

FIGURE 4. **The ubiquitin ligase activity of CHIP is necessary to mediate Ron degradation induced by geldanamycins.** *A*, COS-7 cells were transiently transfected with Ron and either CHIP or the ubiquitylation-defective CHIP Δ U-box. 72 h after transfection, cells were treated with vehicle (−) or 1 μM GA for 6 h and equal amounts of cell lysates were analyzed by immunoblotting (*IB*) with Ron and CHIP antibodies. Representative results from three independent experiments are shown. *B*, COS-7 cells were transiently transfected with Ron and either c-Cbl or c-Cbl-70Z. 72 h after transfection, lysates from cells treated with vehicle (−) or 1 μM GA for 6 h were analyzed by immunoblotting with Ron and c-Cbl antibodies. Representative results from two independent experiments are shown. *C*, FG2 cells were transiently transfected with siRNAs targeted to CHIP transcript or to an unrelated sequence. 48 h after transfection, cells were treated with vehicle (−) or 1 μM GA or 1 μM 17-AAG. Equal quantities of lysates from cells harvested at the indicated times were analyzed by immunoblotting with Ron antibodies. CHIP silencing was verified by immunoblotting with appropriate antibodies and anti-α-tubulin immunoblotting was used as loading control. Densitometry of Ron immunoblotting was performed and values, normalized to the relative α-tubulin control bands, were plotted as percentages of vehicle-treated cells. *White columns*, unrelated siRNA; *black columns*, CHIP siRNA. Each data point represents the mean ± S.E. of three independent experiments.

detached with 1 mM EDTA and resuspended with 2% fetal bovine serum. 1×10^5 cells were plated on the upper side and allowed to migrate for 6 h in the presence of 100 nM 17-AAG toward the lower chamber containing appropriate medium supplemented with 10% fetal bovine serum. Cells remaining in the upper chamber were mechanically removed, and those that migrated to the lower side were fixed and stained as described above.

Transforming Assay—A focus-forming assay was performed on NIH-3T3 fibroblasts (5×10^5 cells) with 5 μg of recombinant plasmid as described previously (10). Two days after transfection, 17-AAG was added to cultures and renewed every 48 h. Cell cultures were maintained at confluence and screened for focus formation 10 ± 18 days after transfection. Spontaneous formation of foci was negligible.

RESULTS

Geldanamycins Target Ron for Degradation—To investigate the sensitivity of Ron to Hsp90 inhibitors, we performed a time course experiment on NIH-3T3 fibroblasts (3T3-Ron) and pancreatic carcinoma FG2 cells, expressing recombinant and endogenous Ron, respectively. After cell exposure to GA for different times, we observed a robust reduction of both precursor and mature form of the receptor within 6 h. It is noteworthy that Ron protein levels declined with similar rates in both cell lines upon GA treatment. Similar effects, at a slightly lesser extent, were observed with the same concentration of the less toxic GA derivative 17-AAG (Fig. 1*A*). Ron destabilization upon Hsp90 inhibition was obtained also by using a chemically unrelated Hsp90 inhibitor, the macrolactone antibiotic radicicol (supplemental Fig. 1).

It has been shown for other RTKs (platelet-derived growth factor receptor and epidermal growth factor receptor) (35) that only the newly synthesized receptor molecules are destabilized by GA. We evaluated if Ron depletion following GA or 17-AAG exposure was due to impaired maturation of the nascent chains only or if also cell surface-exposed receptors were targeted for degradation. By surface biotinylation of 3T3-Ron and FG2 cells, followed by Ron immunoprecipitation, we observed an accelerated decrease of cell surface mature Ron after exposure to GA or 17-AAG for 6 h (Fig. 1*B*). This indicates that GA and 17-AAG, albeit with minor efficacy, are able to destabilize the receptor even after its exposure to the plasma membrane. In NIH-3T3 cells expressing a kinase-defective Ron mutant (31), GA-induced receptor degradation was retained (supplemental Fig. 2), demonstrating that the kinase activity is not required for sensitivity of Ron to GA.

GA-induced degradation of the client proteins is reported to involve the ubiquitin-proteasome pathway (36). Thus, we ana-

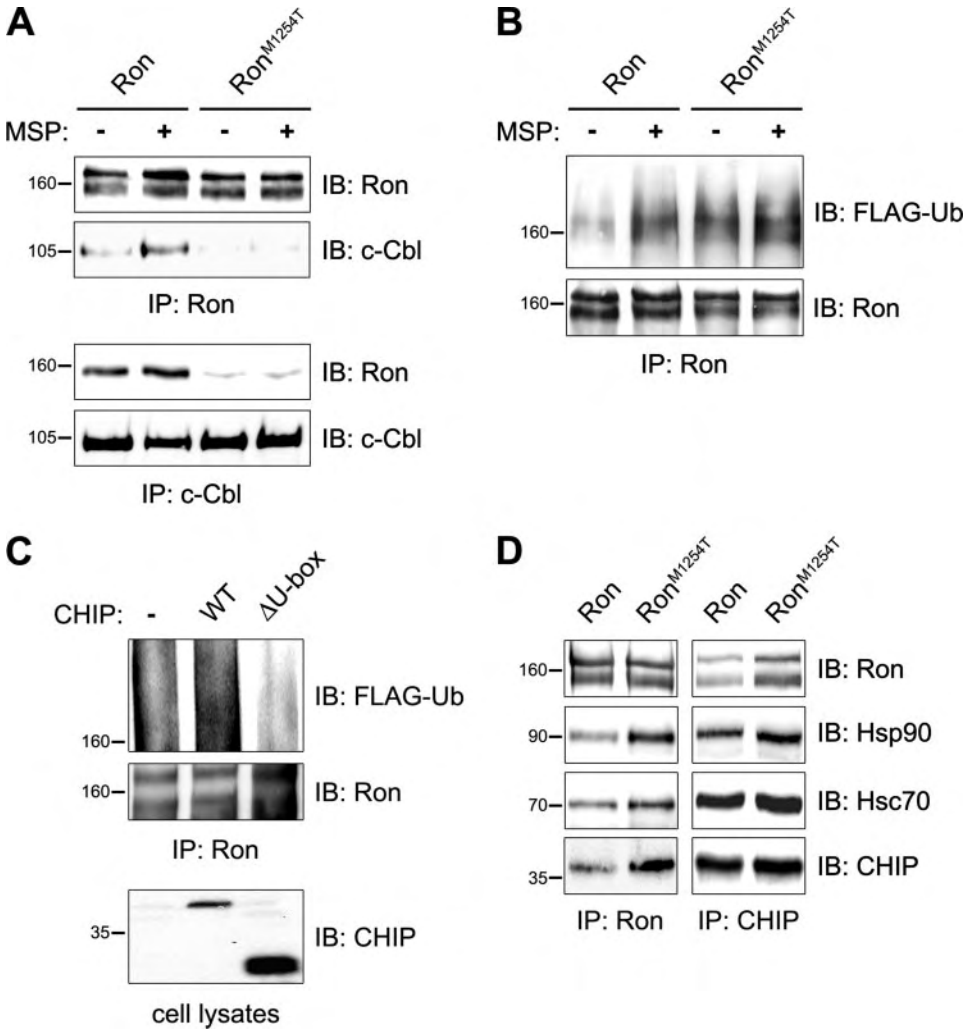

FIGURE 5. **CHIP mediates c-Cbl independent oncogenic Ron^{M1254T} ubiquitylation.** *A*, COS-7 cells were transiently transfected with Ron or Ron^{M1254T}, along with c-Cbl and FLAG-tagged ubiquitin. 72 h after transfection, serum-starved cells were treated with vehicle (−) or 300 ng/ml MSP for 20 min, and equal protein amounts of cell lysates were immunoprecipitated (*IP*) with Ron (*top*) or c-Cbl (*bottom*) antibodies. Associated c-Cbl or Ron were detected with the appropriate antibodies. *B*, Ron immunoprecipitation described in *A* was followed by immunoblotting (*IB*) with FLAG antibodies to detect ubiquitylated receptors. The immunoprecipitated receptor was detected by Ron immunoblotting. *C*, proteins from cell lysates of COS-7 transiently transfected with Ron^{M1254T} and FLAG-tagged ubiquitin, along with CHIP or CHIPΔU-box or empty vector, were subjected to immunoprecipitation with Ron antibodies and analyzed by anti-FLAG and anti-Ron immunoblotting. Anti-CHIP immunoblotting on cell lysates was used to control transfection efficiency. *D*, COS-7 cells were transiently transfected with Ron or Ron^{M1254T} along with CHIP. 72 h after transfection equal protein amounts of cell lysates were immunoprecipitated with Ron or CHIP antibodies and presence of CHIP, Ron, Hsp90, or Hsc70 in the immunocomplexes was detected with the appropriate antibodies. Ron, Ron^{M1254T}, and CHIP expression was monitored by immunoblotting. All results shown are representative of at least three independent experiments.

lyzed Ron ubiquitylation upon GA or 17-AAG treatment of 3T3-Ron and FG2 cells. In these conditions, a marked ubiquitylation of the receptor was observed as early as 15 min after drug addition (Fig. 2*A*). This indicates that receptor ubiquitylation is an early step in GA-induced Ron degradation and suggests that a specific E3 ligase is involved. Moreover, pretreatment of both cell lines with the proteasome inhibitor MG-132 impaired Ron depletion induced by geldanamycins (Fig. 2*B*), indicating that this destabilizing effect on Ron requires proteasomal activity. Conversely, when cells were pretreated with the lysosomal inhibitor concanamycin A, GA retained full activity on Ron (supplemental Fig. 3). Our results show that cell surface-exposed mature Ron is destabilized by GA-induced kinase-independent degradation, involving the ubiquitin-proteasome pathway.

Ron Associates with a Chaperone Complex Containing the E3 Ubiquitin Ligase CHIP—We aimed at identifying the ubiquitin ligase responsible for GA-induced Ron ubiquitylation. Among several ligases, we focused our attention on CHIP, since this E3 enzyme mediates degradation of signaling proteins, relying on the association with chaperone proteins Hsp90 and Hsc70 (20, 37). We verified if Ron and CHIP were recruited in stable complexes with these chaperone proteins. We co-transfected COS-7 cells with cDNAs encoding both Ron and CHIP. Immunoblotting analysis on Ron immunoprecipitates demonstrated that the receptor associates with endogenous Hsp90 and Hsc70 as well as with CHIP (Fig. 3*A*).

CHIP has the ability to bind Hsc70 by means of the amino-terminal tetratricopeptide domain, whereas its E3 ubiquitin ligase activity is mediated by its carboxyl-terminal U-box domain (38). To better characterize the interaction between the receptor and the ubiquitin ligase, we tested the ability of CHIP proteins harboring a mutation in the tetratricopeptide (K30A) or lacking the U-box (ΔU-box) domain to interact with Ron. The K30A mutant, which does not bind to either Hsp90 or Hsc70 (20), failed to co-immunoprecipitate with Ron. This suggests that these chaperone intermediates are involved in the Ron-CHIP interaction. Conversely, the deletion of the U-box domain did not impair the complex formation (Fig. 3*A*).

To verify whether CHIP could directly mediate Ron ubiquitylation, we performed an *in vitro* ubiquitylation assay on immunocomplexes from 3T3-Ron fibroblasts, by using purified GST-CHIP fusion proteins in the presence of biotinylated ubiquitin and E1 and E2 enzymes. Wild type (GST-CHIP), but not U-box-deleted (GST-CHIPΔU-box), fusion protein catalyzed the receptor ubiquitylation. No ubiquitylation was observed in the presence of GST protein alone as well as when the reaction was performed in absence of immunoprecipitated Ron (Fig. 3*B*). This demonstrates that CHIP can serve as an E3 ligase for Ron. Taken together, these results indicate that in live cells Ron forms a complex with

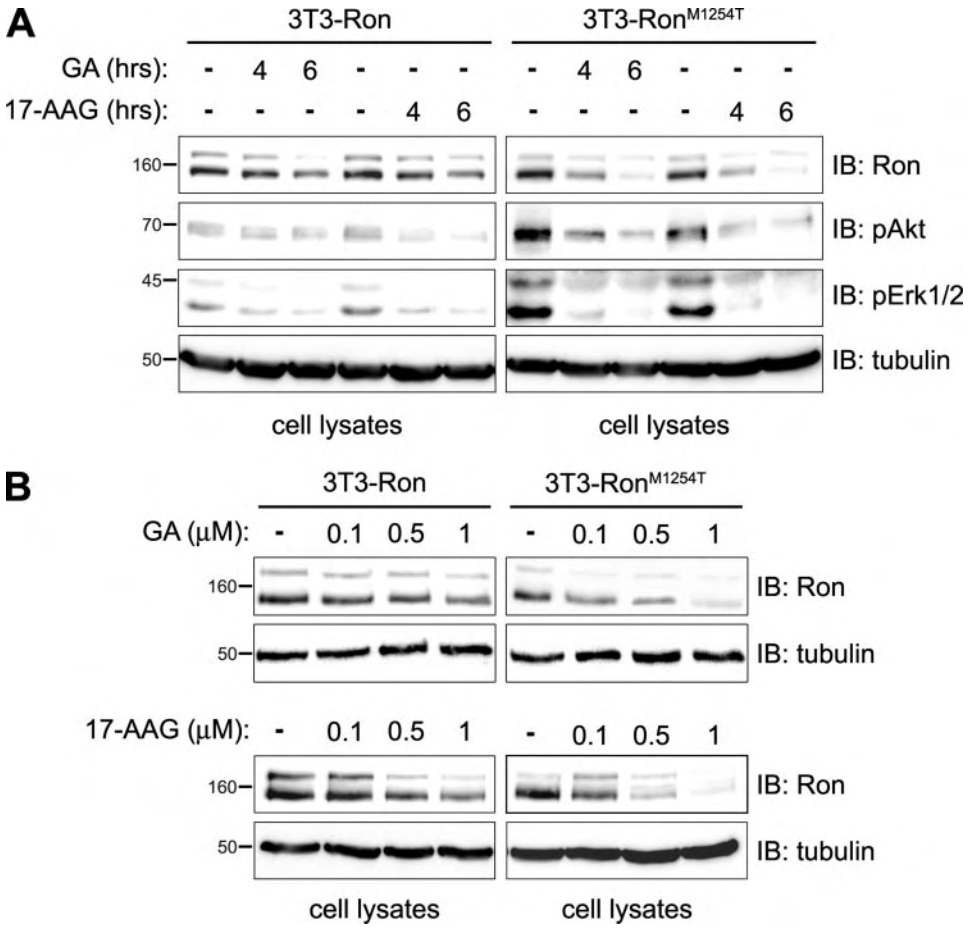

FIGURE 6. **Oncogenic Ron^{M1254T} displays higher sensitivity to geldanamycins than wild-type receptor.** *A*, 3T3-Ron and 3T3-Ron^{M1254T} cells were treated with vehicle (−) or 1 μM GA, or 1 μM 17-AAG for the indicated times. Equal amounts of cell lysates were analyzed by immunoblotting (*IB*) with Ron, phospho-Akt, and phospho-Erk1/2 antibodies. α-Tubulin immunoblotting was used as loading control. *B*, 3T3-Ron and 3T3-Ron^{M1254T} cells treated with vehicle (−) or increasing amounts of GA, or of 17-AAG for 6 h. Equal amounts of cell lysates were analyzed by immunoblotting with Ron antibodies. Anti-α-tubulin immunoblotting was used as loading control. All results shown are representative of at least four independent experiments.

the chaperones Hsp90 and Hsc70, which mediate receptor association with the E3 ubiquitin ligase CHIP.

CHIP Mediates Ron Degradation Induced by Geldanamycins—We evaluated the involvement of CHIP in GA-induced Ron degradation by using COS-7 cells expressing the wild-type E3 ligase or the deletion mutant CHIPΔU-box, which despite its lack of ubiquitin ligase activity still associates with the receptor. Overexpression of the dominant negative CHIPΔU-box resulted in abrogation of GA-induced Ron degradation (Fig. 4*A*).

We previously reported that the E3 ubiquitin ligase c-Cbl physically interacts with Ron, promoting its ligand-dependent ubiquitylation and down-regulation (31). To verify the role for c-Cbl in receptor destabilization driven by GA, we performed the parallel experiment in COS-7 transfected with c-Cbl or the dominant negative c-Cbl-70Z (39). Impairment of c-Cbl activity had no effect on GA-induced Ron degradation (Fig. 4*B*).

To confirm the key role of CHIP in GA-mediated Ron destabilization, we analyzed cells deprived of CHIP by expression of targeted siRNAs. FG2 cells were engineered by means of vectors to express siRNAs designed to selectively inactivate CHIP transcripts or targeted to an unrelated sequence as control. Cells expressing CHIP-targeted siRNAs displayed markedly reduced levels of CHIP. In these conditions, Ron was refractory to the degradation induced by GA, whereas in cells expressing control siRNAs, receptor degradation still occurred. Similar results were obtained with the same concentration of 17-AAG (Fig. 4*C*). We conclude that the ubiquitin ligase activity of CHIP is necessary to mediate Ron degradation induced by geldanamycins.

CHIP Is Responsible for Oncogenic Ron^{M1254T} c-Cbl-independent Ubiquitylation—We next addressed the role of CHIP-chaperone complex on the negative regulation of the oncogenic mutant Ron^{M1254T}. This mutant harbors a point mutation responsible for constitutive activation of the kinase and for overcoming the requirement for the multifunctional docking site of the Ron receptor (10, 11).

In COS-7 cells co-expressing c-Cbl and Ron^{M1254T}, the mutant receptor failed to co-immunoprecipitate the ubiquitin ligase, even upon MSP stimulation. Likewise, in the reciprocal experiment, wild-type Ron, but not Ron^{M1254T}, was present in c-Cbl immunoprecipitates of the same cells (Fig. 5*A*). On the basis of these results, we evaluated if the lack of association with c-Cbl could affect Ron^{M1254T} ubiquitylation. In COS-7 cells co-transfected with wild-type or mutant receptor along with c-Cbl and a tagged form of ubiquitin (FLAG-Ub), the ubiquitylation of Ron^{M1254T} was preserved and was ligand-independent (Fig. 5*B*).

To verify if Ron^{M1254T} ubiquitylation *in vivo* relies on the ubiquitin ligase activity of CHIP, we overexpressed CHIP or the defective ligase CHIPΔU-box in COS-7 cells. Endogenous CHIP was sufficient to promote Ron^{M1254T} ubiquitylation, which was increased by overexpression of recombinant CHIP and almost totally abrogated in cells overexpressing CHIPΔ U-box. This demonstrates that CHIP is a functional E3 ubiquitin ligase for this oncogenic receptor (Fig. 5*C*).

On the basis of these data, we sought evidence of the association of Ron^{M1254T} with the chaperone complex containing CHIP. We co-transfected COS-7 cells with cDNAs encoding either Ron^{M1254T} or wild-type Ron and CHIP. Hsp90, Hsc70, and CHIP were more abundant in Ron immunocomplexes from cells expressing the oncogenic receptor, and the stronger interaction between CHIP and Ron^{M1254T} was confirmed by the reciprocal experiment (Fig. 5*D*).

These data altogether indicate that Ron and Ron^{M1254T} differentially interact with the E3 ligase CHIP, which is responsi-

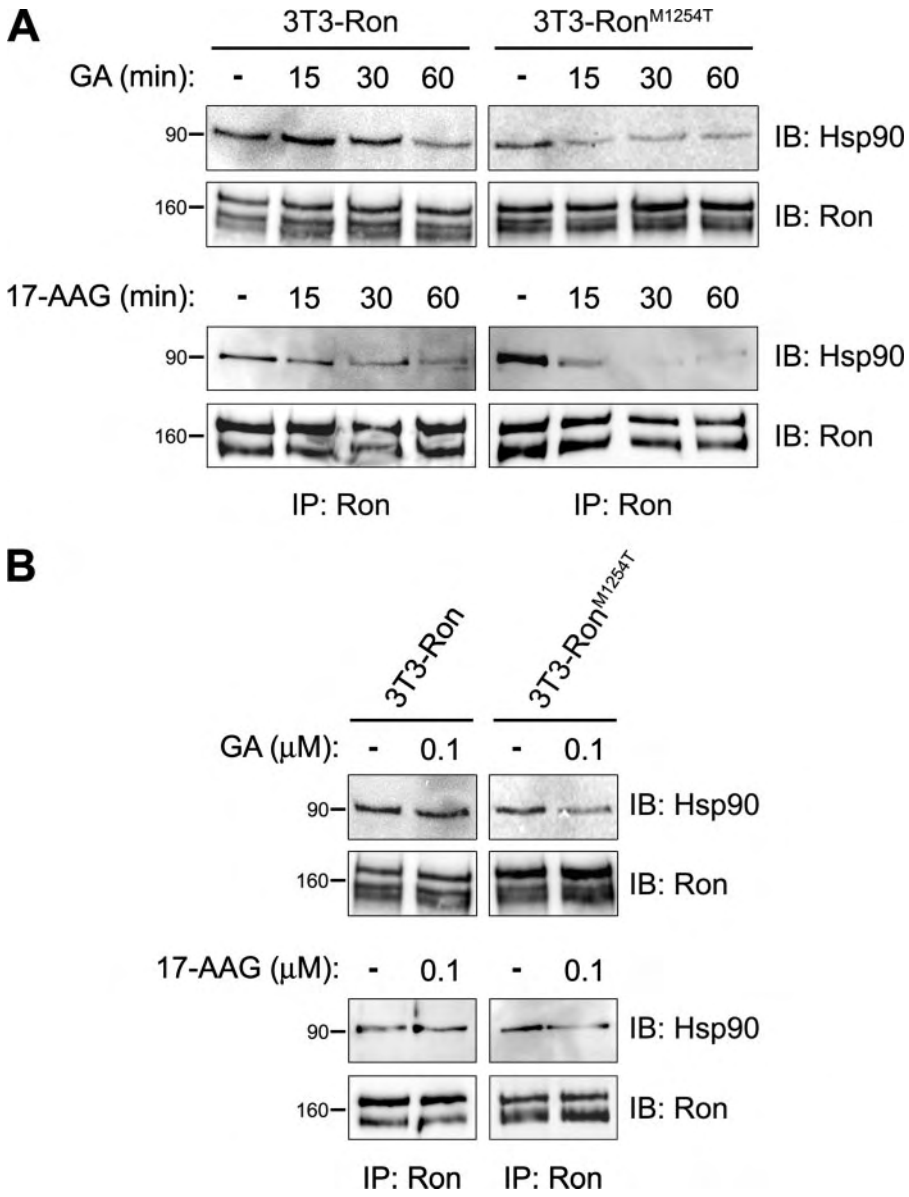

FIGURE 7. **Hsp90 dissociation from Ron^{M1254T} is more rapid and occurs at lower geldanamycin concentrations compared with wild-type receptor.** *A*, 3T3-Ron and 3T3-Ron^{M1254T} cells were treated with vehicle (−) or 1 μM GA or with 1 μM 17-AAG for the indicated times. Equal protein amounts of cell lysates were subjected to immunoprecipitation (*IP*) with Ron antibodies, and associated Hsp90 was detected by immunoblotting (*IB*) with the appropriate antibodies. The immunoprecipitated receptor was detected by Ron immunoblotting. *B*, proteins from cell lysates of 3T3-Ron and 3T3-Ron^{M1254T} treated with vehicle (−) or increasing amounts of GA or of 17-AAG for 6 h were subjected to Ron immunoprecipitation. Associated Hsp90 was detected by immunoblotting with the appropriate antibodies. The immunoprecipitated receptor was detected by Ron immunoblotting. All results shown are representative of at least three independent experiments.

ble for the c-Cbl- and ligand-independent ubiquitylation of the oncogenic receptor.

Oncogenic M1254T Substitution Increases Ron Sensitivity to Geldanamycins—Since oncogenic Ron^{M1254T} is recruited into the CHIP-chaperone complex even more efficiently than wild-type Ron, we tested the activity of GA and 17-AAG on the stability of the wild-type receptor and of its oncogenic counterpart.

The treatment of 3T3-Ron and 3T3-Ron^{M1254T} cells with both inhibitors revealed an accelerated degradation rate for the mutant receptor, as compared with wild-type Ron (Fig. 6*A*). Interestingly, Ron^{M1254T} degradation was paralleled by an evident dephosphorylation of Akt and Erk1/2 effectors (Fig. 6*A*). We further evaluated the relative sensitivity of wild-type and oncogenic Ron to these inhibitory drugs in a dose-response experiment. GA or 17-AAG concentration as low as 0.1 μM was efficient in degrading the mutant Ron^{M1254T} after 6 h of treatment, whereas at least a 1 μM concentration was required to induce detectable degradation of the wild-type receptor (Fig. 6*B*).

The destabilizing effects of GA have been attributed to altered association of Hsp90 with its client proteins (40). Therefore, we tested Ron interaction with Hsp90 upon GA or 17-AAG treatment of 3T3-Ron and 3T3-Ron^{M1254T} cells in a short term experiment (up to 60 min). In both cell types, the receptor co-precipitated with Hsp90, and geldanamycins caused an evident decrease in the amount of Hsp90 associated with Ron immunocomplexes. However, the dissociation of the Ron^{M1254T}-Hsp90 complex occurs earlier, starting within 15 min of drug exposure, as compared with the Ron-Hsp90 complex (Fig. 7*A*). Consistently, by using the lowest effective concentration of GA and 17-AAG (0.1 μM) able to induce degradation of Ron^{M1254T} but not of wild-type Ron, we observed dissociation of Hsp90 from the mutant receptor only (Fig. 7*B*). These results indicate that the oncogenic M1254T substitution in the Ron receptor is associated with increased sensitivity to geldanamycins and with a more dynamic interaction with Hsp90.

Geldanamycins Hamper Growth, Migration, and Transforming Activity of Oncogenic Ron—The amino acid substitution M1254T confers to Ron *in vitro* transforming potential, including growth and migration in a ligand-independent way (10). We tested if the GA derivative suitable for clinical use 17-AAG could hamper these biological effects in 3T3-Ron^{M1254T}. In a 72-h proliferation assay, the higher proliferation rate of 3T3-Ron^{M1254T} cells compared with 3T3-Ron cells was considerably reduced in the presence of low concentrations (0.1 μM) of 17-AAG. As expected, the growth rates of nontransformed 3T3 and 3T3-Ron cells were similar, and, consistently, the reduction of growth rate observed in these cells upon 17-AAG was com-

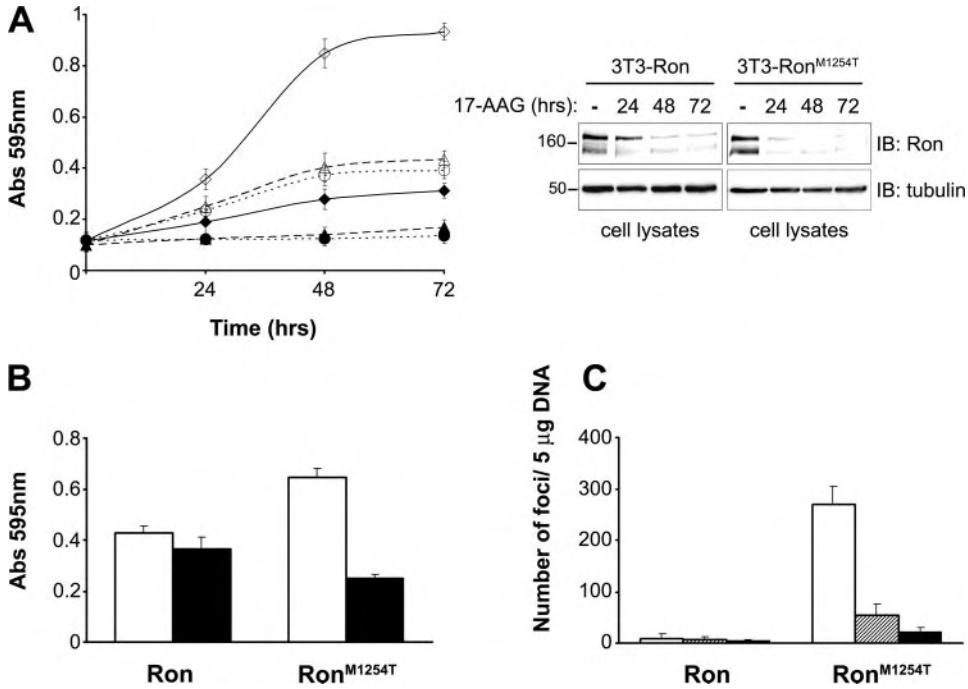

FIGURE 8. **17-AAG potently affects growth, migration, and transformation of cells expressing oncogenic Ron^{M1254T}.** *A*, NIH-3T3 fibroblasts (*dotted curve*), 3T3-Ron (*dashed curve*), and 3T3-Ron^{M1254T} (*solid curve*) cells were plated on 96-well plates and cultured in medium supplemented with 10% fetal bovine serum in presence of vehicle (*white symbols*) or 100 nM 17-AAG (*black symbols*). After 0, 24, 48, and 72 h of drug addition, cells were fixed and stained in crystal violet, and absorbance at 595 nm was measured. OD is expressed as mean $A_{595} \pm$ S.E. of three independent experiments (*left panel*). Protein levels from 3T3-Ron and 3T3 Ron^{M1254T} cell lysates were determined by immunoblotting (*IB*) at same times and conditions of the growth curve (*right panel*). *B*, 3T3-Ron and 3T3-Ron^{M1254T} cells were plated on the *upper side* of 8-μm pore size Transwell® chambers and allowed to migrate for 6 h in the presence of vehicle (*white columns*) or 100 nM 17-AAG (*black columns*) toward the lower chamber containing appropriate medium supplemented with 10% fetal calf serum and coated with fibronectin. Cells that migrated toward the lower chamber were fixed and stained as described in *A*. OD is expressed as mean $A_{595} \pm$ S.E. of three independent experiments. *C*, NIH-3T3 fibroblasts were transfected as described under "Experimental Procedures" with Ron- or Ron^{M1254T}-encoding plasmid. Two days after transfection, vehicle (*white columns*), 10 nM 17-AAG (*hatched columns*), or 50 nM 17-AAG (*black columns*) were added and renewed every 48 h. Cell cultures were maintained at confluence and screened for focus formation 10 $\pm$ 18 days after transfection. Spontaneous formation of foci was negligible. All of the experiments were performed in triplicate, and mean $\pm$ S.E. number of foci is displayed.

parable. Immunoblotting analysis of Ron protein levels under the same experimental conditions confirmed the higher sensitivity of oncogenic Ron^{M1254T} to 17-AAG, even if degradation of also the wild-type receptor occurred upon the prolonged drug exposure (Fig. 8*A*).

In a migration assay, performed in the presence of serum, 3T3-Ron^{M1254T} cells migrated more efficiently than 3T3-Ron cells. The presence of 17-AAG hampered the haptotactic migration of both cell types, and the inhibition was by far more evident in cells expressing the Ron oncogenic form (Fig. 8*B*).

We have previously shown that Ron^{M1254T} has a strong transforming activity when expressed in NIH-3T3 fibroblasts (10). A focus-forming assay was performed in the presence or absence of low doses of 17-AAG. As expected, Ron^{M1254T}-transfected cells displayed a high transforming activity, which was completely abolished by 17-AAG treatment (Fig. 8*C*).

We conclude that the clinically relevant inhibitor 17-AAG is a potent negative regulator of cell proliferation, migration, and transformation, typically induced by the Ron^{M1254T} oncogenic form.

DISCUSSION

Ubiquitylation and down-regulation represent a major deactivation pathway for RTKs, whose impairment may be a mechanism in cancer (41).

Dysregulated signaling of Ron, the tyrosine kinase receptor for MSP, due to over-activation or loss of negative regulation, is involved in tumor progression and metastasis. Overexpression and subsequent aberrant activation of Ron have been observed in primary breast carcinomas (42), non-small cell lung tumors (43), and colorectal adenocarcinomas (44). Silencing *ron* gene expression by RNA interference has been shown to hamper *in vivo* tumor formation of established colorectal carcinoma cells (45). Moreover, it has been reported that Ron expression is positively associated with histological grading, larger size, and tumor stage in bladder cancer specimens (13).

We have previously demonstrated a ligand-induced c-Cbl-dependent mechanism for the down-regulation of Ron (31). Here we identify a novel degradation pathway for Ron. This mechanism involves proteasomal activity, the Hsp90/Hsc70 chaperones and the U-box ubiquitin ligase CHIP. The whole process of receptor degradation is triggered by the small molecule inhibitors of Hsp90 benzoquinone ansamycins via dissociation of the Ron-chaperone complex. The requirement of this complex for Ron stability is confirmed by the destabilizing effects observed also with the Hsp90 inhibitor radicicol, which is chemically unrelated to geldanamycins.

It has been reported that Hsp90 and its cohort of co-chaperones play a regulatory role in conformational maturation and in maintenance of structural integrity of a variety of cellular proteins (17). We show here for the first time that Ron is present in a stable but dynamic complex with the Hsp90/Hsc70-based chaperone machinery, also containing the E3 ligase CHIP. As shown for ErbB2 (20, 40), this complex is required for maintaining Ron receptor stability. This is confirmed by the activity of the Hsp90-inhibitory drugs geldanamycin or 17-AAG, which force disruption of the Ron-Hsp90 interaction, followed by receptor ubiquitylation and degradation. Moreover, conversely to what occurs with c-Cbl-mediated degradation (31), geldanamycin does not require the Ron kinase activity for its action, since the "kinase-dead" Ron^{K1114M} is highly sensitive to this Hsp90 inhibitor.

The effect of geldanamycin has been restricted to the ability of destabilizing newly synthesized EGFR or platelet-derived growth factor receptor molecules (35, 46). On the other hand, it has been also demonstrated that geldanamycin enhances the loss of mature cell surface ErbB2 protein (40, 47), suggesting a lack of univocal mean to target different receptors. Our results clearly indicate that mature Ron exposed at plasma membrane is a target of geldanamycin, as in the case of ErbB2. This is in accordance with the association of mature Ron with the E3 ligase CHIP, which has been characterized as a mediator of geldanamycin action for ErbB2 degradation (20, 47). However, based on our data, we cannot exclude that also the uncleaved precursor of the Ron receptor may be affected by geldanamycins.

Several evidences indicate that the ternary complex of the substrates with chaperones and ubiquitin ligase is targeted to the proteasome for degradation (16). Moreover, recently it has been reported that proteasomal activity is required for ErbB2 internalization but that receptor degradation takes place in lysosomes (48). Our results on Ron confirm that geldanamycin-mediated receptor degradation requires the integrity of the proteasomal pathway but that the lysosomal involvement is dispensable.

A destabilizing effect of geldanamycins has been described for the HGF/SF receptor Met, homologous to Ron (29, 49), but the E3 ligase regulating this process has not been identified yet. Conversely, our results clearly show that Ron is a substrate of CHIP both *in vitro* and *in vivo*. Furthermore, by CHIP RNA interference and by use of a truncated CHIP mutant, we demonstrate that CHIP is necessary for Ron degradation, following Hsp90 inhibition by geldanamycins.

This mechanism of Ron depletion is reminiscent of that shown for ErbB2 (47) and for mutated EGFR (28). Also Ron can harbor oncogenic mutations in a conserved region of the kinase domain (10). One of these substitutions (M1254T) shifts substrate specificity and overcomes the requirement for the multifunctional docking site (11).

We show here that the oncogenic Ron^{M1254T} receptor escapes from c-Cbl mediated down-regulation. Notwithstanding it is efficiently ubiquitylated and becomes degraded upon geldanamycin treatment. Oncogenic Ron degradation occurs even more rapidly than for the nonmutated receptor and at lower doses of the Hsp90 inhibitor. The higher sensitivity of Ron^{M1254T} to geldanamycins may be explained by the stronger interaction of Ron^{M1254T} with Hsp90 and CHIP, compared with wild-type Ron. Similar results were observed also for EGFR mutants (28), v-Src (50), and mutated p53 (51). As hypothesized for other kinases (28), the reason for the greater association of the mutated receptor to the chaperone complex, may reside more on a inherently less stable structure rather than on its altered phosphorylation state.

The effect of Hsp90 inhibition by geldanamycin has been thoroughly investigated and clarified in terms of altered association of the chaperone to its client proteins, which are thus degraded (52). In the case of ErbB2, geldanamycin activity has been associated to a parallel increase of Hsp/Hsc70 association to the receptor (20). We did not observe any reciprocal exchange between Hsp90 and Hsc70 in the binding to either Ron or Ron^{M1254T}. On the other hand, we show the first evidence of a marked and significant difference in dissociation rate from Hsp90, between wild-type and oncogenic Ron receptors, upon geldanamycins treatment. We hypothesize that the ADP/ATP cycling rate of the Hsp90-Ron^{M1254T} complex is higher than that of Hsp90 complex containing Ron. This may explain the higher sensitivity of the oncogenic mutant to geldanamycins. This highlights Ron^{M1254T} as an ideal target for the antioncogenic activity of these drugs.

Cells expressing oncogenic Ron^{M1254T} display ligand-independent, strong constitutive Erk1/2 and phosphatidylinositol 3-kinase/Akt signaling, leading to elevated levels of growth and migration. The less toxic GA-derivative 17-AAG markedly inhibits these signaling pathways, resulting in a strong reduction of growth and migration rates, induced by oncogenic Ron^{M1254T} signaling. We cannot exclude that degradation of intracellular proteins, possibly Ron^{M1254T} effectors, may also contribute to these effects. Nevertheless, this confirms the very high sensitivity of the oncogenic receptor and of its signaling to geldanamycins, resulting in robust inhibition of dysregulated biological activities.

Recently, it has been demonstrated that geldanamycins inhibit HGF/SF-dependent, urokinase-type plasminogen activator-mediated cell scattering and invasion, thus affecting typical tumor cell properties (30). Consistently, our results demonstrate that 17-AAG abrogates the transforming ability of oncogenic Ron. Even if further studies on xenographed immunodeficient mice are required to substantiate the inhibition of Ron oncogenic properties, the overall effects observed in cultured cells strongly suggest that Ron-dependent tumorigenesis is a sensitive target of geldanamycin or its derivatives. We identified a novel Ron destabilization pathway, which highlights the important role of ansamycin antibiotics as potential pharmacological tools, able to target altered Ron expression and dysregulation in cancers.

Acknowledgments—We thank Elena Boggio and Sabrina Pinato for assistance, Simona Corso and Luca Tamagnone for assistance and access to lentiviral methodology and facilities, and Dr. Hamid Band for GST-CHIP constructs.

REFERENCES

1. Blume-Jensen, P., and Hunter, T. (2001) *Nature* **411,** 355–365
2. Bennasroune, A., Gardin, A., Aunis, D., Cremel, G., and Hubert, P. (2004) *Crit. Rev. Oncol. Hematol.* **50,** 23–38
3. Lamorte, L., and Park, M. (2001) *Surg. Oncol. Clin. N. Am.* **10,** 271–288, viii
4. Rowinsky, E. K. (2004) *Annu. Rev. Med.* **55,** 433–457
5. Wang, M. H., Ronsin, C., Gesnel, M. C., Coupey, L., Skeel, A., Leonard, E. J., and Breathnach, R. (1994) *Science* **266,** 117–119
6. Gaudino, G., Follenzi, A., Naldini, L., Collesi, C., Santoro, M., Gallo, K. A., Godowski, P. J., and Comoglio, P. M. (1994) *EMBO J.* **13,** 3524–3532
7. Danilkovitch-Miagkova, A., Miagkov, A., Skeel, A., Nakaigawa, N., Zbar, B., and Leonard, E. J. (2001) *Mol. Cell Biol.* **21,** 5857–5868
8. Santoro, M. M., Gaudino, G., and Marchisio, P. C. (2003) *Dev. Cell* **5,** 257–271
9. Wei, X., Hao, L., Ni, S., Liu, Q., Xu, J., and Correll, P. H. (2005) *J. Biol. Chem.* **280,** 40241–40251
10. Santoro, M. M., Penengo, L., Minetto, M., Orecchia, S., Cilli, M., and

Gaudino, G. (1998) *Oncogene* **17,** 741–749
11. Santoro, M. M., Penengo, L., Orecchia, S., Cilli, M., and Gaudino, G. (2000) *Oncogene* **19,** 5208–5211
12. Wang, M. H., Wang, D., and Chen, Y. Q. (2003) *Carcinogenesis* **24,** 1291–1300
13. Cheng, H. L., Liu, H. S., Lin, Y. J., Chen, H. H., Hsu, P. Y., Chang, T. Y., Ho, C. L., Tzai, T. S., and Chow, N. H. (2005) *Br. J. Cancer* **92,** 1906–1914
14. Persons, D. A., Paulson, R. F., Loyd, M. R., Herley, M. T., Bodner, S. M., Bernstein, A., Correll, P. H., and Ney, P. A. (1999) *Nat. Genet.* **23,** 159–165
15. Peace, B. E., Toney-Earley, K., Collins, M. H., and Waltz, S. E. (2005) *Cancer Res.* **65,** 1285–1293
16. Kamal, A., Boehm, M. F., and Burrows, F. J. (2004) *Trends Mol. Med.* **10,** 283–290
17. Wegele, H., Muller, L., and Buchner, J. (2004) *Rev. Physiol. Biochem. Pharmacol.* **151,** 1–44
18. Siligardi, G., Hu, B., Panaretou, B., Piper, P. W., Pearl, L. H., and Prodromou, C. (2004) *J. Biol. Chem.* **279,** 51989–51998
19. Connell, P., Ballinger, C. A., Jiang, J., Wu, Y., Thompson, L. J., Hohfeld, J., and Patterson, C. (2001) *Nat. Cell Biol.* **3,** 93–96
20. Xu, W., Marcu, M., Yuan, X., Mimnaugh, E., Patterson, C., and Neckers, L. (2002) *Proc. Natl. Acad. Sci. U. S. A.* **99,** 12847–12852
21. Stebbins, C. E., Russo, A. A., Schneider, C., Rosen, N., Hartl, F. U., and Pavletich, N. P. (1997) *Cell* **89,** 239–250
22. Schneider, C., Sepp-Lorenzino, L., Nimmesgern, E., Ouerfelli, O., Danishefsky, S., Rosen, N., and Hartl, F. U. (1996) *Proc. Natl. Acad. Sci. U. S. A.* **93,** 14536–14541
23. Basso, A. D., Solit, D. B., Munster, P. N., and Rosen, N. (2002) *Oncogene* **21,** 1159–1166
24. Gorre, M. E., Ellwood-Yen, K., Chiosis, G., Rosen, N., and Sawyers, C. L. (2002) *Blood* **100,** 3041–3044
25. Goetz, M. P., Toft, D., Reid, J., Ames, M., Stensgard, B., Safgren, S., Adjei, A. A., Sloan, J., Atherton, P., Vasile, V., Salazaar, S., Adjei, A., Croghan, G., and Erlichman, C. (2005) *J. Clin. Oncol.* **23,** 1078–1087
26. Workman, P. (2004) *Cancer Lett.* **206,** 149–157
27. Mimnaugh, E. G., Chavany, C., and Neckers, L. (1996) *J. Biol. Chem.* **271,** 22796–22801
28. Shimamura, T., Lowell, A. M., Engelman, J. A., and Shapiro, G. I. (2005) *Cancer Res.* **65,** 6401–6408
29. Webb, C. P., Hose, C. D., Koochekpour, S., Jeffers, M., Oskarsson, M., Sausville, E., Monks, A., and Vande Woude, G. F. (2000) *Cancer Res.* **60,** 342–349
30. Xie, Q., Gao, C. F., Shinomiya, N., Sausville, E., Hay, R., Gustafson, M., Shen, Y., Wenkert, D., and Vande Woude, G. F. (2005) *Oncogene* **24,** 3697–3707
31. Penengo, L., Rubin, C., Yarden, Y., and Gaudino, G. (2003) *Oncogene* **22,** 3669–3679
32. Ballinger, C. A., Connell, P., Wu, Y., Hu, Z., Thompson, L. J., Yin, L. Y., and Patterson, C. (1999) *Mol. Cell Biol.* **19,** 4535–4545
33. Waterman, H., Levkowitz, G., Alroy, I., and Yarden, Y. (1999) *J. Biol. Chem.* **274,** 22151–22154
34. Brummelkamp, T. R., Bernards, R., and Agami, R. (2002) *Science* **296,** 550–553
35. Sakagami, M., Morrison, P., and Welch, W. J. (1999) *Cell Stress Chaperones* **4,** 19–28
36. Sepp-Lorenzino, L., Ma, Z., Lebwohl, D. E., Vinitsky, A., and Rosen, N. (1995) *J. Biol. Chem.* **270,** 16580–16587
37. Fan, M., Park, A., and Nephew, K. P. (2005) *Mol. Endocrinol.* **19,** 2901–2914
38. Jiang, J., Ballinger, C. A., Wu, Y., Dai, Q., Cyr, D. M., Hohfeld, J., and Patterson, C. (2001) *J. Biol. Chem.* **276,** 42938–42944
39. Waterman, H., and Yarden, Y. (2001) *FEBS Lett.* **490,** 142–152
40. Xu, W., Mimnaugh, E., Rosser, M. F., Nicchitta, C., Marcu, M., Yarden, Y., and Neckers, L. (2001) *J. Biol. Chem.* **276,** 3702–3708
41. Bache, K. G., Slagsvold, T., and Stenmark, H. (2004) *EMBO J.* **23,** 2707–2712
42. Maggiora, P., Marchio, S., Stella, M. C., Giai, M., Belfiore, A., De Bortoli, M., Di Renzo, M. F., Costantino, A., Sismondi, P., and Comoglio, P. M. (1998) *Oncogene* **16,** 2927–2933
43. Willett, C. G., Wang, M. H., Emanuel, R. L., Graham, S. A., Smith, D. I., Shridhar, V., Sugarbaker, D. J., and Sunday, M. E. (1998) *Am. J. Respir. Cell Mol. Biol.* **18,** 489–496
44. Zhou, Y. Q., He, C., Chen, Y. Q., Wang, D., and Wang, M. H. (2003) *Oncogene* **22,** 186–197
45. Xu, X. M., Wang, D., Shen, Q., Chen, Y. Q., and Wang, M. H. (2004) *Oncogene* **23,** 8464–8474
46. Supino-Rosin, L., Yoshimura, A., Yarden, Y., Elazar, Z., and Neumann, D. (2000) *J. Biol. Chem.* **275,** 21850–21855
47. Zhou, P., Fernandes, N., Dodge, I. L., Reddi, A. L., Rao, N., Safran, H., DiPetrillo, T. A., Wazer, D. E., Band, V., and Band, H. (2003) *J. Biol. Chem.* **278,** 13829–13837
48. Lerdrup, M., Hommelgaard, A. M., Grandal, M., and van Deurs, B. (2006) *J. Cell Sci.* **119,** 85–95
49. Maulik, G., Kijima, T., Ma, P. C., Ghosh, S. K., Lin, J., Shapiro, G. I., Schaefer, E., Tibaldi, E., Johnson, B. E., and Salgia, R. (2002) *Clin. Cancer Res.* **8,** 620–627
50. Xu, Y., Singer, M. A., and Lindquist, S. (1999) *Proc. Natl. Acad. Sci. U. S. A.* **96,** 109–114
51. Esser, C., Scheffner, M., and Hohfeld, J. (2005) *J. Biol. Chem.* **280,** 27443–27448
52. Isaacs, J. S., Xu, W., and Neckers, L. (2003) *Cancer Cell* **3,** 213–217

Available online at www.sciencedirect.com
ScienceDirect
Virus Research xxx (2006) xxx–xxx
Virus Research
www.elsevier.com/locate/virusres

Short communication

Alpha- and betapapillomavirus E6/E7 genes differentially modulate pro-inflammatory gene expression

Marco De Andrea [a,b,1], Michele Mondini [a,b,1], Barbara Azzimonti [b], Valentina Dell'Oste [b], Serena Germano [c], Giovanni Gaudino [c], Tiziana Musso [a], Santo Landolfo [a], Marisa Gariglio [b,*]

[a] *Department of Public Health and Microbiology, Medical School of Torino,Via Santena 9, 10126 Torino, Italy*
[b] *Department of Clinical and Experimental Medicine, Medical School of Novara, Via Solaroli 17, 28100 Novara, Italy*
[c] *DISCAFF & DFB Center, University of Piemonte Orientale "A. Avogadro", Via Bovio 6, 28100 Novara, Italy*

Received 19 June 2006; received in revised form 28 September 2006; accepted 28 September 2006

Abstract

Keratinocytes, the target cell of human papillomavirus (HPV) infection, can produce numerous cytokines and pro-inflammatory molecules which are important for the generation of an effective immune response. How this biological response, which involves the tumor stroma, is affected by the HPV oncoproteins within the epithelial cell itself is not clear. Here it is shown that oncoproteins of different HPV genotypes (alpha- versus beta-HPV genus) alter the expression of pro-inflammatory molecules in early passage primary human keratinocytes and the immortalized cell line HaCaT. HPV5 E6/E7 oncoproteins significantly induced interleukin-8 (IL-8), monocyte chemoattractant protein-1 (MCP-1) and intercellular adhesion molecule-1 (ICAM-1) expression. By contrast, the same molecules were down-regulated or not modulated in HPV16 E6/E7 transduced keratinocytes. Interestingly, HPV38 oncoproteins expression resulted in a lower induction of pro-inflammatory molecules, resembling the behavior displayed by the mucosal carcinogenic HPV16. Finally, inducible nitric oxide synthase (iNOS) expression levels and nitric oxide (NO) production were induced at similar levels by all the HPV genotypes tested. These results further emphasize the different biological activities among HPV genotypes, and offer new insights into HPV-associated skin diseases.

Keywords: Cytokines; Immune evasion; Inflammation; Nitric oxide; Papillomavirus; Skin diseases

Human papillomaviruses (HPVs) are small double-stranded DNA viruses found in a wide variety of proliferative lesions of epithelial origin, and can be grouped into either mucosal or cutaneous HPV types based on tissue tropism. Infection with a subset of high-risk mucosal HPV (HPV16, 18, 31, 33 being the most widespread) is the major risk factor for the development of cervical cancer (zur Hausen, 2002). Several experimental studies have indicated that much of the transforming potential of high-risk HPVs and their ability to stimulate proliferation arises from the biological effects of their E6 and E7 oncoproteins. However, HPV *per se* is not sufficient to permanently transform epithelial cells and to give rise to invasive cervical cancer. The host's cell-mediated immune response influences both susceptibility to and regression of HPV infections. Several studies have described a localized immune dysfunction accompanying cervical HPV infection, suggesting that the high-risk mucosal genotypes may interfere with recruitment or activation of lymphocytes and macrophages (O'Brien and Saveria Campo, 2002).

The cutaneous HPV types are phylogenetically distant from the mucosal types. Evidence for their involvement in non-melanoma skin cancer (NMSC) originated from studies of patients suffering from the rare hereditary disease epidermodysplasia verruciformis (EV), that results from abnormal susceptibility to infection with specific HPV types commonly referred to as EV-HPV types (Akgul et al., 2006). Although EV-HPV types were previously considered to be restricted to EV patients, it has became increasingly evident that they also occur at high frequency in the healthy general population, in patients with NMSC, and in patients with psoriasis. According to the most updated *Papillomaviridae* classification, the EV-HPVs and phylogenetically related types are grouped together into the *Betapa-*

* Corresponding author. Tel.: +39 0321 660649; fax: +39 0321 620421.
E-mail address: gariglio@med.unipmn.it (M. Gariglio).
[1] These authors contributed equally to this work.

0168-1702/$ – see front matter © 2006 Elsevier B.V. All rights reserved.
doi:10.1016/j.virusres.2006.09.010

pillomavirus genus, while the mucosal genotypes belong to the *Alphapapillomavirus* genus (de Villiers et al., 2004). Attempts to identify mechanisms by which the beta-HPV genotypes can contribute to NMSC development revealed a rather weak transforming potential in vitro. No single HPV genotype predominates in skin cancers and so far, there has been no evidence of high-risk types analogous to cervical cancer for the beta-genus (Harwood and Proby, 2002; Pfister, 2003). Thus, the mechanisms of HPV induced skin carcinogenesis are still not fully established and differ substantially from the much better explored genital oncogenesis.

Keratinocytes, the target cell of HPV infection, can produce numerous cytokines which are important for the generation of an effective immune response and thus may contribute to controlling the development of squamous intraepithelial lesions. How the biological response, which involves the tumor stroma, is affected by the HPV oncoproteins within the epithelial cell itself is not clear (Balkwill et al., 2005).

The present study was undertaken to evaluate whether the expression of HPV oncoproteins from either alpha- or beta-genus could be associated with altered expression of pro-inflammatory molecules in human epithelial cells. To this end, normal human epidermal keratinocytes (NHEK) and the non-transformed spontaneously-immortalized cell line HaCaT were transduced with recombinant retroviruses containing the E6 and E7 genes from the indicated genotypes. The rationale for comparing NHEK with HaCaT cells lies in the fact that the immortal cell lines (such as HaCaT) and tumor-derived cell lines (such as HeLa, Caski, SiHa) used in other studies harbour alterations in various molecular pathways that may lead to abnormal responses following HPV infection. HPV5 and 38 were chosen for this investigation, as they broadly represent the beta-genotypes (ex EV-HPVs) in the *Papillomaviridae* family that are involved in skin cancer. HPV16, belonging to the alpha-genus, was included as the prototype of mucosal high-risk genotype. High-titer recombinant retroviruses were generated by transient transfection of Phoenix cells with pLXSN vector containing the E6/E7 open reading frame from HPV5, 16 and 38 and used to infect NHEK or HaCaT cells as previously described (Pear et al., 1993). After G418 selection, the presence of the transgenes was confirmed by RT-PCR analysis. As shown in Fig. 1, E6 and E7 genes were transcribed at similar levels in each cell culture. As negative control, cells were infected with the empty parental vector virus. NHEK from two different pools were used independently to exclude variation due to the specific genetic background. To investigate at the molecular level whether transduction of the E6 and E7 genes induced changes in mRNA expression of pro-inflammatory genes, real-time RT-PCR was performed. Gene expression was determined with commercial assays from Applied Biosystems. The housekeeping gene hypoxanthine phosphoribosyltransferase 1 was used to normalize for the variations in cDNA. PCR on each sample was performed in triplicate. The results were analyzed with a relative expression software tool (REST-384) (Pfaffl et al., 2002) and down-regulations were calculated as minus reciprocal expression ratio. In our culture conditions, IL-8 mRNA expression levels were increased 7.7- and 5.5-fold by HPV5

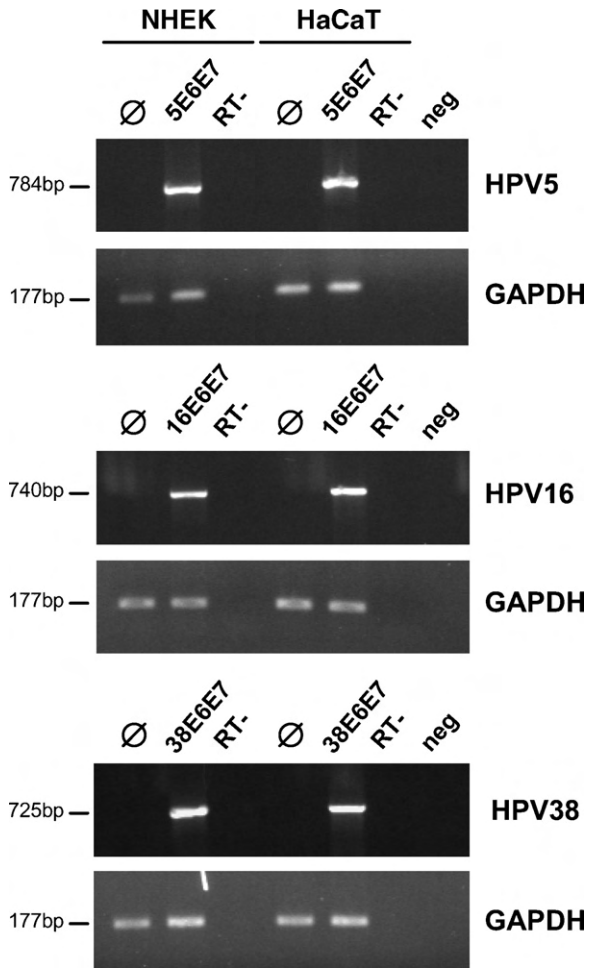

Fig. 1. Analysis of E6E7 transcription levels in NHEK and HaCaT cells transduced with E6/E7 from HPV5, 16 and 38. Ø, cells infected with the vector-only virus. RT-, control reaction in which reverse transcriptase enzyme was omitted in the RT step to exclude genomic contaminations. Glyceraldehyde-3-phosphate dehydrogenase (GAPDH) amplification was performed to normalized variation in cDNA. The results shown are from a representative experiment of three independent infections from two separate pools of cells.

E6/E7 compared to the control in both NHEK and HaCaT cells, respectively, as shown in Fig. 2A. A different picture emerged with the other two HPV genotypes. HPV38 E6/E7 induced a slight increase (3.1-fold) in IL-8 mRNA expression in NHEK, whereas it did not significantly change its levels in HaCaT. By contrast, HPV16 E6/E7 decreased IL-8 mRNA levels in NHEK (4.4-fold), while it slightly up-regulated its expression in HaCaT cells. When the levels of secreted IL-8 were assessed by ELISA using the Quantikine Human IL-8 Immunoassay (R&D Systems) in cell supernatants (Fig. 2B), consistent with the mRNA expression analysis, HPV5 E6/E7 proteins significantly enhanced the release of IL8 in NHEK compared to control cells transduced with the empty vector (820 pg/mg versus 410 pg/mg, respectively). HPV16 E6/E7 proteins decreased IL-8 production when compared to empty vector-transduced NHEK. A similar pattern of IL-8 release was observed with HaCaT cells. Thus, IL-8, one of the most potent neutrophil chemoattractants involved in the early stages of the inflammatory response, was found to be significantly increased at

Please cite this article in press as: De Andrea, M. et al., Alpha- and betapapillomavirus E6/E7 genes differentially modulate pro-inflammatory gene expression, Virus Res. (2006), doi:10.1016/j.virusres.2006.09.010

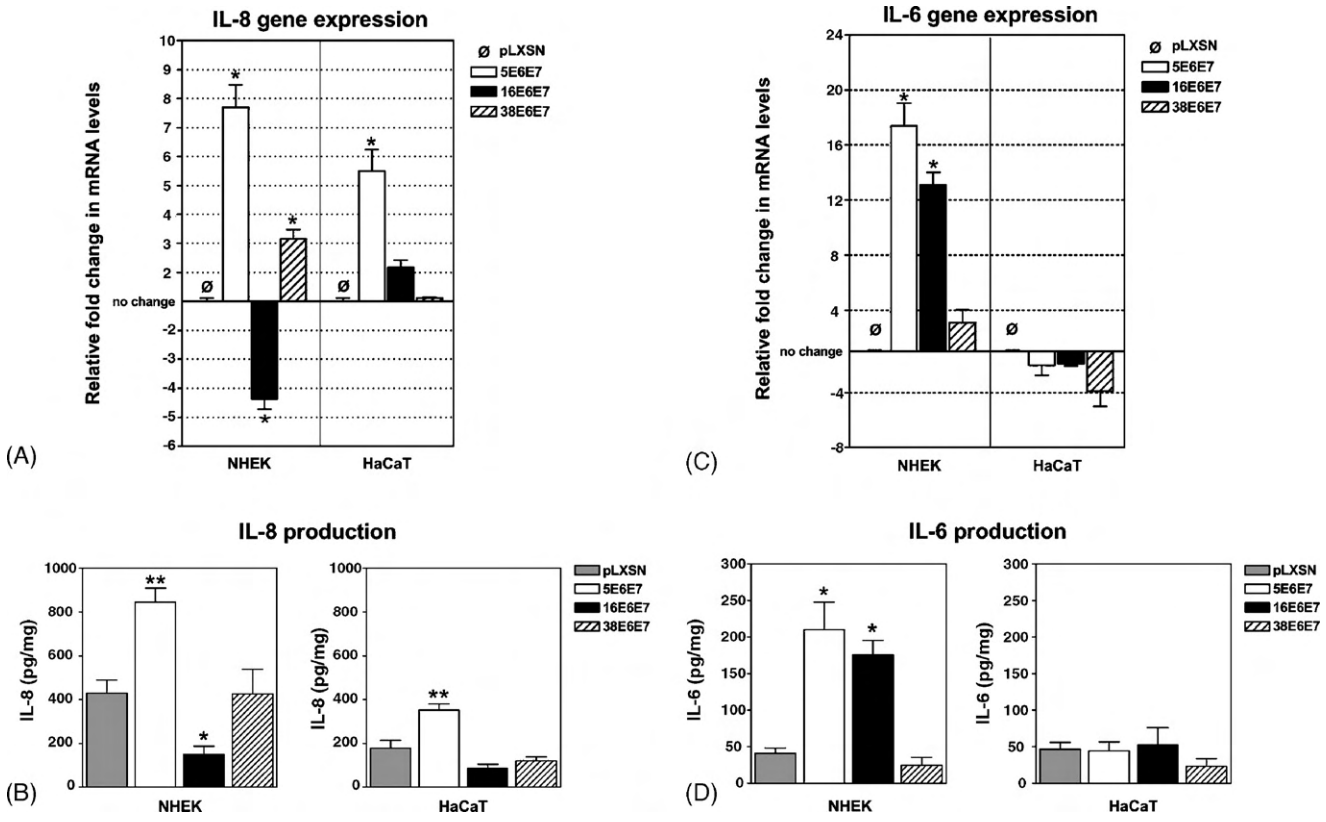

Fig. 2. Comparison of IL-8 and IL-6 mRNA and protein levels in NHEK and HaCaT cells transduced with E6/E7 from HPV5, 16 and 38 as indicated. pLXSN, cells infected with the vector-only virus. (A and C) Total RNA was extracted and mRNA transcript levels were determined by real-time RT-PCR. Expression was normalized to the endogenous control gene HPRT1, and is shown as mean ± S.E. fold changes relative to control-infected cells. (B and D) ELISA analysis was conducted on supernatants of the cells to detect IL-8 and IL-6 expression. Cytokines were normalized to the total amount of secreted protein. Results shown in the four panels are an average of three independent infections from two separate pools of cells with standard errors displayed (*$p < 0.05$, **$p < 0.01$).

both mRNA and protein levels by E6/E7 oncoproteins from the beta-genotype HPV5, while HPV16 E6/E7 down-regulated its production in both the cell lines tested. Controversial data exist about IL-8 modulation by HPV16 oncoproteins. Some authors reported that the expression of HPV16 E6 and E7 increased the secretion of IL-8, while others did not observe any significant variation in its expression (Nees et al., 2001; Toussaint-Smith et al., 2004). Reporter data also showed that HPV16 E6/E7 represses IL-8 promoter activity through effects on CREB binding protein/p300 and P/CAF (Huang and McCance, 2002).

Some cervical carcinoma cell lines have shown to synthesize IL-6 (Castrilli et al., 1997), a cytokine that plays a key role in inflammation being the main inducer of acute phase proteins (Iglesias et al., 1995). To determine if IL-6 production could be influenced by E6/E7 expression in our experimental system, its expression was analysed at both mRNA and protein levels. As shown in Fig. 2C, IL-6 mRNA levels were significantly up-regulated (17.4-fold) by HPV5 E6/E7 expression and to a lower extent by HPV16 oncoproteins (13.1-fold). HPV38 E6/E7 gave rise to the lowest induction rate (3.1-fold). By contrast, in HaCaT cells IL-6 mRNA was weakly down-regulated by all three HPV genotypes. Analysis of IL-6 secretion from these cells by ELISA, using Quantikine Human IL-6 Immunoassay (R&D Systems), showed that levels of IL-6 protein in the cell supernatants corresponded to levels of mRNA expression (Fig. 2D).

Although MCP-1 expression is induced after infection by a variety of RNA and DNA viruses, its suppression by high-risk mucosal HPV has been reported both *in vitro* and *in vivo* (Kleine-Lowinski et al., 2003). Consistent with this finding, it was found that MCP-1 mRNA levels were down-regulated in HPV16 E6/E7 transduced NHEK, but in striking contrast, it was strongly up-regulated in HPV16 E6/E7 transduced HaCaT cells (Fig. 3A). Similarly, HPV38 E6/E7 down-regulated its expression in NHEK, but not in HaCaT cells. Analysis of chemokine secretion from these cells by ELISA, using Quantikine Human MCP-1/CCL2 Immunoassay (R&D Systems), showed that levels of MCP-1 protein in the cell supernatants corresponded to levels of mRNA expression (Fig. 3B). These controversial results between NHEK and HaCaT further emphasize the importance of studying cellular HPV responses in primary human cells rather than immortalized or tumor-derived cells. The selective induction of MCP-1 after HPV5 E6/E7 transduction of NHEK may have an important implication for the pathogenesis of skin inflammatory disorders associated with the presence of beta-HPV genotypes, such as EV or psoriasis.

The intercellular adhesion molecule-1 (ICAM-1, CD54) is a member of the immunoglobulin gene superfamily. A previous report showed that HPV16-immortalized and carcinoma-

Please cite this article in press as: De Andrea, M. et al., Alpha- and betapapillomavirus E6/E7 genes differentially modulate pro-inflammatory gene expression, Virus Res. (2006), doi:10.1016/j.virusres.2006.09.010

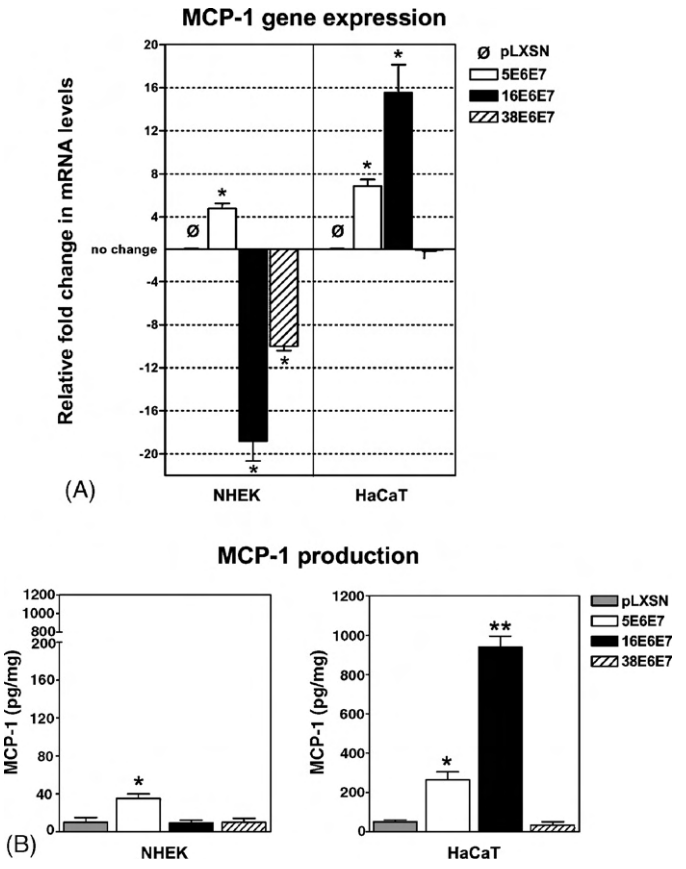

Fig. 3. Comparison of MCP-1 mRNA and protein levels in NHEK and HaCaT cells transduced with E6/E7 from HPV5, 16 and 38 as indicated. pLXSN, cells infected with the vector-only virus. (A) Total RNA was extracted, and MCP-1 mRNA transcript levels were determined by real-time RT-PCR. Expression was normalized to the endogenous control gene HPRT1, and is shown as mean ± S.E. fold changes relative to control-infected cells. (B) ELISA analysis was conducted on supernatants of the cells to detect MCP-1 expression. MCP-1 was normalized to the total amount of secreted protein. The results shown in panels A and B are an average of three independent infections from two separate pools of cells with standard errors displayed (*$p < 0.05$, **$p < 0.01$).

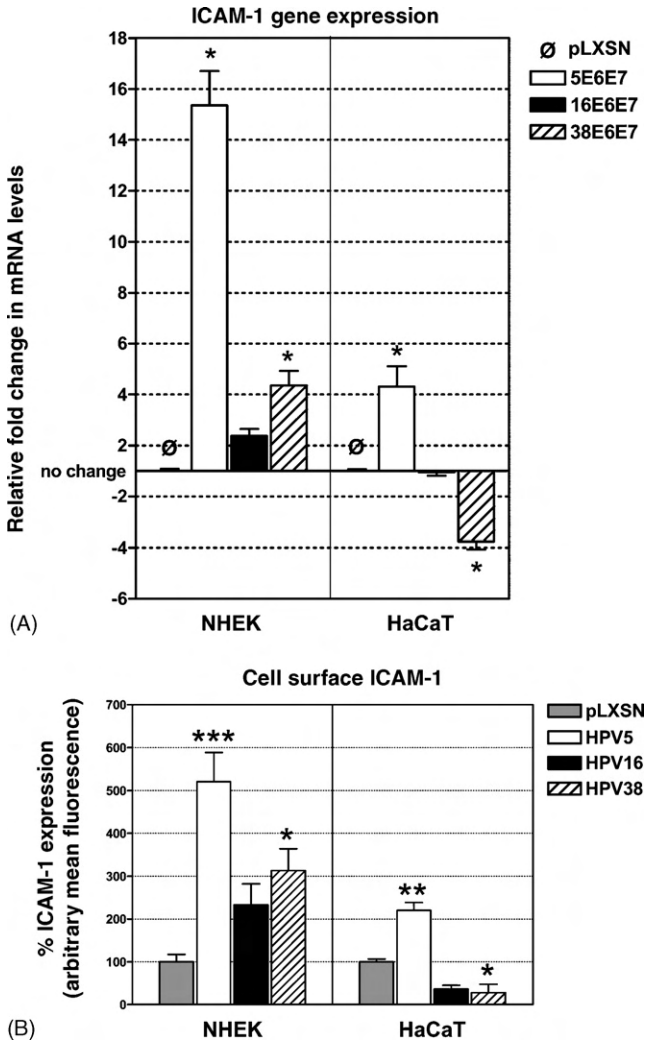

Fig. 4. Comparison of ICAM-1 mRNA and protein levels in NHEK and HaCaT cells transduced with E6/E7 from HPV5, 16 and 38 as indicated. pLXSN, cells infected with the vector-only virus. (A) Total RNA was extracted, and MCP-1 mRNA transcript levels were determined by real-time RT-PCR. Expression was normalized to the endogenous control gene HPRT1, and is shown as mean ± S.E. fold changes relative to control-infected cells. (B) ICAM-1 expression was measured by using a flow cytometer. Data are presented as percent compared to empty vector-transduced cells. The results shown in panels A and B are an average of three independent infections from two separate pools of cells with standard errors displayed (*$p < 0.05$, **$p < 0.01$, ***$p < 0.001$).

derived cell lines exhibited partial or complete loss of ICAM-1 inducibility after exposure to IFN-γ (Woodworth and Simpson, 1993). Consistent with this report, both NHEK and HaCaT cells transduced with HPV16 E6/E7 did not show a significant variation in the ICAM-1 RNA levels in comparison with control-infected cells (Fig. 4A). By contrast, its expression was markedly enhanced in HPV5 E6/E7 transduced cells, although the magnitude of the induction was higher in NHEK (15.5-fold) in comparison to HaCaT cells (4.2-fold). A different picture was observed with HPV38 E6/E7 transduced cells, being up-regulated in NHEK (4.2-fold) but down-regulated in HaCaT cells (3.8-fold). The effects of HPV oncoproteins on the expression of ICAM-1 antigen was also determined by FACS analysis as previously described (Roy et al., 1998). Basal ICAM-1 expression levels were very low in unstimulated cells. Consistent with mRNA analysis, ICAM-1 antigens were significantly up-regulated by HPV5 oncoproteins in both NHEK and HaCaT cells (Fig. 4B).

A variety of viruses have been reported to induce iNOS (inducible nitric oxide synthase), leading to nitric oxide (NO) production that has been shown to play a relevant role in viral clearance, immunopathology and generation of DNA damage (Machida et al., 2004; Reiss and Komatsu, 1998). To examine whether NO is also involved in HPV pathogenesis, we first determined the level of iNOS mRNA in HPV-transduced cells using real-time RT-PCR. As illustrated in Fig. 5A, transduction of E6/E7 from all three genotypes dramatically enhanced the levels of iNOS mRNA in HaCaT cells. Similar results were obtained in NHEK, although in this cellular model HPV5 oncoproteins gave rise to the maximum induction (16-fold) in comparison to the other genotypes. To confirm that the iNOS induction seen was functionally significant, supernatant levels of NO_2^-/NO_3^-, which are the final products of NO *in vivo*, were determined using a colorimetric assay kit (Cayman Chem-

Please cite this article in press as: De Andrea, M. et al., Alpha- and betapapillomavirus E6/E7 genes differentially modulate pro-inflammatory gene expression, Virus Res. (2006), doi:10.1016/j.virusres.2006.09.010

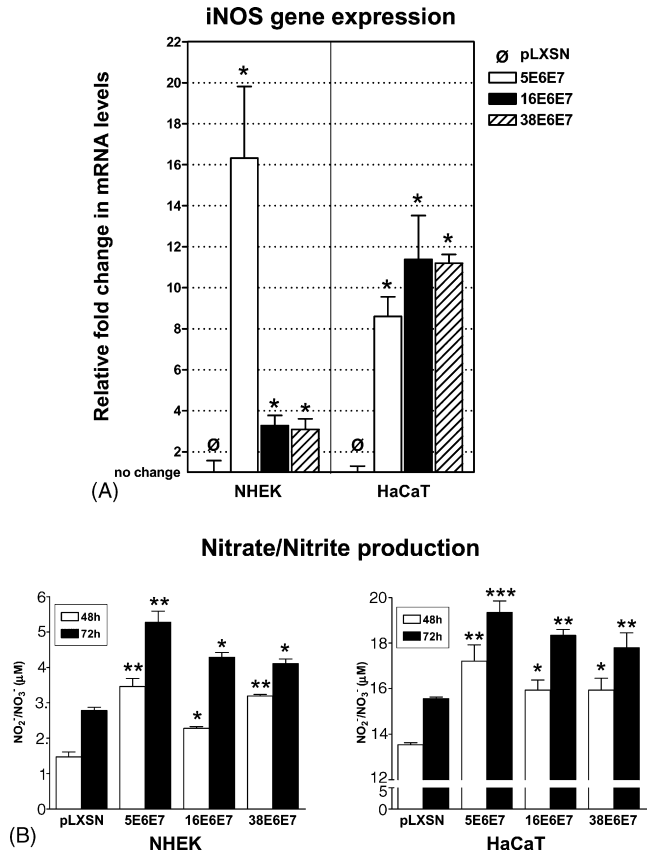

Fig. 5. Induction of iNOS gene expression and NO production in NHEK and HaCaT cells stably transduced with E6/E7 from HPV5, 16 and 38. pLXSN, cells infected with the vector-only virus. (A) Total RNA was extracted, and iNOS mRNA transcript levels were determined by real-time RT-PCR. Expression was normalized to the endogenous control gene HPRT1, and is shown as mean ± S.E. fold changes relative to control-infected cells. (B) NO_2^-/NO_3^- production in cell culture medium collected at 48 and 72 h after plating. The results shown in panels A and B are an average of three independent infections from two separate pools of cells with standard errors displayed (*$p < 0.05$, **$p < 0.01$, ***$p < 0.001$).

ical, Ann Arbor, USA). Consistent with the mRNA analysis, the amount of nitrites and nitrates produced by E6/E7 transduced cells, from all three HPV genotypes, was significantly higher than those in the control cells (Fig. 5B). These results demonstrated that E6/E7 transduction enhanced the production of nitrites and nitrates as a result of iNOS activation.

In addition, modulation of tumor necrosis factor (TNF)-α, another proinflammatory cytokine, was also evaluated. In our experimental system, we did not detect any significant variation of TNF-α expression at both mRNA and protein levels by all three HPV genotypes (data not shown).

This is the first report that compares the expression of pro-inflammatory genes by E6/E7 proteins between alpha- and beta-HPV genotypes in primary human keratinocytes. Our results suggest that HPV16 E6/E7 oncoproteins may contribute to the development of cervical cancer not only by disrupting cell cycle regulation but also by creating a microenvironment that reduces host's immune surveillance and therefore fosters cell growth. By contrast, both mRNA and protein analysis showed that HPV5 E6/E7 oncoproteins altered the keratinocytes gene expression in favour of factors that have been shown to promote strong inflammation. Indeed, expression of IL-8, IL-6, MCP-1 and ICAM-1, all potent inducers of the cross-talk between keratinocytes and inflammatory cells, increased in HPV5 E6 and E7 expressing cells. It is well established that the host immune response is vital in protection against papillomavirus, and failure of virus clearance leading to its persistence is attributable to a poor immunological response (O'Brien and Saveria Campo, 2002). Consistent with this hypothesis, in this study it has been demonstrated that HPV16 may escape host immune surveillance by inhibiting MCP-1 and IL-8 expression. By contrast, the same inflammatory mediators that are released by HPV5 E6/E7 transduced cells activate local professional antigen-presenting cells such as Langerhans cells in the skin, allowing them to efficiently process and present foreign antigen to naïve T cells, thus initiating an effector lymphocyte response via the expansion of virus-specific lymphocytes. Worthy of note, the lower induction of pro-inflammatory molecules observed with HPV38, the only beta-genotype that is able to immortalize primary human keratinocytes through alteration of p53 and pRb function, resembles the behavior displayed by the mucosal carcinogenic HPV16 (Caldeira et al., 2003). These results further emphasize the different biological activities among genotypes, and offer new insights into HPV-associated skin diseases.

Acknowledgements

This work was supported by Associazione Italiana per la Ricerca sul Cancro (AIRC), Special Oncology Project "Compagnia di San Paolo", MIUR ("Programma 40%" to S.L.), and Regione Piemonte "Ricerca Sanitaria Finalizzata e Applicata (CIPE)". M.M. is a recipient of a Research Fellowship from "Fondazione Internazionale di Ricerca in Medicina Sperimentale, Turin". V.D.O. is a recipient of a Ph.D. Fellowship from "Fondazione Cassa di Risparmio di Vercelli". The authors thank M. Tommasino, J. ter Schegget and L. Struijk for providing retroviral constructs, and U. Dianzani for helpful discussion.

References

Akgul, B., Cooke, J.C., Storey, A., 2006. HPV-associated skin disease. J. Pathol. 208 (2), 165–175.

Balkwill, F., Charles, K.A., Mantovani, A., 2005. Smoldering and polarized inflammation in the initiation and promotion of malignant disease. Cancer Cell 7 (3), 211–217.

Caldeira, S., Zehbe, I., Accardi, R., Malanchi, I., Dong, W., Giarre, M., de Villiers, E.M., Filotico, R., Boukamp, P., Tommasino, M., 2003. The E6 and E7 proteins of the cutaneous human papillomavirus type 38 display transforming properties. J. Virol. 77 (3), 2195–2206.

Castrilli, G., Tatone, D., Diodoro, M.G., Rosini, S., Piantelli, M., Musiani, P., 1997. Interleukin 1alpha and interleukin 6 promote the in vitro growth of both normal and neoplastic human cervical epithelial cells. Br. J. Cancer 75 (6), 855–859.

de Villiers, E.M., Fauquet, C., Broker, T.R., Bernard, H.U., zur Hausen, H., 2004. Classification of papillomaviruses. Virology 324 (1), 17–27.

Harwood, C.A., Proby, C.M., 2002. Human papillomaviruses and non-melanoma skin cancer. Curr. Opin. Infect. Dis. 15 (2), 101–114.

Please cite this article in press as: De Andrea, M. et al., Alpha- and betapapillomavirus E6/E7 genes differentially modulate pro-inflammatory gene expression, Virus Res. (2006), doi:10.1016/j.virusres.2006.09.010

Huang, S.M., McCance, D.J., 2002. Down regulation of the interleukin-8 promoter by human papillomavirus type 16 E6 and E7 through effects on CREB binding protein/p300 and P/CAF. J. Virol. 76 (17), 8710–8721.

Iglesias, M., Plowman, G.D., Woodworth, C.D., 1995. Interleukin-6 and interleukin-6 soluble receptor regulate proliferation of normal, human papillomavirus-immortalized, and carcinoma-derived cervical cells in vitro. Am. J. Pathol. 146 (4), 944–952.

Kleine-Lowinski, K., Rheinwald, J.G., Fichorova, R.N., Anderson, D.J., Basile, J., Munger, K., Daly, C.M., Rosl, F., Rollins, B.J., 2003. Selective suppression of monocyte chemoattractant protein-1 expression by human papillomavirus E6 and E7 oncoproteins in human cervical epithelial and epidermal cells. Int. J. Cancer 107 (3), 407–415.

Machida, K., Cheng, K.T., Sung, V.M., Shimodaira, S., Lindsay, K.L., Levine, A.M., Lai, M.Y., Lai, M.M., 2004. Hepatitis C virus induces a mutator phenotype: enhanced mutations of immunoglobulin and protooncogenes. Proc. Natl. Acad. Sci. U.S.A. 101 (12), 4262–4267.

Nees, M., Geoghegan, J.M., Hyman, T., Frank, S., Miller, L., Woodworth, C.D., 2001. Papillomavirus type 16 oncogenes downregulate expression of interferon-responsive genes and upregulate proliferation-associated and NF-kappaB-responsive genes in cervical keratinocytes. J. Virol. 75 (9), 4283–4296.

O'Brien, P.M., Saveria Campo, M., 2002. Evasion of host immunity directed by papillomavirus-encoded proteins. Virus Res. 88 (1–2), 103–117.

Pear, W.S., Nolan, G.P., Scott, M.L., Baltimore, D., 1993. Production of high-titer helper-free retroviruses by transient transfection. Proc. Natl. Acad. Sci. U.S.A. 90 (18), 8392–8396.

Pfaffl, M.W., Horgan, G.W., Dempfle, L., 2002. Relative expression software tool (REST) for group-wise comparison and statistical analysis of relative expression results in real-time PCR. Nucleic Acids Res. 30 (9), e36.

Pfister, H., 2003. Chapter 8: Human papillomavirus and skin cancer. J. Natl. Cancer Inst. Monogr. 31, 52–56.

Reiss, C.S., Komatsu, T., 1998. Does nitric oxide play a critical role in viral infections? J. Virol. 72 (6), 4547–4551.

Roy, S., Sen, C.K., Kobuchi, H., Packer, L., 1998. Antioxidant regulation of phorbol ester-induced adhesion of human Jurkat T-cells to endothelial cells. Free Radic. Biol. Med. 25 (2), 229–241.

Toussaint-Smith, E., Donner, D.B., Roman, A., 2004. Expression of human papillomavirus type 16 E6 and E7 oncoproteins in primary foreskin keratinocytes is sufficient to alter the expression of angiogenic factors. Oncogene 23 (17), 2988–2995.

Woodworth, C.D., Simpson, S., 1993. Comparative lymphokine secretion by cultured normal human cervical keratinocytes, papillomavirus-immortalized, and carcinoma cell lines. Am. J. Pathol. 142 (5), 1544–1555.

zur Hausen, H., 2002. Papillomaviruses and cancer: from basic studies to clinical application. Nat. Rev. Cancer 2 (5), 342–350.

Please cite this article in press as: De Andrea, M. et al., Alpha- and betapapillomavirus E6/E7 genes differentially modulate pro-inflammatory gene expression, Virus Res. (2006), doi:10.1016/j.virusres.2006.09.010

IMATINIB MESYLATE WITH GEMCITABINE AND PEMETREXED: A NOVEL APPROACH TO MESOTHELIOMA THERAPY

Pietro Bertino[1], Camillo Porta [2], Dario Barbone[1], Serena Germano[1], Sara Busacca[1], Sabrina Pinato[1], Giancarlo Tassi[3], Roberto Favoni[4], Giovanni Gaudino[1#], and Luciano Mutti[5#]

[1] DISCAFF Department and DFB Center, University of Piemonte Orientale "A. Avogadro", Novara, Italy

[2] Medical Oncology, IRCCS San Matteo University Hospital, Pavia, Italy

[3] Chest Medicine Unit, Brescia Hospital, Brescia, Italy

[4] National Cancer Institute, Genoa, Italy

[5] Local Health Unit 11 Piemonte/Institute for Research and Care "S. Maugeri" Foundation, Pavia, Italy.

# these authors gave equal contribution

Financial support: Associazione Italiana per la Ricerca sul Cancro (AIRC), Buzzi Foundation for the study of Mesothelioma, Italian Group for the Study and Therapy for Mesothelioma (G.I.Me.), Novartis Pharma

Corresponding author:

Giovanni Gaudino, DISCAFF & DFBC, Via Bovio, 6 – 28100 Novara - Italy

Phone:+39.0321.375815 - Fax:+39.0321.375821; e-mail: giovanni.gaudino@unipmn.it

Keywords: Pleural Neoplasm; Protein Kinase Inhibitors; Chemotherapy; Drug Synergism

Word count: 2470 words

ABSTRACT

Malignant Mesothelioma is a cancer refractory to current therapies. Imatinib Mesylate (STI571, Glivec™) is a selective inhibitor of tyrosine kinases as bcr-abl, kit, fms and Platelet Derived Growth Factor Receptor β (PDGFRβ). PDGFRβ is often overexpressed in Mesothelioma cells and is a therapeutic target for Imatinib in some solid tumors. The aim of this study is to assess whether Imatinib alone or combined with chemotherapeutic agents may be successful for mesothelioma therapy. Mesothelioma cells from pleural effusions of patients were treated with Imatinib alone or in combination with chemotherapeutics. We show here that Imatinib induces cytotoxicity and apoptosis selectively on PDGFRβ positive Mesothelioma cells, *via* blockade of receptor phosphorylation and interference with the Akt pathway. Among chemotherapeutics tested in combination, Imatinib synergizes with Gemcitabine and Pemetrexed. We provide a rationale for a novel translational approach to mesothelioma therapy, relying on enhancement of tumor chemosensitivity, via inhibition of Akt.

INTRODUCTION

Malignant Mesothelioma (MMe) is an asbestos-related malignant tumor, whose incidence is dramatically expected to raise in the next decade in Europe (1, 2), while in U.S.A. it has already increased in frequency by 90% in the last years (3). Due to its biological aggressiveness, MMe is unfortunately fatal except in rare cases, with a median survival of 12.6 months (4, 5).

Despite multimodality therapy with surgery, chemotherapy and radiotherapy has improved survival in the early stages of the disease (6) and a pemetrexed-containing chemotherapeutic regimen proved to be of benefit for advanced patients (7), novel and more effective systemic therapies for this tumor are definitively needed.

A number of growth factors such as Hepatocyte Growth Factor (HGF) (8, 9), Vascular Endothelial Growth Factor (VEGF) (10, 11), Insulin-like Growth Factor -1 and -2 (12, 13) have been shown to play a significant role in the development and progression of MMe. Moreover several findings underscore the crucial role of Platelet Derived Growth Factor (PDGF) A and B in MMe cell growth, reviewed in (14). High expression level of PDGFRβ was demonstrated in MMe cells, but not in normal Human Mesothelial Cells (HMC), mostly expressing PDGFRα (15). Furthermore, increased expression of PDGF A and B were detected at higher levels in MMe cells compared to HMC (16) and a significant reduction in MMe cell growth or migration was observed by blocking PDGF A and PDGF B (17). c-kit expression on MMe cells has been demonstrated by some authors, although its role in this tumor is very controversial (18-20). M-CSF production by mesothelial cells has been already shown (21) and inhibition of c-fms receptor by Imatinib has been demonstrated (22).

Many Cytokines are released in the microenvironment by tumor stromal cells (23) and PDGF paracrine stimulation has been demonstrated in human tumors and MMe in particular

(24-26). PDGFRβ activated by PDGF B can induce PI3K/Akt signaling (27), which seems to be crucial for survival of MMe cells (28).

Imatinib is a selective inhibitor for a subset of tyrosine kinases, including bcr-abl, as well as c-kit, PDGFRβ (29), as well as c-fms (22, 30). PDGF receptors are expressed by several tumor cells and have been identified as potential therapeutic targets for Imatinib (31).

Gemcitabine, Cisplatin, Etoposide, Doxorubicin and, more recently, Pemetrexed have been demonstrated to be active for MMe treatment. Combined therapy Cisplatin/Pemetrexed and Cisplatin/Gemcitabine have been demonstrated more effective than each single agents used alone (32). The aim of the present study is to investigate a translational approach which assesses assessing the possible efficacy of Imatinib, as a single agent or in combined therapy for MMe.

Methods

Cell cultures. MMP cells and primary Human Mesothelial Cells (HMC) were characterized and cultured as previously described (9). REN cells were kindly provided by Dr. Albelda and ISTMES2 were from the IST cell depository of Genoa (Italy).

Drugs. Imatinib was kindly provided by Novartis (Basel, Switzerland); Gemcitabine and Pemetrexed by Lilly (Indianapolis, IN). Commercially available Cisplatin, Doxorubicin and Etoposide were from Alexis (Lausen, Switzerland).

Signal transduction. Cells were grown in 0.2 % Foetal Bovine Serum (FBS) for 24 h, then pre-incubated for 90 min in presence or absence of 10 μM Imatinib. To the same medium 20 ng/ml purified PDGF (R&D, Milan, Italy) or 20% FBS for 15 min at 37° C were added. Immunoblotting was performed by using 50 μg of cell lysates as previously described (9). Antibodies used were: PDGFRβ, phospho-PDGFRβ, c-Kit, c-fms (Santa Cruz Biotechnology,

USA), phospho-Akt-Ser473 (Cell Signaling, USA), phosphotyrosine (UBI, USA) and phospho-Erk1/2 (Sigma, USA). Reactions were detected by Enhanced Chemiluminescence System (ECL, Amersham, UK).

Cytotoxicity and apoptosis. Subconfluent cells were exposed for 48 h to medium supplemented with 2% FBS, with or without different drugs at concentrations ranging from $1x10^{-10}$ M to $1x10^{-3}$ M (33-35). Cell viability was assessed by MTT assay (36). LC50 values were calculated using Origin software (Microcal Software, USA) and applied to the "50% Isobologram" method (37). Apoptosis was evaluated by TUNEL analysis (DeadEnd™ Colorimetric TUNEL system, Promega, USA), following treatment with Imatinib, alone or combined with Gemcitabine or Pemetrexed, accordingly with the specific LC50 values determined by MTT analysis in each cell type, as follows. MMP: Imatinib $3x10^{-7}$M, Gemcitabine $5x10^{-7}$M, Pemetrexed $6.5x10^{-6}$M. REN: Imatinib $1x10^{-6}$M, Gemcitabine $5x10^{-9}$M, Pemetrexed $1x10^{-5}$M. ISTMES2: Imatinib $4x10^{-6}$M, Gemcitabine $1x10^{-9}$M, Pemetrexed $5x10^{-6}$M.

Statistical analysis. Data are expressed as mean percentage ± Standard Deviation (SD) of three independent experiments. We used χ-square test to evaluate statistical differences. P values ≤ 0.05 were considered significant.

Results

PDGFRβ, c-kit and c-fms are expressed by MMe cells. We evaluated the expression of PDGFRβ, c-Kit (tyrosine kinase receptor for Stem Cell Factor) and c-Fms (Macrophage Colony Stimulating Factor Receptor) by immunoblotting analysis on a panel of six MMe cell lines. Between PDGF receptors, only PDGFRβ, but not PDGFRα, was expressed in MMe cells examined. We select three MMe cell lines for their different representative expression

pattern (Fig. 1A). In MMP and in REN cells PDGFRβ was expressed at higher level than in ISTMES2 cells, while untransformed Human Mesothelial Cells (HMC) did not express the PDGFRβ receptor. The expression of c-Kit and c-fms occurred at higher levels in MMP cells, while in REN and ISTMES2 expression of these receptors was reduced. HMC only displayed very low level of c-fms.

Imatinib-mediated PDGFRβ inhibition selectively affects Akt. MMe cells positive for PDGFRβ, were also tested by immunoprecipitation with PDGFRβ antibodies followed by immunoblotting with phosphotyrosine antibodies, after growing cells in low serum conditions. MMe cells displayed negligible levels of tyrosine phosphorylation whereas addition of recombinant PDGF B increased the receptor phosphorylation of all cells (Fig. 1 B, upper panel). Neither c-Kit nor c-fms phosphorylation was detectable in all MMe cells (data not shown).

Then, we tested if treatment with Imatinib could possibly interfere with signaling pathways elicited by this receptor. In low serum conditions, only MMP cells displayed autonomous Akt activity (determined as Ser^{473} phosphorylation), whereas upon PDGF stimulation tyrosine phosphorylation of PDGFRβ along with Akt phosphorylation were increased, but markedly inhibited by 10 μM Imatinib, in all MMe cells examined. Basal Erk1/2 activity was slightly enhanced after PDGF in MMP and, a lesser extent, in REN cells, while both activities were barely affected by treatment with Imatinib 10 μM (Fig. 1B lower panel).

Conversely, Akt inhibition was complete and comparable to what obtained by treatment with the PI3K inhibitor Wortmannin at concentration of 100 nM (Fig 1 C). Interestingly, Akt activity in MMP cells, expressing also HGFR/Met (9), was increased by addition of recombinant HGF (100 ng/ml), but not affected by Imatinib (Fig 1 D). This indicates a selective blockade of the PDGFRβ dependent Akt signaling by Imatinib.

Imatinib reduces cell viability of MMe cells expressing PDGFRβ. In view of the crucial role played by Akt in determining survival of HMC and MMe cells (28), we postulated that Imatinib could negatively affect PDGFRβ-positive MMe cells viability. Upon 48 h incubation with up to 10 μM Imatinib, cell viability, tested by MTT assay, markedly decreased, with a LC50 of $1.84x10^{-5}$ M for MMP cells. Gemcitabine and Pemetrexed have been already demonstrated particularly effective in combination with Cisplatin for MMe chemotherapy (32). Therefore we tested the cytotoxic effect induced by these two agents, in presence of different concentrations of Imatinib. As expected, Gemcitabine and Pemetrexed caused death of MMe cells, determined by MTT assay, in dose-dependent manner. The presence of Imatinib modified the profile of the dose-response curves, with a shift toward lower LC50 values and by decreasing the fraction of drug resistant cells (Fig 2 A).

Imatinib synergizes with Gemcitabine and Pemetrexed in inducing MMe cell death.

Activation of tyrosine kinase receptors by ligands induces phosphatidylinositol-3 kinase (PI3K) and Akt activities, exerting several biological effects, including increased cell survival with relevant effects on human carcinogenesis (38, 39). We recently demonstrated that Akt plays a major survival role for MMe cells (28). Therefore, based on the clear-cut toxic effect induced by Imatinib on MMe cells, mediated by the inhibition of the PI3K/Akt pathway, we hypothesized that this inhibitor may also reinforce cytotoxicity generated by other cytotoxic agents.

Thus, combined treatments of Imatinib with other chemotherapeutics were analyzed by the isobologram plot method (37). Interestingly, only Imatinib/Gemcitabine and Imatinib/Pemetrexed combinations showed a marked synergism in reducing MMP and REN cell viability, compared to the effects observed with single agents alone. This was revealed by

lining of all LC50 values on a concave upward curve, below the isoeffective plot (Fig. 2 B). In REN cells the synergistic effect is still appreciable, although at lower extent, while in ISTMES2 cells the effect of Imatinib/chemotherapeutics was antagonistic.

The effectiveness of these combined treatments was confirmed when cell death was investigated by TUNEL. The combination of Imatinib with Gemcitabine or Pemetrexed induced a significant increase in apoptosis ($p \leq 0.05$), compared to each chemotherapeutic drug alone (Tab. 1). On the contrary, no synergistic effect was observed with any of other chemotherapeutic drugs (not shown).

Interestingly, the concentrations of the single agents used in the combined treatment were by far lower than those obtainable at therapeutic dosages.

Table 1. TUNEL analysis of apoptosis induced in MMe cells by single drugs or by drug combination.

Treatment	MMP	REN	ISTMES2
Untreated control	**2.46 ± 1.13**	**1.94 ± 0.74**	**1.34 ± 0.47**
Imatinib	**3.56 ± 1.54**	**2.94 ± 1.01**	**3.04 ± 0.93**
Gemcitabine	**4.04 ± 1.99**	**5.01 ± 2.71**	**4.14 ± 1.68**
Pemetrexed	**3.44 ± 2.33**	**2.98 ± 1.20**	**2.34 ± 1.22**
Imatinib + Gemcitabine	**7.80 ± 1.85 (*)**	**11.66 ± 2.53 (*)**	**2.36 ± 1.51**
Imatinib + Pemetrexed	**10.94 ± 1.90 (*)**	**6.66 ± 1.20 (*)**	**1.38 ± 0.79**

Data are expressed as the percentage of Biotin-dU positive nuclei for 100 counted cells at a magnification of 100X. Different concentrations of drugs were used, as described in Material and Methods

(*) Statistically significant ($p \leq 0.05$) difference between Gemcitabine or Pemetrexed alone vs. Imatinib/Gemcitabine or Imatinib/Pemetrexed combinations.

Discussion

We described here some preclinical and clinical results, providing the rationale for a novel approach to refractory MMe. Our findings preliminarily provided further evidences supporting that PDGFRβ is broadly expressed on MMe cells but not in the normal counterpart HMC (15). Therefore, expression of PDGFRβ in MMe cells offered the rationale for testing the tyrosine kinase inhibitor Imatinib, as a *smart drug* addressed to these tumor cells. The autonomous tyrosine phosphorylation of this receptor in MMP and REN cells, which are sensitized to Imatinib cytototoxic effects, addresses toward the role of either a paracrine or autocrine PDGFRβ-activating mechanisms, leading to PI3K/Akt signaling.

A paracrine loop has been described as an activating mechanism leading to tyrosine kinase receptor activity in MMe cells (9) and stromal microenvironment has been shown to be a fundamental source of activating ligands for PDGFR in human tumors (23). Thereby, activation in MMe cells of Akt is a crucial signaling pathway for MMe carcinogenesis (28, 40) and even though this may also be dependent on several other tyrosine kinase receptor activities (41), our findings demonstrate how specifically interference with PDGFRβ pathway exerts relevant cytotoxic effects and makes it a priority target for MMe therapy.

PDGFRβ activating loops have been described in many human tumors and stressed as a cause of spontaneous tumors in humans (42) and other preclinical studies on several human solid tumors revealed the efficacy of Imatinib as a cytotoxic agent (33, 35, 43, 44) On the contrary of what happens in CML and GIST, where the carcinogenic role of the fusion protein BCR-ABL (44) and activating mutations of c-Kit (45), respectively provide the rationale for a targeted therapy, we demonstrate that in MMe cells the activation (autocrine or paracrine) of a receptor is sufficient to arrange a targeted therapy. As opposite, in no conditions MMe cells displayed activated c-Kit or c-fms, ruling out that the cytotoxic effect we described here primarily occurred via c-Kit or c-fms signaling interference. Conversely, in other solid

tumors, e.g. SCLC, only the activated form of c-Kit (due to ligand binding or to activating mutations) was predictive of clinical response (46).

Our results clearly indicate that PDGFRβ expression in MMe cells is mandatory for the sensitivity to Imatinib and for the synergy observed between Imatinib and Gemcitabine or Pemetrexed. However, when all three receptors sensitive to Imatinib are co-expressed in the same cell type, as in MMP, the synergistic effect is higher than in REN cells where only two of them are expressed (PDGFRβ and c-Kit). effect is synergizing

Expression of active PDGFRβ in MMe cells has been demonstrated by many authors (reviewed in (14)), providing a reliable target for most of patients with MMe.

Our in vitro findings on synergisms between Imatinib and some chemotherapeutics active on MMe cells provide further evidences with even more promising therapeutic implications. Gemcitabine and Pemetrexed are well known active agents on MMe cells (47) and their combination with Imatinib discloses intriguing implications. Particularly the synergism revealed here indicates that very low doses of chemotherapeutic agents should be sufficient to exert therapeutic effects.

Given our previous findings (28) the most relevant mechanism underlying the observed *in vitro* synergy is the Imatinib-dependent PDGFRβ inhibition. This in turn leads to Akt inhibition resulting in MMe cell sensitization to low concentrations of Gemcitabine. However, it is conceivable that other biological effects could play a role in humans. Reduction of the intratumoral interstitial fluid pressure by Imatinib has been demonstrated (48, 49) *in vivo*, as well as the Imatinib interference with VEGF expression and associated neoangiogenesis (50).

The present study shows that a specific tyrosine kinase inhibitor, such Imatinib, can be an effective therapeutic tool, by enhancing tumor chemosensitivity *via* Akt inhibition, even in

previously refractory MMe. It also suggests that Akt signaling is a key target for an effective therapy for refractory MMe.

Albeit some steps forward have been done in MMe therapy (7), results are still unsatisfactory and MMe remains an ideal field to test new therapeutic approaches (47). Our work provides a strong rationale for a new model for approaching MMe therapy.

Acknowledgements

This work was supported by research grants from AIRC (Associazione Italiana per la Ricerca sul Cancro) and from MARF (Mesothelioma Applied Research Foundation) to G.G.. We thank the Buzzi Foundation (Casale Monferrato, Italy) for financial help. This work is part of G.I.Me. (Gruppo Italiano per lo Studio e la Terapia del Mesotelioma) and A.I.P.O. (Associazione Italiana Pneumologi Ospedalieri) network program.

We gratefully thank Dr. Patrizia Morbini, Institute of Pathology, San Matteo University Hospital, Pavia, Italy.

References

1. Peto J, Decarli A, La Vecchia C, Levi F, Negri E. The European mesothelioma epidemic. Br J Cancer 1999;79(3-4):666-72.

2. Treasure T, Sedrakyan A. Pleural mesothelioma: little evidence, still time to do trials. Lancet 2004;364(9440):1183-5.

3. Fisher SG, Weber L, Carbone M. Cancer risk associated with simian virus 40 contaminated polio vaccine. Anticancer Res 1999;19(3B):2173-80.

4. Curran D, Sahmoud T, Therasse P, van Meerbeeck J, Postmus PE, Giaccone G. Prognostic factors in patients with pleural mesothelioma: the European Organization for Research and Treatment of Cancer experience. J Clin Oncol 1998;16(1):145-52.

5. Pass HI, Vogelzang N, Hahn S, Carbone M. Malignant pleural mesothelioma. Curr Probl Cancer 2004;28(3):93-174.

6. Lee TT, Everett DL, Shu HK, Jahan TM, Roach M, 3rd, Speight JL, et al. Radical pleurectomy/decortication and intraoperative radiotherapy followed by conformal radiation with or without chemotherapy for malignant pleural mesothelioma. J Thorac Cardiovasc Surg 2002;124(6):1183-9.

7. Vogelzang NJ, Rusthoven JJ, Symanowski J, Denham C, Kaukel E, Ruffie P, et al. Phase III study of pemetrexed in combination with cisplatin versus cisplatin alone in patients with malignant pleural mesothelioma. J Clin Oncol 2003;21(14):2636-44.

8. Klominek J, Baskin B, Liu Z, Hauzenberger D. Hepatocyte growth factor/scatter factor stimulates chemotaxis and growth of malignant mesothelioma cells through c-met receptor. Int J Cancer 1998;76(2):240-9.

9. Cacciotti P, Libener R, Betta P, Martini F, Porta C, Procopio A, et al. SV40 replication in human mesothelial cells induces HGF/Met receptor activation: a model for viral-related carcinogenesis of human malignant mesothelioma. Proc Natl Acad Sci U S A 2001;98(21):12032-7.

10. Strizzi L, Catalano A, Vianale G, Orecchia S, Casalini A, Tassi G, et al. Vascular endothelial growth factor is an autocrine growth factor in human malignant mesothelioma. J Pathol 2001;193(4):468-75.

11. Cacciotti P, Strizzi L, Vianale G, Iaccheri L, Libener R, Porta C, et al. The presence of simian-virus 40 sequences in mesothelioma and mesothelial cells is associated with high levels of vascular endothelial growth factor. Am J Respir Cell Mol Biol 2002;26(2):189-93.

12. Pass HI, Mew DJ, Carbone M, Donington JS, Baserga R, Steinberg SM. The effect of an antisense expression plasmid to the IGF-1 receptor on hamster mesothelioma proliferation. Dev Biol Stand 1998;94:321-8.

13. Hoang CD, Zhang X, Scott PD, Guillaume TJ, Maddaus MA, Yee D, et al. Selective activation of insulin receptor substrate-1 and -2 in pleural mesothelioma cells: association with distinct malignant phenotypes. Cancer Res 2004;64(20):7479-85.

14. Garlepp MJ, Leong CC. Biological and immunological aspects of malignant mesothelioma. Eur Respir J 1995;8(4):643-50.

15. Langerak AW, van der Linden-van Beurden CA, Versnel MA. Regulation of differential expression of platelet-derived growth factor alpha- and beta-receptor mRNA in normal and malignant human mesothelial cell lines. Biochim Biophys Acta 1996;1305(1-2):63-70.

16. Pogrebniak HW, Lubensky IA, Pass HI. Differential expression of platelet derived growth factor-beta in malignant mesothelioma: a clue to future therapies? Surg Oncol 1993;2(4):235-40.

17. Klominek J, Baskin B, Hauzenberger D. Platelet-derived growth factor (PDGF) BB acts as a chemoattractant for human malignant mesothelioma cells via PDGF receptor beta-integrin alpha3beta1 interaction. Clin Exp Metastasis 1998;16(6):529-39.

18. Horvai AE, Li L, Xu Z, Kramer MJ, Jablons DM, Treseler PA. c-Kit is not expressed in malignant mesothelioma. Mod Pathol 2003;16(8):818-22.

19. Butnor KJ, Burchette JL, Sporn TA, Hammar SP, Roggli VL. The spectrum of Kit (CD117) immunoreactivity in lung and pleural tumors: a study of 96 cases using a single-source antibody with a review of the literature. Arch Pathol Lab Med 2004;128(5):538-43.

20. Catalano A, Rodilossi S, Rippo MR, Caprari P, Procopio A. Induction of stem cell factor/c-Kit/slug signal transduction in multidrug-resistant malignant mesothelioma cells. J Biol Chem 2004;279(45):46706-14.

21. Lanfrancone L, Boraschi D, Ghiara P, Falini B, Grignani F, Peri G, et al. Human peritoneal mesothelial cells produce many cytokines (granulocyte colony-stimulating factor [CSF], granulocyte-monocyte-CSF, macrophage-CSF, interleukin-1 [IL-1], and IL-6) and are activated and stimulated to grow by IL-1. Blood 1992;80(11):2835-42.

22. Taylor JR, Brownlow N, Domin J, Dibb NJ. FMS receptor for M-CSF (CSF-1) is sensitive to the kinase inhibitor imatinib and mutation of Asp-802 to Val confers resistance. Oncogene 2006;25(1):147-51.

23. Sawyers C. Targeted cancer therapy. Nature 2004;432(7015):294-7.

24. Heldin CH, Westermark B. Mechanism of action and in vivo role of platelet-derived growth factor. Physiol Rev 1999;79(4):1283-316.

25. Yu J, Ustach C, Kim HR. Platelet-derived growth factor signaling and human cancer. J Biochem Mol Biol 2003;36(1):49-59.

26. Shih AH, Holland EC. Platelet-derived growth factor (PDGF) and glial tumorigenesis. Cancer Lett 2005.

27. Johnson MD, Okedli E, Woodard A, Toms SA, Allen GS. Evidence for phosphatidylinositol 3-kinase-Akt-p7S6K pathway activation and transduction of mitogenic signals by platelet-derived growth factor in meningioma cells. J Neurosurg 2002;97(3):668-75.

28. Cacciotti P, Barbone D, Porta C, Altomare DA, Testa JR, Mutti L, et al. SV40-dependent AKT activity drives mesothelial cell transformation after asbestos exposure. Cancer Res 2005;65(12):5256-62.

29. George D. Platelet-derived growth factor receptors: a therapeutic target in solid tumors. Semin Oncol 2001;28(5 Suppl 17):27-33.

30. Dewar AL, Cambareri AC, Zannettino AC, Miller BL, Doherty KV, Hughes TP, et al. Macrophage colony-stimulating factor receptor c-fms is a novel target of imatinib. Blood 2005;105(8):3127-32.

31. Abou-Jawde R, Choueiri T, Alemany C, Mekhail T. An overview of targeted treatments in cancer. Clin Ther 2003;25(8):2121-37.

32. Tomek S, Manegold C. Chemotherapy for malignant pleural mesothelioma: past results and recent developments. Lung Cancer 2004;45 Suppl 1:S103-19.

33. Krystal GW, Honsawek S, Litz J, Buchdunger E. The selective tyrosine kinase inhibitor STI571 inhibits small cell lung cancer growth. Clin Cancer Res 2000;6(8):3319-26.

34. Zhang P, Gao WY, Turner S, Ducatman BS. Gleevec (STI-571) inhibits lung cancer cell growth (A549) and potentiates the cisplatin effect in vitro. Mol Cancer 2003;2(1):1.

35. Gonzalez I, Andreu EJ, Panizo A, Inoges S, Fontalba A, Fernandez-Luna JL, et al. Imatinib inhibits proliferation of Ewing tumor cells mediated by the stem cell factor/KIT receptor pathway, and sensitizes cells to vincristine and doxorubicin-induced apoptosis. Clin Cancer Res 2004;10(2):751-61.

36. Mosmann T. Rapid colorimetric assay for cellular growth and survival: application to proliferation and cytotoxicity assays. J Immunol Methods 1983;65(1-2):55-63.

37. Tallarida RJ. Drug synergism: its detection and applications. J Pharmacol Exp Ther 2001;298(3):865-72.

38. Stein RC. Prospects for phosphoinositide 3-kinase inhibition as a cancer treatment. Endocr Relat Cancer 2001;8(3):237-48.

39. Yu Y, Alwine JC. Human cytomegalovirus major immediate-early proteins and simian virus 40 large T antigen can inhibit apoptosis through activation of the phosphatidylinositide 3'-OH kinase pathway and the cellular kinase Akt. J Virol 2002;76(8):3731-8.

40. Rascoe PA, Cao X, Daniel JC, Miller SD, Smythe WR. Receptor tyrosine kinase and phosphoinositide-3 kinase signaling in malignant mesothelioma. J Thorac Cardiovasc Surg 2005;130(2):393-400.

41. Corso S, Comoglio PM, Giordano S. Cancer therapy: can the challenge be MET? Trends Mol Med 2005;11(6):284-92.

42. Sebti SM, Hamilton AD. Design of growth factor antagonists with antiangiogenic and antitumor properties. Oncogene 2000;19(56):6566-73.

43. Wang WL, Healy ME, Sattler M, Verma S, Lin J, Maulik G, et al. Growth inhibition and modulation of kinase pathways of small cell lung cancer cell lines by the novel tyrosine kinase inhibitor STI 571. Oncogene 2000;19(31):3521-8.

44. Druker BJ, Sawyers CL, Kantarjian H, Resta DJ, Reese SF, Ford JM, et al. Activity of a specific inhibitor of the BCR-ABL tyrosine kinase in the blast crisis of chronic myeloid leukemia and acute lymphoblastic leukemia with the Philadelphia chromosome. N Engl J Med 2001;344(14):1038-42.

45. Heinrich MC, Corless CL, Demetri GD, Blanke CD, von Mehren M, Joensuu H, et al. Kinase mutations and imatinib response in patients with metastatic gastrointestinal stromal tumor. J Clin Oncol 2003;21(23):4342-9.

46. Dy GK, Miller AA, Mandrekar SJ, Aubry MC, Langdon RM, Jr., Morton RF, et al. A phase II trial of imatinib (ST1571) in patients with c-kit expressing relapsed small-cell lung cancer: a CALGB and NCCTG study. Ann Oncol 2005.

47. Vogelzang NJ, Porta C, Mutti L. New agents in the management of advanced mesothelioma. Semin Oncol 2005;32(3):336-50.

48. Pietras K, Ostman A, Sjoquist M, Buchdunger E, Reed RK, Heldin CH, et al. Inhibition of platelet-derived growth factor receptors reduces interstitial hypertension and increases transcapillary transport in tumors. Cancer Res 2001;61(7):2929-34.

49. Pietras K, Rubin K, Sjoblom T, Buchdunger E, Sjoquist M, Heldin CH, et al. Inhibition of PDGF receptor signaling in tumor stroma enhances antitumor effect of chemotherapy. Cancer Res 2002;62(19):5476-84.

50. Beppu K, Jaboine J, Merchant MS, Mackall CL, Thiele CJ. Effect of imatinib mesylate on neuroblastoma tumorigenesis and vascular endothelial growth factor expression. J Natl Cancer Inst 2004;96(1):46-55.

Figure legends

Fig.1 - PDGFRβ expression in MMe cells. (A) Immunoprecipitation followed by immunoblotting with PDGFRβ antibodies on HMC and the three established MMe cell lines. Controls: HDF, Human Dermal Fibroblasts expressing PDGFRβ and CCRF, CCRF-HSB-2, human leukemic lymphoblast cells, expressing c-Kit and c-Fms. (B) Immunoblotting with the indicated antibodies on whole lysates of MMP cells in low serum (-) or stimulated with PDGF in presence or absence of 10 μM Imatinib or (C) of 100 nM Wortmannin; (D) Immunoblotting with P-Akt (P-Ser 473) antibodies of MMP cells stimulated by 50 ng/ml HGF in presence or absence of 10 μM Imatinib.

Fig. 2 – Imatinib synergizes with Gemcitabine and Pemetrexed. (A) Cell viability of Gemcitabine (left) and Pemetrexed (right) in presence of different concentration of Imatinib. For Imatinib/Gemcitabine combination: ●, $1x10^{-7}$ M; ▲, $2.5x10^{-6}$ M; ▼, $1x10^{-4}$ M. For Imatinib/Pemetrexed combination: ●, $3x10^{-7}$ M; ▲, $6x10^{-7}$ M; ▼, $1.5x10^{-6}$ M. (B) 50%

isobologram plot for Imatinib in combination with Gemcitabine (*left)* and Pemetrexed (*right*) on the indicated cells.

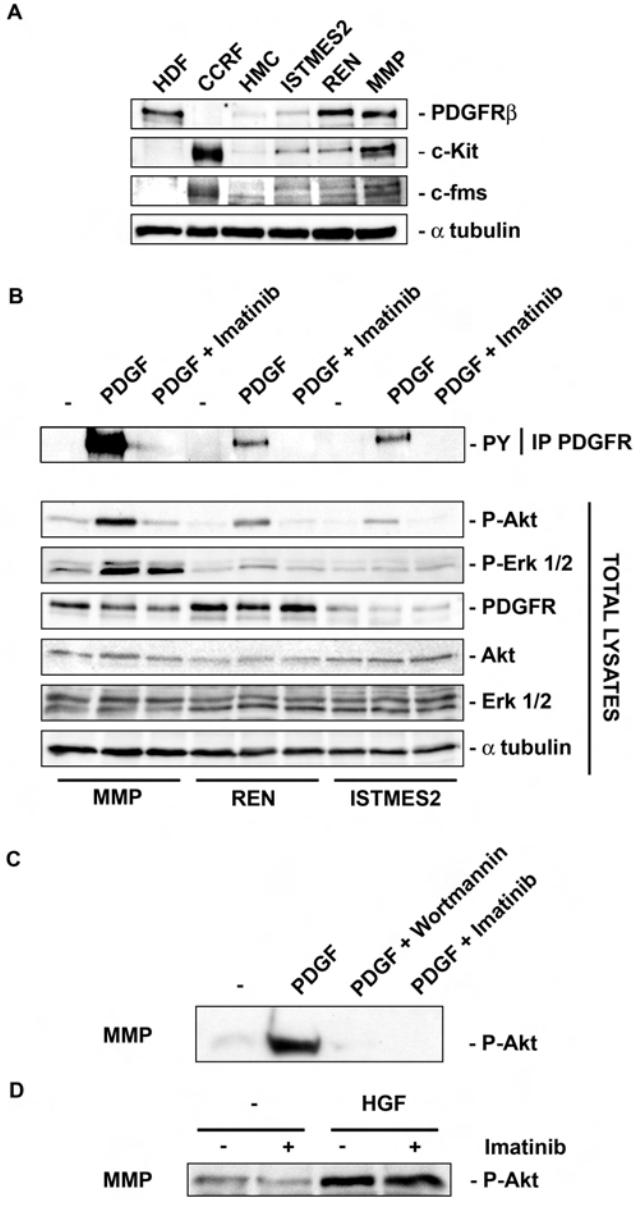

Bertino et al.Fig.1

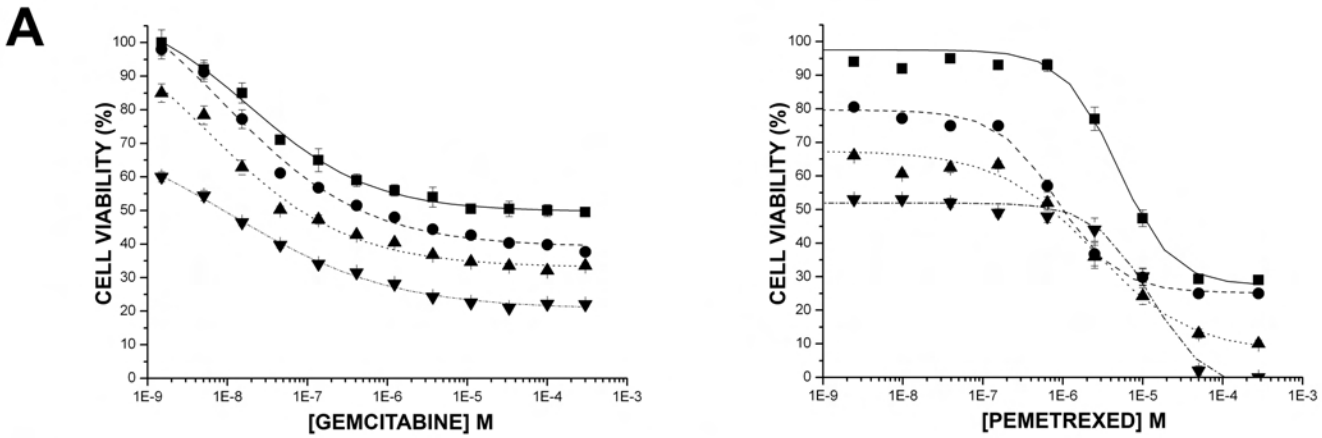

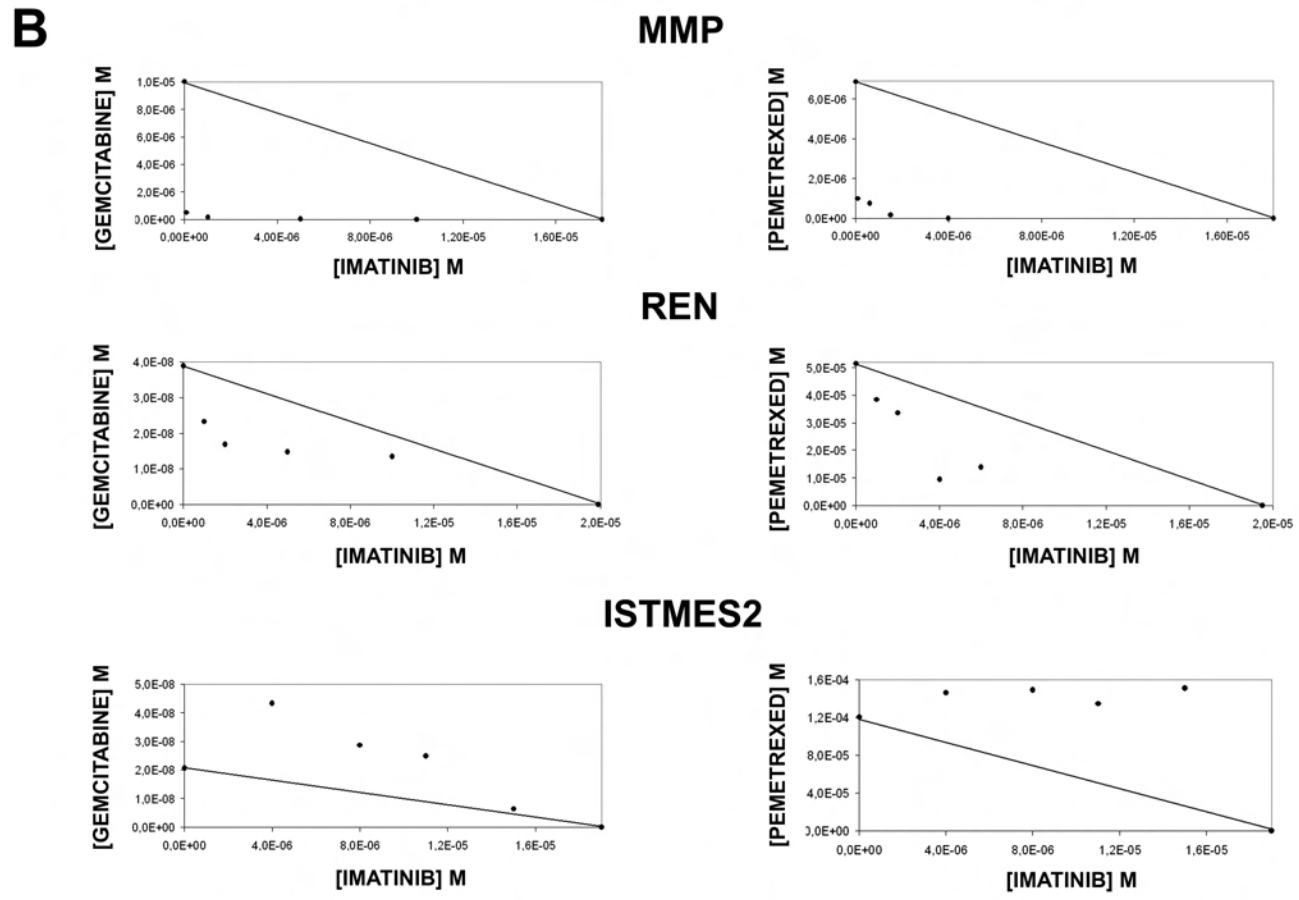

Bertino et al. Fig.2

Int. J. Cancer: **120,** 000–000 (2007)

Erionite and asbestos differently cause transformation of human mesothelial cells

P. Bertino[1], A. Marconi[2], L. Palumbo[2], B. Bruni[2], D. Barbone[1], S. Germano[1], A.U. Dogan[3,4], G. F. Tassi[5], C. Porta[6], L. Mutti[7] and G. Gaudino[1]*

[1]*Department of DISCAFF and DFB Center, University of Piemonte Orientale ''A. Avogadro'', Novara, Italy*
[2]*Department of Environment and Primary Prevention, ISS, Roma, Italy*
[3]*Department of Geological Engineering, Ankara University, Turkey*
[4]*Department of Chemical and Biochemical Engineering, University of Iowa, Iowa City, IA*
[5]*Chest Medicine Unit, Brescia Hospital, Brescia, Italy*
[6]*Medical Oncology, IRCCS San Matteo University Hospital, Pavia, Italy*
[7]*Local Health Unit, 11 Piemonte, Italy*

Malignant mesothelioma (MM) is an aggressive tumor associated with environmental or occupational exposure to asbestos fibers. Erionite is a fibrous zeolite, morphologically similar to asbestos and it is assumed to be even more carcinogenic. Onset and progression of MM has been suggested as the result of the cooperation between asbestos and other cofactors, such as SV40 virus infection. Nevertheless, several cases of MM were associated with environmental exposure to erionite in Turkey, where SV40 was never isolated in MM specimens. We show here that erionite is poorly cytotoxic, induces proliferating signals and high growth rate in human mesothelial cells (HMC). Long term exposure to erionite, but not to asbestos fibers, transforms HMC *in vitro*, regardless the presence of SV40 sequences, leading to foci formation in cultured monolayers. Cells derived from foci display constitutive activation of Akt, NF-κB and Erk1/2, show prolonged survival and a deregulated cell cycle, involving cyclin D1 and E overexpression. Our results reveal that erionite is able *per se* to turn HMC into transformed highly proliferating cells and disclose the carcinogenic properties of erionite, prompting for a careful evaluation of environmental exposure to these fibers. The genetic predisposition to the effect of erionite is a separate subject for investigation.
© *2007 Wiley-Liss, Inc.*

Key words: asbestos; zeolite; erionite; mesothelioma; cell transformation

Environmental or occupational exposure to asbestos fibers may cause chronic respiratory diseases, including interstitial lung fibrosis and pleural malignant mesothelioma (MM).[1,2] Pedigree and mineralogical studies indicate that the high incidence of MM in a number of Cappadocia villages in Turkey is caused, in genetically predisposed individuals, by exposure to fibrous erionite. This is a highly pathogenic form of the naturally occurring zeolite, similar in appearance and properties to asbestos.[3,4] Erionite is a strong mutagen,[5] considered more carcinogenic than asbestos fibers in man and rodents,[6] possibly due to the peculiar property of accumulating iron on its surface, despite its very small content of this element.[7] It is well documented that erionite from Oregon has genotoxic properties[8] and induces high incidence of MM in rats after both intrapleural inoculation or inhalation,[9] although there are no epidemiological data correlating the presence of erionite to MM in Oregon.

Similarly to what occurs with asbestos, exposure to erionite fibers leads to generation of reactive oxygen metabolites from macrophages[10] and to increased mRNA levels of the early response c-fos and c-jun proto-oncogenes in mesothelial cells.[11,12] MAPK signaling significantly contributes to pivotal cell functions as cell proliferation and death in response to toxic and inflammatory agents.[13] Similarly, PI3K/Akt and NF-κB signaling play a crucial role in determining cell fate after exposure to toxic agents[14,15] and are activated by asbestos fibers as well.[16,17] Interestingly, TNF-α inhibits asbestos-induced cytotoxicity *via* a NF-κB-dependent pathway.[18] These results underscore the key role played by NF-κB in asbestos-induced oncogenesis of human mesothelial cells (HMC). Epidermal growth factor receptor (EGFR) overexpression and activation have been linked to asbestos-induced proliferation.[19] Autocrine loops for both EGFR and platelet derived growth factor receptor (PDGFR) have been also reported in MM cells.[20] Moreover, we previously demonstrated that an autocrine circuit involving hepatocyte growth factor (HGF) and its receptor Met contributes to HMC transformation[21] and others showed that Met is overexpressed in MM cells.[22]

In vitro studies demonstrated that SV40 and asbestos fibers cooperate to determine HMC transformation,[23] *via* PI3K/Akt signaling.[24] Therefore, here we compared the proliferating and transforming efficacy of short- and long-term exposures of HMC to erionite, amosite, chrysotile or glass fibers, in absence of SV40 infection. Moreover, to achieve a better understanding on the mechanism by which these fibers determine cell transformation, we further evaluated tyrosine kinase receptor expression and signal transduction in HMC transformed by the different fibers.

Our data reveal that erionite fibers have higher intrinsic transformation ability than asbestos fibers and give a possible explanation for the high incidence of MM in 3 small villages in Turkey, where SV40 virus infection of MM cells has never been detected.[3,4,25,26]

Material and methods

Fibers

The sample of erionite fibers from Karain, provided by co-author Dr. Umran Dogan (Ankara, Turkey), was associated with considerable amounts of nonfibrous particles and bundles, with diameter greater than 3 μm and length-to-width ratio (L/W) less than 3:1. The fraction of fibrous material with L/W of 3:1 or greater in this sample is less than 10% by weight, because erionite in Karain occurs as a minor constituent of a volcanic amorphous rock, from which the erionite mineral originates.[4,9,27–29] The erionite sample from Oregon, kindly provided by Dr. J. W. Skidmore (Glamorgan, UK), was almost totally made of fibrous particles.

No milling, crushing or ultrasound processing was performed prior to size analysis. Representative portions of each erionite sample was weighted (5 ± 0.5 mg) and dispersed in 20 ml of filtered, deionized, distilled water. About 0.45 ml of the dispersion

Grant sponsors: AIRC (Associazione Italiana per la Ricerca sul Cancro), MARF (Mesothelioma Applied Research Foundation), Buzzi Foundation (Casale M., Italy).
The last two authors equally contributed to this work.
***Correspondence to:** Department of DISCAFF and DFB Center, University of Piemonte Orientale ''A. Avogadro'', Via Bovio, 6-28100 Novara, Italy. Fax: +39-0321-375821.
E-mail: giovanni.gaudino@unipmn.it
Received 8 June 2006; Accepted after revision 2 February 2007
DOI 10.1002/ijc.22687
Published online 00 Month 2007 in Wiley InterScience (www.interscience.wiley.com).

J_ID: IJC Wiley Ed. Ref. No.: 06-1230.R2 Customer A_ID: 22687 Date: 1-MARCH-07 Stage: I Page: 2

was filtered on a policarbonate filter (0.1 μm), dried, placed on aluminum stub and plated with gold in a sputter coater.

Each sample was examined using a Philips XL30 scanning electron microscope (SEM) at different magnifications, to determine dispersion and visibility of the fibers. Central fields with adequate fibers dispersion were selected for each sample and length (L) and width (W) of fibers were measured directly on the SEM screen with the ruler of the microscope. Fiber bundles with L/W of 3:1 or greater were considered as single fibers. L and W measurements of about 500 fibers were recorded for each fibrous sample. The size analysis of glass fibers was similarly performed.

Size distribution of UICC asbestos samples (Chrysotile B and Amosite) were acquired from previous data obtained by transmission electron microscopy.[30]

Erionite (Karain-Turkey and Oregon-USA), amosite, chrysotile (UICC asbestos samples) and glass fibers were dispersed in PBS at 2.0 mg/ml, before autoclaving. Then, amosite, chrysotile and glass fibers, but not erionite fibers, were triturated 8 times through a 22-gauge needle.

Cell cultures

Two primary HMC cell cultures, obtained from patients with heart failure were cultured in Ham's F-12 medium, supplemented with 10% fetal bovine serum (FBS–GIBCO, Rockville, MD) at 37°C in a 5% CO_2-humidified atmosphere. HMC were used between the second and the sixth passage. Both cultures gave similar results in all assays performed, as previously characterized.[24]

DNA-neosynthesis

HMC cells were exposed to medium containing 2% FBS supplemented with fibers in presence of 10 μM BrdU (Bromo-deoxy-Uridine). Incorporation in neosynthesized DNA was evaluated after 24 hr by the cell proliferation kit (Roche, Basel, Switzerland). Data are expressed as mean increase of DNA-neosynthesis over untreated controls.

Cytotoxicity and DNA *adducts*

Cells were seeded on multiwell plates and 5×10^3 cell/well were exposed for 24 or 48 hr to fibers at densities ranging from 2 to 10 μg/cm^2 in presence of 2% FBS. Experiments performed on foci derived cells were conducted in presence of 100 μM VP16 (Etoposide, Sigma-Aldrich, St. Louis, MO), for 24 hr. Cytotoxicity was assessed by MTT assay, performed in quadruplicate, as previously described.[31] Normalized cytotoxicity percentages were obtained according to the ratio: [1-(A_{570} mean values of extracts from exposed samples/A_{570} mean values of extracts from control cell samples)] $\times$ 100.

DNA adducts were evaluated by high-performance liquid chromatography (HPLC), in the presence or absence of 10 mM *N*-Acetyl-L-cysteine (L-NAC) (Sigma-Aldrich, St. Louis, MO), on extracts from cells exposed for 5 hr at 10 μg/cm^2 to the indicated fibers and are expressed as amount of 8-OHdG per 10^5 dG, as previously described.[32]

Exposure to fibers

Short term exposure. Stimulation of sub-confluent cells for 24 hr with medium containing 20% FBS supplemented with fibers at concentrations ranging from 0.1 to 10 μg/cm^2.

Long term exposure. Two cycles of treatment, 72 hr each, with low concentrations of fibers. In details, 1 day after plating at 80% confluence in 25 ml flasks, cells were exposed to 2.5 μg/cm^2 of each fiber for 72 hr. Then, cells were washed twice with PBS and cells were transferred in larger (75-and 150-cm^2) flasks and let growing in medium containing 10% FBS for additional 4 days. Afterwards, the same fiber treatment was repeated as above and cells were grown up to 2 months, by 1:4 periodical passages. Treatments were made in triplicate.

Apoptosis

Sub-confluent cells were exposed to Ham's medium supplemented with 2% FBS, containing fibers (10 μg/cm^2) or 100 μM VP16 (Etoposide, Sigma-Aldrich, St. Louis, MO) for 24 hr. Nuclei fragmentation was evaluated by staining cells grown on cover slips with 8 μg/ml Hoechst solution (Calbiochem, San Diego, CA) in dark conditions for 1 hr. Samples were fixed in –20°C cold acetone:methanol for 15 min, washed in PBS, mounted in 50% glycerol/PBS and observed with a Leica immunofluorescence microscope. Cells displaying nuclear fragmentation were counted on 10 fields out of at least 50 cells in the same slide. Values are expressed as percentages of Hoechst staining positive HMC over total counted cells. Caspase activity was evaluated by staining cells with CaspACE FITC-VAD-FMK *in situ* marker (Promega, Madison, WI), followed by flow cytometry.

Signal transduction

Immunoblotting was performed by loading 50 μg of cell lysates in reducing conditions. After separation on SDS-PAGE and transfer to nitrocellulose (Hybond, Amersham, Buckinghamshire, UK), filters were probed with phospho-p38 (Thr180-Tyr182), phospho-NF-κB p65 (Ser536), phospho-JNK (Thr183-Tyr185), phospho-Akt (Ser473), phospho-Erk1/2 (Thr202-Tyr204), Akt, Erk1/2 antibodies from Cell Signalling Technology, Beverly, MA, α-Tubulin antibodies from Sigma-Aldrich as loading controls, Met, EGFR, PDGFRβ, NF-κB p65, JNK, p38, Cyclin D1 and E antibodies from Santa Cruz Biotechnology, Santa Cruz, CA. Detection was performed by the enhanced chemiluminescence system (ECL, Amersham).

Focus forming assay

Cells that survived the ''long term'' exposure to fibers, were followed 8 weeks, then a focus forming assay was performed in triplicate in 6-well dishes. Cells were plated at a density of 3×10^4/well and grown in 10% FBS Ham's medium. The number of foci per number of seeded cells is expressed as mean number ± standard deviation (SD). Foci arisen from confluent cells were taken and successfully established in cultures as single clones. Biochemical and biological characterization of foci were performed on a pool of clones, with a representative mixture of cells from each original focus.

Cell proliferation

Cells were grown on 24-well plates at a density of 3×10^4/well in Ham's medium supplemented with 2% FBS and containing the indicated fibers (1.25 μg/cm^2). Cells were fixed in 11% glutaraldehyde after 0, 24, 48 and 72 hr exposure and stained in crystal violet staining was eluted in 10% acetic acid and absorbance at 595 nm (A595) was measured in an ELISA plate reader.[33]

Immunochemical staining

Sub-confluent cells plated on glass slide flaskets (NUNC, Rochester, NY) were exposed to Ham's medium supplemented with 2% FBS and containing fibers (10 μg/cm^2) for 24 hr and subsequently fixed in 10% formalin. After 1 hr incubation with Ki67 antibodies (Neomarkers, Freemont, CA) at room temperature, biotin-streptavidin immunostaining was performed with UltraVision detection system, according to the manufacturer's instructions. Ki67 positive cells were counted on 10 fields with at least 50 cells in the same slide. Values are expressed as percentages of Ki67 positive cells over total counted HMC.

Cell cycle

Cells were synchronized by 0.1 μg/ml Colcemyd (Sigma-Aldrich) treatment for 24 hr, and then kept in normal medium for 4 days before analysis. They were washed in PBS, fixed in 50% ethanol and stained for 30 min at room temperature with 50 μg/ml propidium iodide (PI-Sigma-Aldrich) in 0.1 M PBS pH 7.2

ID: vasanss Date: 1/3/07 Time: 17:31 Path: J:/Production/IJC#/Vol00000/070117/3B2/C2IJC#070117

J_ID: IJC Wiley Ed. Ref. No.: 06-1230.R2 Customer A_ID: 22687 Date: 1-MARCH-07 Stage: I Page: 3

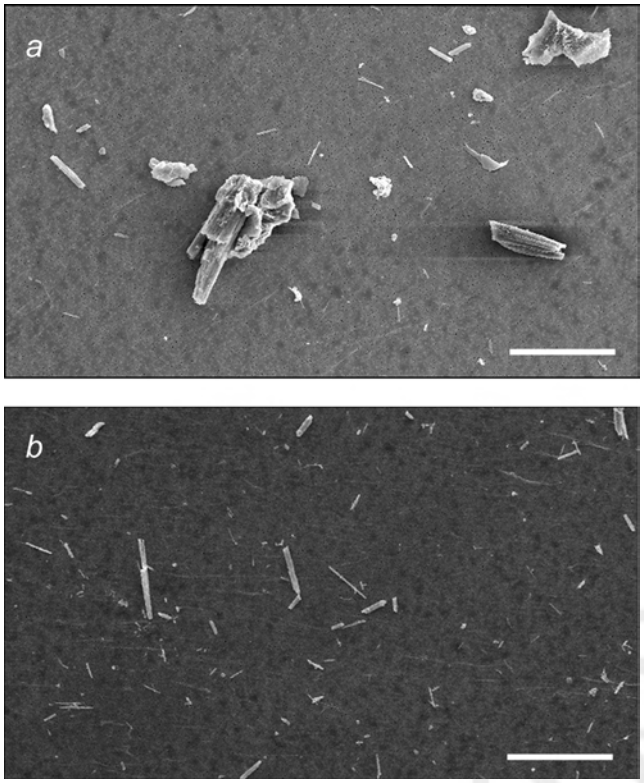

FIGURE 1 – SEM analysis of erionite fiber samples. SEM analysis of Karain (*a*) and Oregon (*b*) fiber samples at ×500 magnification. Central fields with adequate dispersion of fibers were selected for each sample. Bar: 50 μm.

containing 0.5 mg/ml RNAse. 10,000 events per sample were analyzed by flow cytometry.

Statistics

Data from cytotoxicity, DNA adducts, cell cycle, DNA neosynthesis, proliferation assays and caspase activity were expressed as mean ± standard deviation (SD) of at least 3 independent experiments. Statistical differences were evaluated by analysis of variance (ANOVA), followed by Tukey's HSD. Statistical analysis of Ki67 immunostaining and Hoechst staining assays was performed by Fisher's exact test among different groups, as indicated in the text. In all statistical evaluation the significance threshold was specified in the text. All statistical tests were two-sided.

Results

Most of erionite fiber samples fall in a mineralogical category with lower cytotoxicity than asbestos fibers

Karain erionite is a minor constituent of a volcanic rock, which is mainly Si-rich glass.[4,9,27–29] In addition, montmorillonite, and traces of quartz, feldspar, opal, clay (illite), carbonates were found associated with rock and soil samples from Karain.[27,28] For these reasons, the preparation of an adequately fiber-enriched sample for our tests was not possible. Nevertheless, in accordance with previous studies,[28] most of the matrix particulate material associated to the erionite used here is amorphous glass and few clay, carbonate and feldspar minerals. The erionite sample was characterized as having acceptable balance error, to verify that the data obtained fit with chemical composition and structure of the tested mineral.

TABLE I – NUMBER OF FIBRES IN DIFFERENT DIMENSIONAL CATEGORIES BY SEM

Fibre diameter (μm)	Fibre length, μm (%)		
	≤5	>5–8	>8
Oregon erionite (n = 495)			
>1.5	1 (0.2)	3 (0.6)	41 (8.2)
>0.5–1.5	36 (7.2)	55 (11.1)	69 (14.0)[1]
≤0.5	117 (23.6)	94 (19.0)	79 (16.1)[1]
Karain erionite (n = 500)			
>1.5	1 (0.2)	8 (1.6)	82 (16.4)
>0.5–1.5	38 (7.6)	69 (13.8)	97 (19.4)[1]
≤0.5	87 (17.4)	85 (17.0)	33 (6.6)[1]

[1]Proportion of fibres falling into the dimensional category with highest neoplastic response.

TABLE II – SIZE DISTRIBUTION (%) OF UICC ASBESTOS SAMPLES[23]

UICC sample	$L \geq 8$ μm	$D \leq 1.5$ μm
Chrysotile B	88	100
Amosite	70	99

From SEM examination the fraction of Karain fibrous material with L/W of 3:1 or greater resulted to be in the range 5–10%. In the erionite sample from Oregon this fraction resulted about 75%, with nonfibrous particles being mostly of amorphous nature (Fig. 1), in accordance with previous studies.[34] F1

The distribution of fiber sizes of the erionite samples are shown in the Table I. The fraction of fibers ($L > 8$ μm and $W \leq 1.5$ μm) with the dimensional category suggested as having the highest carcinogenic potential in rats ($L > 8$ μm and $W \leq 1.5$ μm)[35] was 26.0 and 30.1% in the Karain and Oregon samples, respectively. As shown in Table II, the size distribution of UICC asbestos samples (chrysotile B and amosite) reveals that all particles were asbestiform fibers with diameters smaller than 1 μm. However, the fraction of fibers with $L > 8$ μm was 88 and 70% for chrysotile and amosite, respectively. T1 T2

Calculations made on the basis of size distributions of Karain and Oregon erionite fibers revealed that the dust in size range considered more biologically active was constituted of ~19 and 180 fibers per microgram (F/μg) respectively, whereas the UICC chrysotile sample had about 1.5×10^5 and UICC amosite 1.2×10^5 F/μg. Noteworthy, the number of Oregon erionite fibers expressed in F/μg was very close to the value (150 F/μg) previously reported.[8]

Therefore, the fraction of more biologically active fibers was considerably lower in the case of erionite fibers, as compared to UICC asbestos samples, particularly in the case of erionite from Karain. In the glass fiber sample only a very small percentage (about 1%) of fibers were included in the more pathogenic size range.

Erionite induces low cell death but high DNA *neosynthesis*

We compared cytotoxicity induced by Karain (Turkey) and Oregon (USA) erionite fibers with that of asbestos fibers (amosite and chrysotile) and of glass fibers, used as relatively inert control. HMC were exposed for short term (24 hr) to fiber suspensions ranging from 0.1 up to 10 μg/cm^2, and cytotoxicity was evaluated by MTT assay. Our data show that dose-dependent cytotoxicity occurred in HMC exposed to erionite fibers, although by far lower than that induced by amosite. The differences evaluated at 5 and 10 μg/cm^2 at 24 hr are statistically significant ($p \leq 0.001$). Conversely, chrysotile-induced cytotoxicity was comparable with that of erionite. As expected, no detectable cytotoxicity was induced by glass fibers. After 48 hr the cytotoxic response was uniformly increased and differences among amosite and erionite fibers in

ID: vasanss Date: 1/3/07 Time: 17:31 Path: J:/Production/IJC#/Vol00000/070117/3B2/C2IJC#070117

J_ID: IJC Wiley Ed. Ref. No.: 06-1230.R2 Customer A_ID: 22687 Date: 1-MARCH-07 Stage: I Page: 4

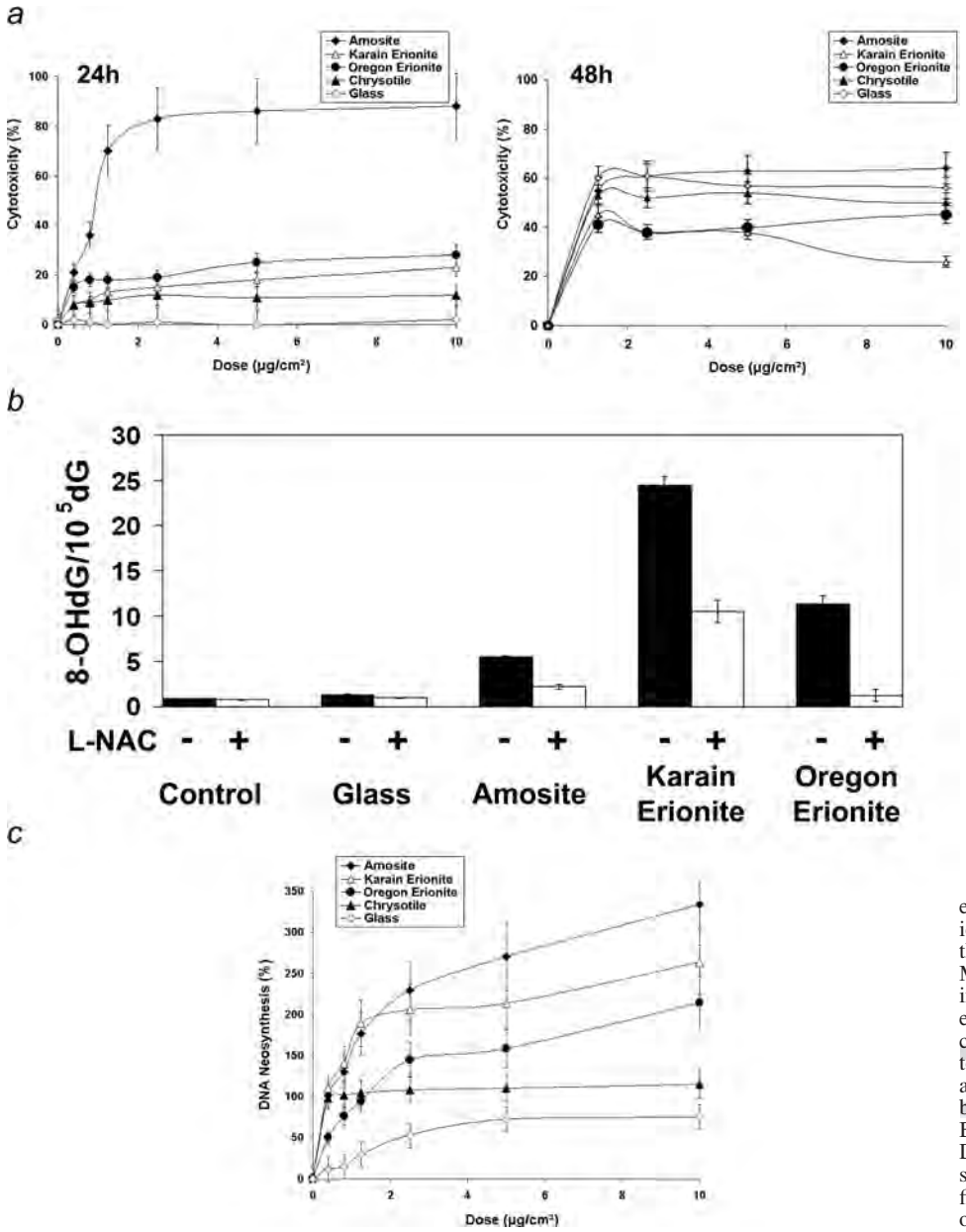

FIGURE 2 – Short term exposure to erionite and asbestos induces cytotoxicity, DNA adducts and DNA neosynthesis. (*a*) Cytotoxicity evaluated by MTT assay at different doses of the indicated fiber types, after short term exposure of 24 and 48 hr. (*b*) DNA content of 8-OHdG in HMC exposed to the indicated fibers, in presence or absence of L-NAC, evaluated as number of adducts formed per 10^5 dG. (*c*) BrdU incorporation in neosynthesized DNA of HMC cells, after 24 hr exposure to different doses of the indicated fiber types, expressed as percentage over untreated control.

inducing cell death were less evident, albeit erionite fibers at 5 μg/cm^2 still significantly displayed lower cytotoxicity levels than amosite ($p \leq 0.005$) and even than glass ($p \leq 0.05$) (Fig. 2*a*). These results were confirmed when apoptosis was evaluated by counting apoptotic cells after Hoechst staining. A higher number of nuclei showing typical chromatin condensation was observed upon cell exposure to pro-apoptotic agent VP16 (11.3%) and to amosite (12.4%), than in cells exposed to Karain erionite (3.9%), Oregon erionite (5.6%) or to glass beads (2.5%). These differences were statistically significant ($p \leq 0.001$). The possible effects of oxidative stress by fibers were examined by 8-hydroxy-2′-deoxyguanosine (8-OHdG) evaluation with HPLC and UV/amperometric detection. Interestingly, amosite and erionite fibers significantly induced DNA damage as compared to unexposed controls or to glass ($p \leq 0.001$). However, the amount of adducts induced by both erionite fibers was by far higher than that induced by amosite ($p \leq 0.001$). When the exposure to fibers was conducted in presence of the anti-oxidant agent *N*-Acetyl-L-Cysteine (L-NAC), the amount of DNA adducts significantly decreased for amosite and erionite fibers ($p \leq 0.001$), (Fig. 2*b*). This strongly indicates that oxygen reactive species play a role in DNA damage induced by exposure to fibers. Moreover, cell exposure to amosite or erionite fibers at 10 μg/cm^2 induced significantly higher BrdU incorporation in comparison with exposure to glass beads ($p \leq 0.005$) or chrysotile ($p \leq 0.05$), (Fig. 2*c*).

Only erionite-induced DNA *neosynthesis leads to cell proliferation*

Cell proliferation was monitored in HMC cultures to verify whether the considerable DNA neosynthesis observed upon erionite exposure was due either to compensatory synthesis of DNA, to repair fiber-induced chromosome damage, or to actual cell proliferation.

We observed an evident, although not statistically significant, increase in cell proliferation rate after 24 hr upon exposure to both types of erionite fibers, as compared to amosite, chrysotile and

ID: vasanss Date: 1/3/07 Time: 17:31 Path: J:/Production/IJC#/Vol00000/070117/3B2/C2IJC#070117

J_ID: IJC Wiley Ed. Ref. No.: 06-1230.R2 Customer A_ID: 22687 Date: 1-MARCH-07 Stage: I Page: 5

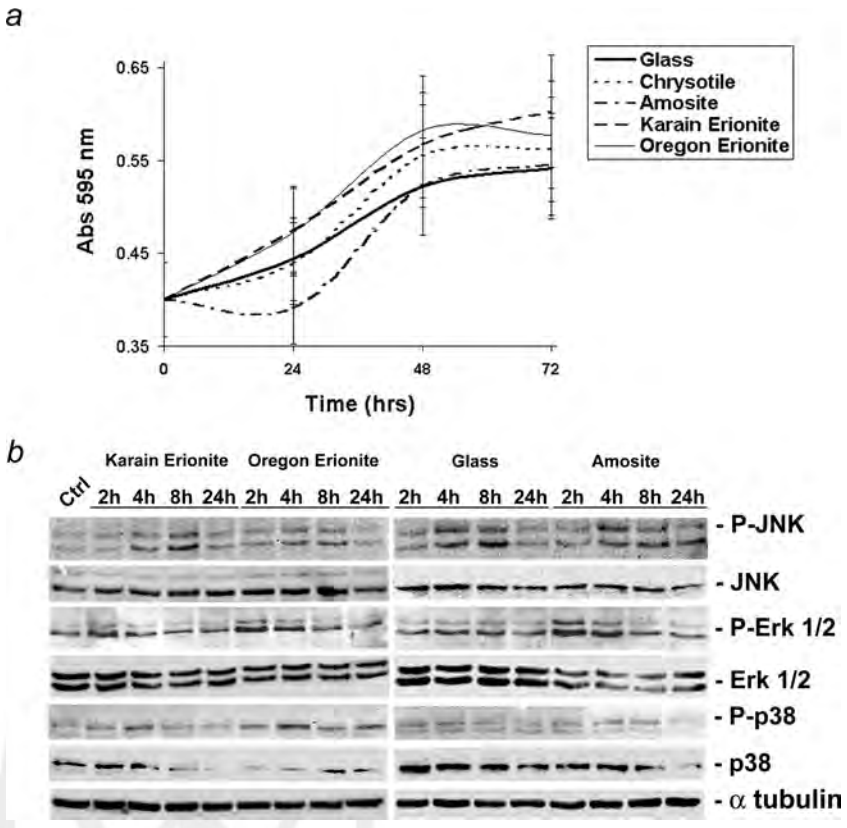

FIGURE 3 – Erionite-induced DNA neosynthesis is not only compensation for DNA damage. (*a*) Cell growth curve of HMC exposed to the indicated fibers and monitored at 24, 48 and 72 hr. Cell number was estimated by Abs595 nm values of the adsorbed crystal violet. (*b*) Immunoblotting with phospho-JNK, phospho-ERK1/2 and phospho-p38 antibodies on total lysates of HMC exposed to the indicated fibers for 2, 4, 8 and 24 hr. The expression levels of JNK, ERK1/2 and p38 were also examined by immunoblotting and α-tubulin content is also reported as loading control.

glass fibers exposure. After 72 hr, these differences were still evident, even though cells were sub-confluent and attained the growth plateau (Fig. 3*a*). Also Ki67 staining, a known cell proliferation marker, was determined upon 24 hr exposure to amosite, glass and both types of erionite fibers. Higher percentages of Ki67-positive cells were found in HMC cultures exposed to Karain erionite (6.2%) and to Oregon erionite (5.0%), as compared to amosite (2.6%) or glass (2.1%) fibers, as well as to untreated cells (3.2%). The differences in Ki67 staining induced by both erionite fibers compared to other fiber types are statistically significant ($p \leq 0.005$). Moreover, transient Jnk phosphorylation was observed 4 hr after exposure to any fiber type (10 μg/cm^2), suggesting a nonspecific stress response (Fig. 3*b*). Jnk phosphorylation decreased after 8 hr, except in the case of amosite, which evoked instead a sustained Jnk activity, as expected from its high level of cytotoxicity. Erk1/2 and p38 phosphorylation was not detectable after exposure to glass fibers, whereas Erk1/2 phosphorylation was sustained up to 8 hr after exposure to amosite. In cells exposed to erionite fibers Erk1/2 signaling was more transient. The activity of p38 was by far more evident in cells exposed to erionite than amosite, especially in consideration of a reduced p38 expression in erionite treated cells (Fig. 3*b*). In cells exposed to amosite fibers we observed: reduced proliferation rate (Fig. 3*a*), increased cell death (Fig. 2*a*) and significantly lower staining of Ki67, but also elevated BrdU incorporation (Fig. 2*c*) and sustained Erk1/2 activity (Fig. 3*b*). One possible interpretation of these data is that DNA neosyntesis occur in cells nevertheless dying, as a consequence of amosite damage.

As regards erionite fibers, we conclude that DNA-neosynthesis observed after short term exposure to fibers is not only compensatory in consequence of erionite-induced DNA damage, but also allows HMC proliferation. Moreover, the exposure to erionite fibers, displaying low cytotoxicity and high production of reactive oxygen species, exerts on HMC the highest transforming potential.

TABLE III – FOCI FORMED AFTER 60 DAYS ''LONG TERM'' EXPOSURE TO DIFFERENT FIBRE TYPES

Treatment	Frequency of focus formation[1]
Untreated	–[2]
Glass	–[2]
Amosite	–[2]
Chrysotile	–[2]
Karain erionite	$1.0 \times 10^{-4} \pm 0.65 \times 10^{-4}$
Oregon erionite	$0.3 \times 10^{-4} \pm 0.46 \times 10^{-4}$

[1]Number of transformed foci per treated cell.–[2]No foci developed from 3×10^5 cells exposed to fibres.

Erionite fibers ''long-term'' exposure promotes HMC transformation per se

It has been demonstrated that prolonged exposure of SV40 positive-HMC to asbestos fibers may induce transformation.[23,24] We aimed to verify whether exposure to low doses of erionite fibers could induce mesothelial transformation and if SV40 is required, as for asbestos fibers. We treated HMC according to a ''long term'' exposure protocol (see Methods). Two months after the ''long term'' exposure, only cells exposed to erionite fibers underwent loss of cell contact inhibition and several foci arose from the culture. No statistically significant differences were observed between the 2 types of erionite fibers in focus formation. No foci resulted after exposure to amosite, chrysotile and glass fibers (Table III). These cells acquired a clear-cut novel morphology, similar to what we previously described[24] for cells exposed to asbestos (Fig. 4*a* left). Cells obtained from foci were cultured up to 29 passages for HMC-Karain erionite and 48 passages for HMC-Oregon erionite. These cells maintained the phenotype described earlier, grew in low serum, displayed anchorage-independent soft-agar growth and showed a significantly higher proliferation rate than HMC (at 48 hr, $p \leq 0.05$ for

ID: vasanss Date: 1/3/07 Time: 17:31 Path: J:/Production/IJC#/Vol00000/070117/3B2/C2IJC#070117

J_ID: IJC Wiley Ed. Ref. No.: 06-1230.R2 Customer A_ID: 22687 Date: 1-MARCH-07 Stage: I Page: 6

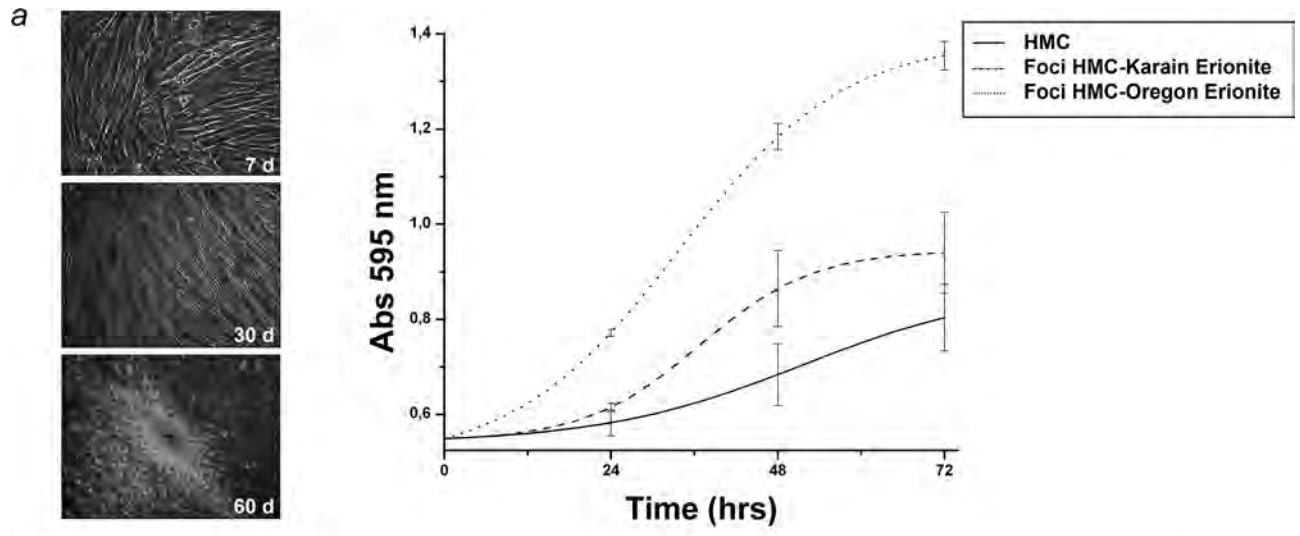

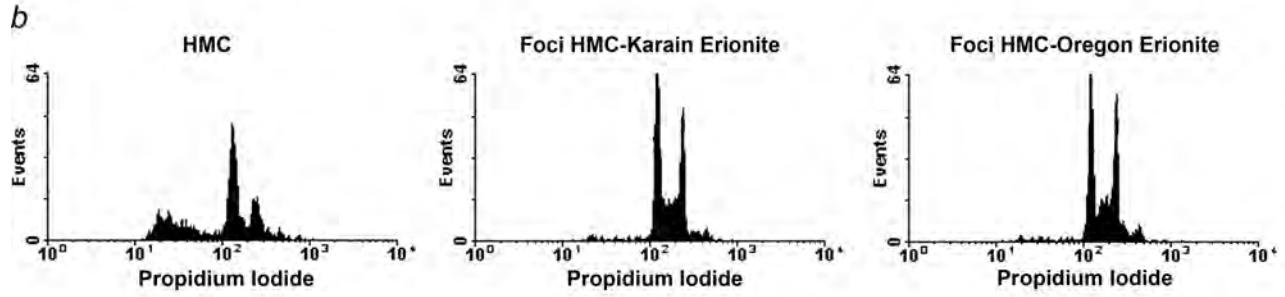

	sub-G1	G1	S	G2-M
HMC	31.81 ± 2,72	44.03 ± 3,01	6.20 ± 1,25	18.29 ± 1,43
Foci HMC-Karain Erionite	3.65 ± 1,07	49.50 ± 2,96	18.60 ± 1,51	29.73 ± 2,81
Foci HMC-Oregon Erionite	3.72 ± 0,89	51.74 ± 3,04	19.27 ± 1,61	26.88 ± 2,68

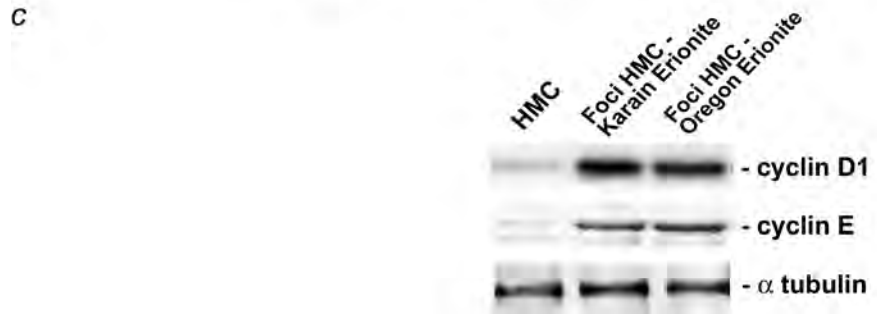

FIGURE 4 – Erionite fibers ''long-term'' exposure *per se* promotes HMC transformation. (*a*) Left: representative pictures of HMC 7, 30 and 60 days after the long-term exposure to Karain erionite fibers, showing the different acquired morphology. Right: proliferation assay of pooled cell clones from foci obtained after long term exposure to both types of erionite fibers. Cell number was estimated by Abs595 nm values of the adsorbed crystal violet. (*b*) Cell cycle analysis of synchronized HMC and cells derived from foci elicited by exposure to the two types of erionite. The percentages of cells in the different phases of the cell cycle are given in details below the cytograms. (*c*) Immunoblotting on total lysates of HMC and of foci derived cells probed with cyclin D1 and cyclin E antibodies. Same filter and loading controls of Figure 5, determined by α-tubulin immunoblotting.

HMC-Karain erionite and $p \leq 0.005$ for HMC-Oregon erionite; Fig. 4*a* right).

Cell cycle analysis revealed that cells obtained from foci, which escaped serum-dependency for growth, exhibited disappearance of subG1-S hypoploid phase, displayed a strong increase of S-phase entry (Fig. 4*b*). The differences between percentages of foci cells and HMC in subG$_1$-phase and in S-phase are statistically significant ($p \leq 0.001$). Moreover, we observed over expression of cyclins D1 and E, involved in G1/S cell cycle transition (Fig. 4*c*). In foci derived cells HGFR/Met, EGFR and PDGFRβ were expressed at higher extent than in HMC, as determined by immunoblotting. Analysis of cell signaling revealed that these cells displayed Akt, Erk1/2 and NF-κB activities at higher levels than in untransformed HMC (Fig. 5). Moreover, cells derived from foci became significantly more resistant ($p \leq 0.001$ for HMC-Karain Erionite and $p \leq 0.005$ for HMC-Oregon Erionite) than HMC to

F5

ID: vasanss Date: 1/3/07 Time: 17:32 Path: J:/Production/IJC#/Vol00000/070117/3B2/C2IJC#070117

J_ID: IJC Wiley Ed. Ref. No.: 06-1230.R2 Customer A_ID: 22687 Date: 1-MARCH-07 Stage: I Page: 7

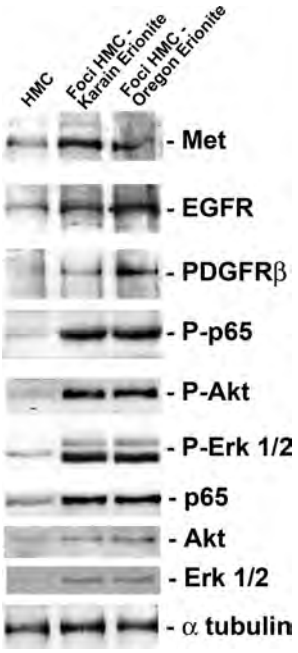

FIGURE 5 – Characterization of cells derived from foci. Immunoblotting on total lysates of HMC performed using either antibodies directed against growth factor receptors (Met/HGFR, EGFR, PDGFRβ) and phospho-specific antibodies recognizing the active form of intracellular effectors (P-p65 NF-κB, P-Akt, P-Erk1/2). Levels of p65, Akt and Erk1/2 were also determined by immunoblotting. The content of cellular proteins has been normalized by α-tubulin immunoblotting.

the pro-apoptotic agent VP16 (Etoposide), as determined by MTT assay (Fig. 6*a*). As well, induction of Caspase activity, evaluated by flow cytometry, was significantly reduced in foci ($p \leq 0.001$) as compared with untransformed HMC (Fig. 6*b*).

We conclude that even relatively low concentrations of erionite fibers can cause transformation of HMC.

Discussion

Our results show that erionite has clear intrinsic transforming properties, associated with low cytotoxicity and high oxygen reactive species formation, combined with high DNA neo-synthesis and high cell proliferation rate. Cell transformation is demonstrated by foci formation in cultures exposed to erionite but not to amosite fibers. Transformed cells obtained from erionite induced foci are highly proliferating and resistant to apoptosis. HGFR/Met, EGFR and PDGFRβ are highly expressed as well, and the intracellular signalling effectors NF-κB, Akt and Erk are also activated.

The characterization by SEM analysis of the fibers used, reveals that the proportion of fibers with $L > 8$ μm and $W \leq 1.5$ μm, close to the dimensional category associated with the highest biological activity,[35] was considerably lower for erionite compared to UICC asbestos samples, very rich of fibers in the ''biologically active'' size range. The nonfibrous material present in our erionite samples should not have a substantial pathogenic influence.[36] However, we cannot exclude a possible potentiating effect by some components of this material to the action of the fibrous fraction.[37]

It has been demonstrated that the number of erionite fibers required to develop peritoneal mesothelioma in rats was orders of magnitude lower than that observed for asbestos fibers.[38] This explained the higher carcinogenic potential observed for erionite, even at considerably lower concentration than asbestos.[6]

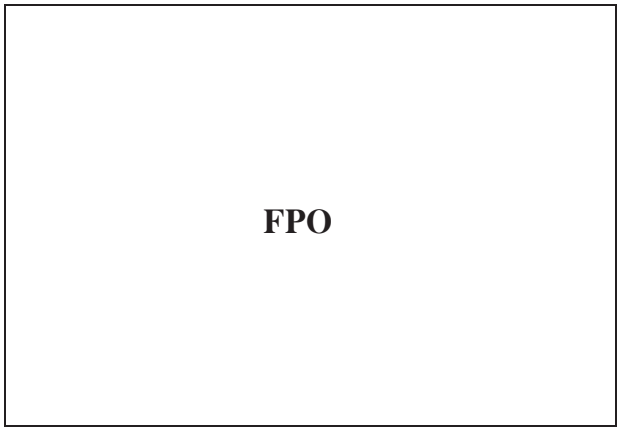

FIGURE 6 – Cells from foci become resistant to toxics. (*a*) Cytotoxicity of the indicated cell types (HMC and cells derived from foci), after exposure to 100 μM VP16, evaluated by MTT assay. (*b*) Cytofluorimetric analysis of caspase activity, by using the CaspACE FITC-VAD-FMK marker, of HMC and cells derived from foci, after exposure to 100 μM VP16. The percentage of caspase activity increase is indicated on the right.

In the present work, the comparison of asbestos with erionite fibers indicate that amosite induces relevant HMC cytotoxicity, possibly because of their longer fibers or high iron content.[39] Conversely, only erionite fibers promote HMC transformation, possibly because these fibers are less cytotoxic than amosite, having a lower content of iron.[7] Chrysotile fibers, in spite of their reduced cytotoxicity, are unable to cause cell proliferation, as previously reported.[40] Even short term exposure for 24 hr to erionite fibers induced low cytotoxicity, allowing a high proliferation rate, associated with formation of DNA adducts.

Upon fiber exposure several intracellular signals are generated. Jnk was increased by all fiber types, suggesting a nonspecific stress response and its activity was sustained only upon amosite exposure, probably because of the high cytotoxic property of these fibers. The transient patterns of Erk1/2 activity observed in HMC exposed to amosite fibers were similar to those previously reported for crocidolite exposure,[16] which has the same cytotoxicity pattern of amosite.[24] Erionite- and amosite-dependent Erk1/2 activity was consistent with cell proliferation evoked by these fibers.[12] Higher p38 activity in HMC upon exposure to erionite, can be explained with the highest oxidative stress caused by these fibers[41] and is consistent with highest levels of 8OH-dG observed here in the same conditions.

In view of the high level of BrdU incorporation in cells otherwise displaying high percentage of cell death, we interpret DNA incorporation as caused by neo-synthesis of DNA in cells that eventually are dying, as a consequence of amosite induced damage, rather than as enhancement of mitogenesis. Conversely, the 2 types of erionite display the lowest cytotoxicity values, combined with DNA neosynthesis and cell proliferation, evaluated both by growth curve and Ki67 marker. Moreover, genotoxic properties of erionite fibers have been reported[8] and are confirmed by our data on 8-OHdG adduct levels, which are significantly higher in cells exposed to erionite fibers of both types. Altogether, these results account for high transforming activity of the few erionite fibers in the pathogenic size range.

Cells from foci induced by erionite displayed the properties of *in vitro* full transformation, *i.e.* changes in morphology, growth in soft agar, high number of passages in culture and increased proliferation rate. Moreover, these cells had autonomous NF-κB, Erk1/2 and Akt activities. Whereas MAPK activity is likely associated to increased cell proliferation rate, NF-κB and Akt are responsible of the increased resistance to cytotoxic agents, as suggested by the

ID: vasanss Date: 1/3/07 Time: 17:32 Path: J:/Production/IJC#/Vol00000/070117/3B2/C2IJC#070117

rescue of sensitivity upon treatment with specific PI3K and NF-κB inhibitors (not shown). Noteworthy, recently it has been demonstrated a key role for NF-κB in asbestos carcinogenesis in HMC.[18] The presence of activated p65 NF-κB subunit in erionite-induced foci described here is in agreement with these results. Similarly, these cells expressed high levels of HGFR/Met, EGFR and PDGFRβ, suggesting their possible role in sustaining cell survival.

Asbestos is certainly a universally accepted causative agent of MM,[2] although several evidences suggest that SV40 virus may cooperate with asbestos in HMC transformation[23,24] and in the onset of MM.[42] We show here that erionite fibers are able to induce HMC transformation *per se*, regardless SV40 infection. This may explain the high incidence of MM in Cappadocia, a region of Turkey where SV40 virus was never isolated.[3,4,25,26] Erionite is a ubiquitous zeolite, also present in Oregon, USA, where SV40 has been identified in several human specimens.[26] Although amosite is considered a potent human carcinogen, we show here that, according to other similar findings,[23] amosite is not clearly transforming by itself. However, the high level of DNA neosynthesis, as that induced by amosite in these *in vitro* experiments, can induce infidelity of DNA replication and frequent mismatches. Furthermore other agents (such as SV40) can act as critical co-factors, allowing these damaged cells to survive and to progressively acquire biological transformation.

In conclusion, the mineralogical characteristics of erionite fibers (size, surface area and structure) associated with their high transforming capability, highlight the importance of a careful evaluation of the hazard represented by exposure to low concentrations of other similar fibers, to which human beings could be exposed.

Acknowledgements

We thank Dr. J.W. Skidmore (MRC Pneucomoniosis Unit, Llandough Hospital, Penarth, Wales) for providing erionite samples. We also thank Dr. M. Rinaldi for advice on the statistical analysis. This work is part of a G.I. Me. (Gruppo Italiano per lo studio e la terapia del Mesotelioma) network program.

References

1. Mossman BT, Gee JB. Asbestos-related diseases. N Engl J Med 1989;320:1721–30.
2. Mossman BT, Kamp DW, Weitzman SA. Mechanisms of carcinogenesis and clinical features of asbestos-associated cancers. Cancer Invest 1996;14:466–80.
3. Dogan AU, Dogan M, Emri S. Erionite. In: Encyclopedia of toxicology, 2nd edn., vol. 2. Oxford: Elsevier, 2005.
4. Dogan AU, Baris YI, Dogan M, Emri S, Steele I, Elmishad AG, Carbone M. Genetic predisposition to fiber carcinogenesis causes a mesothelioma epidemic in Turkey. Cancer Res 2006;66:5063–8.
5. Okayasu R, Wu L, Hei TK. Biological effects of naturally occurring and man-made fibres: in vitro cytotoxicity and mutagenesis in mammalian cells. Br J Cancer 1999;79:1319–24.
6. Carthew P, Hill RJ, Edwards RE, Lee PN. Intrapleural administration of fibres induces mesothelioma in rats in the same relative order of hazard as occurs in man after exposure. Hum Exp Toxicol 1992;11: 530–4.
7. Eborn SK, Aust AE. Effect of iron acquisition on induction of DNA single-strand breaks by erionite, a carcinogenic mineral fiber. Arch Biochem Biophys 1995;316:507–14.
8. Poole A, Brown RC, Turver CJ, Skidmore JW, Griffiths DM. In vitro genotoxic activities of fibrous erionite. Br J Cancer 1983;47:697–705.
9. Wagner JC, Skidmore JW, Hill RJ, Griffiths DM. Erionite exposure and mesotheliomas in rats. Br J Cancer 1985;51:727–30.
10. Long JF, Dutta PK, Hogg BD. Fluorescence imaging of reactive oxygen metabolites generated in single macrophage cells (NR8383) upon phagocytosis of natural zeolite (erionite) fibers. Environ Health Perspect 1997;105:706–11.
11. Janssen YM, Heintz NH, Marsh JP, Borm PJ, Mossman BT. Induction of c-fos and c-jun proto-oncogenes in target cells of the lung and pleura by carcinogenic fibers. Am J Respir Cell Mol Biol 1994;11: 522–30.
12. Timblin CR, Guthrie GD, Janssen YW, Walsh ES, Vacek P, Mossman BT. Patterns of c-fos and c-jun proto-oncogene expression, apoptosis, and proliferation in rat pleural mesothelial cells exposed to erionite or asbestos fibers. Toxicol Appl Pharmacol 1998;151:88–97.
13. Johnson GL, Lapadat R. Mitogen-activated protein kinase pathways mediated by ERK, JNK, and p38 protein kinases. Science 2002;298: 1911–2.
14. Tsuruo T, Naito M, Tomida A, Fujita N, Mashima T, Sakamoto H, Haga N. Molecular targeting therapy of cancer: drug resistance, apoptosis and survival signal. Cancer Sci 2003;94:15–21.
15. Waddick KG, Uckun FM. Innovative treatment programs against cancer. II. Nuclear factor-κB (NF-κB) as a molecular target. Biochem Pharmacol 1999;57:9–17
16. Berken A, Abel J, Unfried K. β1-integrin mediates asbestos-induced phosphorylation of AKT and ERK1/2 in a rat pleural mesothelial cell line. Oncogene 2003;22:8524–8.
17. Janssen YM, Barchowsky A, Treadwell M, Driscoll KE, Mossman BT. Asbestos induces nuclear factor κ B (NF-κ B) DNA-binding activity and NF-κ B-dependent gene expression in tracheal epithelial cells. Proc Natl Acad Sci USA 1995;92:8458–62.
18. Yang H, Bocchetta M, Kroczynska B, Elmishad AG, Chen Y, Liu Z, Bubici C, Mossman BT, Pass HI, Testa JR, Franzoso G, Carbone M. TNF-α inhibits asbestos-induced cytotoxicity via a NF-κB-dependent pathway, a possible mechanism for asbestos-induced oncogenesis. Proc Natl Acad Sci USA 2006;103:10397–402.
19. Pache JC, Janssen YM, Walsh ES, Quinlan TR, Zanella CL, Low RB, Taatjes DJ, Mossman BT. Increased epidermal growth factor-receptor protein in a human mesothelial cell line in response to long asbestos fibers. Am J Pathol 1998;152:333–40.
20. Bermudez E, Everitt J, Walker C. Expression of growth factor and growth factor receptor RNA in rat pleural mesothelial cells in culture. Exp Cell Res 1990;190:91–8.
21. Cacciotti P, Libener R, Betta P, Martini F, Porta C, Procopio A, Strizzi L, Penengo L, Tognon M, Mutti L, Gaudino G. SV40 replication in human mesothelial cells induces HGF/Met receptor activation: a model for viral-related carcinogenesis of human malignant mesothelioma. Proc Natl Acad Sci USA 2001;98:12032–7.
22. Tolnay E, Kuhnen C, Wiethege T, Konig JE, Voss B, Muller KM. Hepatocyte growth factor/scatter factor and its receptor c-Met are overexpressed and associated with an increased microvessel density in malignant pleural mesothelioma. J Cancer Res Clin Oncol 1998;124:291–6.
23. Bocchetta M, Di Resta I, Powers A, Fresco R, Tosolini A, Testa JR, Pass HI, Rizzo P, Carbone M. Human mesothelial cells are unusually susceptible to simian virus 40-mediated transformation and asbestos cocarcinogenicity. Proc Natl Acad Sci USA 2000;97:10214–19.
24. Cacciotti P, Barbone D, Porta C, Altomare DA, Testa JR, Mutti L, Gaudino G. SV40-dependent AKT activity drives mesothelial cell transformation after asbestos exposure. Cancer Res 2005;65:5256–62.
25. Emri S, Kocagoz T, Olut A, Gungen Y, Mutti L, Baris YI. Simian virus 40 is not a cofactor in the pathogenesis of environmentally induced malignant pleural mesothelioma in Turkey. Anticancer Res 2000;20:891–4.
26. De Rienzo A, Tor M, Sterman DH, Aksoy F, Albelda SM, Testa JR. Detection of SV40 DNA sequences in malignant mesothelioma specimens from the United States, but not from Turkey. J Cell Biochem 2002;84:455–9.
27. Mumpton FA. A reconnaissance study of the association of zeolites with mesothelioma occurrences in central Turkey, United States Department of the Interior Geological Survey, 1979.
28. Dogan M. Sources and types of mineral dust in regions of Turkey with endemic malignant mesothelioma. Indoor Built Environ 2003; 12:377–83.
29. Dogan M, Dogan AU. Asbestos mineralogy and health effects. In: Malignant mesothelioma: advances in pathogenesis, diagnosis, and translation therapies. New York: Springer, 2005.
30. Kohyama N, Shinohara Y, Suzuki Y. Mineral phases and some reexamined characteristics of the International Union Against Cancer standard asbestos samples. Am J Ind Med 1996;30:515–28.
31. Mossman BT. In vitro approaches for determining mechanisms of toxicity and carcinogenicity by asbestos in the gastrointestinal and respiratory tracts. Environ Health Perspect 1983;53:155–61.
32. Toyokuni S, Sagripanti JL. Association between 8-hydroxy-2′-deoxyguanosine formation and DNA strand breaks mediated by copper and iron. Free Radic Biol Med 1996;20:859–64.
33. Kueng W, Silber E, Eppenberger U. Quantification of cells cultured on 96-well plates. Anal Biochem 1989;182:16–9.
34. Wright WE, Rom WN, Moatamed F. Characterization of zeolite fiber sizes using scanning electron microscopy. Arch Environ Health 1983;38:99–103.
35. Stanton MF, Laynard M, Tegeris A, Miller E, May M, Kent E. Carcinogenicity of fibrous glass: pleural response in the rat in relation to fiber dimension. J Natl Cancer Inst 1977;58:587–603.

AQ2

36. Becher R, Hetland RB, Refsnes M, Dahl JE, Dahlman HJ, Schwarze PE. Rat lung inflammatory responses after in vivo and in vitro exposure to various stone particles. Inhal Toxicol 2001;13:789–805.
37. Johnson NF, Edwards RE, Munday DE, Rowe N, Wagner JC. Pluripotential nature of mesotheliomata induced by inhalation of erionite in rats. Br J Exp Pathol 1984;65:377–88.
38. Davis JM, Bolton RE, Miller BG, Niven K. Mesothelioma dose response following intraperitoneal injection of mineral fibres. Int J Exp Pathol 1991;72:263–74.
39. Kamp DW, Graceffa P, Pryor WA, Weitzman SA. The role of free radicals in asbestos-induced diseases. Free Radic Biol Med 1992;12:293–315.
40. Marchevsky AM, Wick MR. Current controversies regarding the role of asbestos exposure in the causation of malignant mesothelioma: the need for an evidence-based approach to develop medicolegal guidelines. Ann Diagn Pathol 2003;7:321–32.
41. Maples KR, Johnson NF. Fiber-induced hydroxyl radical formation: correlation with mesothelioma induction in rats and humans. Carcinogenesis 1992;13:2035–9.
42. Mayall FG, Jacobson G, Wilkins R. Mutations of *p53* gene and SV40 sequences in asbestos associated and non-asbestos-associated mesotheliomas. J Clin Pathol 1999;52:291–3.

AQ1: Kindly check whether the short title is OK as given.

AQ2: Kindly provide the editor names as well as the page numbers for References 3 and 29 (Edited book part type references).

AQ3: Kindly check whether the corresponding information is OK as typeset.

ED1: Please provide artwork for Figure 6.